THESIS FOR THE DEGREE OF DOCTOR OF PHILOSOPHY WITH INTERNATIONAL MENTION FOR THE UNIVERSITY OF SEVILLE

Proposal and Calibration of a Biodynamic Model of Human-Structure Interaction by the Resolution of the Inverse Dynamic Problem. Application to Pedestrian Bridges.

Javier Fernando Jiménez Alonso

Department of Continuum Mechanics and Structural Analysis

School of Engineering

UNIVERSITY OF SEVILLE

Seville, Spain 2015

Proposal and calibration of a biodynamic model of human-structure interaction by the resolution of the inverse dynamic problem. Application to pedestrian bridges.

PhD's Thesis in the Dynamic of Structures and Earthquake Engineering program.

Javier Fernando Jiménez Alonso

Advisor: Prof. Dr. Andrés Sáez Pérez.

Department of Continuum Mechanics and Structural Analysis

School of Engineering

University of Seville

Abstract

In this thesis a biomechanical crowd-structure interaction model is proposed and further implemented in order to adequately estimate the energy exchange between pedestrians and footbridge. The proposed model focuses on both the vibrations in the vertical and lateral directions and it allows to take into account the change of the modal properties of the structure due to the presence of pedestrians, thus improving the numerical estimation of the response of the structure under pedestrian flows. It further permits to analyze in more detail the lateral lock-in phenomenon. The model involves two sub-models, namely (i) a pedestrian-structure interaction sub-model plus (ii) a crowd sub-model. The first sub-model follows from a modal projection of a two degree of freedom system that simulates the behavior of each pedestrian, on the vibration modes of the structure. The parameters of this model are estimated from the accelerations recorded on a real footbridge by implementing an inverse dynamic approach. For the second sub-model, the crowd behavior is simulated via a multi-agent method. The performance of the resulting overall model is assessed by correlating the experimental and numerical dynamic behavior of two real footbridges. In particular two phenomena are analyzed in detailed: (i) the change in the first vertical natural frequency of a real footbridge induced by the pedestrian-structure interaction and (ii) the occurrence of the lateral lock-in phenomenon due to the pedestrian action. The proposed model leads to numerical results that exhibit good agreement with the obtained experimental values. Therefore, it becomes a valuable tool to account for the change on the modal properties of a footbridge induced by the crowd-structure interaction phenomenon. The consideration of this factor allows estimating more accurately the dynamic response of the footbridge under the pedestrian action, analyzing in more detailed the occurrence of the lateral lock-in phenomenon or improving the efficiency in the design of passive and active dampers if their installation was necessary to guarantee an adequate comfort level on the footbridge.

Keywords: *simplified biomechanical model, human-structure interaction, crowd dynamics, change of natural frequencies, operational modal analysis, model updating, parameter identification, lateral lock-in phenomenon*

PREFACE

This Thesis has been carried out at the Department of Continuum Mechanics and Structural Analysis at the University of Seville. The work has been supervised by Full Professor Dr. Andrés Sáez Perez. I always owe my deepest gratitude to Andrés for encouraging and supporting me constantly during the development of this work. This research would not have been possible without his infinite patient and helpful guidance for the organization of the papers. Thank him for his time, effort and friendship. I feel really lucky for having had the opportunity to develop this work under his tutelage.

Additionally, I would like to express some lines of gratitude to those who have contributed to the development of the research carried out by the author of this Thesis.

To Prof. Alvaro Cunha, who provided me a nice workplace during my research stay at the *Laboratory of Vibrations and Structural Monitoring* (*ViBest*) of the *University of Porto* (*Portugal*), allowing me to improve my knowledge of the operational modal analysis methodology and perform several experimental tests of great importance for the development of this work. The results I collected during my research stay constitute a vital part of my Thesis and would not have been possible without the support of Associate Professor Elsa Caetano and Assistant Professor Filipe Magalhães.

To Prof. Alexander Pavic, for receiving me into his group of the *Vibration Engineering Section* of the *University of Exeter* (*U.K.*) during my second research stay allowing me to introduce myself in the interesting field of the control of civil engineering structures.

To my parents, Antonio and Maria del Carmen, who taught me the value of the education and who made a remarkable effort for us, their children, so that we could have all the opportunities that they did not have.

To my colleagues (past and present) at the Department of Building Structures of the University of Seville and at the Bridge Engineering Firm, IDES, for their constant support.

This thesis is based on scientific papers which have already been accepted for publication in relevant scientific journals or presented at international conference with peer-review. Finally, two additional papers, currently under review, have been included.

Last but not least, I am very grateful for the loving support of my family, in particular my brilliant and comprehensive wife, Patricia, and our two lovely daughters, Claudia and Lorena. I hope that one day I could compensate the time that I stool them for the development of this work.

To Maribel for her continuous support, for me and my family, during these difficult years.

My gratitude goes also to other relatives and friends that have helped me to overtake successfully all the difficulties for the achievement of this Thesis.

Seville, October 2015
Javier Fernando Jiménez Alonso

ACKNOWLEDGEMENTS

This work was partially funded by the Spanish Ministry for Science under research project DPI2014-53947-R.

THESIS

This Thesis consists of an extended summary and the following appended papers:

Paper A	J.F. Jiménez-Alonso and A. Sáez
	A direct-pedestrian structure interaction model to characterize the human induced vibrations on slender footbridges
	Informes de la Construcción, Vol. 66 (Extra 1). m007
Paper B	J.F. Jiménez-Alonso, A. Sáez, E. Caetano, F. Magalhães
	Vertical crowd–structure interaction model to analyze the change of the modal properties of a footbridge
	Journal of Bridge Engineering. ASCE (in press)
Paper C	J.F. Jiménez-Alonso and A. Sáez
	Model updating for the selection of the retrofit method of an ancient bridge (Almeria, Spain).
	Structural Engineering International. IABSE (in press).
Paper D	J.F. Jiménez-Alonso and A. Sáez
	Controlling the human-induced longitudinal vibrations of a Nielsen-truss footbridge via the modification of its natural frequencies
	Under review
Paper E	J.F. Jiménez-Alonso, A. Sáez, E. Caetano and A. Cunha
	Lateral crowd-structure interaction model to analyze the lateral lock-in phenomenon on a real footbridge
	Under review
Paper F	J.F. Jiménez-Alonso, E. Caetano and A. Cunha
	Dynamic testing of Carpinteira footbridge at Colvihã (Portugal)
	5th International Operational Modal Analysis Conference (Guimarães, Portugal) 13-15 May 2013
Paper G	J.F. Jiménez-Alonso and A. Sáez
	Assessment of the dynamic behavior of Palmas Altas footbridge at Seville (Spain)
	37th IABSE Symposium. Madrid (Spain) 3-5 September 2014

The appended papers were prepared in collaboration with co-authors. The author of this Thesis is responsible for the major progress of work in these papers, including the development/deduction of solutions and numerical methods, performing the numerical simulations and experimental tests and writing the main parts of the papers.

Table of Contents

PART I

EXTENDED SUMMARY

I. Extended summary

1. Introduction.

The excitation originated by the pedestrian walking action is the main cause of the vibratory problems on footbridges (*Bachmann and Amman, 1987*). Although the magnitude of a single pedestrian load is limited, the possible resonant phenomenon, originated by the agreement of the pedestrian step frequency with some of the natural frequencies of the structure may cause high levels of vibration.

In modern civil engineering, the improvement of the resistant conditions, the use of new structural systems and the current aesthetic requirements have prompted that these structures are increasingly likely to experience pedestrian-structure interaction problems. Although, at the end of the last century, there were a lot of papers about cases of vibratory problems on structures originated by the pedestrian action (*Bachmann and Amman, 1987; Wolmuth and Surtees, 2003*), it was the closing of the Millennium footbridge (London, 2000) (*Dallard et al., 2001*), the main cause that made that the scientific community became aware of the importance of the problem.

Three are the main factors that control this problem: (i) first, the source of excitation, being necessary to distinguish, between the behavior of a single pedestrian and a group of them; (ii) second, the support system, the footbridge, characterized by its modal parameters (mass, damping and stiffness); and (iii) third, the receiver (the pedestrian). The complexity of the resultant forces is due to the fact that they are generated and controlled by the human being (Figure 1).

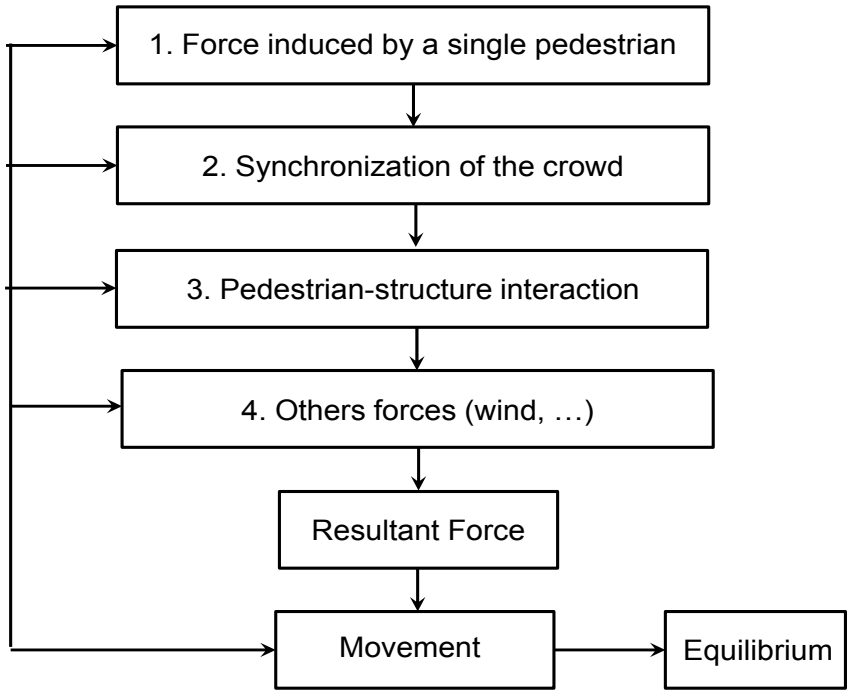

Figure 1. Layout of the auto-excitation process of the pedestrian load.

Given the high sensitivity of the pedestrians to vibrations, there are not many reported cases (*Wolmuth and Surtees, 2003*) where this phenomenon had as effect the failure of the structure, since, the excitation normally stopped under high levels of accelerations, and therefore, the problem usually needed to be dealt as a serviceability limit state problem (comfort) rather than as an ultimate limit state problem (failure).

The treatment given to the problem by the international standards has basically focused on avoiding its occurrence, recommending that the natural frequencies of the footbridge stay away from the range of frequencies that characterizes the pedestrian walking step. This recommendation cannot always be checked, being therefore necessary to guarantee that the footbridge attains certain comfort level. These comfort levels were normally established in function of the maximum acceleration that the pedestrian can bear in each spatial direction, according to the use assigned to the structure. In this manner, a certain comfort level will be checked if the accelerations on the deck, under different both pedestrian densities and step frequencies, was lower than the limit values established by the standards. Otherwise, it will be necessary to modify the mass, stiffness or damping of the structure in order to guarantee an adequate dynamic behavior.

In Table 1, the ranges of natural frequencies, established by several international standards, where it is necessary to check the comfort level of the structure, are shown.

Table 1. Ranges of frequencies for the pedestrian-structure interaction according to different international standards.

Standards	Vertical [Hz]	Lateral [Hz]
LRFD American Guide (2009)	<3.00	
Eurocode 1 (2002)	1.60-2.40	0.80-1.20
Eurocode 5 (2003)	<2.50	0.80-1.20
DIN-Fachbericht 102 (2003)	1.60-2.40/3.50-4.50	
SIA 260 (2003)	1.60-4.50	<1.30
BS 5400 (2006)	<5.00	<1.50
Austroads (2012)	1.50-3.00	
Hong Kong Guide (2009)	1.50-2.30	
Ontario Guide (1995)	<3.00	
Setra (2006)	1.00-2.60/2.60-5.00	0.30-1.30/1.30-2.50
Synpex (2007)	1.25-2.30/2.50-4.60	0.50-1.20
EHE-08 (2008)	<5.00	
EAE (2011)	1.60-2.40/3.50-4.50	0.60-1.20
IAP-11 (2011)	1.25-4.60	0.50-1.20

In this Thesis a new crowd-structure interaction model will be proposed, calibrated and validated in order to estimate more accurately the dynamic response of footbridges under the pedestrian action. The model takes into account all the aspects that govern the crowd-structure interaction problem, specially, it allows considering the change of the modal properties of the structure due to the presence of the pedestrians. The estimation of the parameters of the model has been performed from the results of experimental tests conducted on real footbridges. In order to validate the proposal, the crowd-structure interaction model has been

implemented to analyze the change of the modal properties and the lateral lock-in phenomenon on two real footbridges.

1.1 Motivation.

The main motivation for the development of this work was the phenomenon happened on the footbridge situated close to the Martin Carpena sport pavilion (Malaga, Spain) (**Paper D**). The change of its use conditions originated a comfort problem in the longitudinal direction of the structure, so additional measures had to be adopted. In order to control its dynamic response under high pedestrian flows in longitudinal direction it was necessary to modify its natural frequencies increasing the stiffness of the footbridge. The crowd action was simulated using the methodology proposed by the more recent international standards (*Setra, 2006*; *Butz et al., 2007*). The performance was validated experimentally checking that the longitudinal natural frequency of the structure was out of the range that characterizes the walking pedestrian longitudinal force. The improvement of the dynamic behavior of the structure was better than anticipated by the numerical estimations. This fact aroused the interest of the author in the vibratory problem and specially in analyzing the aspects of the problem that were not adequately addressed on the international standards.

After a detailed study of the state of the art of the subject, the author realized that one of main factors included in a simplified way in the existing models was the effect of the pedestrians on the modal properties of the footbridge.

In this manner, the author decided to start a research work in order to develop a new crowd-structure interaction model that took into account this issue.

This Thesis collects the work done by the author during the last four years in order to develop, calibrate and validate a proposal for a new crowd-structure interaction model.

1.2 Objectives.

As it was mentioned above, the main objective of this Thesis is to develop, calibrate and validate a new proposal of crowd-structure interaction model that allows considering the change of the modal properties of the structure induced by the crowd-structure interaction. In order to achieve this main objective the following requirements were established:

(i) the proposed model should be able to deal with the different aspects of the vibratory problems induced by the pedestrian-structure interaction on footbridges in a compact form. The model should be robust enough in order to give response to different situations associated with the pedestrian-structure interaction.

(ii) the pedestrian-structure interaction model should be as simple as possible in order to be applied easily in design offices. In this manner, the behavior of the structure should be defined by the results obtained from its finite element model and the behavior of each pedestrian by a simple system with a reduced number of degrees of freedom.

(iii) the proposed model should be formulated in two sub-models. A first sub-model where the pedestrian-structure interaction is addressed and a second sub-model

that governs the interaction among pedestrians. The interaction between both sub-models should be also achieved in a simple manner.

(iv) the pedestrian-structure interaction should be solved directly in order to reduce as much as possible the computational time.

(v) the estimation of the parameters of the proposed pedestrian-structure interaction model should be based on the results of experimental pedestrian or crowd tests conducted on real footbridges, in order to take into account in the proposed model their actual dynamic behavior.

In order to achieve these objectives several skills, away from the bridge engineering, have been acquired. For the development of this work, the following tools have been used:

(i) operational modal analysis methodology to obtain experimentally the modal parameters of a footbridge (**Paper F**; **Paper G**).

(ii) model updating technique to reduce the level of uncertainties of the finite element model (**Paper C)**.

(iii) resolution of inverse dynamic problems to estimate the modal parameters of the proposed pedestrian-structure interaction model (**Paper A**; **Paper B**; **Paper E**).

(iv) global optimization algorithms in order to minimize the value of the objective function used by the model updating and the identification process.

(v) signal processing in order to filter and denoise the experimental measures to reduce the uncertainties of the identification process.

Additionally, a thorough review of the state of the art of the subject (**Paper D**) has preceded the development of the proposed pedestrian-structure interaction model.

The Thesis has focuses on vertical and lateral directions, since, according to the reported cases, are the direction more affected by the vibrations induced by the pedestrian-structure interaction.

The work is organized as follows: A summary of the state of the art of the vibratory problems on footbridge induced by the crowd-structure interaction is presented in section 2. The proposed crowd-structure interaction model is presented in section 3, by describing: (i) the pedestrian-structure interaction sub-model; (ii) the crowd sub-model; as well as (iii) the interaction mechanisms between both sub-models. The methodology followed in order to estimate the parameters of the proposed pedestrian-structure interaction sub-model is presented in section 4. The experimental estimation of the main parameters that characterize the pedestrian-structure interaction sub-model is described in section 5. In section 6, the validity and accuracy of the overall crowd-structure interaction model is successfully assessed by correlating both the experimental and numerical results for two real applications, the analysis of the change of the first natural frequency of a real footbridge due the crossing of a pedestrian group and the analysis of the lateral lock-in phenomenon on other real footbridge. Finally, some concluding remarks and future research lines are drawn to close the work in section 7.

2. Vibratory problems due to pedestrian flows on footbridges.

In this section a summary of the main aspects of the vibratory problems induced by the crowd-structure interaction is presented. The section includes the different models that have mainly influenced the author for the development of the proposed crowd-structure interaction model. On the other hand, this section constitutes a brief summary of the state of the art about this subject.

2.1. Load models for a single pedestrian.

The first models proposed in order to study the effect of a pedestrian crossing a footbridge were based on the assumption that the pedestrian's action can be approximated by a harmonic force. From this approach arises the proposal of the British standard (*BSI, 2006*), the single model, that later was adopted by other countries, as for instance, Canada (*Ontario, 1995*) and Spain (*RPM-95, 1995*). This model considered that the effect of the passage of a pedestrian on the structure is equivalent to a moving vertical sinusoidal force F_p (in N), with a pedestrian step frequency f_p (in Hz), a pedestrian step velocity v_p (m/s) a

$$F_p(t) = 180\sin\left(2\pi f_p t\right) \quad [1]$$

$$v_p(t) = 0.9 f_p \quad [2]$$

being t the time variable (sec.).

From the end of the last century, several researches have focused their efforts on the characterization of this force more precisely, including additional terms in the Fourier series and considering its effect in the three spatial directions. In the following equations, [3 and 4], and in Table 2 and Figure 2 a summary of the main proposals reported is shown (*Setra, 2006, Butz et al., 2007, Racic et al., 2009*).

$$F_{p,ver}(t) = P_p\left[1 + \sum_{i=1}^{nh} \alpha_{i,ver} \sin\left(2\pi i f_s t - \varphi_{i,ver} - \phi_p\right)\right] \quad [3]$$

$$F_{p,lat}(t) = P_p \sum_{i=1}^{nh} \alpha_{i,lat} \sin\left(\pi i f_s t - \varphi_{i,lat} - \phi_p\right) \quad [4]$$

where

$F_{p,ver}$ is the vertical periodic force due to walking.

$F_{p,lat}$ is the lateral periodic force due to walking.

$P_p = 700$ N is the mean pedestrian's weight (*Butz, et al.,2007*).

$\alpha_{i,ver}$ and $\alpha_{i,lat}$ are the Fourier coefficients of the ith harmonic for vertical and lateral force, dynamic load factors (DLFs)

f_s [Hz] is the step frequency.

$\varphi_{i,ver}$ and $\varphi_{i,lat}$ are phase shift of the ith harmonic.

nh is total number of contributing harmonics.

ϕ_p is the phase shift among pedestrians.

From the analysis of the results provided by Table 2, it can be concluded that at least two harmonics are necessary to characterize adequately the vertical pedestrian force while three harmonics are necessary for the lateral direction. On the other hand, the lateral component of the pedestrian force is characterized by frequencies that are the half of the frequencies transmitted in the vertical direction.

The relationship between the pedestrian velocity (v_p) and the pedestrian step frequency (f_s) has been studied by different authors. The works reported by Butz *et al.* (2007), *Riccardelli and Pizzimenti (2007), Riccardelli et al. (2007)* and *Bertram and Ruina* (2001) may be highlighted. The ultimate proposal, internationally accepted by the scientific community, is governed by the following equation.

$$f_s = 2.93 \cdot v_p - 1.59 \cdot v_p^2 + 0.35 \cdot v_p^3 \qquad [5]$$

Lately, this relationship will be considered in the crowd-structure interaction model proposed in this work.

Table 2. Dynamics Load Factors (DLFs) according to different author for walking action in vertical and lateral direction (*Setra, 2006*; *Butz et al., 2007*; *Racic et al. 2009*).

Author	Fourier Coef./Phase	Commentaries	Action-Direction
Blanchard et al. (1977)	$\alpha_{1,ver}$=0.257		Walking-Vertical
Bachmann & Ammann (1987)	$\alpha_{1,ver}$=0.40-0.50; $\alpha_{2,ver}$= $\alpha_{3,ver}$=0.10	f_s=2.00-4.00 Hz	Walking-Vertical
Schulze (1980)	$\alpha_{1,ver}$=0.37; $\alpha_{2,ver}$=0.10; $\alpha_{3,ver}$=0.12; $\alpha_{4,ver}$=0.04; $\alpha_{5,ver}$ =0.015;	f_s=2.00 Hz	Walking-Vertical
Bachmann et al. (1995)	$\alpha_{1,ver}$=0.40/0.50; $\alpha_{2,ver}$= $\alpha_{3,ver}$=0.10; $\alpha_{1/2,lat}$ =$\alpha_{1,lat}$=$\alpha_{3/2,lat}$=0.10; φ_2=φ_3=pi/2;	f_s=2.00-2.40 Hz f_s=2.00 Hz f_s=2.00 Hz	Walking-Vertical Walking-Vertical Walking -Lateral Walking-Vertical-Lateral
Kerr (1998)	$\alpha_{1,ver}$ =0.40/0.50; $\alpha_{2,ver}$ = $\alpha_{3,ver}$ =0.10;	α_1 according to the frequency	Walking-Vertical
Young (2001)	$\alpha_{1,ver}$=0.37 (f_p-0.95) ≤0.50 $\alpha_{2,ver}$=0.054+0.0088 f_s $\alpha_{3,ver}$=0.026+0.015 f_s $\alpha_{4,ver}$=0.01+0.0204 f_s	Mean values of Fourier Coef.	Walking-Vertical
EC5 (2003)	$\alpha_{1,ver}$=0.40; $\alpha_{2,ver}$=0.20 $\alpha_{1,lat}$= $\alpha_{2,lat}$=0.10		Walking-Vertical Walking-Lateral
SETRA (2006)	$\alpha_{1,ver}$=0.40 $\alpha_{2,ver}$=$\alpha_{3,ver}$=0.04 $\varphi_{2,ver}$=$\varphi_{3,ver}$=pi/2; $\alpha_{1/2,lat}$=$\alpha_{3/2,lat}$ =0.05 $\alpha_{1,lat}$ =$\alpha_{2,lat}$ =0.01		Walking-Vertical Walking-Vertical Walking-Vertical Walking-Lateral Walking-Lateral
SYNPEX (2007)	$\alpha_{1,ver}$=0.0115 f_s^2+0.2803 f_s-0.2902 $\varphi_{1,ver}$ =0.00 [º] $\alpha_{2,ver}$ =0.0669 f_s^2+0.1067 f_s-0.0417 $\varphi_{2,ver}$ = -99.76 f_s^2+478.92 f_s - 387.80 [º] $\alpha_{3,ver}$ =0.0247 f_s^2+0.1149 f_s-0.1518 If f_s<2.00 Hz $\varphi_{3,ver}$ = -150.88 f_s^3+819.65 f_s^2 - 1431.35 f_s+811.93 [º] If f_s≥2.00 Hz $\varphi_{3,ver}$ = 813.12 f_s^3-5357.60 f_s^2 +11726.00 f_s -8505.90 [º] $\alpha_{4,ver}$ =-0.0039 f_s^2+0.0285 f_s-0.0082 $\varphi_{4,ver}$ = -34.19 f_s-65.14 [º]	Fourier Coef. and phases for mean pedestrian loads	Walking-Vertical

2.2. Load models for crowds.

The main limitation of the above models is that they are not able to predict the response of the footbridge when the structure is subjected to a pedestrian flow, being necessary, therefore, to develop models that account for the behavior of the crowd. The methodology used more frequently in the literature consists in multiplying the response of a single pedestrian by a factor that considers globally the effect of the crowd. Among the different proposed models, it is presented below a summary of the most historically influential, according to the author's criterion.

The first considered model was proposed by *Matsumoto et al.* (1978) and takes into account as multiplication factor the magnitude $\sqrt{n_p}$, being n_p the number of pedestrians on the deck at certain instant. This factor establishes, according to a Poisson distribution, the proportion of pedestrians that due to the hazard are moving in phase, avoiding the effect of the rest of individuals. However, this factor was used, without success, in order to predict the response of the T-footbridge (Tokyo) that underwent vibratory problems due to the lateral synchronization of the pedestrians (*Zivanovic et al., 2005*).

Subsequently, the Swiss standards, SIA 260 (2003), presented as novelty the modification of the multiplication factor in function of the pedestrian density. In that sense, it proposes: (i) up to 10 pedestrians, a linear law with several sections and a maximum value of 3; (ii) up to a pedestrian density of 0.30 P/m^2 (Persons/m^2) it accepts the above proposal and (iii) up to about this point it establishes a parabolic law with a maximum factor of 20. Therefore, the pedestrian density determines a regime change of the pedestrian behavior: while values lower than 0.30 P/m^2 allows the free movement of the pedestrians, as the pedestrian density increases their free movement becomes difficult, so that the pedestrians tend to synchronize.

The Eurocode (2002) establishes, similarly to the Swiss standards, three load models according to the expected pedestrian density. The first model, DLM1, which is the basis of the rest, is used to characterize the action of a single pedestrian, being its action defined as a moving sinusoidal force with two spatial components: one vertical, of value 280 N and one lateral, with magnitude 70 N. Both the pedestrian step frequency and the pedestrian velocity follow the criterion of the British standard (*BSI, 2006*). The second model, DLM2, characterizes the action of a group of up to 15 pedestrians. The response of the footbridge under the action of the group is calculated multiplying the response of the model DLM1 by a factor, with a maximum value of 3, which takes into account the probability that a resonance phenomenon occurs on the structure due to the action of the group of pedestrians. The modification of the modal properties of the footbridge due to the pedestrian effect is quantified through the addition, at the point with a maximum modal deflection, of a point load of 800 kg. The last model, DLM3, applicable to scenarios under a continuous pedestrian flow, characterizes the action of the crowd through a harmonic load equivalent to the weight of a pedestrian density 0.60 P/m^2 multiplied by two factors in order to account for the possible resonance between the pedestrians and the structure, as well as the transitory character of the load. The first factor, adopts a variable value ranging between 0.05-0.30 and the second factor is equal to 0.75. The equivalent load is only applied in the part of the structure where the modal deformation has the same sign as the load and its effect

is unfavorable. The pedestrian load is applied to the same frequency than the model DLM1. Finally, the model assumes that the pedestrian flow produces an increase of the modal mass of the structure of 40 kg/m^2.

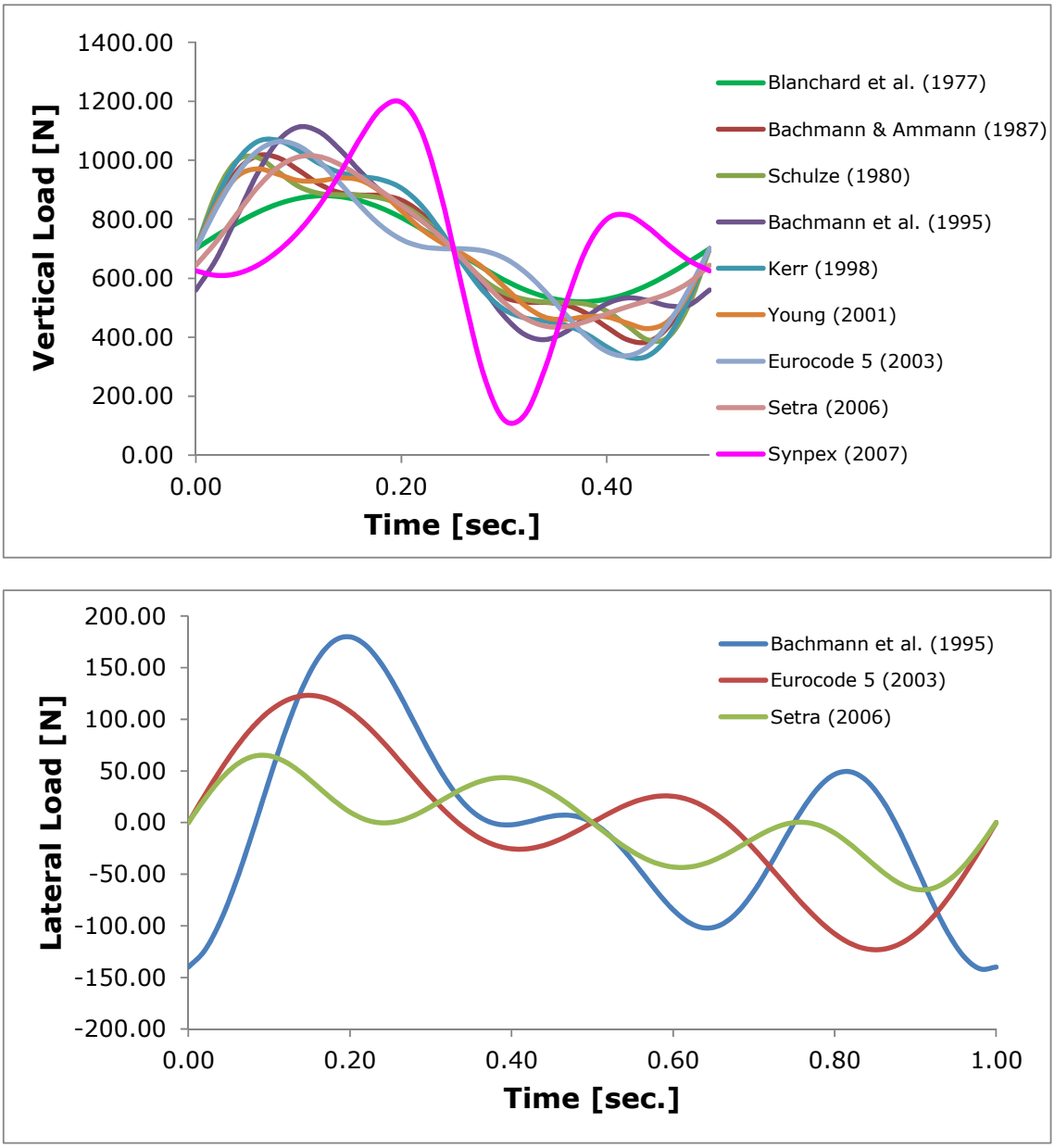

Figure 2. Vertical and Lateral pedestrian walking force according to different authors (*Setra, 2006; Butz et al., 2007 and Racic et al., 2009*).

The French standard, Setra (2006), based on both the research conducted on the Solferino footbridge (Paris, France) and laboratory tests on treadmills, presents a new methodology that has been widely adopted by researchers and designers. The methodology has been accepted equally by the European Research Project, *SYNPEX* (*Butz et al., 2007*). The proposed method simulates the effect of the pedestrian flows as an equivalent uniform distributed load applied according the considered vibration mode and whose value is equal to the effect of the group of pedestrians that are synchronized among them. This magnitude is named as *equivalent number of pedestrians*, n'. In order to determine the number of pedestrians on the

footbridge, the structure is classified according to the expected traffic level. In Table 3, the four possible traffic types are specified (d=pedestrian density=Persons/m^2) which allow generating on the structure the different load scenarios. A comfort level will be associated with each traffic level.

The equivalent uniform load applied on the deck of the structure is obtained from the following equation.

$$p(t) = G \cdot \cos(2 \cdot \pi \cdot f_{foot} \cdot t) \cdot n_p' \cdot \psi \qquad [6]$$

where

G is the component of the pedestrian load ($G = 280$ N for the vertical walking and $G = 35$ N for the lateral walking).

f_{foot} is the natural frequency of the structure under consideration.

n_p' is the equivalent number of pedestrians according to Table 3.

ψ is the reduction coefficient to take into account the probability that the footfall frequency approaches the natural frequency under consideration (Figure 3).

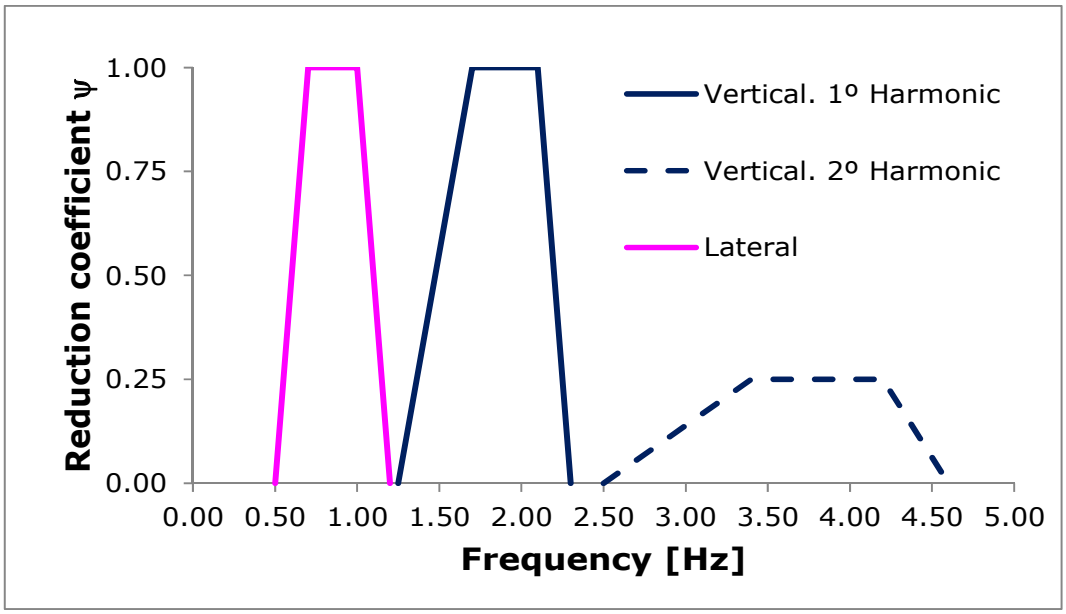

Figure 3. Reduction factor ψ versus the natural frequency of the structure (Butz et al., *2007*).

The equivalent number of pedestrian depends on the pedestrian density on the structure, the natural frequency under consideration and the ratio between the structural and the critical damping, ζ. In Table 3, several proposals for its determination are shown.

Table 3. Equivalent number of pedestrians, n_p', according to French code (Setra, 2006).

		Range of natural frequencies [Hz]			
Traffic Class	d [P/m^2]	1.70-2.10	1.00-1.70 2.10-2.60	2.60-5.00	<1.00 >5.00
IV	<0.20	---	---	---	---
III	0.50	$10.8\sqrt{n_p\zeta}$	---	---	---
II	0.80	$10.8\sqrt{n_p\zeta}$	$10.8\sqrt{n_p\zeta}$	$10.8\sqrt{n_p\zeta}$	---
I	1.00	$1.85\sqrt{n_p}$	$1.85\sqrt{n_p}$	$1.85\sqrt{n_p}$	---

Meanwhile, the structural damping ratios for different construction types can been obtained from Table 4 (*Setra, 2006 and Butz et al., 2007*).

Table 4. Damping structural ratios for Service and Ultimate Limit states (*Setra, 2006 and Butz et al., 2007*).

Construction type	**S.L.S.**		**U.L.S.**
	$\zeta_{\min}$ [%]	ζ_{med} [%]	$\zeta_{\max}$ [%]
Reinforced concrete	0.80	1.30	5.00
Prestressed concrete	0.50	1.00	2.00
Composite steel-concrete	0.30	0.60	2.00
Welded steel	0.20	0.40	2.00
Screwed steel	0.20	0.40	4.00
Timber	1.00	1.50	4.00
Stress-ribbon	0.70	1.00	2.00
Elastomers	----	----	7.00

Thus, the most advanced international standards (*Setra, 2006 and Butz et al., 2007*) estimate the modification of the dynamic properties of the footbridge due to the pedestrian flows only by considering the modification of the modal mass of the structure, adding directly the passive mass implied by the pedestrians. The effect of the second harmonic that characterizes the pedestrian step is only considered in footbridges under pedestrian densities larger than 0.80 P/m^2.

However, these international standards present the following limitations: (i) a simplified estimation of the change of the dynamic properties of the footbridge due to the presence of the pedestrians, (ii) the consideration of the synchronization phenomenon from an experimental relationship obtained from tests on only one real footbridge, (iii) DLFs obtained from laboratory test, (iv) a formulation that does not fit well to the case where several vibration modes of the footbridge are in the range that characterizes the pedestrian-structure interaction, and (v) they do not take into account the effect of the non-synchronized pedestrians.

In the present Thesis a crowd-structure interaction will be proposed and calibrated in order to overcome the above limitations.

2.3. Synchronization and lock-in.

In the context of the pedestrian-structure interaction, the synchronization reflects the tendency of the pedestrians to walk with the same spacing and phase among them, while the lock-in reflects the tendency of the pedestrians in coupling their step with the vibratory movement of the structure. This phenomenon can have a deliberate character (vandalism) or unintentional. This last case, responsible of many of the vibratory problems of footbridges detected during the last years, can be generated by two different mechanisms, according to the scheme shown in Figure 4.

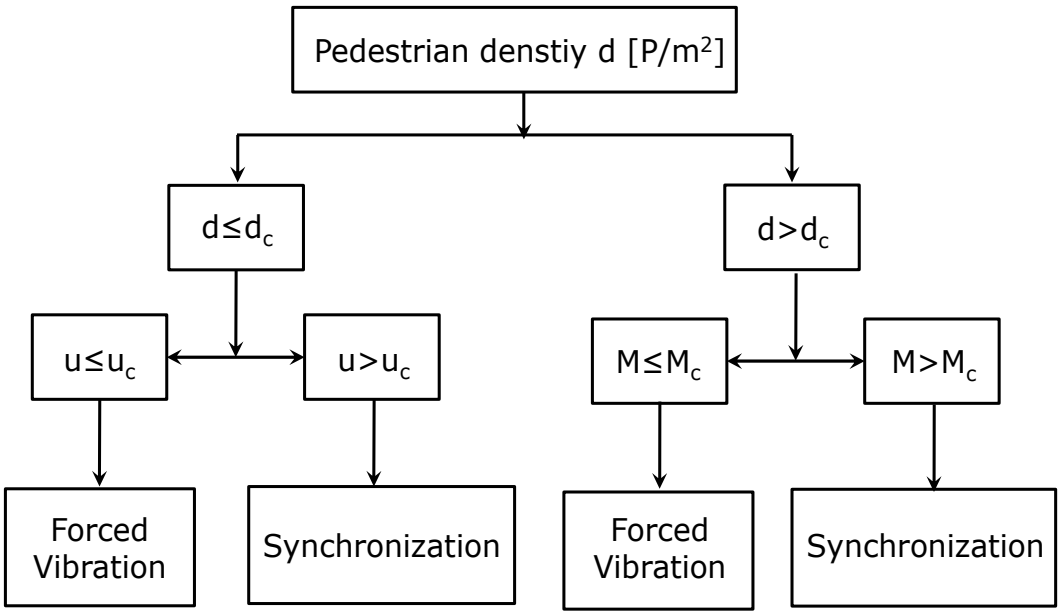

Figure 4. Flowchart of unintentional of pedestrian-structure synchronization (*Racic et al., 2009*).

The first synchronization mechanism may occur when the pedestrian density on the footbridge, d, is lower than a critical value, d_c (limit density for which the movement of a pedestrian is influenced by the rest of the group), and the value of the amplitude of the deck induced by the pedestrians, u**,** was upper a limit value, u_c, that marks the limit value from the pedestrians tend to synchronize with the motion of the deck.

On the other hand, a second mechanism, that originates the synchronization, may occur, under high pedestrian densities, if the mass provided by the pedestrians, M, is upper a critical value, M_c, equal to the mass of the pedestrians which inertial force may induce a vibration amplitude, u_c.

In the following sections, a literature review of the main existing models for the analysis of the lock-in phenomenon in footbridges is presented. The practical application of these studies, adopted by the current standards, is also described.

2.3.1. Models for the simulation of the synchronization and lock-in.

The study of the problem of synchronization between pedestrians and the footbridge, the lock-in phenomenon, has been performed historically independently to the simulation of the behavior of the crowd, or in the best case, an additional checking criterion has been established (*Setra, 2006 and Butz et al., 2007*). The first reported phenomenon of this type occurred in a German footbridge (1972), during its opening, when a vibration mode of 1.10 Hz was excited by 300-400 pedestrians, as it is described by Bachmann and Ammann (1987) in their book. The comfort level of the footbridge was guaranteed by the addition of several tuned mass dampers without giving additional importance to the phenomenon.

Next, a literature review of the most relevant models for the analysis of the phenomenon is presented summarized.

One of the first models, proposed by *Fujino et al.* (1993), was developed from the results of the study of the lateral lock-in phenomenon in the T-footbridge (Tokyo). By the analysis of video images of 2000 pedestrians crossing the structure, they estimated that 20% of the pedestrians were synchronized with the footbridge, with a maximum lateral displacement of the deck of 10 mm and a lateral natural frequency of 0.90 Hz. It was established, for the first time, as cause of the vibratory problem the synchronization between the pedestrians and the structure. From these results, a general calculation rule was presented, establishing a fixed value of the synchronization of 20% (among pedestrian with each other and with the structure) and a value of the mean lateral force generated by a pedestrian of 35 N. The model did not consider neither the increase of the synchronization with the amplitude of the movement of the deck nor the effect of the pedestrians that only was synchronized with each other but not with the deck.

This model was unsuccessfully applied for the study of the dynamic behavior of the Millennium footbridge (London) during its design phase. After the vibratory problems detected in it, large scale and laboratory tests were performed in order to calibrate a new proposal for simulating the pedestrian behavior. The pedestrian action, according to Dallard (*Dallard et al., 2001*), may be approximated as a force that depends on the velocity of the deck and a negative coefficient of pedestrian damping. In this way, the increase of the pedestrians on the footbridge produces a reduction of the global damping of the structure, to such an extent that a dynamic instability state may be reached, which is additionally favored by the complementary synchronization process experienced by the pedestrians. The concept of the equivalent number of pedestrians is introduced as the number of pedestrians that eliminate the damping of the system. The practical application of this model is reflected by the Arup formula. The Millennium footbridge experienced a lateral movement of 50 mm with a natural frequency of 0.80 Hz in the lateral span and a lateral movement of 75 mm with a natural frequency of 1.00 Hz in the central span, synchronizing the movement of 50% of the pedestrians that crossed the structure. The resulting value of the lateral force transmitted by each pedestrian, 30 N, is similar to the value proposed by *Fujino et al.* (1993). On the other hand, the model provided, a limit value of the pedestrian density of 1.50 P/m^2, from which is so hard to walk on the deck that the dynamic effects are negligible. Nevertheless, the model presents some limitations: (i) the model ignores the energy transmitted by the not-synchronized pedestrians with the structure, (ii)

it does not take into account the change of the modal properties of the structure due to the presence of the pedestrians, (iii) the change of the behavior of the pedestrians with the vibration level of the structure is not considered and (iv) the value of the equivalent pedestrian damping is only estimated for one footbridge and specific range of frequencies.

In order to consider in a more appropriate manner the change of the behavior of the pedestrians induced by the vibration level, *Nakamura et al.* (2004) modified Dallard's proposal (*Dallard et al., 2001*) in order to take into account that, according to the observations performed on the T and M footbridges (Tokyo), from certain value of the lateral displacement, 10 mm, the pedestrians modified their step to guarantee an adequate comfort level, further reducing the lateral force originated by their step. In that way, a saturation factor is introduced in each pedestrian lateral force that avoids that the force increases linearly with the velocity of the deck indefinitely. This proposal reduces the ratio of the increase of the velocity when the velocity increases until making it null. Although this model is an improvement as compared to the previous proposals, it has as main limitation the necessity of knowing the maximum displacement of the structure to scale the saturation ratio, while shares the other limitations of the previous models.

Subsequently, the French standard (*Setra, 2006*) proposed a more compact model considering the results of two types of tests, on treadmills at laboratory and large scale pedestrian tests on Solferino footbridge (Paris). As conclusions of these two sets of tests: (i) an experimental relationship that allows estimating the number of synchronized pedestrians on the footbridge was proposed, as well as (ii) a new criterion in order to determine the sensitivity of the footbridge to the lateral lock-in phenomenon. It was verified, in this sense, that a change of regime in the pedestrian behavior occurs, from forced to synchronized vibration, with a maximum synchronization ratio of 60% for a lateral acceleration of the deck between 0.10-0.15 m/s^2. This limit acceleration has been adopted as a criterion in order to determine the sensitivity of the footbridge to the lateral lock-in.

In the last five years, several more sophisticated models, not yet implemented in the international standards, have appeared providing a new approach to the problem. Among these models, the most influential ones for the development of this Thesis are described, in summary, in the following paragraphs

In the first model, proposed by Macdonald (*Macdonald, 2008*) and based on the inverse pendulum model by Baker (*Baker, 2002*), the pedestrian is modelled as a lumped mass attached to the footbridge by an inclined bar (Figure 5). The pedestrian under the lateral vibrations modifies the tilt of his legs, searching his stability, increasing the lateral component of the walking pedestrian force and being able to attain a dynamic instability situation. The proposed model has been accepted to describe the initiation of the phenomenon, but the effect of modification of the pedestrian step due to large lateral vibrations is not included in the proposal. Despite its limitations, there are evolutions of the model (*Morbiato et al., 2011*) with greater complexity and precision.

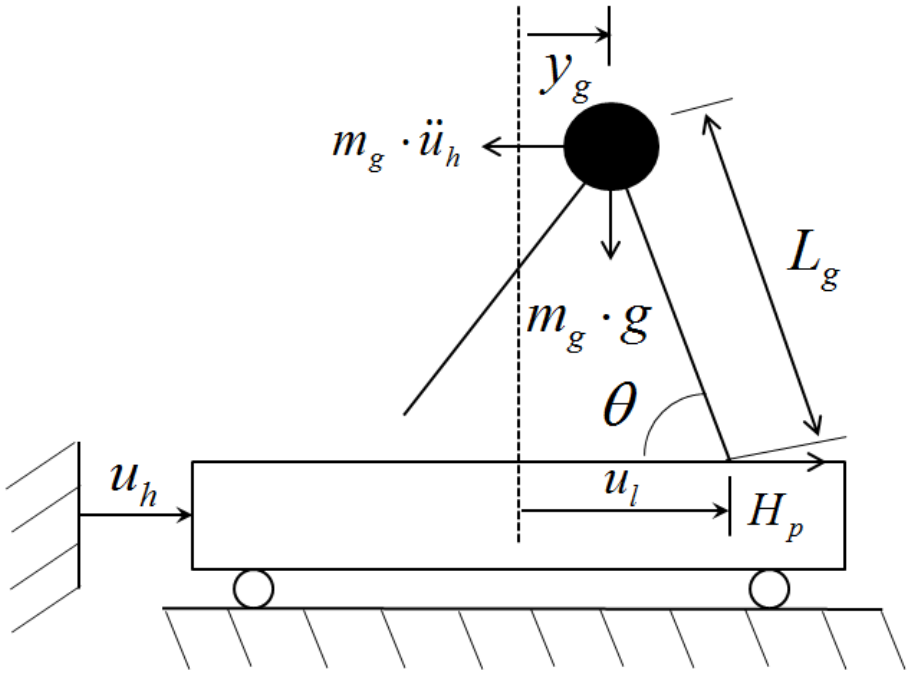

Figure 5. Inverted pendulum model proposed by *Baker (2002*).

In Figure 5 the Macdonald's model is shown, where

u_h is the lateral displacement of the deck.

$\ddot{u}_h$ is the lateral acceleration of the deck.

L_g is the distance between the centre of gravity of the pedestrian and his/her more advanced heel.

g is the acceleration of the gravity.

m_g is the pedestrian mass.

θ is the angle of the pedestrian's leg with the horizontal axis.

H_p is the horizontal force generated by each pedestrian.

y_g is the horizontal position of the centre of mass.

u_l is the horizontal position of the more advanced heel.

Finally, the latest trend focuses on the development of models based on computational mechanics. Among these models, the one proposed by Piccardo and Tubino (*Piccardo and Tubino, 2008*) presents a parametric mechanism where an equivalent pedestrian force, which magnitude is function of the vibration of the deck and the natural frequency of the footbridge. Other interesting model, utilized as a starting point for future developments was reported by Bruno and Venuti (*Venuti et al., 2007*) that consists in the decomposition of a nonlinear coupled

multiphysics model in two interacting subsystems. The first subsystem, the structure, is modelled by a multiple degrees of freedom dynamic system where the applied force depends on the existing pedestrian density and the lateral acceleration of the deck. The second subsystem, the pedestrians, is modelled by a macroscopic unidimensional model, where the pedestrian flow is simulated by a continuous fluid. The lateral lock-in condition is introduced into the system applying the criterion established by the French standard (*Setra, 2006*). The model has been validated successfully on the T-footbridge (Tokyo). It is a very complete model, which includes both the analysis of the lateral lock-in phenomenon and the action of the pedestrians non-synchronized with the structure. However it does not take into account the modification of the modal parameters of the structure due to the presence of the pedestrians. An evolution of this model is Carrol's proposal (*Carrol et al., 2012*) where the Macdonald's inverse pendulum model is coupled with a discrete law of pedestrian behaviour.

The previous models have a difficult practical application in the project of footbridges so the international standards have adopted only in a simplified way the results of the above proposals.

In the present thesis, a new model is proposed in order to reduce the existing limitations of the models described above as well as to improve the estimation of the dynamic behavior of a footbridge under pedestrian flows.

2.3.2. Synchronization and vertical lock-in.

In order to estimate the sensitivity of a footbridge under the phenomenon of the vertical lock-in, Newland (Newland*, 2003*; Newland*, 2004*) proposed an adaptation of the Scruton's number (*Cremona et al., 2002*), normally used in wind engineering. The proposed relationship is expressed by the following equation:

$$S_{cp} = \frac{2 \cdot \zeta \cdot M_p}{m_p} \qquad [7]$$

where

S_{cp} is the Scruton's number for the pedestrian case.

M_p, is the mass of the footbridge by unit length.

m_p, is the mass of the pedestrians by unit length.

So that,

$$S_{cp} > \alpha \cdot \beta \qquad [8]$$

where

α is the ratio between the movement of the centre of gravity of a pedestrian that circulate on a vibratory footbridge and the movement experienced by its deck. The

value of this parameter has been fixed experimentally in 2/3 in the pedestrian-structure interaction range.

β is a factor that takes into account the percentage of pedestrians synchronized on a footbridge in function of the movement experienced by the structure. Its value is obtained from the following equation derived from the tests performed in the Millennium footbridge (London).

$$\beta = 0.0133 \cdot u_v + 0.3 \qquad [9]$$

With u_v being the maximum displacement of the deck in mm.

However, the results of the researches developed to date in relation with the vertical synchronization lead to the conclusion; this phenomenon rarely occurs. Thus the above equations (7-9) are usually used only to analyse the sensitivity of a footbridge under the pedestrian action in the vertical direction.

2.3.3. Synchronization and lateral lock-in.

The Dallard's model (*Dallard et al., 2001*) and the proposal of the French standard (*Setra, 2006*) have been the two more used criteria by the designers in order to analyze the sensitivity of the structure to the lateral lock-in phenomenon.

The Arup formula determines the critical number of pedestrians, N_E, in a crowd, that generates the lateral lock-in phenomenon.

$$N_E = \frac{8 \cdot \pi \cdot f_{foot} \cdot \zeta \cdot m_r}{k} \qquad [10]$$

where

k is a constant estimated as 300 sN/m

f_{foot} is the natural frequency for the affected lateral vibration mode.

ζ is the modal damping ratio for the affected lateral vibration mode.

m_r is the modal mass ratio for the affected lateral vibration mode.

The lateral lock-in phenomenon occurs if the number of pedestrians on the footbridge is greater than the above critical number and some natural frequency of the footbridge is inside the range 0.50-1.20 Hz.

The French standard (*Setra, 2006*) establishes a simple rule in order to analyse the sensitivity of the footbridge to the lateral lock-in phenomenon. According to this code, the phenomenon occurs if some natural frequency of the footbridge is inside the previously defined range and the lateral acceleration of the footbridge under a pedestrian flow is about 0.10-0.15 m/s^2.

The equivalence of both proposals has been demonstrated following their application on real footbridges (*Caetano et al., 2010*).

2.4. The perception of the vibration.

The main receiver of the vibrations that occur on the footbridge under a pedestrian flow is the own pedestrian. The human response to vibrations is a really complex phenomenon, since its nature presents a double variability (*Zivanovic et al., 2005*): different subjects react differently to the same vibratory process (inter- subject variability) and the same subject will change its state of sensitivity depending on the moment he experiences the phenomenon (intra-subject variability). From the first studies made in the early 1930s, researchers and designers of this type of structure, as Wallay and Leonard (*Zivanovic et al., 2005*) established that it was completely uneconomical to design a footbridge under the constraint that its users did not experience any vibration, and that certain sensitivity thresholds must be considered in the design roles.

The first proposal, adopted by several European standards, as the British (*BSI, 2006*) and Spanish codes (*RPM-95, 1995*), in order to establish the value of the maximum vertical allowable acceleration, $a_{\lim}$, comes from the results of a research developed by Leonard (*Zivanovic et al. 2005*) on an isostatic beam under the passage of 40 pedestrians and excited sinusoidally with a maximum amplitude of 5 mm and a range of frequencies between 1-14 Hz. The results of this study allowed *Blanchard et al.* (*Zivanovic et al., 2005*) obtaining the following relationship:

$$a_{\lim} = 0.5 \cdot \sqrt{f_{foot}} \ \text{m/s}^2 \qquad [11]$$

If the natural frequencies of the footbridge are outside of the pedestrian-structure interaction range, *Tilly et al.* (*Zivanovic et al., 2005*) recommend increasing this limit to double the value obtained from the above equation.

In the lateral direction, Nakamura (2004) based on the measurements recorded in T and M footbridges developed a deep study of the sensitivity of pedestrians to lateral vibrations. In terms of the maximum lateral displacement ($d_{lat,lim}$) and the associated acceleration ($a_{lat,lim}$), established the comfort levels shown in Table 5.

Table 5. Lateral Comfort classes according to Nakamura (2004).

Degree	$d_{lat,lim}$ [mm]	$a_{lat,lim}$ [m/s^2]
Tolerable	10.00	0.00-0.30
Minimum	45.00	0.30-1.35
Unacceptable	70.00	1.35-2.10

The first international standards that introduced a limitation associated with the maximum lateral acceleration experienced by the pedestrians on the structure were the Eurocode (*Eurocode, 2002*) and the Chinese standard (*Hong Kong, 2009*), that established a maximum limit of 0.15 m/s^2.

In the last ten years, given the social importance acquired by the footbridges, as unifying elements of the urban environment, and the better experimental knowledge of the pedestrians' behaviour, several standards have emerged in order to collect in a more detailed way the limits that ensure the compliance of the different comfort levels. In that sense, the proposal of the French standard (*Setra, 2006*) stood out again, subsequently adopted by the European project, *SYNPEX*

(*Butz et al.*, 2007) and even by the recent Spanish standard (IAP-11, 2011). The limit acceleration values proposed by these standards are shown in Table 6. The limit vertical ($a_{ver,lim}$) and lateral ($a_{lat,lim}$) acceleration according to the considered comfort level are established in Table 6.

Table 6. Comfort classes (*Setra, 2006 and Butz et al., 2007*).

Level	Degree	$a_{ver,lim}$ [m/s^2]	$a_{lat,lim}$ [m/s^2]
CL1	Maximum	<0.50	<0.10
CL2	Medium	0.50-1.00	0.10-0.30
CL3	Minimum	1.00-2.50	0.30-0.80
CL4	Unacceptable	>2.50	>0.80

In lateral direction, the lateral lock-in criterion must be overlapped to the above limits (Table 6).

2.5. Dynamic properties of the structures under pedestrian action.

Currently, one of the main weaknesses of the existing models is that they consider in a very simplified way the change of the modal parameters of the footbridge induced by the pedestrian-structure interaction. This Thesis proposes a crowd-structure interaction model that takes into account this effect in order to improve the numerical estimation of the dynamic response of the footbridge under the pedestrian action.

However, there are several studies, as reported by Jones et al. (2010), describing the effect of passive pedestrians on stadium stands in the dynamic vertical behaviour of such structures in terms of a static single degree of freedom (SDOF) system. The results of these studies have been used as starting point for the development of the pedestrian-structure interaction model considered in this work.

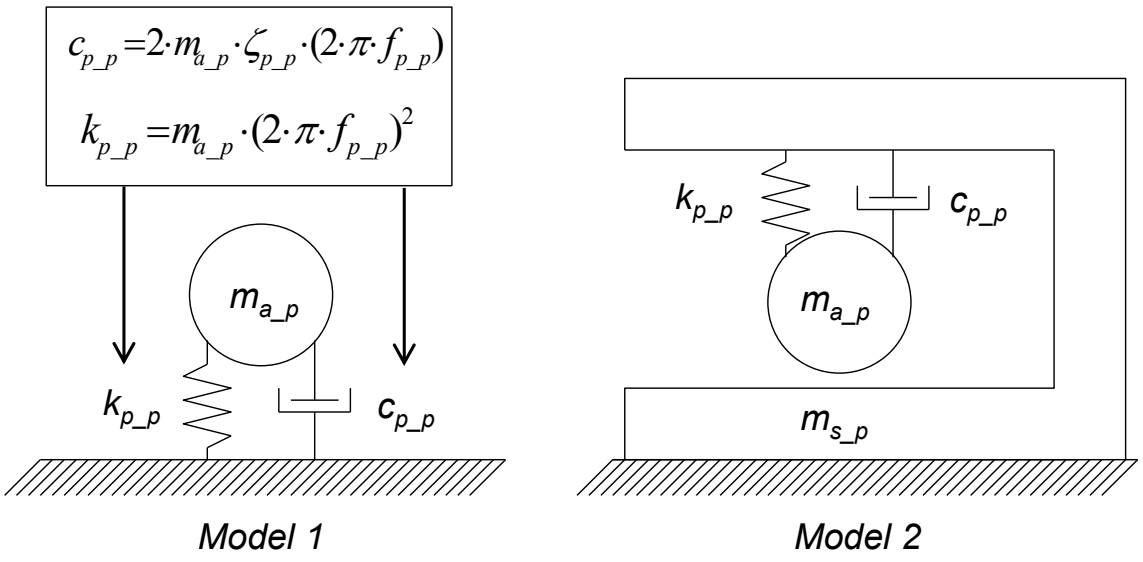

Figure 6. Simplified dynamic models of passive pedestrians on stadiums stands (*Jones et al.* (2010)).

In Figure 6 and Table 7, a scheme of the used models, the estimated values of their modal parameters and their range of variation are shown (Jones et al. (2010)), where f_{p_p} is the passive human natural frequency, ζ_{p_p} is the passive equivalent human damping ratio and m_{a_p} and m_{s_p} indicate the percentage of passive sprung and unsprung masses respectively of the human body. The main difference between the two passive pedestrian models is the distribution of the total mass of the pedestrian, considering only a sprung component in the "Model 1" and, both sprung and unsprung components in the "Model 2".

Table 7. Dynamic properties for SDOF models of passive pedestrians on stadium stands (Jones et al., 2010).

Author	Model	m_{a_p} [%]	m_{s_p} [%]	ζ_{p_p} [%]	f_{p_p} [Hz]
Foschi et al. (1995)	1	100.00	0.00	53.00	3.30
Al-Foqaha'a (1997)	1	100.00	0.00	34.00	3.50
Al-Foqaha'a (1997)	2	90.00	10.00	36.00	3.70
Brownjohn (1999)	1	100.00	0.00	37.00	4.90
Falati (1999)	1	100.00	0.00	50.00	10.43
Zheng and Brownjohn (2001)	1	100.00	0.00	39.00	5.24
Matsumoto and Griffin (2003)	1	100.00	0.00	69.00	5.74
Matsumoto and Griffin (2003)	2	90.00	10.00	61.00	5.88
Minimum		90.00	0.00	34.00	3.30
Maximum		100.00	10.00	69.00	10.43

The minimum and maximum values of each parameter have been included in Table 7. These extrema values allow establishing a range of variation of these parameters.

2.6. The control of the vibratory response.

In order to guarantee an adequate comfort level of the structure, it must be checked that under the different design scenarios, the dynamic response of the footbridge leads to accelerations lower than the limit value that characterizes the required comfort level (*Setra, 2006; Butz et al., 2007*). If this condition is not met additional measures must be applied in order to improve the dynamic behavior of the footbridge (*Slaich, 2005*). In that sense, one or more of the modal parameters of the footbridge (its mass, stiffness and damping) are usually modified (*Butz et al., 2007*) in order to control the dynamic response of the structure under pedestrian flows.

2.6.1. Modification of the mass induced by pedestrian action.

The addition of mass to the deck of the footbridge can improve its dynamic behavior under pedestrian flows, due to the increase of the modal mass, since the accelerations that occur on the deck are inversely proportional to the mobilized modal mass (*Setra, 2006*). The efficiency of the method is greater in footbridges with short spans and high pedestrian densities in order to control the second harmonic that characterizes the pedestrian force (*Setra, 2006; Butz et al., 2007*).

On the basis of the spectral design model, *Butz (2006)* developed an empirical expression for the determination of the required modal mass, M_i (kg), for a given pedestrian traffic to ensure a required comfort level under the assumption that some natural frequency of the structure is in the range that characterizes the walking pedestrian action.

$$M_i \geq \frac{\sqrt{n_p} \cdot \left(k_1 \cdot \zeta^{k_2} + 1.65 \cdot k_3 \cdot \zeta^{k_4}\right)}{a_{\lim}} \qquad [12]$$

where

k_1 to k_4 are constants, as given in Table 8.

$a_{\lim}$ is the limit acceleration according to the considered comfort level (Table 6).

and, n_p, is the number of pedestrians.

Table 8. Constants for required modal mass (*Butz, 2006*).

	Vertical-Torsion				Lateral			
d [P/m^2]	k_1	k_2	k_3	k_4	k_1	k_2	k_3	k_4
<0.50	0.7603		0.050					
1.00	0.5700	0.4680	0.040	0.675	0.1205	0.4500	0.0120	0.6405
1.50	0.4000		0.035					

2.6.2. Modification of the stiffness induced by pedestrian action.

The value of the natural frequencies of the footbridge is proportional to the square root of the ratio between the modal stiffness and mass of the structure. In this manner, large structural modifications are necessary if the natural frequencies of the footbridge must be located out of the pedestrian-structure interaction range. The current trend in the design of footbridges, under aesthetics, resistant and economic requirements causes that the above criterion is not always feasible in order to guarantee an adequate comfort level (*Slaich, 2005*).

However, there are occasions, where the first natural frequency of the structure is inside the walking pedestrian range, and the second natural frequency is outside that range, where it can be reasonable to reduce the stiffness of the structure so both natural frequencies are outside the pedestrian-structure interaction range and checking additionally that the static deflection of the footbridge is compatible with its use (*Setra, 2006 and Butz et al., 2007*).

The most common strategies in order to modify the natural frequencies of the footbridge, from the viewpoint of the stiffness, are (*Setra, 2006 and Butz et al., 2007*): (i) increase the degree of statically indetermination, (ii) provide structural characteristics to protection or surface elements, and (iii) use cable systems with a stabilizing function (*Setra, 2006*). It is recommended in footbridges with a width larger than 4.00 m and spans with lengths above 50.00 m, to install a lateral load transmission system, as an effective method to control the lateral lock-in phenomenon (*Low, 2008*). Finally, at high seismicity areas, the increase of the

stiffness of the structure in order to avoid vibratory problems induced by pedestrians may cause, by contrast, an increase of the seismic action (*Slaich, 2005*).

2.6.3. Modification of the damping induced by pedestrian action.

The increase of the structural damping has been, until the date, the most used method to control the vibrations induced by pedestrians on footbridges (*Fujino et al., 1993; Dallard et al., 2001 and Caetano et al., 2010*). This increment can be achieved either by the actuation on internal elements of the structure, or by the implementation of external control devices of different nature according to their performance: active, semi-active, hybrid or passive devices (*Moutinho et al., 2010*). The most usual is the use of passive dampers as: (i) viscous dampers (*Butz et al., 2007 and Taylor, 2003*), (ii) tuned mass, liquid or liquid column dampers (*Fujino et al., 1993; Butz et al, 2007 and Caetano et al., 2010*) and (iii) pendulum dampers (*Butz et al., 2007*). However, the use of these passive dampers must be limited since although they allow achieving a high level of damping with a reasonable cost, they present several problems that discourage their widely use. Among these problems, the most important are: (i) the necessity of damping all the natural frequencies of the structure inside the range of pedestrian interaction, (ii) a bad performance may be the cause of a splitting of the natural frequency originally damped, (iii) they are mechanical elements that require maintenance, and (iv) due to their weight it can be non-viable their placement on existing footbridges due to strength reasons (*Meinhardt, 2009*).

3. Proposal of a simplified biomechanical crowd-structure interaction model.

The proposed crowd-structure interaction has been simulated using two individual sub-models (Figure 7): (i) the pedestrian-structure interaction sub-model and (ii) the crowd sub-model.

In the first sub-model, all the dynamics effects induced by the pedestrians on the footbridge are considered. The lateral or vertical acceleration, $\ddot{y}_a$ or $\ddot{z}_a$, experimented by each pedestrian is the output obtained from this model (according to the analysed direction).

In the second sub-model, the crowd is simulated as a behavioural model, providing a description of the individual pedestrian position, $\mathbf{x}_p$, walking pedestrian velocity, $\mathbf{v}_p$, step pedestrian frequency, f_s , and phase among pedestrians, ϕ_p .

In order to take into account the change of the pedestrian behaviour associated with the acceleration level experienced, two additional conditions have been included in this latter sub-model. In vertical direction only a comfort threshold has been included, while in lateral direction a comfort and lateral lock-in thresholds have been considered. The first condition modifies the pedestrian velocity, $\mathbf{v}_p$, according to the comfort level experienced by each pedestrian and the second condition modifies the step pedestrian frequency, f_s , and the phase among pedestrians, ϕ_p , in order to synchronize the movement of the pedestrians and the structure if certain limit is exceeded.

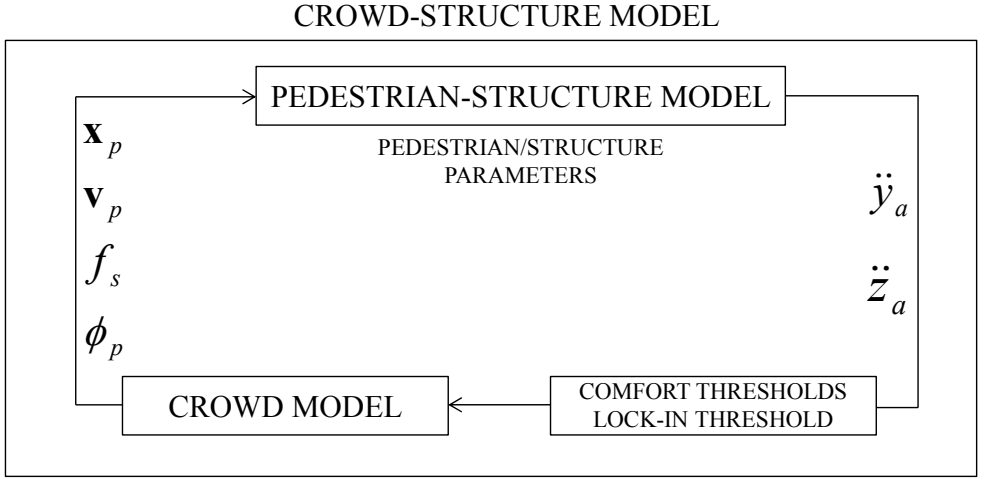

Figure 7. Layout of the biomechanical crowd-structure interaction model.

For each interaction the crowd sub-model determines the position, velocity step frequency and phase of each pedestrian. Subsequently, these four parameters are used as input to define the walking force of each pedestrian-structure model, obtaining as output the lateral o vertical acceleration of each pedestrian. The pedestrian velocity and frequency of each individual is modified according to the

comfort level experimented by each pedestrian and additionally his phase shift if a lateral lock-in threshold is exceeded. Finally, the process is repeated by the updated values of the position, the pedestrian velocity, the step frequency and the phase shift (Figure 7).

3.1. Modelling the pedestrian-structure interaction.

The proposed pedestrian-structure interaction in each direction follows from the application of dynamic equilibrium equations (*Clough and Penzien, 1993; Dominguez, 2001*; *Xia and Zhang, 2005*) to a simplified model of interaction (Figure 8) with sprung (m_a) and unsprung masses (m_s). This methodology has been applied separately for vertical (**Paper A and Paper B**) and lateral (**Paper E**) directions and here it will summarized for the case of vertical direction. Its implementation in the lateral direction is described in **Paper E**. The formulation of the proposed model may be further generalized to the three directions by accordingly modifying both the equation that governs the considered pedestrian load in each direction and the value of the modal parameters that define the TDOF (two degrees of freedom) pedestrian model. In this way, the resulting model would be suitable for the more general 3-D problem and it could therefor take into account the possible interaction in the three spatial directions.

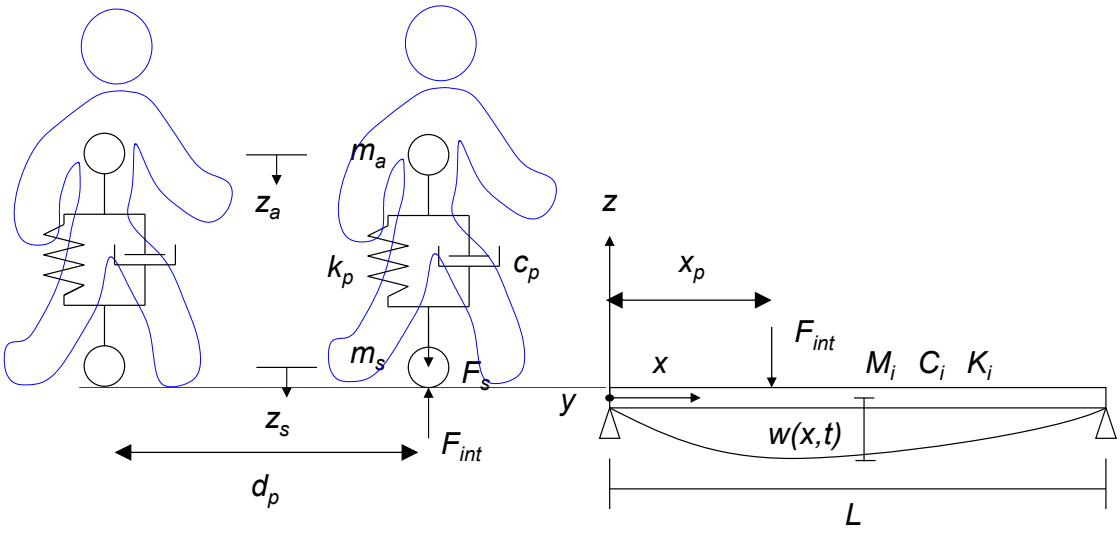

Figure 8. Biomechanical pedestrian-structure interaction model in vertical direction (**Paper B**).

Considering the balance of the system, structure and pedestrian model, the following coupled equations of motion may be written.

$$M_i \ddot{z}_i + C_i \dot{z}_i + K_i z_i = \phi_{NUM\_i}(x_p) \cdot F_{\text{int}} \quad [13]$$

$$m_a \ddot{z}_a + c_p (\dot{z}_a - \dot{z}_s) + k_p (z_a - z_s) = 0 \quad [14]$$

$$m_s \ddot{z}_s + c_p (\dot{z}_s - \dot{z}_a) + k_p (z_s - z_a) = F_{p,ver} - F_{\text{int}} \quad [15]$$

where

m_a is the sprung mass of the pedestrian in the considered direction [kg].

m_s is the unsprung mass of the pedestrian in the considered direction [kg].

$m = m_s + m_a$ is the total mass of the pedestrian in the considered direction [kg].

z_i is the modal displacement of the vibration mode i [m]

z_a is the absolute vertical displacement of the sprung mass [m].

z_s is the absolute vertical displacement of the unsprung mass [m].

k_p is the equivalent stiffness of a pedestrian [N/m].

c_p is the equivalent damping of a pedestrian [sN/m].

$F_{p,ver}$ is the vertical pedestrian force due to walking [N].

F_{int} is the interaction force between the pedestrian and the structure [N].

M_i is the modal mass of the vibration mode *i* [kg].

C_i is the modal damping of the vibration mode *i* [sN/m]

K_i is the modal stiffness of the vibration mode *i* [N/m].

ϕ_{NUM_i} is the vertical component of the numerical vibration mode *i*.

$x_p = v_{px} \cdot t$ is the longitudinal position of the pedestrian [m].

t is the time [sec.]

v_{px} is the longitudinal component of the pedestrian velocity vector [m/s].

d_p is the distance among pedestrians [m].

$w(x,t)$ is the deflection of the footbridge at the position x [m].

L is the length of the footbridge [m].

From Eq.(15) the following expression is obtained for, F_{int} :

$$F_{\text{int}} = F_{p,ver} - m_s \ddot{z}_s - c_p\left(\dot{z}_s - \dot{z}_a\right) - k_p\left(z_s - z_a\right) \qquad [16]$$

and substituting this equation into Eq.(13) yields.

$$M_i\ddot{z}_i + C_i\dot{z}_i + K_i z_i = \phi_{NUM\_i}(x_p)\cdot\left(F_{p,ver} - m_s\ddot{z}_s - c_p\left(\dot{z}_s - \dot{z}_a\right) - k_p\left(z_s - z_a\right)\right) \quad [17]$$

Applying, at the contact point between the pedestrian and the structure, the equations of compatibility of displacements, velocity and acceleration between the structure and the simplified pedestrian-model of interaction:

$$z_s = w(x_p,t) = w(v_{px}\cdot t,t) \quad [18]$$

$$\dot{z}_s = \dot{w}(x_p,t) = \dot{w}(v_{px}\cdot t,t) \quad [19]$$

$$\ddot{z}_s = \ddot{w}(x_p,t) = \ddot{w}(v_{px}\cdot t,t) \quad [20]$$

These quantities may be expressed in terms of the amplitude $z_i(t)$ and the modal shape of the *n* numerical considered vibration modes $\phi_{NUM\_i}(x)$, neglecting the term of variation of the pedestrian velocity along time, as:

$$w(x_p,t) = \sum_{i=1}^{n} z_i(t)\cdot\phi_{NUM\_i}(x_p) \quad [21]$$

$$\dot{w}(x_p,t) = \sum_{i=1}^{n}\dot{z}_i(t)\cdot\phi_{NUM\_i}(x_p) + \sum_{i=1}^{n} z_i(t)\cdot v_{px}\cdot\phi'_{NUM\_i}(x_p) \quad [22]$$

$$\ddot{w}(x_p,t) = \sum_{i=1}^{n}\ddot{z}_i(t)\cdot\phi_{NUM\_i}(x_p) + \sum_{i=1}^{n} 2\cdot\dot{z}_i(t)\cdot v_{p,x}\cdot\phi'_{NUM\_i}(x_p) + \sum_{i=1}^{n} z_i(t)\cdot {v_{p,x}}^2\cdot\phi''_{NUM\_i}(x_p)) \quad [23]$$

$$\phi'_{NUM\_i}(x) = \frac{d\phi_{NUM\_i}(x)}{dx} \quad [24]$$

$$\phi''_{NUM\_i}(x) = \frac{d^2\phi_{NUM\_i}(x)}{dx^2} \quad [25]$$

where

$\phi'_{NUM\_i}(x)$ is the first spatial derivate of the mode of vibration i.

$\phi''_{NUM\_i}(x)$ is the second spatial derivate of the mode of vibration i.

The numerical vibration modes, $\phi_{NUM\_i}(x)$, are obtained in a discrete way using the corresponding finite element method as:

$$\phi_{NUM\_i}(x) = \sum_j \phi_i^j\cdot N_j(x) \quad [26]$$

where $N_j(x)$ are the shape functions and ϕ_i^j are the nodal values.

In the previous expressions, the value of the numerical vibration modes is set to zero when the pedestrian remains outside the structure.

$$\phi_{NUM\_i}(x_p) = 0 \text{ for } \begin{matrix} x_p(t) < 0 \\ x_p(t) > L \end{matrix} \quad [27]$$

The above relations –Eqs.(18) to (23)- are then substituted in the overall dynamic equilibrium equations -Eqs.(13) to (15)- so that, organizing information in a matrix form, the following model of interaction is obtained (see **Paper B** for further details and matrix formulation).

$$\mathbf{M}(t)\cdot\ddot{\mathbf{z}}(t) + \mathbf{C}(t)\cdot\dot{\mathbf{z}}(t) + \mathbf{K}(t)\cdot\mathbf{z}(t) = \mathbf{F}(t) \quad [28]$$

For a group of *k* pedestrians (Figure 8), each of them will be represented by the above simplified interaction model. In the case of a single pedestrian, the proposed model leads to a system *of n+1* equations, corresponding to the considered number of vibration modes *n* plus the simplified interaction equation. Similarly, when considering a group of *k* pedestrians, a system of *n+k* differential equations will need to be solved.

Considering the nature of the resulting system, the use of a method of β-Newmark integration family is proposed, with parameters $\beta = 1/4$ and $\gamma = 1/2$, thus ensuring an unconditionally stable system.

Furthermore, the integration step, Δt, is established according to the usual recommendations (*Clough and Penzien, 1993*; *Dominguez, 2001*) for dynamics models based on modal decomposition technique, as the minimum of the following values.

$$\Delta t = \min\left(\frac{1}{8\cdot f_{\max}}, \frac{L_{\min}}{200\cdot|v_p|}, \frac{L_{\min}}{4\cdot n\cdot|v_p|}, 0.01\right) \text{sec.} \quad [29]$$

with $f_{\max}$ [Hz] being the highest considered vibration frequency of the structure and $L_{\min}$ [m] the minimum span length of the pedestrian bridge.

In order to determine the number of pedestrians that cross the footbridge in phase, a Poisson distribution has been adopted, according to the results by *Matsumoto et al.* (1978). Thus, when a group of n_p pedestrians arrive at the footbridge, the number of pedestrians randomly synchronized is $\sqrt{n_p}$. This synchronization criterion has been adopted originally in the crowd-structure interaction model. Its implementation is achieved by the phase shift parameter, ϕ_p. For a given generation/group of pedestrians, the value of the phase shift of the $\sqrt{n_p}$ randomly synchronized pedestrians has been set equal to zero. For the remaining pedestrians the phase shift has been assigned randomly, using a Gaussian distribution in the range $[0,2\pi]$. Subsequently, in the lateral direction, this parameter will be modified if the lateral lock-in threshold is exceeded.

3.2. Modelling the crowd-behavior.

The pedestrian walking inside a crowd may be modelled using the governing equations of particle dynamics (*Rapaport, 2004*), considering that different social forces interact among pedestrians. This approach has been successfully applied by several authors (*Helbing and Molnár, 1995*; *Carroll et al., 2012*). In this way, the different motivation and influences experimented by the pedestrians are described by several force terms. The model is based on Newton dynamics and is able to represent the following rules in relation with the natural pedestrian movement (see (*Helbing and Molnár, 1995*) for a more involved description): (i) pedestrians normally choose the fastest route, (ii) each pedestrian has an individual speed that may be defined by a Gaussian distribution (iii) and the distance between pedestrians depends on the pedestrian density and the walking pedestrian speed. Figure 9 sketches the social forces acting on a pedestrian in a crowd, as described in detail in the following paragraphs.

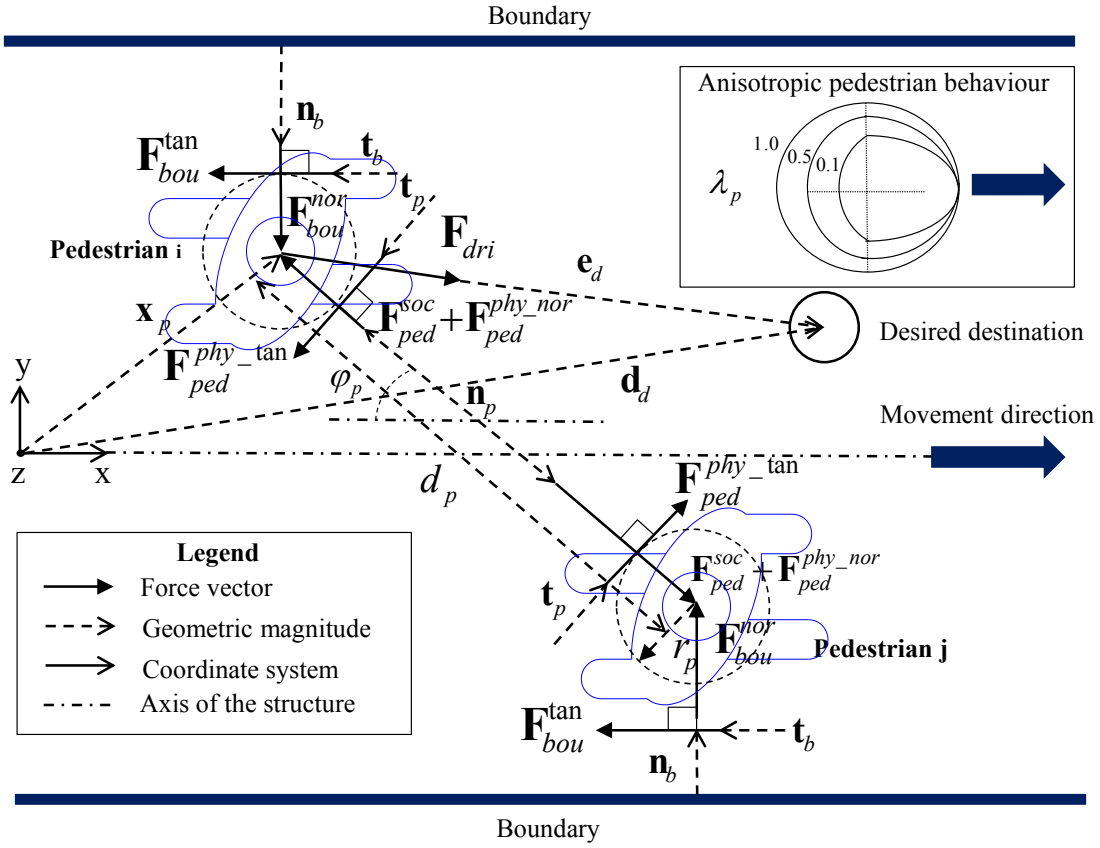

Figure 9. Pedestrian-crowd interaction forces (*Helbing and Molnár, 1995*).

All the parameters for the crowd model considered in this study have been obtained from the reported results provided by different authors (*Helbing and Molnár, 1995*; *Carroll et al., 2012*), as summarized in Table 9 and briefly described next.

Driving force.

Each pedestrian has a certain motivation to reach his desired destination, $\mathbf{d}_d$, with his desired velocity, v_d, which is represented by the driving force, $\mathbf{F}_{dri}$, as:

$$\mathbf{F}_{dri} = m \cdot \left(\frac{v_d \cdot \mathbf{e}_d}{t_r} - \frac{\mathbf{v}_p}{t_r} \right) \quad [30]$$

where $\mathbf{e}_d$ is the desired direction vector, $\mathbf{v}_p$ is the pedestrian step velocity and t_r is the relaxation time of the pedestrian (*Helbing and Molnár, 1995*) (Table 9). The desired direction of the movement may be obtained from the position of the pedestrian in each instant, $\mathbf{x}_p$, and its desired destination according to:

$$\mathbf{e}_d = \frac{\mathbf{d}_d - \mathbf{x}_p}{\left\| \mathbf{d}_d - \mathbf{x}_p \right\|} \quad [31]$$

Interactions among pedestrians.

The interaction among pedestrians originates a repulsive force (*Helbing and Molnár, 1995*), $\mathbf{F}_{ped}$, with two components, a socio-psychological force, $\mathbf{F}_{ped}^{soc}$, and a physical interaction force, $\mathbf{F}_{ped}^{phy}$, as:

$$\mathbf{F}_{ped} = \mathbf{F}_{ped}^{soc} + \mathbf{F}_{ped}^{phy} \quad [32]$$

The socio-psychological force reflects the fact that the pedestrians try to maintain a certain distance to other pedestrians in the crowd. This socio-psychological force depends on the distance between pedestrians, reaching its maximum value at the lowest established distance and tending to zero as such distance increases. The socio-psychological force is defined as:

$$\mathbf{F}_{ped}^{soc} = A_p \cdot \exp\left(\frac{2 \cdot r_p - d_p}{B_p} \right) \cdot \mathbf{n}_p \cdot s_p \quad [33]$$

where

A_p is the interaction strength between pedestrians (Table 9).

B_p is the range of the repulsive interaction between pedestrians (Table 9).

d_p is the distance between two pedestrians.

r_p is the so-called pedestrian radius (Table 9).

$\mathbf{n}_p$ is the normalized vector pointing between pedestrians.

s_p is a form factor to consider the anisotropic behaviour (the pedestrian action in front of the pedestrian is more important than behind him) of the pedestrians, which value may be obtained from:

$$s_p = \lambda_p + (1-\lambda_p)\cdot\frac{1+\cos(\varphi_p)}{2} \quad [34]$$

where λ_p (Table 9) is a potential factor that considers the influence on the pedestrian movement of other pedestrians situated in front of him (Figure 9) and φ_p is the angle between two pedestrians (Figure 9).

The physical interaction force, $\mathbf{F}_{ped}^{phy}$, is only considered in situations of physical contact among pedestrians (if $d_p \le 2\cdot r_p$), associated with situations of high pedestrian densities (≥0.80 P=Person/m^2). The physical interaction force is defined by the superposition of two components: (i) the body force, $\mathbf{F}_{ped}^{phy\_nor}$, that describes the counteracting body action that the pedestrians perform to avoid physical damage due to their physical contact with other individuals, (ii) and the sliding force, $\mathbf{F}_{ped}^{phy\_\tan}$, that represents the pedestrians' tendency to avoid passing other individuals with a high velocity at small distances (*Helbing and Molnár, 1995*). It is defined as:

$$\mathbf{F}_{ped}^{phy} = \mathbf{F}_{ped}^{phy\_nor} + \mathbf{F}_{ped}^{phy\_\tan} \quad [35]$$

$$\mathbf{F}_{ped}^{phy\_nor} = C_p \cdot H\left(2\cdot r_p - d_p\right)\cdot \mathbf{n}_p \quad [36]$$

$$\mathbf{F}_{ped}^{phy\_\tan} = D_p \cdot H\left(2\cdot r_p - d_p\right)\cdot \Delta v_p^t \cdot \mathbf{t}_p \quad [37]$$

where

$\mathbf{F}_{ped}^{phy\_nor}$ is the normal component of the physical interaction force (body force).

$\mathbf{F}_{ped}^{phy\_\tan}$ is the tangential component of the physical interaction force (sliding force).

C_p is the body force strength due to the contact between pedestrians (Table 9).

D_p is the sliding force strength due to the contact between pedestrians (Table 9).

$\mathbf{t}_p$ is a normalized vector perpendicular to $\mathbf{n}_p$.

$\Delta v_p^t = \left\langle \Delta\mathbf{v}_p \cdot \mathbf{t}_p \right\rangle$ is the tangential component of the relative pedestrian velocity, with $\Delta\mathbf{v}_p$ being the difference of vector velocities between two given pedestrians.

and function H is defined as:

$$H(\bullet)\cdot = \begin{matrix} \bullet & if & \bullet > 0 \\ 0 & if & \bullet \le 0 \end{matrix} \qquad [38]$$

Interactions with boundaries.

The interaction with the boundaries gives rise to forces, $\mathbf{F}_{bou}$. These forces are equivalent to the ones resulting from the interaction with other pedestrian, so they can be formulated in a similar fashion as:

$$\mathbf{F}_{bou} = \mathbf{F}_{bou}^{nor} + \mathbf{F}_{bou}^{\tan} \qquad [39]$$

$$\mathbf{F}_{bou}^{nor} = \left\{ A_b \cdot \exp\left(\frac{r_p - d_b}{B_b} \right) + C_b \cdot H\left(r_p - d_b\right) \right\} \cdot \mathbf{n}_b \qquad [40]$$

$$\mathbf{F}_{bou}^{\tan} = D_b \cdot H\left(r_p - d_b\right) \cdot \left\langle \mathbf{v}_p, \mathbf{t}_b \right\rangle \cdot \mathbf{t}_b \qquad [41]$$

where

$\mathbf{F}_{bou}^{nor}$ is the normal component of the boundary interaction force.

$\mathbf{F}_{bou}^{\tan}$ is the tangential component of the boundary interaction force.

A_b is the interaction strength between the pedestrian and the boundary (Table 9).

B_b is the range of the repulsive interaction between the pedestrian and the boundary (Table 9).

d_b is the distance between the pedestrian and the boundary.

C_b is the body force strength due to the contact with the boundary (Table 9).

D_b is the sliding force strength due to the contact with the boundary (Table 9).

$\mathbf{n}_b$ is the normalized vector defined perpendicularly from the pedestrian to the boundary.

$\mathbf{t}_b$ is the vector perpendicular to $\mathbf{n}_b$.

$\langle\ \rangle$ denotes scalar product.

Resultant force.

Finally, the proposed multi-agent model that simulates the behaviour of the crowd consists in the sum of all these partial forces that represent the different influences that the pedestrians suffer when interacting in a crowd. Therefore, the resultant

force, $\mathbf{F}_{pci}$, describes the movement and direction of each pedestrian in the crowd as:

$$\mathbf{F}_{pci} = \mathbf{F}_{dri} + \mathbf{F}_{ped} + \mathbf{F}_{bou} \quad [42]$$

Table 9. Crowd model parameters considered (*Helbing and Molnár, 1995*; *Carroll et al., 2012*).

Parameter	Element	Value
Relaxation time	t_r	0.50 sec.
Interaction strength pedestrians	A_p	2000 N
Interaction range pedestrians	B_p	0.30 m
Potential factor	λ_p	0.20
Contact strength pedestrians	C_p	2000 N
Sliding strength pedestrians	D_p	4800 N
Interaction strength boundaries	A_b	5100 N
Interaction range boundaries	B_b	0.50 m
Contact strength boundaries	C_b	2000 N
Sliding strength boundaries	D_b	4800 N
Radius of pedestrian	r_p	0.20 m

For the generation of pedestrians flows three parameters have been considered: (i) the pedestrian density [P=Person/m^2] established by international standards (*Butz et al., 2007*; *Setra, 2006*) according to the expected pedestrian traffic on the footbridge, (ii) the value of the desired velocity, v_d, of the pedestrians and (iii) the distance between pedestrians, d_p. In this study only a one-way traffic has been considered for simplicity in the generation of the pedestrian flows, although the model may be easily generalized for two-way traffic. The values of the desired velocity of each pedestrian have been obtained from the pedestrian step frequencies, f_s. For the present crowd-structure interaction model the Gaussian distribution of the pedestrian step frequency provided by *Zivanovic et al* (2010) has been adopted, $N(1.87,0.186)$ Hz (where $N(\mu,\sigma)$ is the Gaussian distribution, μ is the mean value and σ is the standard deviation). After assigning a step frequency

to each pedestrian, its desired velocity is determined from the empirical relation given by *Bertram and Ruina* (2001) (*Bruno and Venuti (2009)*), Eq. (5), so that the initial conditions for each pedestrian assume that the pedestrian velocity, v_p, is equal to the desired velocity, v_d. Finally, once the pedestrian density and the desired velocity of each pedestrian are established, the original distance among pedestrians is calculated considering the width of the footbridge and assuming a rectangular-shaped mesh of pedestrians.

Solution procedure.

The resultant crowd-structure interaction force, $\mathbf{F}_{pci}$, acts on each pedestrian during each time iteration *j*. The acceleration vector, $\mathbf{a}_p^j$, follows from

$$\mathbf{a}_p^j = \frac{\mathbf{F}_{pci}^j}{m} \qquad [43]$$

considering a pedestrian mass, m ($= m_s + m_a$). In this Thesis, according to the more recent international standards (*Setra, 2006*; *Butz et al., 2007*) a medium pedestrian's weight of 70 kg has been considered.

The evaluation of the remaining variables that govern the crowd model, $\mathbf{v}_p^{j+1}$ and $\mathbf{x}_p^{j+1}$, is then performed using a multi-step method based on a predictive-corrective method, namely the Gear's algorithm (*Heermann, 1986*), due to the fact that the social forces depend on the velocity and the position of the pedestrians. The algorithm calculates first an approximate value, called a predictor that subsequently is corrected with a corrector value. A more detailed description of the applied algorithm is reported in **Paper B**.

3.3. Crowd-structure interaction.

The crowd-structure interaction has been simulated including two behavioural conditions in the model, a comfort and lateral lock-in thresholds. The comfort condition is applied in both directions (vertical and lateral) while the lateral lock-in condition is only applied in lateral direction. Additionally the comfort condition takes into account the different sensitivity of the pedestrians to the vibrations according to the acting direction. In this manner, in order to reflect in the model the change of the behaviour of each pedestrian due to the modification of his comfort level in lateral direction, a behavioural factor has been applied to the pedestrian velocity. According to the results provided by several studies (*Brownjohn et al. 2004*; *Macdonald, 2008*; *Carrol et al. 2012*) a minimum comfort threshold 0.20 m/s^2 has been selected in our model. In this manner, if the maximum lateral acceleration of each pedestrian, $(\ddot{y}_a)_{\max}$, is above this value, the pedestrian velocity is reduced by a behavioural factor, r_v, which is a function of the acceleration he/she experiences. Following the intuitive assumption, reported by *Carrol et al.* (2012), that the pedestrians are likely to react more firmly as the lateral acceleration they feel is higher, a third order polynomial is proposed. The function, Eq. (44), has been

obtained interpolating the tri-linear function proposed by *Carrol et al.* (2012) in order to simplify the evaluation of this reduction factor.

$$r_v(\ddot{y}_a) = -0.168 \cdot \ddot{y}_a^{\,3} + 0.1897 \cdot \ddot{y}_a^{\,2} - 0.1443 \cdot \ddot{y}_a + 1.0226 \qquad [44]$$

On the other hand, a maximum vertical, $\ddot{z}_{\lim} = 2.50$ m/s^2 (*Setra, 2006*), and lateral limit acceleration, $\ddot{y}_{\lim} = 2.10$ m/s^2 (*Venuti et al, 2007*), have been also considered, so when the experienced lateral acceleration becomes too high, pedestrians stop walking to maintain balance, and they remain stopped until the acceleration level reduces. A reaction time, $t_{rea} = 2.00$ sec., has been established both to stop walking and to remain stationary before beginning to walk again. The variation of the pedestrian velocity during the reaction time has been adopted as a linear function. In order to avoid meaningless small walking velocities, a practical lower limit on walking velocity magnitude has been imposed as suggested by *Carrol et al.* (2012).

$$|v_p| = \begin{cases} 0.1 \cdot |v_d| & if \quad (\ddot{a}_a)_{\max} < \ddot{a}_{\lim} \cap |v_p| \le 0.1 \cdot |v_d| \\ 0 & if \quad (\ddot{a}_a)_{\max} \ge \ddot{a}_{\lim} \end{cases} \qquad [45]$$

where $(\ddot{a}_a)_{\max}$ reflects the maximum acceleration experienced by the pedestrian according to the considered direction, $(\ddot{a}_a)_{\max} = (\ddot{z}_a)_{\max}$ or $(\ddot{a}_a)_{\max} = (\ddot{y}_a)_{\max}$, and $\ddot{a}_{\lim}$ is the limit acceleration that marks the change of the behaviour according to the directional criterion, $\ddot{a}_{\lim} = \ddot{y}_{\lim}$ or $\ddot{a}_{\lim} = \ddot{z}_{\lim}$.

Finally, as lateral lock-in threshold, the criterion suggested by the French standard (*Setra, 2006*) has been considered. If the lateral acceleration experienced by each pedestrian is above 0.15 m/s^2 and his step frequency is within ±10 percent of the lateral natural frequency of the structure (*Ronnquist, 2005*), both his step frequency and phase shift are modified to match the natural frequency of the footbridge and synchronize the movements of the pedestrian and the structure.

4. Inverse dynamic problem approach.

The implementation of the proposed model was not possible if the parameters of the TDOF-system that characterizes the pedestrian-structure interaction were not well-defined. The considered parameters were the walking pedestrian force and the modal parameters of the TDOF-system (the pedestrian sprung mass, the pedestrian damping ratio and the pedestrian natural frequency) in each considered direction (vertical and lateral). Although the value of these parameters might be estimated from the results of similar studies reported in the literature (see sections 2.1 and 2.5) in order to determine their value for the overall proposed model and on a real footbridge, an inverse dynamic problem approach was used.

A usual manner of identifying the parameters of a system is the solution of an inverse problem since the response of the system is the easiest recordable variable (*Maia and Silva, 1997*). In that sense, the current accelerometers allow obtaining the dynamic response of a structure (accelerations) with a high accuracy and under any type of action. Using these recorded accelerations is possible to determine either the inputs of the system, as for instance the applied forces, or even the own system parameters. The estimation of these magnitudes is achieved by the solution of an inverse dynamic problem approach. Among the different existing algorithms (*Maia and Silva, 1997*), for the development of the present work, as identification method the minimization of a least square problem was considered (*Koh and Perry, 2010*), implementing it in the software package Matlab (*Matlab, 2015*). As global minimization method, genetic algorithms (*Nocental and Wright, 1999*) were used and a search domain for each parameter has been established in order to reduce the uncertainties of the estimated values of the considered parameter and thus prevent an ill-conditioned inverse problem.

The general layout of the inverse dynamic problem approach applied is:

- (i) First, the modal parameters of the interacting footbridge were obtained by the updating (*Teughels, 2003*; *Zivanovic et al., 2007*; **Paper C**; **Paper G**) of its finite element model based on the experimental identification of its modal properties (natural frequencies, modal shapes and damping ratios). These magnitudes were estimated by the signal processing of the records of an ambient test by an operational modal analysis algorithm (*Magalhães and Cunha, 2011*; **Paper F**; **Paper G**). The Viana footbridge (Viana do Castelo, Portugal) has been used for this purpose (*Barbosa et al., 2012*). The updating process allows both transforming a real footbridge into a "laboratory" footbridge and the modal shapes into the vibration modes (normalized by the mass matrix).

- (ii) Second, two additional experimental tests, a pedestrian and a crowd test, were conducted at the Viana footbridge. The dynamic response of the footbridge in four points was recorded under the crossing of two (pedestrian test) or fifty (crowd test) pedestrians at different step frequencies controlled by a metronome. In order to reduce the noise level of the recorded signals, a level 7 decomposition of the signal using the Continuous Wavelet Transform (CWT) based on Daubechies family was applied (CWT) (*Gopalakrishnan and Mitra, 2014*). Subsequently, the principle of Stein's Unbiased Risk Estimate was considered. The reconstruction of the signal was performed using the original approximation coefficients of level 7 and the modified detail coefficients of level from 1 to 7. The reduction of the noise level

reduces the uncertainty of the parameter estimation obtained by the solution of an inverse dynamic problem (*Koh and Perry, 2010*).

- (iii) Third, the results of the two mentioned experimental tests were used to define the objective function of the global minimization algorithm. Different objective functions were used in each direction (**Paper B** and **Paper E**) due to the different signal-noise ratio and the absence of the self-weight component of the pedestrian walking lateral force. In sections 4.1 and 4.2 a more detailed description of the objective function considered in each direction (vertical and lateral) is presented.

- (iv) On the other hand, the definition of the objective functions is completed by the numerical estimation of the dynamic response of the Viana footbridge under a numerical simulation of the mentioned pedestrian and crowd tests by the implementation of the proposed crowd-structure interaction model on the updated finite element model of the Viana footbridge.

- (v) Finally, a search domain for each parameter was established and the estimation of the parameters of the proposed TDOF-system was obtained by minimizing the objective functions defined in each direction.

In the following two sections (4.1 and 4.2) a more detailed description of the selected objective functions, design variables and identification process for the parameter identification in each direction is presented.

4.1. Inverse dynamic problem: parameter identification in vertical direction.

In order to define the objective function for the parameter identification of the TDOF-system in vertical direction (**Paper B**), the recorded dynamic response of the Viana footbridge during the experimental pedestrian test was analysed by its transformation to the frequency domain. It was checked that the dynamic response of the footbridge was characterized by a harmonic series that included both the first two frequencies that characterizes the pedestrian step and the first two natural frequencies of the footbridge in vertical direction. In this manner, as the recorded vertical accelerations contained information of the two components of the proposed TDOF-system, pedestrian and structure, the objective function, in this direction, was defined as the mean square error between the experimental ($a_{v,i}^{\exp}$, where *i* is the considered section) and numerical ($a_{v,i}^{num}$) vertical accelerations obtained, in four points of the Viana footbridge, under the crossing of two pedestrians at different controlled step frequencies. As design variables the first two VDLF ($\alpha_{1,ver}$ and $\alpha_{2,ver}$) of the pedestrian walking vertical force and the three modal parameters that characterizes the TDOF-system in vertical direction (the pedestrian sprung mass, $m_{a,ver}$, the pedestrian damping ratio, $\zeta_{p,ver}$, and the pedestrian natural frequency, $f_{p,ver}$) were considered. In Figure 10 the layout of the identification procedure is shown.

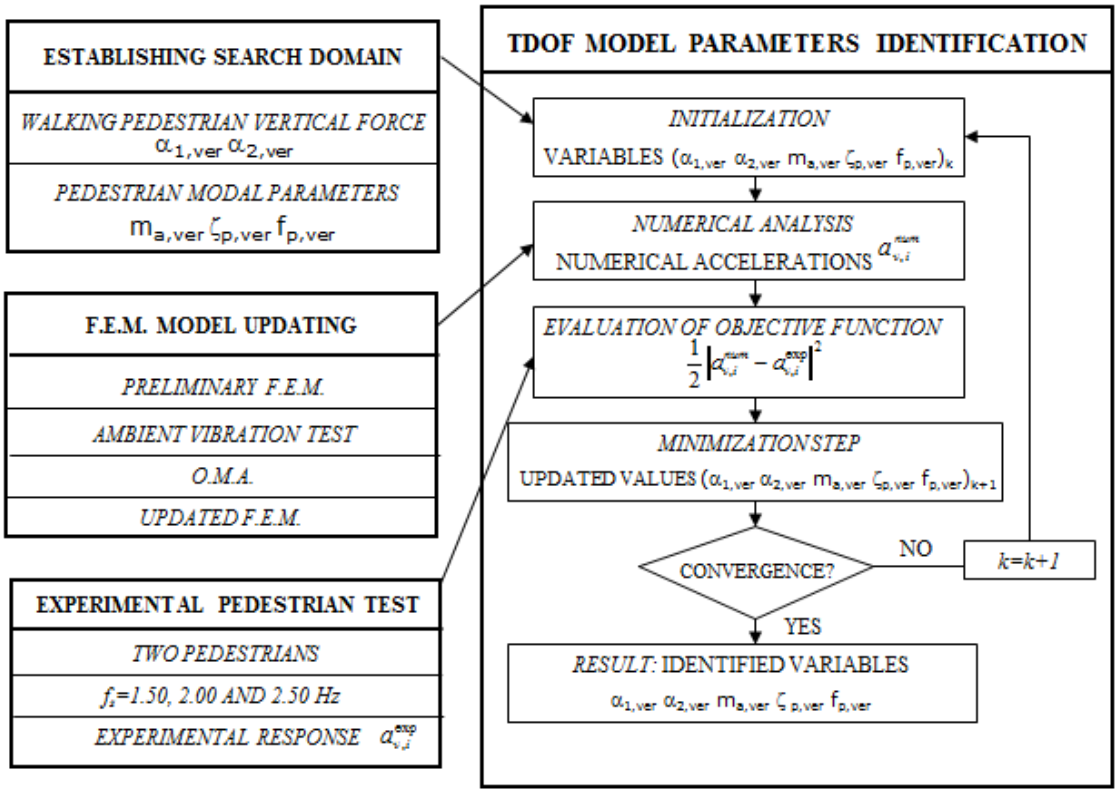

Figure 10. Flowchart of the identification procedure in vertical direction.

An iterative process to reduce the differences between the experimental and numerical vertical accelerations was performed, under the rules of genetic algorithms (*Koh and Perry, 2010*; *Nocental and Wright, 1999***)**, The estimated values of parameters of the pedestrian-structure interaction model, in vertical direction, were correlated successfully with: (i) the walking pedestrian vertical force suggested by different authors (summarized in section 2.1) and (ii) a previous estimation of the modal parameters (**Paper A**) obtained from the analysis of the change of the modal properties of a footbridge induced by a controlled group of pedestrians (*Georgakis and Jorgesen, 2013*). On the other hand, the estimated values of the modal parameters were inside the range, established by *Shahabpoor et al.* (2013).

4.2. Inverse dynamic problem: parameter identification in lateral direction.

In order to define the objective function for the parameter identification of the TDOF-system in lateral direction (**Paper E**), the recorded dynamic response of the Viana footbridge during the experimental pedestrian test was analysed again by its transformation to the frequency domain. In this case, however, it was checked that the dynamic response of the footbridge was characterized by a harmonic series that contained only the first three frequencies that characterizes the pedestrian step without a remarkable contribution of the harmonics associated with the lateral natural frequencies of the footbridge. In this manner, the accelerations recorded during the experimental pedestrian test contained information mainly of the walking pedestrian lateral force, being necessary to conduct a second experimental test, a crowd test, in order to characterize the modal parameters of the TDOF-system. In this crowd test, the dynamic response of Viana footbridge under a group of fifty

pedestrians at different step frequencies was recorded in order to study the change of the first lateral natural frequency of the footbridge induced by the pedestrian-structure interaction. Due to this fact, the identification process was divided in two steps, by solving two inverse dynamic problems.

First, as the modal parameters of the pedestrian-structure interaction model have a direct effect on the modal parameters of the footbridge (**Paper A**) as objective function of the first minimization problem, the mean square error between the experimental, $f_{1,lat}^{\exp}$, and numerical, $f_{1,lat}^{num}$, first lateral natural frequency of the Viana footbridge, obtained during the performance of the experimental crowd test and its numerical simulation, was considered. Additionally, as design variables of this first inverse problem, the three modal parameters that characterizes the TDOF-system, in lateral direction (the pedestrian sprung mass, $m_{a,lat}$, the pedestrian damping ratio, $\zeta_{p,lat}$, and the pedestrian natural frequency, $f_{p,lat}$), were considered.

Second, although there are very recent and comprehensive studies of the lateral force induced by pedestrians (*Ingólfsson and Georgakis, 2011*; *Ingólfsson et al., 2011*), these research do not include the effect of the pedestrian-structure interaction. Therefore it was necessary to estimate the walking pedestrian lateral force under this assumption. In this manner a second inverse problem was solved. As objective function of the second minimization problem, the mean square error between the experimental ($psd_{lat,i}^{\exp}$, where *i* is the considered section) and numerical ($psd_{lat,i}^{num}$) power spectral density obtained from the lateral accelerations recorded in the previously mentioned experimental pedestrian tests and its numerical simulation, was considered. As design variables for this second inverse problem, the first three LDLF ($\alpha_{1,lat}$, $\alpha_{2,la}$ and $\alpha_{3,lat}$) and their corresponding phase shifts of the second and third harmonic ($\varphi_{2,la}$ and $\varphi_{3,lat}$) of the pedestrian walking lateral force were considered. In Figure 11 a flowchart of the identification procedure is shown.

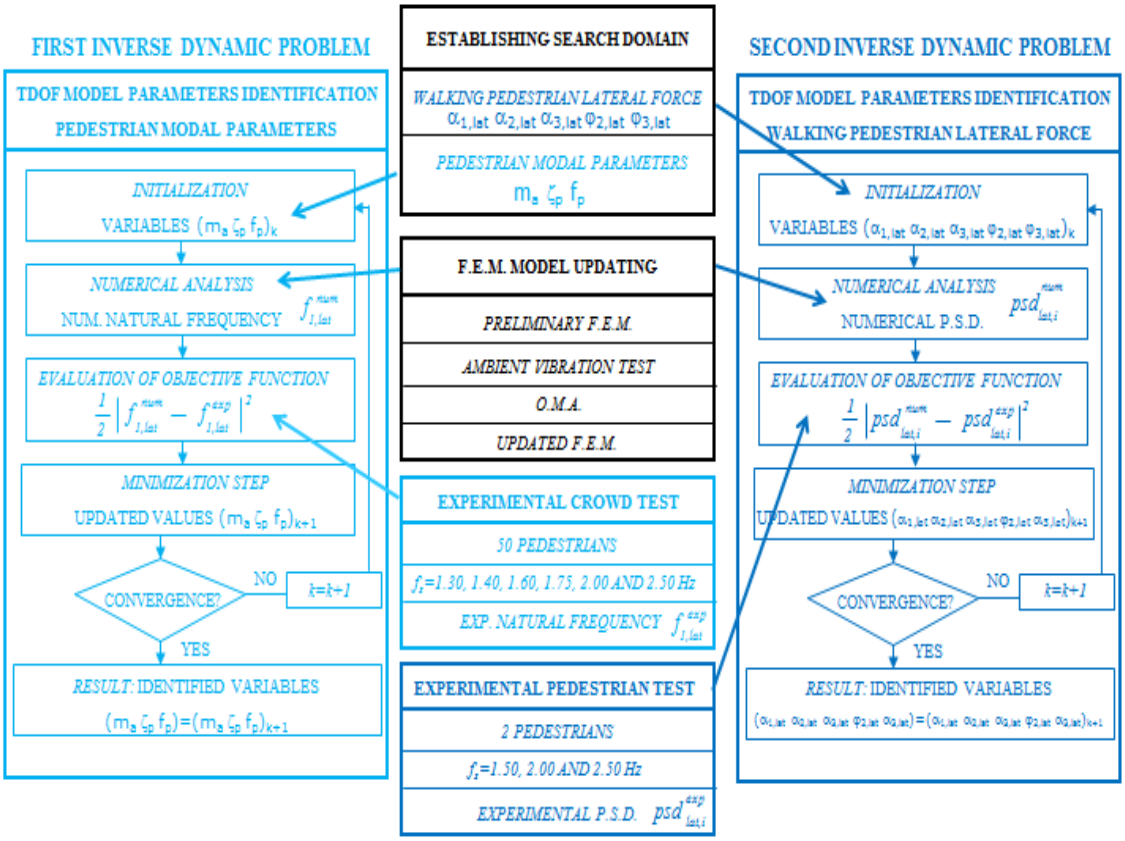

Figure 11. Flowchart of the identification procedure in lateral direction. Light blue marks the modal parameter identification methodology and dark blue the walking pedestrian force identification methodology.

As in the above case (vertical direction), an iterative process to reduce the differences between the experimental and numerical magnitudes was performed, under the rules of genetic algorithms (*Koh and Perry, 2010*; *Nocental and Wright, 1999***)**, In this case, the identification procedure is performed in two steps. First, the modal parameters of the proposed TDOF-system were estimated by the minimization of the relative differences between the experimental and numerical change of the first lateral natural frequency of the Viana footbridge during an experimental crowd test and its numerical simulation. Second, once established the modal parameters of the proposed model, the walking pedestrian lateral force was estimated by the minimization of the relative differences between the experimental and numerical power spectral densities obtained in four points of the Viana footbridge during an experimental pedestrian test and its numerical simulation. The estimated values of the parameters of the pedestrian-structure interaction model, in lateral direction, were correlated successfully with: (i) the walking pedestrian lateral force suggested by different authors (summarized in section 2.1) and the range of pedestrian modal parameters suggested by *Shahabpoor et al.* (2013).

5. Experimental estimation of the parameters of the pedestrian-structure interaction model.

In this section the estimation of the parameters of the proposed TDOF-system was performed in vertical and lateral directions. First, a real footbridge, Viana do Castelo footbridge (*Barbosa et al., 2012*), was converted into a "laboratory" footbridge by the updating of its finite element model based on the experimental modal parameters of the structure obtained from an operational modal analysis performed on the measurements recorded during an ambient test. Second, two experimental tests, a pedestrian and crowd test, were conducted in order to established a basis for the estimation of the parameters of the proposed TDOF-system. Finally, the parameters of the pedestrian-structure interaction model were estimated by the resolution of an inverse problem approach.

5.1. Description and finite element model of the "laboratory" footbridge: Viana footbridge.

The Viana do Castelo footbridge (*Barbosa et al., 2012*) is a moveable cable-stayed bridge. The longitudinal structural scheme of the footbridge consists of two spans of about 36.50 m and 9.00 m respectively suspended by 6 families of two hangers (two retaining ones) from an inclined mast. The deck, with 2.50 m of width, is configured by two rolled steel beams of variable depth braced by circular hollow profiles. The deck floor is covered with wood. The compensation of the main span weight is achieved by placing 11 high density blocks (with a weight of 800 kN) placed in the shorter span. The mast is welded in its base to a cylinder that is connected to a wheel gear bearing that allows the rotational movement of the structure. The pylon is connected to a deep foundation that balances the forces transmitted by the mast. A perspective of the Viana footbridge is shown in Figure 12.

Figure 12. Lateral view of the Viana footbridge (*Barbosa et al., 2012*).

A preliminary numerical finite element (Figure 13) modal analysis was conducted in order to have a first approximation to the dynamic behaviour of the footbridge and to define a starting point required to perform the ambient vibration test.

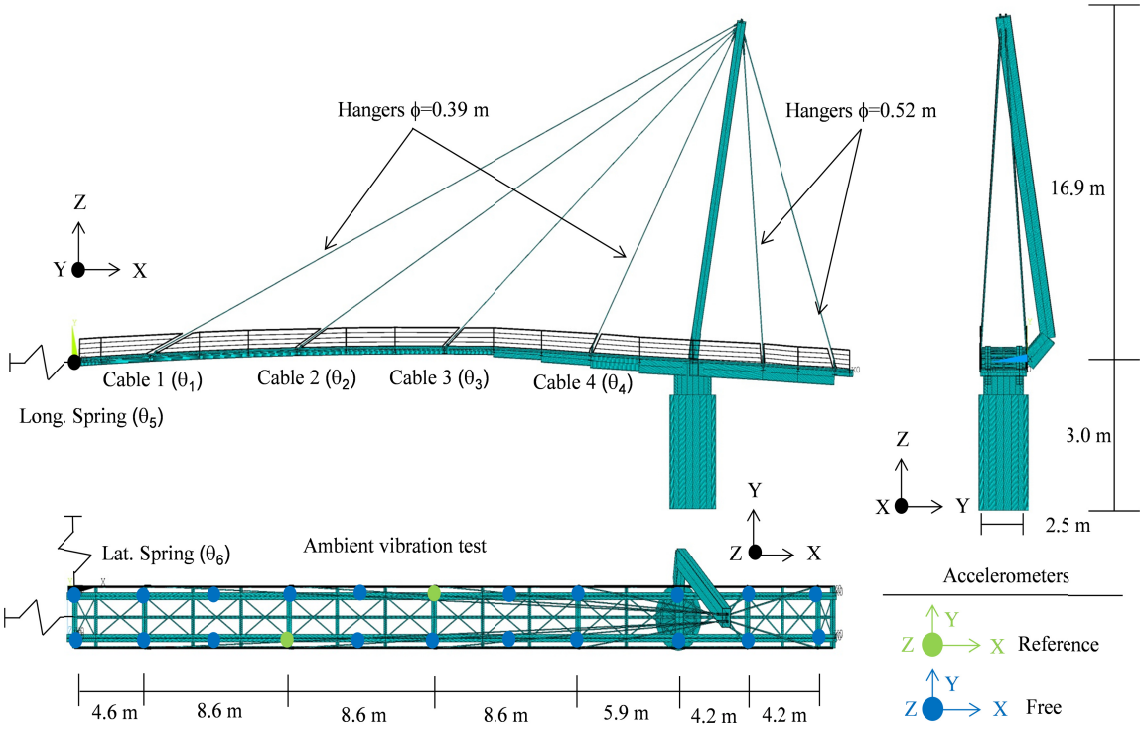

Figure 13. Finite element model, ambient test grid and model updating parameters.

The software package Ansys (*Ansys, 2015*) was used based on a discretization of the structure using 3D-beam elements (BEAM188), except for the hangers where 3D-cable elements (LINK10) were implemented. The nonlinear effects associated with the hangers have been considered for the determination of the numerical natural frequencies and the vibration modes of the structure, by calculating previously the stress level of the hangers under permanent loads and thus estimating its tangent stiffness matrix. The numerical modal analysis of this preliminary FE model leads to the first four numerical vibration modes and associated numerical natural frequencies given in Table 10. In Figure 14 the first four numerical vibration modes are shown (f_{NUM}_i, with *i* being the vibration mode number).

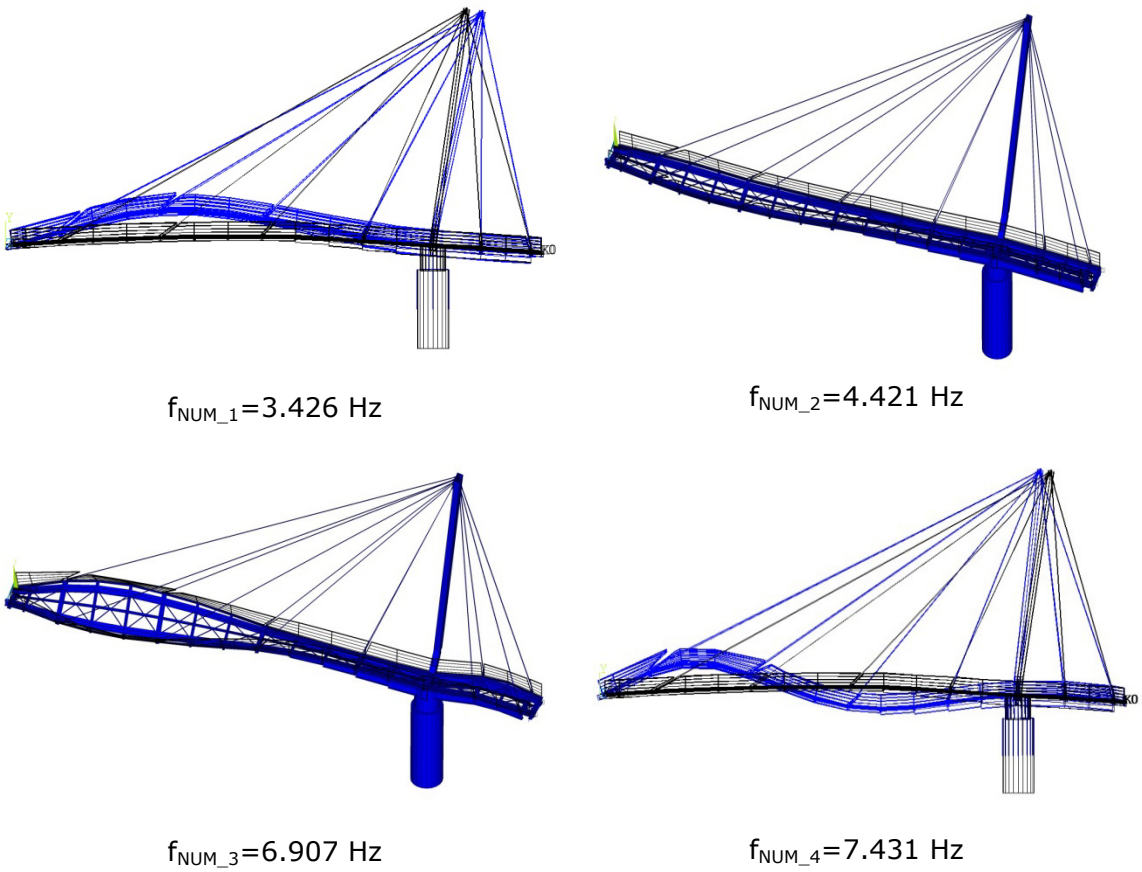

Figure 14. First four numerical vibration modes. Initial FE model.

5.2. Experimental identification of the modal parameters of the "laboratory" footbridge.

In order to obtain experimentally the modal parameters (natural frequencies, damping ratios and modal shapes) of the footbridge, an ambient vibration test was performed. The measurements were recorded in ambient conditions, with the footbridge excited by a light wind. In order to acquire a sufficient level of expertise in the application of this identification technique, the assessment of the dynamic behaviour of others footbridges was conducted by the author during the development of this Thesis. Two representative examples have been included in the document (**Paper F** and **Paper G**). The modal shape coordinates were measured along two gridlines separated transversally 1.68 m. A total of 2x11 points equally distributed along each longitudinal alignment were instrumented. Four high sensitivity tri-axial force balanced accelerometers were used (Figure 15). Using two of these devices as references, measurements were successively made moving the other two accelerometers to the defined instrumentation locations and recording in each point 1000 sec. time series of acceleration sampled at 100 Hz (Figure 13).

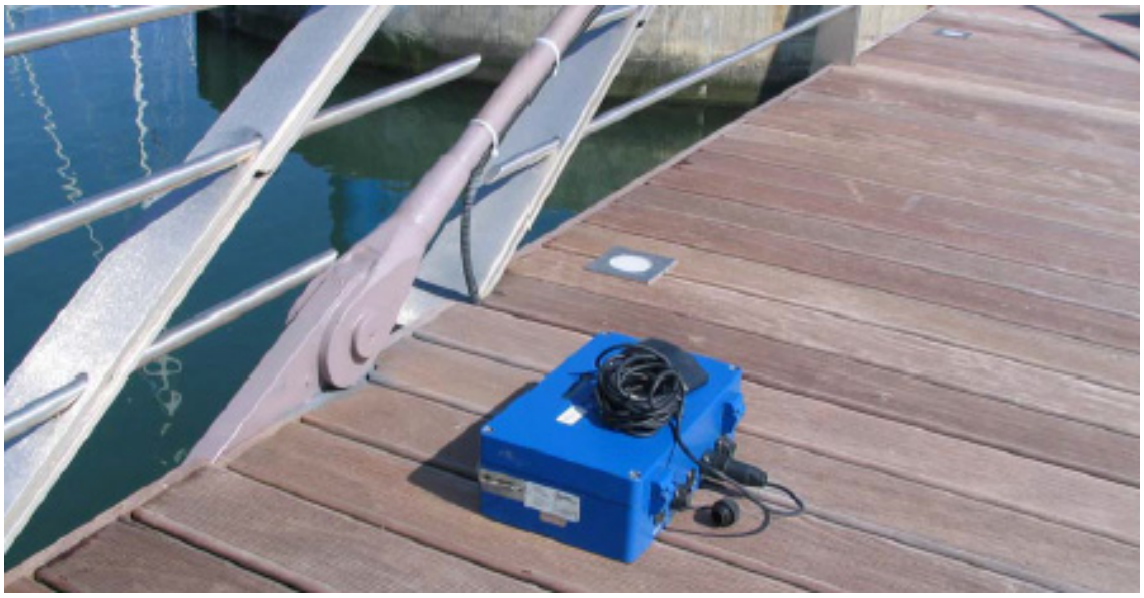

Figure 15. One accelerometer used during ambient/experimental tests.

The experimental identification of the modal parameters was done in the time domain using the Stochastic Subspace Identification method (*Magalhães and Cunha, 2011*), implemented in the software program Artemis (*Artemis, 2015*). Figure 16 illustrates the stabilization diagram of the identification algorithm used. The first four vibration modes were identified and subsequently used for the FE model updating process (see **Paper B**). The obtained numerical and experimental natural frequencies and vibration modes shapes are compared in Table 10 and the correlation between the first four numerical and experimental vibration modes is shown in Figure 17 (with the x axis corresponding to the longitudinal direction of the footbridge). In order to validate the correlation between the numerical and experimental modal parameters, both the relative difference (Δf) between the numerical and experimental frequencies and the modal assurance criterion (*M.A.C.*) were analysed (*Zivanovic et al., 2007*). A good correlation between two modes is achieved when the value of their M.A.C. ratio is greater than 0.90. These two magnitudes may be defined according to Eqs. (46 and 47) as follows:

$$\Delta f = \frac{f_{NUM\_i} - f_{EXP\_i}}{f_{EXP\_i}} \cdot 100 \ \ [\%] \qquad [46]$$

where f_{NUM_i} is the numerical natural frequency and f_{EXP_i} is the experimental natural frequency of the vibration mode *i*.

$$MAC_i = \frac{\left(\phi_{NUM\_i}^T \cdot \phi_{EXP\_i}\right)^2}{\left(\phi_{NUM\_i}^T \cdot \phi_{NUM\_i}\right) \cdot \left(\phi_{EXP\_i}^T \cdot \phi_{EXP\_i}\right)} \qquad [47]$$

where ϕ_{NUM_i} and ϕ_{EXP_i} are the numerical and experimental vibration modes to be compared and ^{T} denotes the transpose.

Although the shapes of the identified vibration modes are in good agreement (with M.A.C. ratios greater than 0.90 in three of the vibration modes), the relative differences, Δf, between the first two numerical and experimental natural frequencies are still significant. Therefore, the initial estimation made on the physical parameters of the structure is not good enough and it becomes necessary to perform a finite element model updating (*Friswell and Mottershead, 1995*; *Teughels, 2003,* **Paper C**) of the footbridge in order to improve the correlation between the numerical and experimental modal parameters.

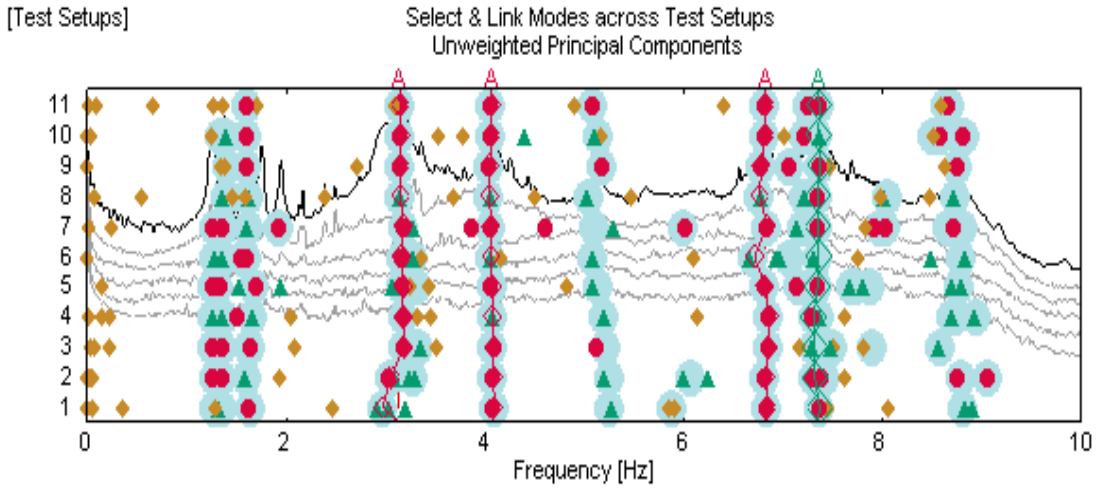

Figure 16. Stabilization diagram of the Stochastic Subspace Identification method.

Finally, in Table 10 an estimation of the damping ratios, ζ_i, associated with the identified vibration modes is also shown (*Magalhães et al., 2010*). These values will be adopted later in the identification process of the parameters of the TDOF-system that models the pedestrian.

Table 10. First four numerical (f_{NUM}) versus experimental (f_{EXP}) vibration modes of the footbridge.

Modes	**f_{NUM} [Hz]**	**f_{EXP} [Hz]**	ζ_i [%]	Δf [%]	**M.A.C.**	**Description**
1	3.426	3.138	1.22	9.17	0.963	First vertical mode
2	4.421	4.068	1.21	8.67	0.985	First lateral mode
3	6.907	6.810	1.10	1.42	0.809	Second lateral mode
4	7.431	7.345	1.39	1.17	0.939	Second vertical mode

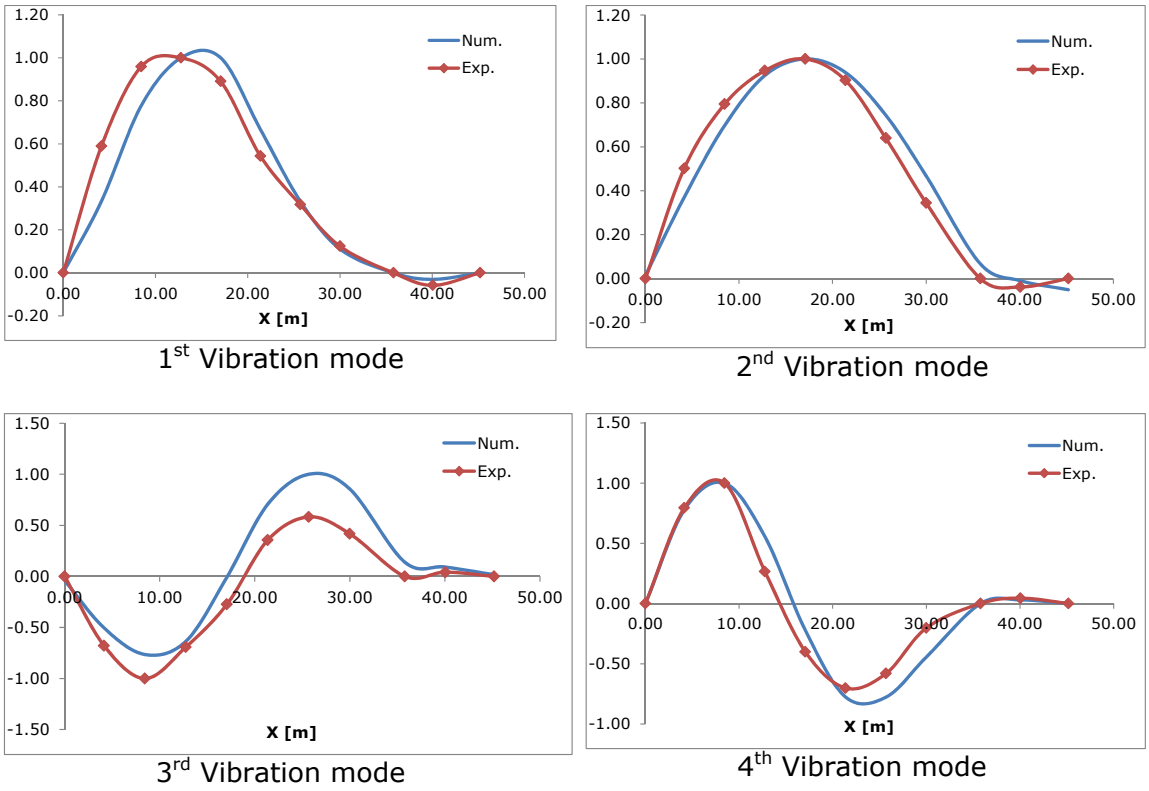

Figure 17. First four numerical (Num.) versus experimental (Exp.) vibration modes.

5.3. Model updating of the "laboratory" footbridge.

As indicated above, in order to reduce the level of uncertainties of the numerical analysis a finite element model updating (*Friswell and Mottershead, 1995*; *Teughels, 2003*; *Zivanovic et al., 2007*, **Paper C**) of the structure has been performed. The four identified vibration modes were considered in the updating process due to the good quality of the experimental data. Both measured natural frequencies and modal coordinate values were taken into account. Therefore, in total 48 residual components were selected for the model updating (the four identified natural frequencies and the eleven coordinates of each identified vibration mode). A more detailed description of the methodology used to perform the model updating can be found in **Paper C** and **Paper G**.

A sensitivity analysis was performed in order to adequately determine the physical parameters of the FE model with greater influence on the identified vibration modes. In this manner, the modal sensitivities with respect to some possible physical variables have been obtained numerically (*Fox and Kapoor (1968)*). The results of this study conclude that the most influential physical parameters on the dynamic behaviour of the footbridge are the stiffness of the four families of main hangers and the soil-structure interaction, modelled by two spring elements (in longitudinal, θ_5, and lateral, θ_6 directions, as Figure 13 illustrates) situated at the extreme of the longer span. As the stiffness of the hangers is conditioned by their stress level, the initial stress state of each considered family (θ_1, θ_2, θ_3 and θ_4)

has also been taken into account as physical variable. In Figure 13 and Table 11, the selected physical variables are shown.

The model updating process has been conducted by solving an optimization problem in the software programs Ansys (*Ansys, 2015*) and Matlab (*Matlab, 2015*). As objective function the mean square error between the experimental and numerical modal parameters (natural frequencies and vibration modes) of the Viana footbridge has been considered. In each iteration, a population of 1000 vectors has been generated that, using the genetic algorithms rules of mutation, reproduction and crossover, has minimized the value of the proposed objective function. The values of the selected parameters have been modified in order to minimize the considered objective function. Additionally, a search domain has been defined to control the variation of each parameter, increasing the efficiency of the optimization algorithm and yet maintaining the physical meaning of the finite element model updating. For the stiffness of the hangers, as a passive behaviour is expected, their medium tension level has been determined under permanent loads, with a value of 250 kPa. Slight variations of this value have been considered expanding the search domain between 0-500 kPa. For the stiffness of the springs (θ_5 and θ_6), given the uncertainty associated with the stiffness of the soil, a wider search domain was considered. So considering, as it is established by the geotechnical report, a variation of the Young's modulus of soil between $E_m = 1-100$ GPa and the geometry of the abutments, the variation of the equivalent stiffness of the springs has been determined θ_5 and $\theta_6 \in \left[10^7 - 10^9\right]$N/m. In Table 11 the range of variation of each parameter and its updated values are shown

Table 11. Updated values of considered physical parameters.

Parameters	Minimum Value	Updated Value	Maximum Value
Tension stress cable 1 (θ_1)	0.00 kPa	112.38 kPa	500.00 kPa
Tension stress cable 2 (θ_2)	0.00 kPa	59.62 kPa	500.00 kPa
Tension stress cable 3 (θ_3)	0.00 kPa	31.62 kPa	500.00 kPa
Tension stress cable 4 (θ_4)	0.00 kPa	147.43 kPa	500.00 kPa
Longitudinal Spring (θ_5)	1.00E7 N/m	6.00E7 N/m	1.00E9 N/m
Lateral Spring (θ_6)	1.00E7 N/m	1.90E8 N/m	1.00E9 N/m

The differences between the numerical and experimental natural frequencies, after the finite element model updating, are very small and the correlation between the numerical and experimental vibration modes are even higher. The relative differences between the updated numerical (f_{UPD}) and experimental (f_{EXP}) modal parameters and the *M.A.C.* values achieved after the model updating process are summarized in Table 12, where the improvement with respect to the initial FE model is clear (see Table 10).

Table 12. First four updated numerical (f_{UPD}) and experimental (f_{EXP}) vibration modes of the footbridge.

Modes	f_{UPD} [Hz]	f_{EXP} [Hz]	Δf [%]	M.A.C.	Description
1	3.136	3.138	-0.06	0.999	First vertical mode
2	4.052	4.068	-0.39	0.999	First lateral mode
3	6.799	6.810	-0.16	0.998	Second lateral mode
4	7.342	7.345	-0.04	0.999	Second vertical mode

Similarly, Figure 18 illustrates the correlation between the updated numerical and the experimental vertical vibration modes, with an excellent agreement.

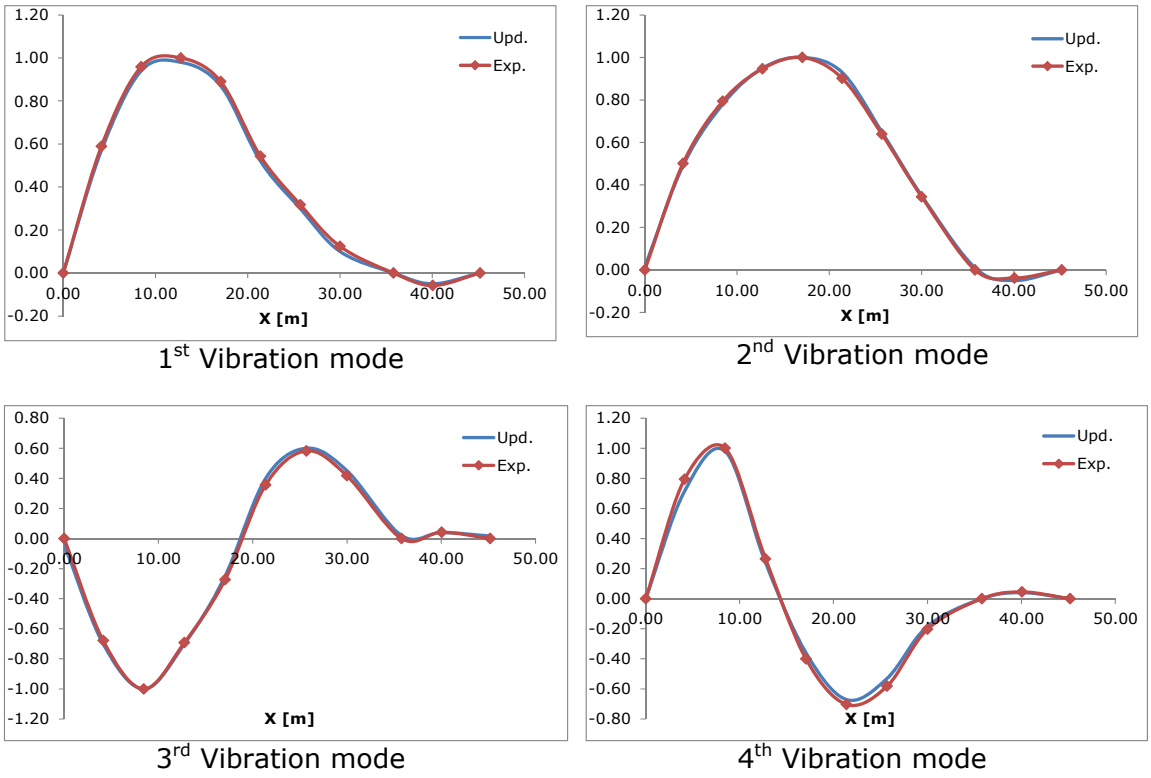

Figure 18. First four updated numerical (Upd.) and experimental (Exp.) vibration modes.

After the development of the model updating, the numerical dynamic behaviour of the footbridge simulates accurately the real response of the structure. This detailed knowledge of the dynamic behaviour of the footbridge allows for adopting this real footbridge as a benchmark or "laboratory" footbridge.

5.4. Experimental pedestrian and crowd tests.

As it has been mentioned above the parameters of the proposed TDOF-system were estimated using an inverse problem approach. The methodology is based on the results of two tests: (i) an experimental pedestrian test, whose results have been used to estimate all the parameters of the proposed TDOF-system in vertical direction and the walking pedestrian lateral force, and (ii) an experimental crowd test, whose results have been used to estimate the modal parameters of the proposed TDOF-system in lateral direction. Additionally, the results of the crowd

test have been used to validate the performance of the proposed crowd-structure interaction model in vertical direction. In the following paragraph a detailed description of these two tests is summarized.

Experimental pedestrian test

The estimation of the all the parameters of the TDOF-system in vertical direction and the walking pedestrian force in lateral direction were made through the results of an experimental pedestrian test. In this test, two pedestrians (A and B), with a pedestrian mass of $m_A = 61.70$ kg and $m_B = 100.50$ kg respectively, were selected. On the deck of the footbridge four triaxial accelerometers were placed at the intersection point between the hangers and the deck (S_1, S_2, S_3 and S_4 in Figure 19). Three time series were recorded for each pedestrian, crossing the footbridge three times at different step frequencies, f_s (1.50, 2.00, 2.50 Hz), controlled by a metronome. In the monitored sections the dynamic response of the structure was measured. In each passage, the initial and end time, that marks the passage of the pedestrian on the structure, was recorded for both localizing the force vibration response corresponding to the passage of each pedestrian and estimating the pedestrian velocity, v_p.

Experimental crowd test

Subsequently, the estimation of the modal parameters of the TDOF-system in lateral direction has been made using the results of an experimental crowd test. In this test, a group of 50 pedestrians crossed the footbridge at different step frequencies (1.30-1.40-1.60-1.75-2-00-2.50 Hz) controlled by a metronome, measuring the dynamic response of the footbridge at the previously mentioned four sections (S_1, S_2, S_3 and S_4 in Figure 19) using tri-axial force balanced accelerometers. During the crowd test the group of 50 pedestrians were distributed in three alignments, maintaining a lateral separation among pedestrians around 0.85 m and a longitudinal distance between pedestrians around 0.50 m. A pedestrian with a metronome led the group in each crossing. A scheme of the pedestrian distribution during the crowd test is shown in Figure 19.

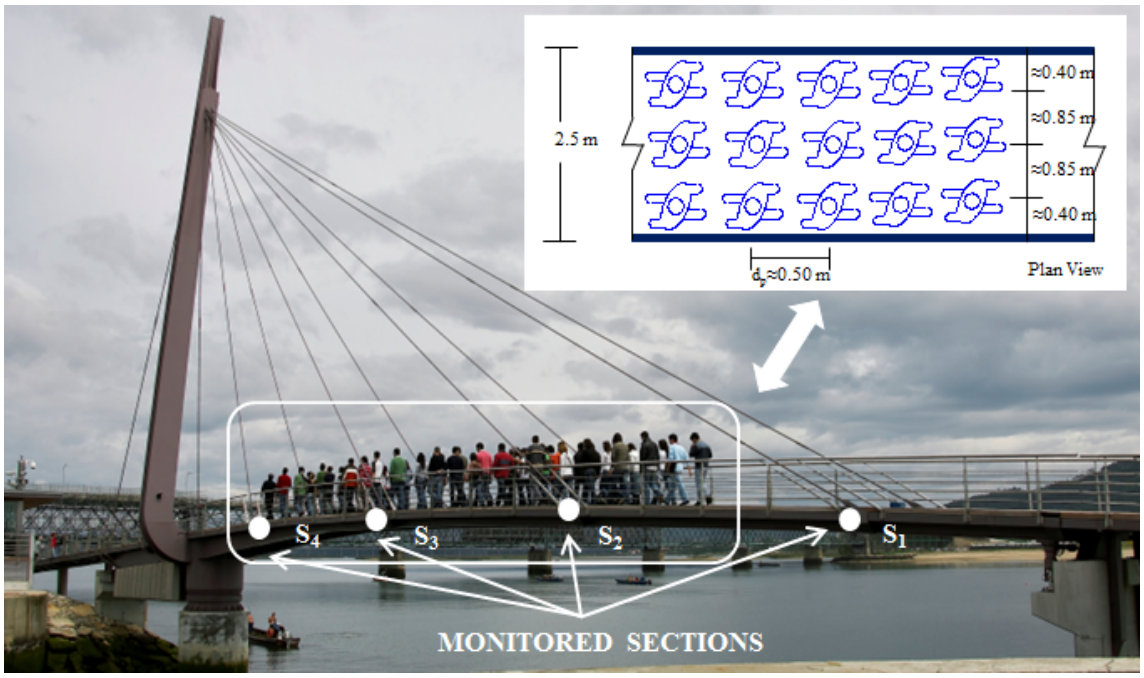

Figure 19. Experimental crowd test at the Viana footbridge.

The results of the experimental crowd test were used additionally to validate the performance of the proposed crowd-structure model in vertical direction.

5.5. Establishing a search domain for the parameters of the pedestrian-structure model.

Two search domains (modal parameters of the pedestrian-structure interaction model and dynamic load coefficients of the pedestrian walking force) were considered in order to reduce the uncertainties of the estimated values of the considered parameters and thus prevent an ill-conditioned inverse problem.

1st Search domain: Modal parameters of the pedestrian-structure interaction model.

According to Table 7, the minimum and maximum values of the parameters of the passive pedestrian models allow defining the search domains for the estimation of the modal parameters of the pedestrian-structure interaction model. The knowledge of the physical problem suggests increasing the above limits in order to take into account the following factors: (i) a reduction of the damping and stiffness of the pedestrian associated with its movement in the lateral direction and (ii) the change in the human body mass distribution between the active and passive states. So, the following search domain was established for the estimation of the modal parameters of the pedestrian-structure interaction model.

- Vertical/lateral pedestrian sprung mass, $m_{a,ver}$ and $m_{a,lat} \in [80-100]\%$.
- Vertical/lateral pedestrian damping ratio, $\zeta_{p,ver}$ and $\zeta_{p,lat} \in [10-69]\%$.
- Vertical/lateral pedestrian natural frequency, $f_{p,,ver}$ and $f_{p,,lat} \in [1-10.43]$ Hz.

2nd Search domain: Walking pedestrian force.

Similarly, according to Table 2, the minimum and maximum values of each dynamic load coefficient allow establishing a search domain for their experimental estimation. In order to take into account that the estimation of these parameters will be performed from measurements carried out on a real footbridge, the above mentioned search domain has been extended.

Thus the following search domains were adopted (vertical and lateral direction):

Vertical Walking Pedestrian Force

- First vertical dynamic load coefficient, $\alpha_{1,ver} \in [0.00 - 0.45]$.
- Second vertical dynamic load coefficient, $\alpha_{2,ver} \in [0.00 - 0.20]$.

Lateral Walking Pedestrian Force

- First lateral dynamic load coefficient, $\alpha_{1,lat} \in [0.00 - 0.10]$.
- Second lateral dynamic load coefficient, $\alpha_{2,lat} \in [0.00 - 0.10]$.
- Third lateral dynamic load coefficient, $\alpha_{3,lat} \in [0.00 - 0.10]$.
- Second lateral phase shift $\varphi_{2,lat} = 0$ or 90^{o}
- Third latera phase shift $\varphi_{3,lat} = 0$ or 90^{o}

5.6. Parameter identification of the pedestrian-structure interaction model: vertical direction.

For the estimation of the parameters of the TDOF-system (*Koh and Perry, 2010*), an inverse dynamic problem was solved (**Paper B**), as it has been described previously. As objective function the relative differences between the experimental and numerical vertical accelerations in four sections of the footbridge were considered. As optimization method, genetic algorithms have been used. The experimental vertical accelerations correspond to the denoised measurements of the above described pedestrian test. The numerical vertical accelerations have been obtained from the implementation of the proposed pedestrian-structure interaction model on the updated finite element model of the Viana footbridge. Figure 20 illustrates the layout of the identification procedure. Six parameters were adopted as design variables:

(i) the first two VDLF that characterize the pedestrian walking force.

(ii) the three modal parameters (pedestrian sprung mass, pedestrian damping ratio and pedestrian natural frequency) that govern the behaviour of the TDOF-system.

(iii) a time lag that allows adjusting the beginning of the crossing of the pedestrian between the experimental and numerical accelerations.

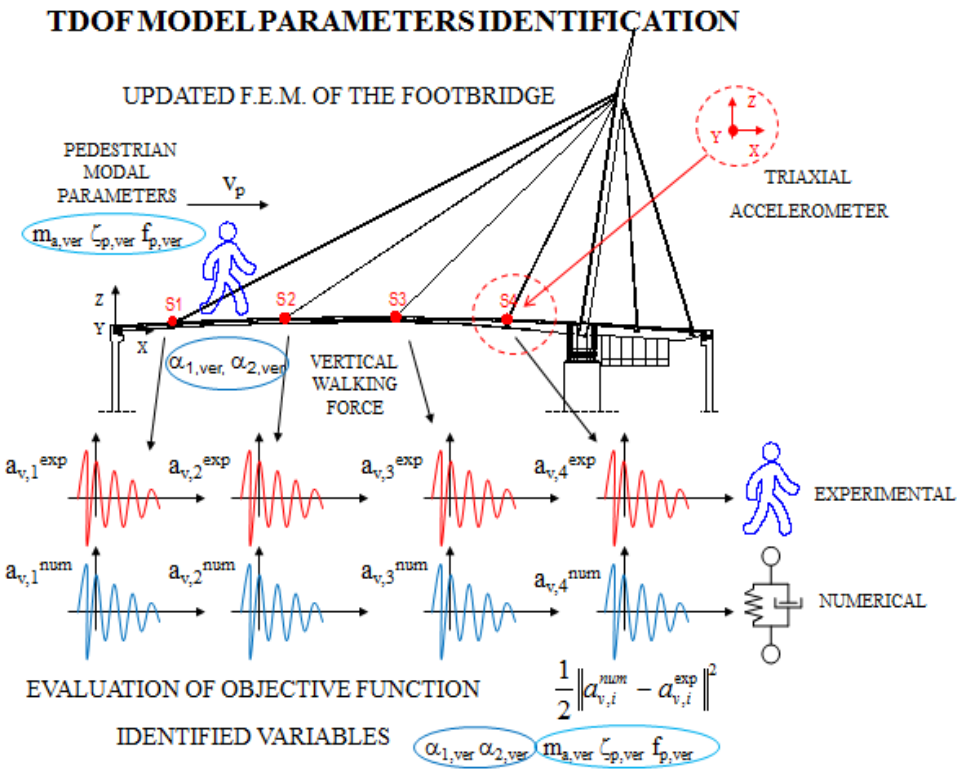

Figure 20. Layout of the parameters identification procedure of the proposed TDOF-system in vertical direction.

For each series, a generation of 1000 individuals has been defined. Each individual modifies, according to the rules of genetic algorithms, the values of its components in order to minimize the defined objective function. The results of the estimation process are summarized in **Paper B**, showing the different estimated parameters versus the pedestrian step frequency. However, due to the number of pedestrians used during the pedestrian test, only a global mean value, μ, and a standard deviation, σ, have been determined $N(\mu,\sigma)$ for each parameter. For the proposed pedestrian-structure model, the following Gaussian distributions have been obtained.

- First VDLF, $\alpha_{1,ver}$, $N(0.237,0.04)$.

- Second VDLF, $\alpha_{2,ver}$, $N(0.043,0.004)$.

- Vertical pedestrian sprung mass, $m_{a,ver}$, $N(87.139,3.809)$ %.

- Vertical pedestrian damping ratio, $\zeta_{p,ver}$, $N(41.44,9.776)$ %.

- Vertical pedestrian natural frequency, $f_{p,ver}$, $N(2.933,0.728)$ Hz.

The proposed values are inside the range, established by *Shahabpoor et al.* (2013) and have a good correlation with a previous study reported in **Paper A**.

Figure 21 illustrates the vertical pedestrian walking force obtained from the proposed identification procedure. The maximum and minimum enveloped values of the vertical forces shown in Figure 2 are also represented.

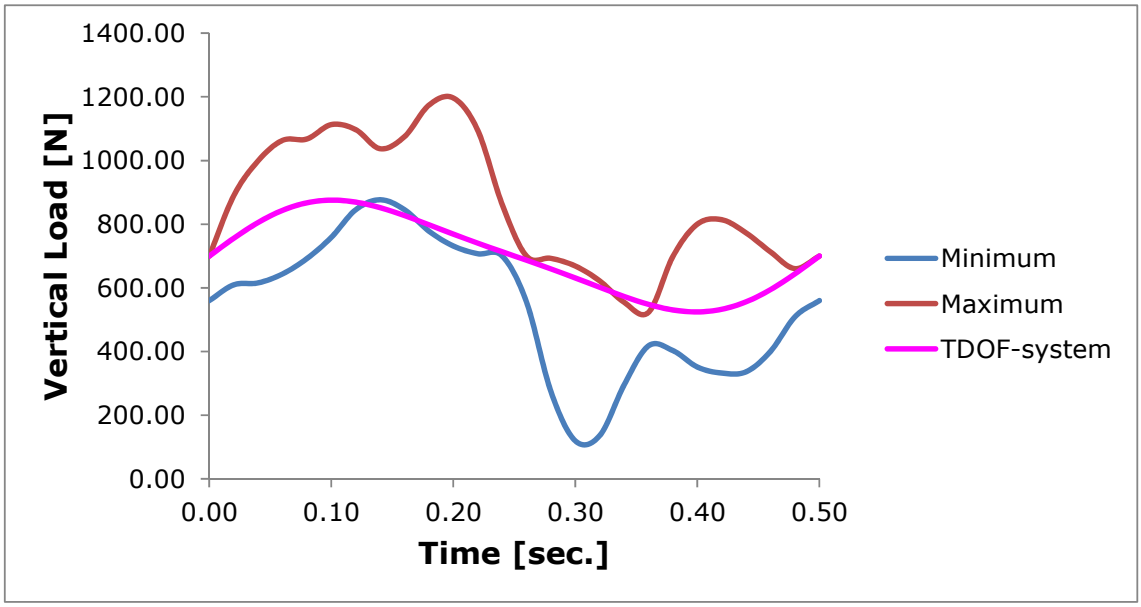

Figure 21. Vertical pedestrian walking force according to the TDOF-system.

5.7. Parameter identification of the pedestrian-structure interaction model: lateral direction.

For the estimation of the modal parameters of the TDOF-system in lateral direction (*Koh and Perry, 2010*), a first inverse problem was solved (**Paper E**), as it was described previously. As objective function the relative differences between the experimental and numerical first lateral natural frequency of the footbridge during the crossing of a group of 50 pedestrians at different step frequencies was considered. As optimization method, genetic algorithms have been used again. In order to determine experimentally the first natural lateral frequency of the footbridge under the crossing of the group of pedestrians, just the forced vibration response of the structure was considered. Only the records at section S_2 (higher modal deflection) were considered. The selected signal was denoised, filtered and processed again by CWT. The maximum value of the wavelet coefficients, in the filtered range of frequencies, was then correlated with the first lateral natural frequency of the structure. This result was validated by the estimation of the natural frequency through the power spectral density of the above signal obtained according to the Peak-Picking method (*Magalhães and Cunha, 2011*). On the other hand, the numerical first lateral natural frequency was obtained from the implementation of the proposed pedestrian-structure interaction model on the updated finite element model of the Viana footbridge. For the determination of the numerical natural frequencies, the classical formulation of the pedestrian-structure interaction model was transformed to the state-space formulation which makes easier the determination of these magnitudes. Finally, the adjustment process allowed obtaining an estimation of the modal parameters of the pedestrian-structure interaction model. The considered values are inside the range established by *Shahabpoor et al.* (2013), that characterizes the modal properties of pedestrian-

structure interaction model The following Gaussian distributions have been obtained ($N(\mu,\sigma)$, being μ the mean value and σ the standard deviation).

- Lateral pedestrian sprung mass, $m_{a,lat}$, $N(73.216,2.736)$ %.
- Lateral pedestrian damping ratio, $\zeta_{p,lat}$, $N(49.116,5.405)$ %.
- Lateral pedestrian natural frequency, $f_{p,lat}$, $N(1.201,0.178)$ Hz.

Figure 22 illustrates the correlation between experimental and numerical results for the change of first lateral natural frequency of the footbridge induced by the crowd-structure interaction phenomenon. Good agreement between both sets of results is observed, with differences below 0.70 % for all the analysed pedestrian walking frequencies. The first lateral natural frequency corresponding to the empty footbridge is included in Figure 22 for reference.

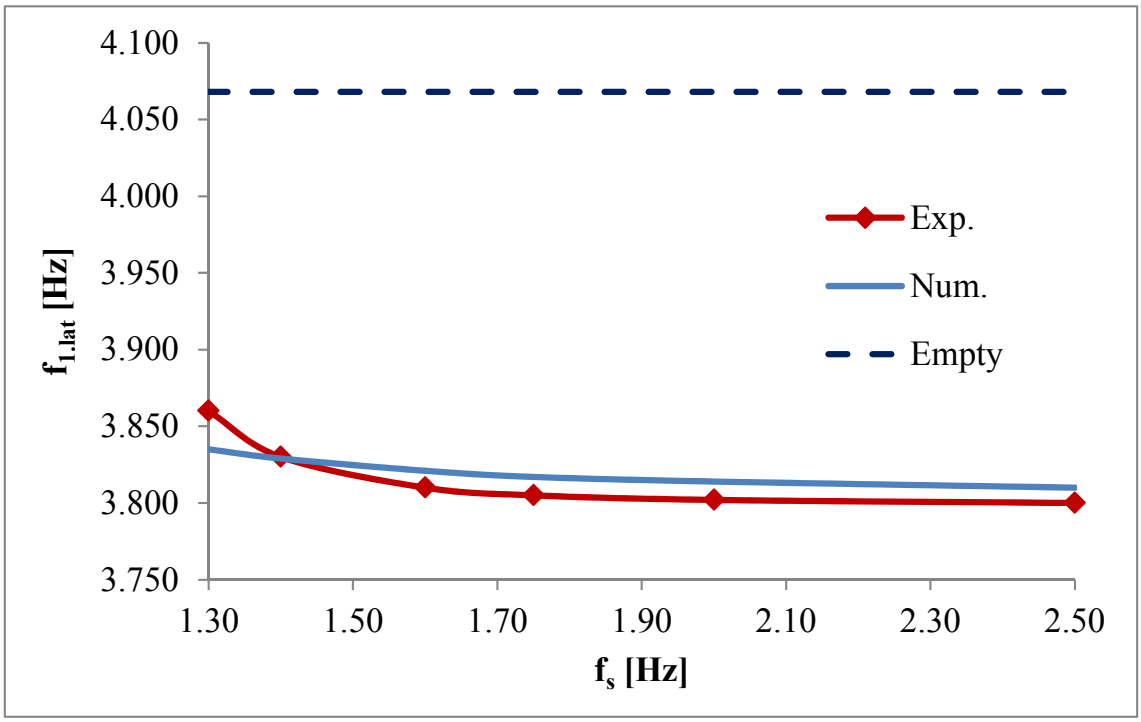

Figure 22. Change of the first lateral experimental (Exp.) and numerical (Num.) natural frequency ($f_{1,lat}$) versus the step frequency [Hz].

From the previous results the following conclusions may be extracted: (i) the stability that the estimated modal parameters present for the different step frequencies, allowing that the proposed crowd-interaction model may be used as a tool for the characterization of the effect of the moving pedestrians on the dynamic behaviour of footbridges in lateral direction and (ii) the good correlation between the experimental and numerical curves (Figure 22) that show the change of the first lateral natural frequency of the footbridge verifies the ability of the proposed model to characterize the pedestrian-structure interaction phenomenon in lateral direction.

For the estimation of the walking pedestrian lateral force of the TDOF-system, a second inverse problem was solved again. In this case, as objective function the mean square error between the experimental and numerical power spectral density obtained from the lateral accelerations recorded in the mentioned four points of the Viana footbridge under the crossing of two pedestrians at controlled step frequencies was considered. The experimental lateral accelerations correspond to the denoised measurements of the above described pedestrian test. The numerical lateral accelerations have been obtained from the implementation of the proposed pedestrian-structure interaction model on the updated finite element model of the Viana footbridge.

The experimental and numerical power spectral density has been obtained from these mentioned accelerations. Six parameters were adopted as design variables:

(i) the first three LDLF that characterize the pedestrian walking lateral force.

(ii) the phase shifts of the second and third harmonic that characterize the pedestrian walking lateral force.

(iii) a time lag that allows adjusting the beginning of the crossing of the pedestrian between the experimental and numerical response.

The estimation of the phase shifts has been made in a discrete way, selecting in each case the option that minimizes the objective function. Figure 23 illustrates the layout of the identification process of the pedestrian walking lateral force of the proposed TDOF-system.

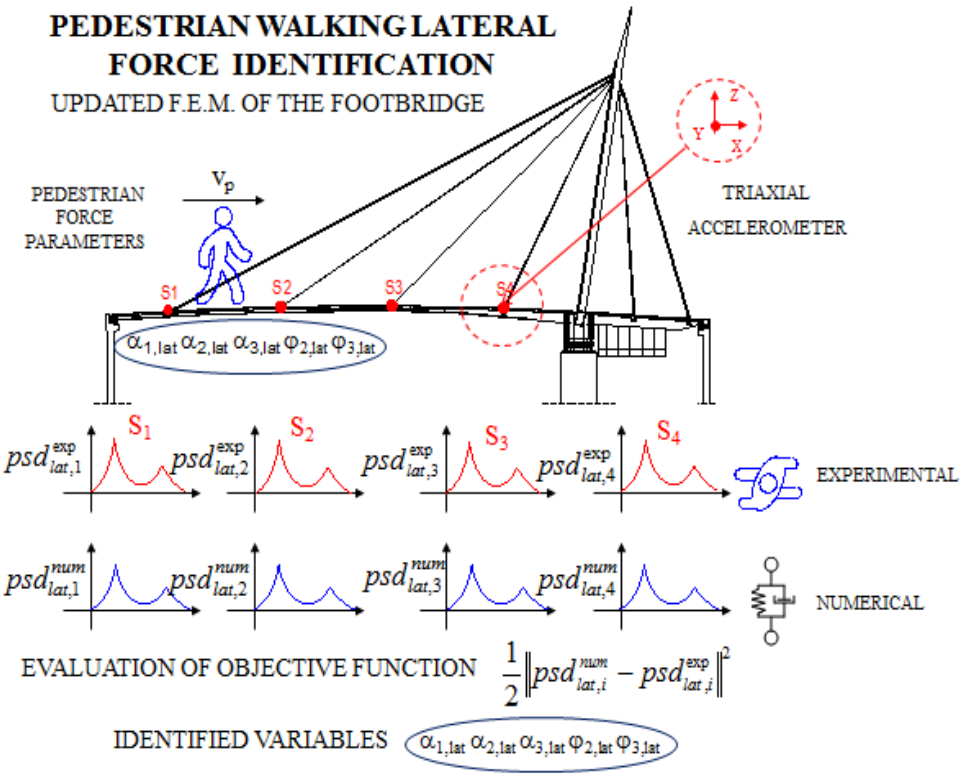

Figure 23. Layout of the walking pedestrian lateral force identification methodology.

In **Paper E**, the results of the estimation process are summarized, showing the different estimated parameters versus the pedestrian step frequency. According to these results, it is possible to obtain a statistical estimation of the design variables that characterize the pedestrian walking lateral force.

- First LDLF, $\alpha_{1,lat}$, $N(0.086,0.017)$.
- Second LDLF, $\alpha_{2,lat}$, $N(0.094,0.009)$.
- Third LDLF, $\alpha_{3,lat}$, $N(0.040,0.019)$.
- Second lateral phase shift $\varphi_{2,lat} = 0$ º.
- Third lateral phase shift $\varphi_{3,lat} = 0$ º.

Figure 24 illustrates the lateral pedestrian walking force obtained from the proposed identification procedure. The maximum and minimum enveloped values of the lateral forces shown in Figure 2 are also represented.

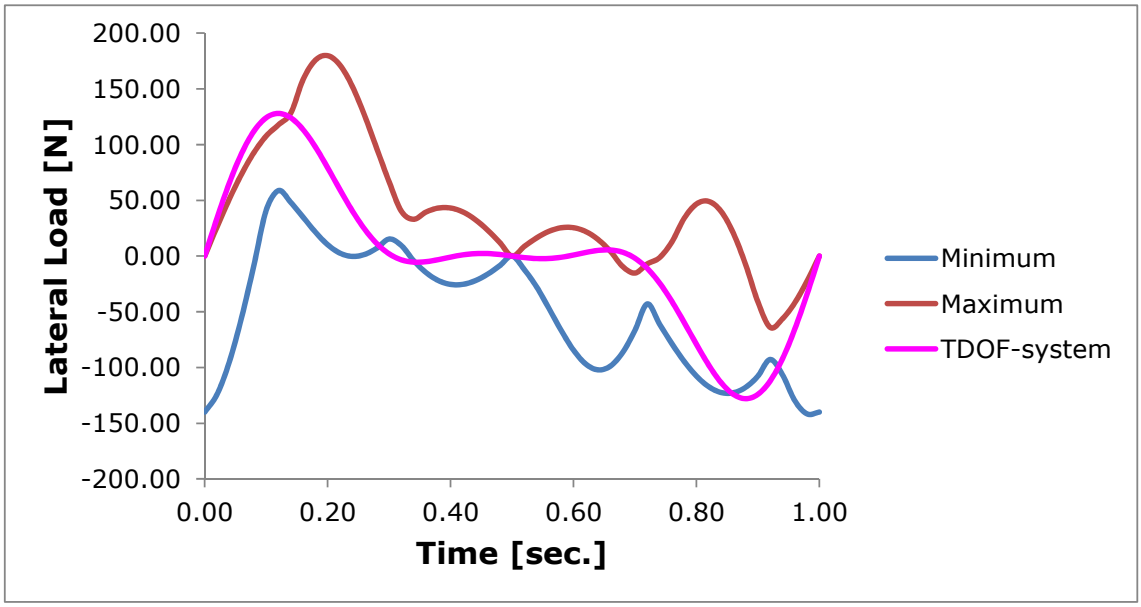

Figure 24. Lateral pedestrian walking force according to the TDOF-system.

For the generation of the pedestrian flows of the crowd-structure interaction model in both directions, the above Gaussian distributions were considered.

6. Validation and main results of this Thesis.

Once obtained the parameters of the proposed TDOF-system in both directions, the definition of the proposed model is complete. The proposed model is validated in this section by correlating the experimental and numerical dynamic response of two real footbridges under the effects induced by the pedestrian action. In vertical direction (**Paper B**), the proposed model was implemented to analyze the dynamic response and the change of the first vertical natural frequency of the Viana footbridge under the previously described crowd test. In lateral direction (**Paper E**), the proposed model was implemented to analyze the lateral lock-in phenomenon on Pedro e Inês footbridge (Coimbra, Portugal), including the estimation of its dynamic response and the change of its first lateral natural frequency due to the pedestrian action.

6.1. Analysis of the change of the modal properties of the Viana footbridge.

The validity and applicability of the proposed crowd-structure interaction model in vertical direction is assessed through its practical application to the following case study (**Paper B**). From the forced recorded response of the previously mentioned crowd test, the experimental analysis of the change of the first vertical natural frequency of the structure, due to the crossing of the group of pedestrians at different step frequencies, was determined. Figure 26 illustrates the experimental analysis of the change of the first vertical natural frequency of the Viana footbridge. Subsequently, the crowd-structure interaction model has been applied to the updated finite element model in order to obtain, first, the vertical numerical acceleration at the mentioned sections and, later, to analyse numerically the change of the first vertical natural frequencies of the footbridge due to the presence of the pedestrians.

The assessment of its performance has been done by correlating the above experimental results with the numerical estimations predicted by the model. For each considered step frequency ten generations of groups with 50 pedestrians were simulated. The number of pedestrians in phase in each new simulation was determined by the evaluation of the parameter ϕ_p. The desired velocity, v_d, of each pedestrian was assigned according to Eq.(5). A pedestrian mass of 70 kg has been considered according to the French code (*Setra, 2006*). As initial spatial distribution of the pedestrians, a rectangular grid was selected, considering an initial distance among pedestrians $d_p = 0.50$ m with an equidistant distribution in the width of the deck. The selected time step is $\Delta t = 0.01$ sec. The numerical vertical acceleration (for three of the 50 pedestrian generations) at section S_2 of the footbridge, for a step frequency of 1.60 Hz, is shown in Figure 25.

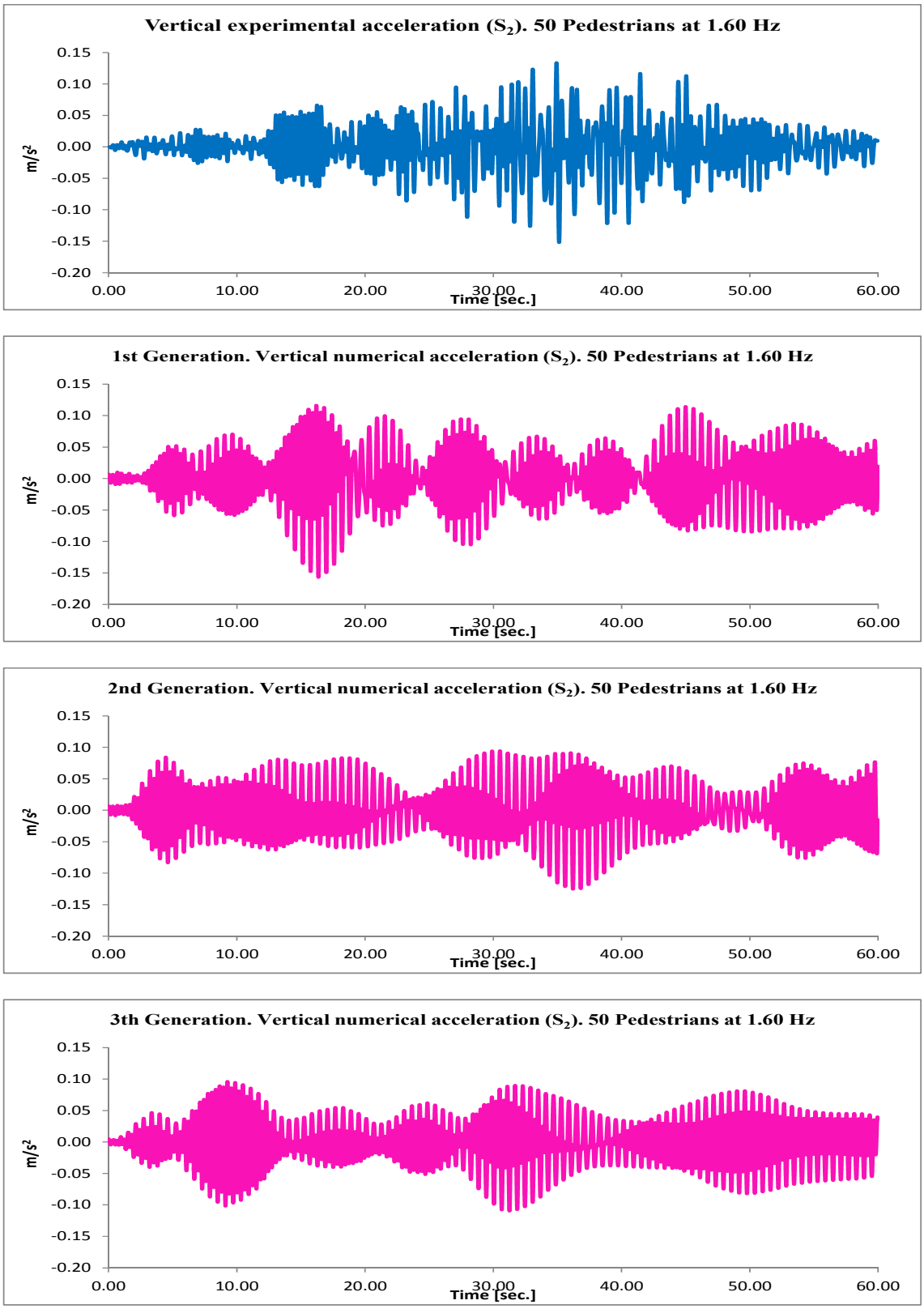

Figure 25. Experimental versus numerical acceleration (three generations) at section S_2 of Viana footbridge under a group of 50 pedestrians (walking frequency of $f_s = 1.60$ Hz).

As Figure 25 shows, the correlation between the experimentally recorded vertical acceleration and the numerically estimated values is adequate, in terms of both the value of the maximum acceleration and its temporal variation.

Finally, the numerically estimated vertical acceleration at section S_2 of the footbridge under a group of 50 pedestrians for different step frequencies was used to identify the first natural frequency of the structure, following the procedure described in **Paper B**. Figure 26 illustrates the correlation between experimental and numerical results for the change of the first vertical natural frequency of the footbridge induced by the crowd-structure interaction phenomenon. The numerical estimation of the change of the first vertical natural frequency was obtained from the mean values of ten simulations for each step frequency. Good agreement between both sets of results is observed, with differences below 1.50 % for all the analysed pedestrian walking frequencies. The first vertical natural frequency corresponding to the empty footbridge is included in Figure 26 for reference.

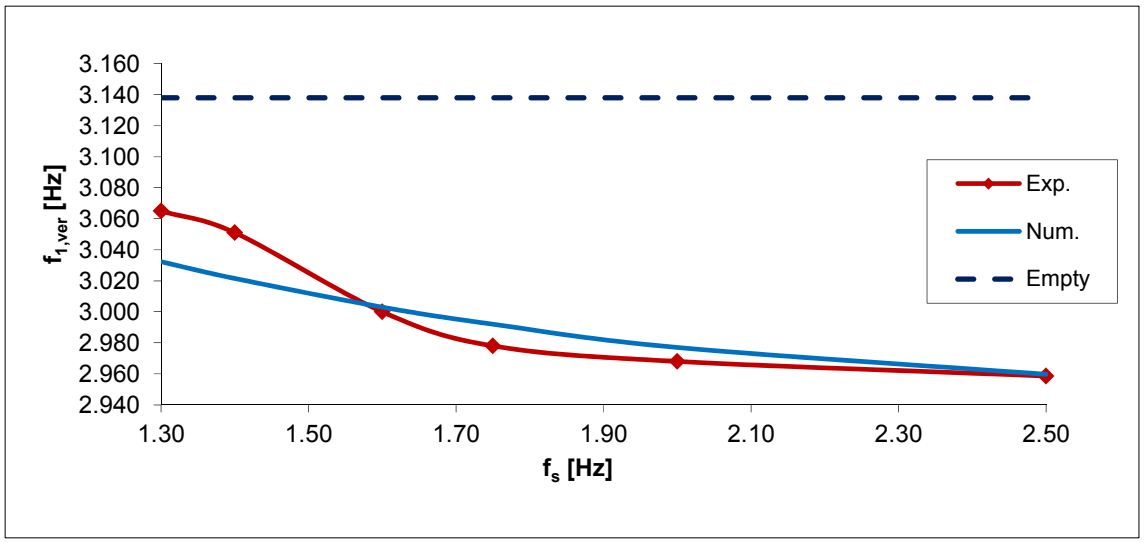

Figure 26. Change of the first vertical, $f_{1,ver}$ [Hz], experimental (Exp.) and numerical (Num.) natural frequency versus the step frequency f_s [Hz].

6.2. Analysis of the lateral lock-in phenomenon on the Pedro e Inês footbridge.

The Pedro e Inês footbridge is located at Coimbra (Portugal). The total length of the structure is 274.5 m, configured by one central arch of 110 m, two lateral semi-arches of 64 m and two transition spans of 30.5 and 6 m (Figure 27). The main feature of the footbridge is the anti-symmetrical configuration of the deck and the arches with respect to the longitudinal axis of the structure. The deck is a concrete-steel composite box-girder with a variable width between 4 and 8 m, what generates a panoramic square at mid-span of the footbridge (Figure 28.a). From its design phase, the numerical studies developed about the footbridge indicated that the structure was prone to vibrations induced by pedestrians in lateral direction. This fact motivated the development of a precise and detailed work for the experimental assessment of its dynamic response and the implementation of a control system in order to guarantee an adequate comfort level for the footbridge.

This work was performed and reported by *Caetano et al.* (2010) and its results have been used in this Thesis in order to validate the proposed crowd-structure interaction model in lateral direction.

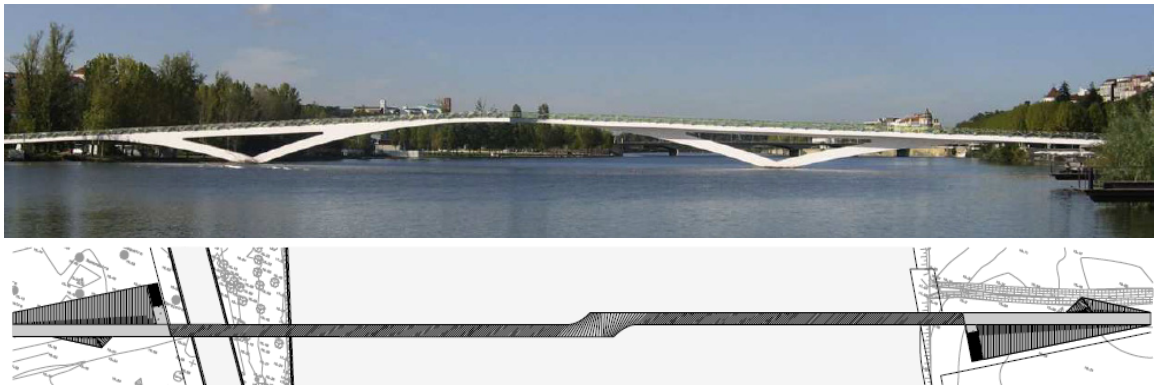

Figure 27. Elevation and plan of the Pedro e Inës footbridge (Caetano et al., 2010).

The footbridge presented a first lateral vibration mode with an experimental natural frequency of 0.91 Hz and an associated damping ratio of 0.55 % that was easily excited by the pedestrian flows. In order to determine experimentally the number of pedestrians that originates the lateral lock-in phenomenon an experimental test was performed. Subsequently, in order to validate the performance of the proposed crowd-structure model, an experimental and numerical analysis of the lateral lock-in phenomenon on the Pedro e Inês footbridge has been correlated. The analysis focused on the beginning of the instability phenomenon, as it is the situation where the effect of the modal parameters of the pedestrians has more influence in the dynamic behaviour of the structure (*Dallard et al., 2001*). The numerical lateral lock-in simulation is obtained from the implementation of the proposed crowd-structure interaction model on an updated finite element model of the Pedro e Inês footbridge reported in the literature (*Caetano et al., 2010*).

Figure 28. a) Perspective of the footbridge and b) experimental lateral lock-in pedestrian test on this footbridge (Caetano et al., 2010).

In the experimental lateral lock-in test, the lateral acceleration, a_{lat}, at mid-span of the footbridge under the crossing of different group of pedestrians was recorded (Figure 28.b). A graphical representation of the maximum lateral acceleration at this position versus the number of pedestrians on the footbridge (Figure 29) allows identifying the instability situation associated with the lateral lock-in phenomenon. As it is reported in the literature (*Caetano et al., 2010*) and it is illustrated in Figure 29 the number of pedestrians that originates the beginning of the lateral lock-in phenomenon is around 75.

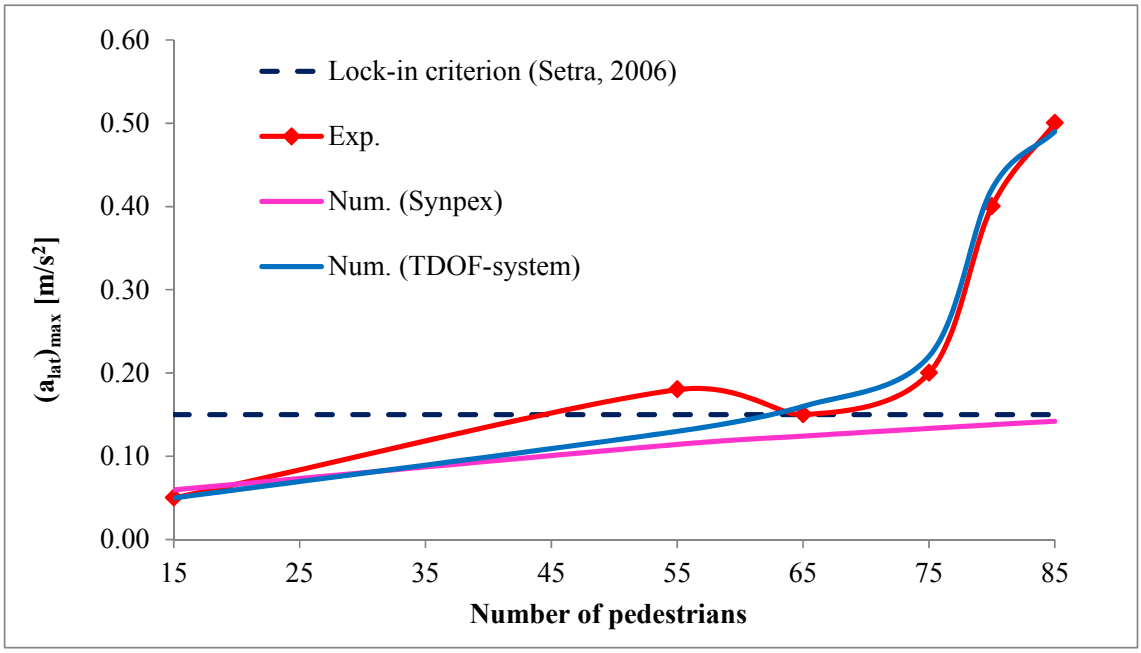

Figure 29. Experimental (Caetano et al. 2010) and numerical variation of the maximum lateral acceleration, $(a_{lat})_{\max}$, at mid-span versus the number of pedestrians.

Subsequently, a numerical lateral lock-in analysis based on the proposed crowd-interaction model was performed. Each considered group of pedestrians was simulated considering as initial spatial distribution a rectangular-shaped grid with an initial distance among pedestrians $d_p = 0.50$ m and a equidistant distribution in the width of the deck. The coordinates of the considered lateral vibration modes of the structure were considered from the results provided by the literature (*Caetano et al. 2010*). In order to account for the change of the structural damping of the footbridge according to its vibration level a parabolic function has been established based on the results obtained by Georgakis and Jorgesen (*Georgakis and Jorgesen, 2014*) in a laboratory footbridge. The range of variation of the damping ratio was comprised between the experimental value obtained in the previously mentioned free vibration test and the limit value under strong vibrations proposed by the more recent international standards (*Butz et al., 2007*; *Setra, 2006*). The maximum numerical lateral acceleration at mid-span versus the number of pedestrians on the footbridge is shown in Figure 29. As Figure 29 shows, the correlation between the experimental lateral maximum accelerations and the numerically estimated maximum values are adequate. Additionally, the estimation of the numerical maximum acceleration obtained applying the methodology proposed by the more

recent international standards *(Butz et al., 2007*; *Setra, 2006*) is shown in Figure 29. The proposed model allows obtaining a more accurate numerical analysis of the lateral lock-in phenomenon than the considered standards. The lateral lock-in criterion established by French standards (*Setra, 2006*) is also illustrated for reference in Figure 29.

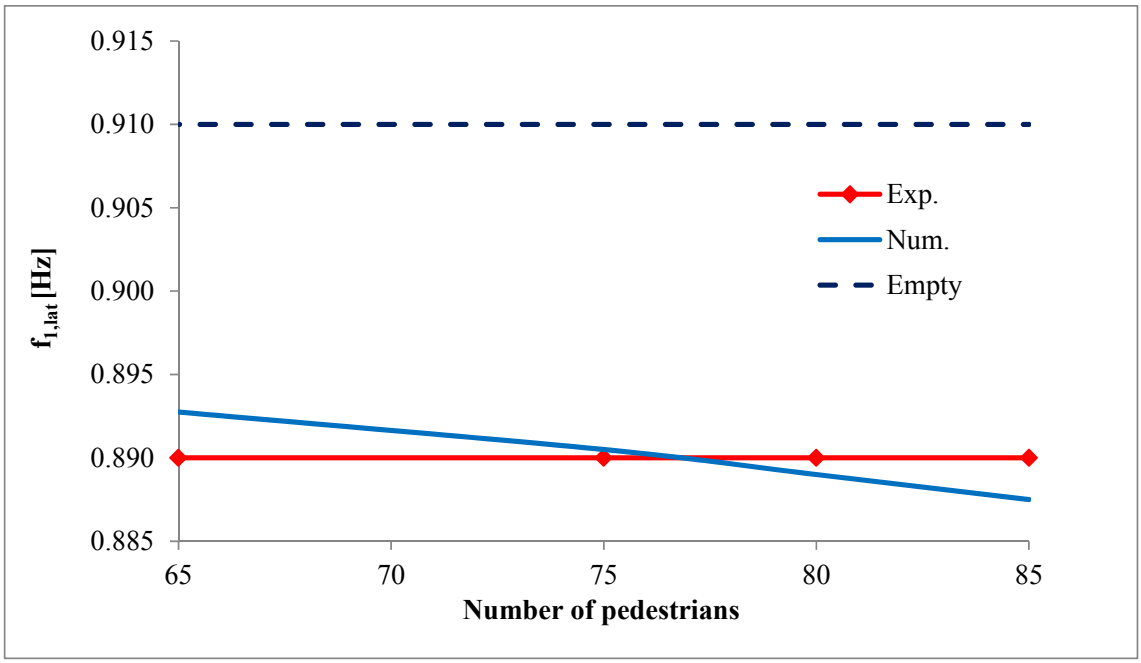

Figure 30. Experimental (*Caetano et al., 2010*) and numerical variation of the first lateral, $f_{1,lat}$, natural frequency of the footbridge versus the number of pedestrians.

Finally, the first lateral numerical natural frequency of the footbridge during the occurrence of the lateral lock-in phenomenon was obtained and it is shown in Figure 26. The experimental first lateral numerical natural frequency (*Caetano et al., 2010*) is also shown in Figure 30. Good agreement between both sets of results is observed, with differences below 0.35 % in the studied range of the number of pedestrians. Additionally, the value of the first lateral natural frequency corresponding to the empty footbridge is illustrated for reference (Figure 30).

7. Conclusions and future research.

7.1 Conclusions.

In this work, a new crowd-structure interaction model has been presented. The proposed model has been validated through the correlation between the experimental and numerical dynamic responses of two real footbridges under the pedestrian action. The proposed model is organized in two sub-models: (i) a pedestrian-structure interaction and (ii) a crowd sub-model. The pedestrian-structure interaction sub-model is defined in terms of a TDOF-system, with sprung and unsprung masses, whose parameters have been estimated experimentally from the results of two experimental tests conducted on the Viana footbridge (Viana do Castelo, Portugal).

As identification technique the solution of an inverse dynamic problem has been utilized, minimizing an objective function defined as the mean square differences between an experimental and numerical magnitude. The estimation of the parameters of the model has been limited to vertical and lateral direction since there are few reported cases of vibratory problems in longitudinal direction.

In vertical direction, the experimental and numerical accelerations on four points of the Viana footbridge under the crossing of two pedestrians at controlled step frequencies have been considered as objective function.

In lateral direction, the identification process has been divided in two steps. In the first step, the modal parameters of the TDOF-system has been estimated considering as objective function the mean square error between the first experimental and numerical lateral natural frequency of the Viana footbridge under the crossing of a group of fifty pedestrians at different controlled step frequencies. Subsequently, in the second step the walking pedestrian lateral force of the proposed model is estimated considering as objective function the mean square differences between the experimental and numerical power spectral density obtained in four points of the Viana footbridge under the crossing of the two mentioned pedestrians.

For the minimization of the above objective functions, as global optimization method, the genetic algorithms have been used in all the cases. The estimated parameters are within the range recommended by previous works in the literature.

The crowd sub-model is defined in terms of a multi-agent model based on the relationships established by the social force model. The interaction between the two sub-models is achieved by imposing two behavioural conditions, a comfort and lateral lock-in thresholds. If the vertical or lateral accelerations experienced by each pedestrian are above certain acceleration limits, the affected pedestrian modifies his step velocity. Additionally, if the lateral accelerations exceed the limit established by the French standard in order to characterize the lateral lock-in phenomenon, the affected pedestrian synchronizes his/her frequency step and phase shift with the movement of the deck.

The proposed model is formulated under the following hypothesis: (i) the parameter of the pedestrian-structure interaction model are assumed constant, so that they do not vary according to the step frequency of each pedestrian, (ii) the

dynamic effects associated to the variation of the pedestrian velocity along time are neglected, and (iii) the direct resolution of the interaction problem has been considered for just the walking action.

A remarkable feature of the model is that it permits an accurate analysis of the change of the dynamic properties of the structure induced by pedestrian flows, being this a key aspect for improving both the numerical estimation of the dynamic response of footbridges under pedestrian action and the efficiency of the damping devices used to control vibratory problems.

In order to validate the proposal, two case studies have been presented. As application in vertical direction, the experimental and numerical change of the first vertical natural frequency of Viana footbridge under a group of 50 pedestrians has been analysed in detail. As application in lateral direction the experimental and numerical analysis of the lateral lock-in phenomenon on Pedro e Inês footbridge (Coimbra, Portugal) has also been performed.

Although the results obtained from the proposed model are adequate, with an excellent correlation between the experimental and numerical results, further studies are recommended in order to better characterize the parameters that define the crowd-structure interaction model. Additional pedestrian tests, including different pedestrians on different footbridges, would also be needed in order to study the sensitivity of the modal parameters of the pedestrian-structure model versus the step frequency and in order to evaluate experimentally the magnitude of the social forces.

7.2. Future research.

Several lines of work may be generated from the subjects treated in this Thesis. This work constitutes a good basis in order to develop the following research lines:

- (i) In order to generalize the use of the crowd-structure model to the longitudinal direction, the estimation of the parameters of the TDOF-system in that direction would be required.

- (ii) Further studies might be conducted in order to estimate more accurately the value of the phase shift parameter ϕ_p, and analyze in detail: (i) its dependence with the damping ratios of the vibration modes of the structure; and (ii) its variation according to the vibration level experienced by each pedestrian.

- (iii) In order to study in more detail the inter and intra-subject variability of the parameters of the pedestrian-structure interaction model, the proposed methodology might be applied to other group of pedestrians on different types of footbridges. This would allow establishing a more robust statistical distribution of these parameters.

- (iv) An important result obtained from this work is the observed relationship between the parameters of the TDOF-system and the step frequency of the pedestrian. This important issue might be analyzed deeply through the application of the mentioned methodology to other groups of pedestrians on different footbridges.

- (v) The value of the parameters of the social force model utilized in the proposed crowd-structure interaction model was considered from the results reported by different authors. As this behavioral model has a more general use, and not only for pedestrians crossing footbridges, an experimental estimation of these magnitudes under the considered conditions (movement of pedestrian on a footbridge) might be useful in order to improve the accuracy of the crowd sub-model. Additionally, the study of the dependence of these parameters with the step frequency and vibration level of the structure might originate a new research line too.

- (vi) The estimation of the parameters of the TDOF-system has been performed considering as estimator the solution of an inverse dynamic problem formulated as the minimization of a least square problem. However, there are other more complex estimators, as for instance Kalman filtering. In this manner, a possible new research line might be the application of these estimators in order to analyze the variation of the parameters of the TDOF-system according to the estimation method.

- (vii) Currently the design of slender footbridges is conditioned by its dynamic behavior, considering the international standards the pedestrian-structure interaction in a very simplified way. The new approach presented in this work may be used during the design phase of this type of structure in order to minimize its budget. A practical research line might focus on studying the increase of the efficiency in the design of this structure thanks to the implementation of the proposed crowd-structure interaction model.

- (viii) The main advantage of the proposed model is that is allows analyzing the change of the modal properties of the structure induced by the crowd-structure interaction. In this manner, the model is a powerful tool in order to improve the efficiency of external damping devices when their presence is necessary to control the dynamic response of the structure. An interesting research line might be the application of the proposed model for the optimization of the parameters of tuned mass dampers on footbridges. The selection of these magnitudes is strongly influence by the natural frequency of the structure to be controlled and this magnitude, as it has been demonstrated in this work, varies with the pedestrian density on the footbridge.

- (ix) The proposed model allows the definition of the comfort level directly on the pedestrians. It opens a new research line in order to redefine the thresholds that configure each comfort level, focusing on the accelerations experienced by the pedestrians instead of the maximum acceleration achieved on the deck.

Bibliography

Al-Foqaha'a, A.A. (1997). Design Criterion for Wood Floor Vibrations Via Finite Element and Reliability Analyses. *PhD Thesis. Washington State University*.

ANSYS Mechanical Release 15.0.

ARTeMIS Extractor Pro 2015.

Austroads (2012). AGBT Guide to Bridge Technology. Austroads Publications Online.

Bachmann ,H.; Ammann W. (1987). Vibrations in structures Induced by Man and Machines p.174. IABSE.

Bachmann, H., Pretlove, A.J., Rainer, H. (1995). Dynamic forces from rhythmical human body motions, in: Vibration Problems in Structures: Practical Guidelines, Birkhäuser, Basel, 1995, Appendix G.

Barbosa, R., Magalhães, F., Caetano, E. Cunha A (2013). The Viana footbridge: Construction and dynamic monitoring, Bridge Engineering, ICE, Vol. 166, Issue 4, pp. 273-290.

Barker, C. (2002). Some observations on the nature of the mechanism that drives the self-excited lateral response of footbridges. *International Conference on the Design and Dynamic Behaviour of Footbridges*. Paris.

Blanchard J., Davies B.L., Smith J.W. (1977). Design criteria and analysis for dynamic loading of footbridges, in: Proceedings of the DOE and DOT TRRL Symposium on Dynamic Behaviour of Bridges, Crowthorne, UK, pp. 90–106.

Bertram, J.E.A., Ruina, A. (2001). Multiple walking speed-frequency relations are predicted by constrained optimization. Journal of Theoretical Biology, Vol. 209 (4), pp. 445-453.

Brownjohn, J.M.W. (1999). Energy dissipation in one-way slabs with human participation. Asia Pacific Vibration Conference'99. Vol. 1, Nanyang Technological University, 2nd SPIE International Conference on Experimental Mechanics, pp. 155-160.

Brownjohn, J.M.W., Fok, P., Roche, M., Omenzetter, P. (2004). Long span steel pedestrian bridge at Singapore Changi airport part 2: crowd loading tests and vibration mitigation measures. The Structural Engineer 82 (16), pp. 28-34.

Bruno, L., Venuti, F., "Crowd-structure interaction in footbridges: modelling, application to a real case-study and sensitivity analysis". Journal of Sound and Vibration, Vol. 323 (1-2), pp. 475-493. 2009.

BSI, Steel, concrete and composite bridges. Part 2: Specification for loads, BS 5400+2: 2006. British Standards Institution.

Butz, Ch. (2006). Beitrag zur Berechnung fussgängerinduzierter Brückenschuringungen, Schriftenreihe des Lehrstuhls für Stahlbau und Leichtmetallbau der RWTH Aachen Helft 60.

Butz CH., Heinemeyer, CH.; Goldack, A.; Keil, A.; Lukic, M.; Caetano, E.; Cunha, A.. Advanced Load Models for Synchronous Pedestrian Excitation and Optimised Design Guidelines for Steel Footbridges (SYNPEX). RFCS-Research Project RFS-CR-03019. 2007.

Caetano, E., Cunha A., Magalhaes F. Moutinho, C. (2010). Studies for controlling human-induced vibration of the Pedro e Inês footbridge, Portutal. Part 1: Assesment of dynamic behaviour. Engineering Structures, 32: 1069-1081. doi:10.1016/j.engstruct.2009.12.034.

Caetano, E., Cunha A., Magalhaes F. Moutinho, C. (2010). Studies for controlling human-induced vibration of the Pedro e Inês footbridge, Portutal. Part 2: Implementation of tuned mass dampers. Engineering Structures, 32: 1082-1091. doi:10.1016/j.engstruct.2009.12.033.

Carrol, S.P., Owen, J.S,, Hussein, M.F.M. (2012). Modelling crowd-bridge dynamic interaction with a discretely defined crowd. *Journal of Sound and Vibration, 331* (1): 2685-2709. doi:10.1016/j.jsv.2012.01.025.

Cremona, C., Foueriat, J.C. (2002). *Comportement au vent des ponts*. Paris. Presses de l'ecole nationale des Ponts et chaussëes.

Clough R., Penzien J. (1993). Dynamic of Structures. McGraw-Hill, Inc.

Dallard, P.,Fitzpatrick, A.J., Le Bourva, S., Low, A., Ridsill Smith, R., Willford, M., Flint, A. (2001). The London Millenium Footbridge. *The Structural Engineer*, *79*(22): 17-33.

Deutsches Institut Fuer Normung (2003). DIN+Fachbericht 102, Betonbrücken.

Domínguez, J. (2001). Dynamic of high speed train bridges: calculation methods and study of the resonance. Ph. D. Thesis. Escuela Técnica Superior de Ingenieros de Caminos, Canales y Puertos de Madrid (UPM). (In Spanish).

European Committee for Standardization CEN: prEN1991+2:2002, Eurocode 1 – Actions on structures, Part 2: Traffic loads on bridges.

European Committee for Standardization CEN: prEN1995+2:2003, Eurocode 5 – Design of timber structures, Part 2: Bridges.

Falati, S. (1999). The Contribution of Non-structural Component of the Overall Dynamic Behaviour of Concrete Floor Slabs. *PhD Thesis. University of Oxford*.

Foschi, R.O., Neumann, G.A., Yao, F., Folz, B. (1995). Floor vibration due to occupants and reliability based design guidelines. *Canadian Journal of Civil Engineering* Vol. 22 (3) pp- 471–479.

Fox, R., Kapoor M.. Rate of change of eigenvalues and eigenvectors. AIAA Journal, 6:2426-2429, 1968.

Friswell, M.I., Mottershead, J.E.. Finite Element Model Updating in Structural Dynamics. Kluwer Academic Publishers. 1995.

Fujino Y., Pacheco B., Nakamura S. and Warnitchai P. (1993). Synchronization of Human Walking Observed during Lateral Vibration of a Congested Pedestrian Bridge. *Earthquake Engineering and Structural Dynamics, 22*: 741-758.

Georgakis, C., Jorgesen, N.G. (2013). Topics in Dynamics of Bridges, Volume 3: Proceedings of the 31st IMAC. A Conference on Structural Dynamics, 2013. Chapter 4. Change in Mass and Damping on Vertically Vibrating Footbridges Due to Pedestrians. The Society for Experimental Mechanics, Inc.

Gopalakrishnan, S., Mitra, M. (2014). Wavelet Methods for Dynamical Problems. With Application to Metallic, Composite and Nano-Composite Structures. CRC Press.

Heermann, D. W. (1986) Computer simulation methods: in theoretical physics. Springer-Verlag New York, Inc. New York, NY, USA.

Helbing, D., Molnár, P. (1995). Social force model for pedestrian dynamics. Physical Review, 51(5):4282-4286.

Ingólfsson, E.T., Georgakis, C.T. (2011). A stochastic load model for pedestrian-induced lateral forces on footbridges. Engineering Structures, Vol. 33 (12), pp. 3454-3470.

Ingólfsson, E.T., Georgakis, C.T., Ricciardelli, F., Jönsson, J.. (2011) Experimental identification of pedestrian-induced lateral forces on footbridges. Journal of Sound and Vibration, Vol. 330, pp. 1265-1284.

Instrucción de acero estructura (EAE) (2011). Ministerio de Fomento. Madrid (España).

Instrucción de acciones puentes de carretera (IAP-11) (2011). Ministerio de Fomento. Madrid (España).

Instrucción de hormigón estructural (EHE) (2008). Ministerio de Fomento. Madrid (España)

Jones, C.A., Reynolds, P., Pavic, A. (2010). Vibration serviceability of stadia structures subjected to dynamic crowd loads: A literature review. *Journal of Sound and Vibration*, Vol. 330, pp. 1531-1566.

Kerr, S.C. (1998) Human Induced Loading on Staircases. PhD Thesis, Mechanical Engineering Department. University College London.

Instrucción de hormigón estructural (EHE+08) (2008). Ministerio de Fomento. Madrid (España).

LFRD Guide Specifications for Design of Pedestrian Bridges (2009). American Association of State Highway and Transportation Officials. Washington (EEUU).

Low, A. (2008). Soft issues in the design of long span footbridges and cycle bridges. Footbridge 2008. Porto.

Koh Ghee C., Perry M.C. (2010). Structural Identification and Damage Detection using Genetic Algorithms. CRC Press, Taylor&Francis Group.

Macdonald, J.H.C. (2008). Pedestrian-induced vibrations of the Clifton Suspension Bridge, UK. Proceedings of the ICE-Bridge Engineering 161 (2), pp. 69-77.

Macdonald J.H.G. (2008). Lateral excitation of bridges by balancing pedestrians. *Proceedings of the Royal Society*.

Magalhães, F., Cunha, A.. Explaining Operational Modal Analysis with data from an arch bridge. Mechanical Systems and Signal Processing, Invited Tutorial Paper, Volume 25, Issue 5, pp. 1431-1450 , 2011.

Magalhães, F., Cunha, A., Caetano, E., Brincker, R. Damping estimation using free decays and ambient vibration tests. Mechanical Systems and Signal Processing, Volume 24, Issue 5, pp. 1274–1290, July 2010.

Maia N., Silva J. (1997). Theoretical and Experimental Modal Analysis. Instituto Superior Técnico, Portugal, Research Studies Press, LTD.

Matlab R2015a. . http://www.mathworks.com/.

Matsumoto, Y., Griffin, M.J. (2003). Mathematical models for the apparent masses of standing subjects exposed to vertical whole-body vibration. *Journal of Sound and Vibration* Vol. 260 (3) pp. 431-451.

Matsumoto Y., Nishioka, H., Shiojiri, H., Matsuzaki, K. (1978). Dynamic design of footbridges. IABSE Proceedings 1-15.

Meinhardt, C. (2009), Application of tuned mass dampers for bridge deck. *Footbridge Vibration Design*. London. CRC Press Taylor&Francis Group.

Morbiato, T., Vitaliani, R., Saetta, A. (2011). Numerical analysis of a synchronization phenomenon: Pedestrian-structure interaction. *Computers and Structures, 89* (1): 1649-1663. doi:10.1016/j.compstruc.2011.04.013.

Moutinho, C., Cunha, A., Caetano, E. (2010). Analysis and control of vibrations in a stress-ribbon footbridge. *Structural Control and Health Monitoring* 18:619–634. doi:10.1002/stc.390

Nakamura, S. (2004). Model for lateral excitation of footbridges by synchronous walking, *Journal of Structural Engineering, 130*(1): 32-37.

Newland D.E. (2003). Pedestrian excitation of bridges- Recent Results. 10th International Congress on Sound and Vibration, Stockholm, Sweden.

Newland D.E. (2004). Pedestrian excitation of bridges. Proceedings of the Institution of Mechanical Engineers, Part C: *Journal of Mechanical Engineering Science* Vol. 218: 477-492.

Nocental J., Wright S.J. (1999). Numerical Optimization. Springer, New York, USA.

Ontario highway bridge design code (1995) The Highway Engineering Division, Ontario (Canada).

Piccardo, G., Tubino, F. (2008). Parametric resonance of flexible footbridges under crowd-induced lateral excitation. *Journal of Sound and Vibration, 311*(1-2): 353-371.

Racic, V., Pavic, A., Brownjonh, J.M.W. (2009). Experimental identification and analytical modelling of human walking forces: Literature review. *Journal of Sound and Vibration, 326* (1): 1-49. doi:10.1016/j.jsv.2009.04.020.

Rapaport, D.C. (2004). The art of molecular dynamic. Cambridge University Press.

Riccardelli, F., Briatico, C., Ingólfsson, E.T., Georgakis, C. (2007). Experimental validation and calibration of pedestrian loading models for footbridges. *Proceedings of the 2th International Conference on Experimental Vibration Analysis for Civil Engineering Structures*. Porto, 24-26 October.

Riccardelli, F., Pizzimenti, D. (2007). Lateral Walking-induced forces on footbridges. *Journal of Bridge Engineering*. Vol. 12, nº6, pp.677-688.

Ronnquist, A. (2005). .Pedestrian Induced Lateral Vibrations on Slender Footbridges. PhD Thesis. Norwegian University of Science and Technoloy.

Recomendaciones para el proyecto de puentes metálicos para carreteras (RPM-95) (2003). Ministerio de Fomento. Madrid (España).

Schulze, H. (1980). Dynamic effects of the live load on footbridges (in German). Signal und Schiene, Vol. 24, (2), pp. 91-93 and (3) pp. 143-147.

Setra (2006). Guide méthodologique passerelles piétonnes (Technical guide footbridges: Assessment of vibrational behavior of footbridges under pedestrian loading), Setra.

SIA 260 (2003) Basis of structural design. Swiss Society of Engineers and Architects SIA.

Slaich, M. (2005). Guidelines for the Design of Footbridges. Footbridges 2005. Venice.

Shahabpoor, E., Pavic, A., Racic, V. (2013). Modelling effect of pedestrians walking on dynamic properties of structures. IMAC XXXI: A Conference and Exposition on Structural Dynamics, 11-14 February, Orange County, California, USA.

Structures Design Manual for Highways and Railways (2009). The Government of Hong Kong. Special Administrative Region.

Taylor, D. (2003). Damper retrofit of the London Millennium Footbridge, a case study in biodynamic design. In the Proceedings of the 73th Shock and Vibration Symposium, San Diego, California, USA.

Teughels, A., (2003). Inverse Modelling of Civil Engineering Structures Based on Operational Modal Data. Ph. D. Thesis, Katholieke Universiteit Leuven.

Venuti, F., Bruno, L., Bellomo, N. (2007). Crowd dynamics on a moving platform: Mathematical modelling and application to lively footbridges. *Mathematical and Computer Modelling, 45*(3-4): 252-269.

Wolmuth, B., Surtees, J. (2003). Crowd-related failure of bridges. *Civil Engineering*, *156*(3): 116-123.

Xia, H., Zhang, N. (2005). Dynamic analysis of railway bridge under high-speed trains. *Computers and Structures*, Vol. 83 (23-34), pp. 1891-1901.

Young, P. (2001). Improved floor vibration prediction methodologies, ARUP Vibration Seminar.

Zheng, X., Brownjohn, J.M.W. (2001). Modelling and simulation of human-floor system under vertical vibration. Smart Structures and Materials 2001: Smart Structures and Integrated Systems. SPIE.

Zivanovic, S., Pavic, A., Ingolfsson, E. (2010). Modelling spatially unrestricted pedestrian traffic on footbridges. Journal of Structural Engineering, Vol. 136 (10), pp. 1296-1308.

Zivanovic, S., Pavic A., Reynolds P. (2007). Finite element modelling and updating of a lively footbridge: The complete process. Engineering Structures, Vol. 301(1-2), pp. 126-145.

Zivanovic, S., Pavic, A., Reynolds, R. (2005). Vibration serviceability of footbridges under human-induced excitation: a literature review. *Journal of Sound and Vibration, 279* (1-2): 1-74.

PART II

APPENDED PAPERS

II. Appended papers.

Paper A: A direct-pedestrian structure interaction model to characterize the human induced vibrations on slender footbridges

The original version of this paper can be found in

doi: 10.3989/ic.2014.v66.iExtra-1

Journal name: Informes de la construcción

ISI 2014 Classification: Q4 (53/59) Construction and Building Engineering. Impact Factor: 0.273

SCIMAGO 2014 Classification: Q3 (121/215) Civil Engineering SJR: 0.345

ISSN: 0020-0883

Informes de la Construcción
Vol. 66, EXTRA 1, m007
diciembre 2014
ISSN-L: 0020-0883
doi: http://dx.doi.org/10.3989/ic.13.110

A direct pedestrian-structure interaction model to characterize the human induced vibrations on slender footbridges

Un modelo directo de interacción peatón-estructura para caracterizar las vibraciones inducidas por peatones en pasarelas esbeltas

J. F. Jiménez-Alonso(*), A. Sáez(*)

ABSTRACT

Although the scientific community had knowledge of the human induced vibration problems in structures since the end of the 19th century, it was not until the occurrence of the vibration phenomenon happened in the Millennium Bridge (London, 2000) that the importance of the problem revealed and a higher level of attention devoted. Despite the large advances achieved in the determination of the human-structure interaction force, one of the main deficiencies of the existing models is the exclusion of the effect of changes in the footbridge dynamic properties due to the presence of pedestrians. In this paper, the formulation of a human-structure interaction model, addresses these limitations, is carried out and its reliability is verified from previously published experimental results.

Keywords: *Slender footbridges; human induced vibration; pedestrian-structure interaction; dynamic behaviour change.*

RESUMEN

Aunque la comunidad científica tenía conocimiento de los problemas vibratorios inducidos por peatones en estructuras desde finales del siglo XIX, no fue hasta la ocurrencia de los eventos vibratorios acontecidos en la pasarela del Milenio (Londres, 2000), cuando la importancia del problema se puso de manifiesto y se le comenzó a dedicar un mayor nivel de atención. A pesar de los grandes avances alcanzados en la caracterización de la fuerza de interacción peatón-estructura una de las principales deficiencias de los modelos existentes es la exclusión del cambio en las propiedades dinámicas de la pasarela por la presencia de peatones. En este artículo, se presenta la formulación de un modelo de interacción peatón-estructura que intenta dar respuesta a dichas limitaciones, y su validación a partir de resultados experimentales previamente publicados por otros autores.

Palabras clave: Pasarelas esbeltas; vibraciones inducidas por seres humanos; interacción peatón-estructura; modificación de comportamiento dinámico.

(*) University of Seville (España).
Persona de contacto/*Corresponding author*: jfjimenez@us.es (J. F. Jiménez-Alonso)

Cómo citar este artículo/*Citation:* Jiménez-Alonso, J. F., Sáez, A. (2014). A direct pedestrian-structure interaction model to characterize the human induced vibrations on slender footbridges. *Informes de la Construcción*, 66(EXTRA-1): m007, doi: http://dx.doi.org/10.3989/ic.13.110.

Recibido/*Received*: 19/07/2013
Aceptado/*Accepted*: 19/11/2013

1. INTRODUCTION

The phenomenon of interaction between pedestrians and bridges is known since, at the end of the 19th century (1), a group of 60 soldiers excited, under their step, a bridge located in the British town of Broughton. Although the scientific community did not stop studying this issue, it was the occurrence of the phenomenon happened in the Millennium Bridge (London) that stressed the importance of the problem and led to a higher level of attention (2). In most cases, the effect that the pedestrians induce on the footbridge has been idealized like a moving variable force on the structure (3). The variability of the above mentioned load tries to have in consideration the variation of the level of pressures that takes place between the pedestrian and the deck during the phenomenon of the step. However, in all these models, either the effect that the pedestrians have on the dynamic characteristics of the structure is neglected, or such effect is considered by means of very simplified finger rules. Consequently, these models do not incorporate appropriately the energetic exchange that takes place between both systems during the step of the pedestrian flows on the structure. Nevertheless, in the existing publications (3) there are clear indications about the importance of the dynamic interaction phenomena, with evidence that both the frequencies and the modes of vibration of the structure are affected by the step of pedestrian groups. In the case of structures subjected to large pedestrian flows, the correct estimation of the change of their dynamic properties due to the pedestrian crossing is very important during the design phase, in order to adjust as much as possible the natural frequencies of the structure outside the range of pedestrian step frequencies and, in the case of an intervention on an existing footbridge, in order to improve its comfort level (4) (5).

In the present work, a methodology for the correct characterization of the whole dynamic behavior is proposed, by implementing a human-structure interaction model with three degrees of freedom, in order to characterize the movement of the gravity center of the pedestrian in the three spatial directions. The problem of energetic exchange is addressed in a direct form, realizing the modal projection of the coordinates in contact between the pedestrian and the structure, and maintaining the physical coordinates of the gravity center of the pedestrian. The model considers, in the same way, the local effect of the step by means of the modal projection of the corresponding interaction force.

This procedure of resolution allows, on the one hand, to uncouple the equations of the dynamic system that governs the behavior of the structure, thus facilitating the effective application of the model from the modal characteristics of the footbridge, as obtained from any commercial software based on the finite element method; and on the other hand, it allows to estimate in a direct form both the dynamic characteristics of the structure during the pedestrian step, as well as the components of the pedestrian center of gravity acceleration. Furthermore, additional parameters, such as the sign of pedestrian damping introduced into the system, may be included in the model. Finally, a validation example of the proposed model is presented, where the change of the dynamic behaviour of a real laboratory footbridge during a variable flow of pedestrians is favorably compared with the model predictions.

2. ANALYSIS OF CURRENT STANDARDS

Currently, the most advanced international codes about the dynamic behaviour of slender footbridges (4) (5) determine that, in a wide way, if the natural frequencies of the structure is in the range of pedestrian walking step frequency (1.25-2.30 Hz for vertical vibrations and 0.50-1.20 Hz for horizontal vibrations) the acceleration, in that direction, needs to be determined and checked against acceleration limits (Table 1) to guarantee an appropriate comfort level for each design scenario. Furthermore, to avoid lateral synchronization the acceleration in this direction must be below 0.10-0.15 m/s^2.

The design scenario is established by the expected pedestrian traffic (Table 2) and the situation or importance of the structure. The comfort level is determined by the owner of the structure, and normally a medium comfort level must be guaranteed for all traffic classes, except for pedestrian densities above 1.00 P (Person)/m^2 where a minimum comfort is acceptable.

The pedestrian induced action is represented as an oscillatory distributed load $p(t)$, defined as:

$$p(t) = G \cdot \cos(2 \cdot \pi \cdot f \cdot t) \cdot n'_p \cdot \psi \quad [1]$$

where:

G, is the considered component of the step force (G=280 N vertical, 140 N longitudinal and 35 N lateral) (4) (5).
f, is the natural frequency of the structure under consideration.
n'_p, is the equivalent pedestrians number, defined by

$$n'_p = 10.80 \cdot \sqrt{\zeta \cdot n_p} \quad \text{for traffic classes TC1-TC3 or} \quad [2]$$

$$n'_p = 1.85 \cdot \sqrt{n_p} \quad \text{for traffic classes TC4-TC5.} \quad [3]$$

ψ, is the reduction coefficient that takes into account the probability that the footfall frequency approaches the natural frequency under consideration.
ζ, is the structural damping ratio.
n_p, is the number of the pedestrians on the loaded surface S ($n_p = S \cdot density$).
S, is the loaded surface that depends on the shape of the normal mode under consideration.

Table 1. Defined comfort classes with limit acceleration ranges (5).

Level	Degree	Vertical acceleration	Horizontal acceleration
CL1	Maximum	<0.50 m/s^2	<0.10 m/s^2
CL2	Medium	0.50-1.00 m/s^2	0.10-0.30 m/s^2
CL3	Minimum	1.00-2.50 m/s^2	0.30-0.80 m/s^2
CL4	Discomfort	>2.50 m/s^2	>0.80 m/s^2

Table 2. Traffic classes (5).

Classes	Density d [P/m^2]	Characteristics
TC1	< 15 P	15 single persons
TC2	< 0.20 P/m^2	Comfortable and free walking
TC3	< 0.50 P/m^2	Unrestricted walking, significantly dense traffic
TC4	< 1.00 P/m^2	Uncomfortable situation, obstructed walking
TC5	< 1.50 P/m^2	Unpleasant walking, very dense traffic

However, this methodology presents some limitations:

- the equivalent pedestrian number (pedestrian moving in phase with the structure) has been determined by the experimental results of only one footbridge (5).
- the change in the dynamic structural properties that the pedestrians flow causes is considered through a finger rule (addition of all the pedestrian mass density to the structure mass matrix).
- the interaction between pedestrians and the structure is only slightly considered, so the international standards do not consider adequately the synchronization phenomenon between pedestrians or between these ones and the structure.

The estimations carried out, under this methodology, normally overestimate the real results (5).

3. PROPOSAL OF A HUMAN-STRUCTURE INTERACTION MODEL

In this section a method for the simulation of the interaction between the pedestrian and the footbridge is proposed. It follows from the application of the dynamic equilibrium equations to a simplified model of interaction with sprung and unsprung masses (Figure 1).

For n modes of vibration $\varphi_i(x)$, the total response of the structure may be decomposed in terms of the amplitude of the different modes $y_i(t)$ as:

[4] $$w(x,t)=\sum_{i=1}^{n} y_i(t)\cdot\varphi_i(x)$$

[5] $$\dot{w}(x,t)=\sum_{i=1}^{n}\dot{y}_i(t)\cdot\varphi_i(x)+\sum_{i=1}^{n} y_i(t)\cdot v\cdot\varphi_i'(x)$$

[6] $$\ddot{w}(x,t)=\sum_{i=1}^{n}\ddot{y}_i(t)\cdot\varphi_i(x)+\sum_{i=1}^{n}2\cdot\dot{y}_i(t)\cdot v\cdot\varphi_i'(x)+\sum_{i=1}^{n} y_i(t)\cdot v^2\cdot\varphi_i''(x)$$

where

[7] $\varphi_i'(x)=\dfrac{d}{dx}\varphi_i(x)$ is the spatial derivate of the mode of vibration i.

[8] $\varphi_i''(x)=\dfrac{d^2}{dx^2}\varphi_i(x)$ is the second spatial derivate of the mode of vibration i.

and it is neglected, due to its low magnitude, the temporal variation of the step speed v.

Considering the equilibrium of the system, structure and pedestrian model, the following coupled equation system may be obtained.

[9] $$M_i\ddot{y}_i+C_i\dot{y}_i+K_i y_i=\varphi_i(vt)\cdot F_{\text{int}}$$

[10] $$m_a\ddot{y}_a+c(\dot{y}_a-\dot{y}_s)+k(y_a-y_s)=0$$

[11] $$m_s\ddot{y}_s+c(\dot{y}_s-\dot{y}_a)+k(y_s-y_a)=F_s-F_{\text{int}}$$

Thus, F_{int} follows from the above equation to yield.

[12] $$F_{\text{int}}=F_s-m_s\ddot{y}_s-c(\dot{y}_s-\dot{y}_a)-k(y_s-y_a)$$

And substituting this equation into the equilibrium equation of the structure.

[13] $$M_i\ddot{y}_i+C_i\dot{y}_i+K_i y_i=\varphi_i(vt)\cdot\left(F_s-m_s\ddot{y}_s-c(\dot{y}_s-\dot{y}_a)-k(y_s-y_a)\right)$$

Applying the equations of compatibility of displacements, velocity and acceleration between the structure and the simplified model of interaction.

[14] $$y_s=w(x,t)$$

[15] $$\dot{y}_s=\dot{w}(x,t)$$

[16] $$\ddot{y}_s=\ddot{w}(x,t)$$

Substituting these relations in the overall dynamic equilibrium equation of the structure and organizing information in a matrix form, the following model of interaction is obtained.

[17] $$M(t)\cdot\ddot{y}(t)+C(t)\cdot\dot{y}(t)+K(t)\cdot y(t)=F(t)$$

Considering the nature of the resulting system, the use of a method of β-Newmark integration family is proposed, with parameters $\beta=1/4$ and $\gamma=1/2$, thus ensuring an unconditionally stable system.

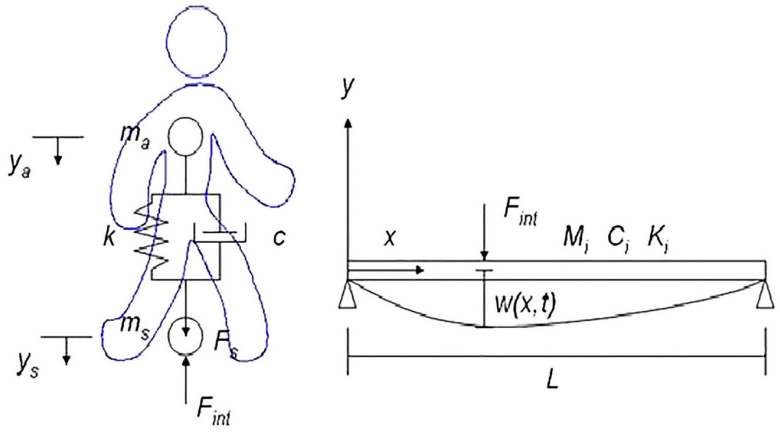

m_a	sprung mass
m_s	unsprung mass
m	total mass
y_a	displacement sprung mass
y_s	displacement unsprung mass
$w(x,t)$	deflection of the structure
k	equivalent pedestrian stiffness
c	equivalent pedestrian damping
v	step speed
F_{int}	interaction force
F_s	step force (see section IV)
M_i	modal mass of the vibration mode i
C_i	modal damping of the ibration mode i
K_i	modal stiffness of the vibration mode i
$\phi_i(x)$	vibration mode i

Figure 1. Pedestrian-structure interaction model.

In the previous expressions, the value of the vibration modes is zero, when the pedestrian remains outside the structure.

[18] $\varphi_i(x) = 0 \text{ for } 0 \geq x \geq L$ for , with L being the length of the structure

In the proposed method, $\varphi_i(x)$ is obtained, in a discrete way, using the finite element method, collecting the modal displacements and derivates in each of the nodes of the structure. To obtain a continuous function of the modes they are determined from the shape functions consistent with the finite element approximation. For the footbridge, the interpolation functions are cubic adopting the Bernoulli hypothesis for the beam elements.

[19] $$\varphi_i(x) = \sum_j \varphi_i^j \cdot N_j(x)$$

Where $N_j(x)$ are the shape functions and φ_i^j are the nodal values.

For a group of k pedestrians (Figure 2), we may further represent each one by the above simplified interaction model.

When a group of pedestrians is considered in the calculations, the number of differential equations to solve increases. In the case of a single pedestrian, the proposed model leads to a system of n+1 equations, corresponding to the considered number of vibration modes n plus the appropriate simplified interaction mechanical element system. Similarly, when considering a group of k pedestrians, a system of $n+k$ differential equations will need to be solved. It is important to note that the equations for the modes of vibration of the structure vary in terms of the position of pedestrians. At every instant, the numbers of pedestrian on the deformed shape must be calculated, as well as the value of the amplitude, slope and curvature corresponding to their position.

As a preliminary validation of the proposed formulation, the previously defined parameters will be estimated from the results available in the literature for comparable studies (6), as summarized in next sections. Finally, the experimental and numerical dynamic characteristics of a laboratory footbridge, under three controlled group of pedestrians, will be compared in order to determine the parameters and goodness of the proposed model.

The validation will be carried out, for simplicity, in the vertical direction, although the extracted results are easily extrapolated to the other directions.

4. DETERMINATION OF THE WALKING FORCES

The movement of the body mass and the put-down, rolling and push-off of the feet of one pedestrian generate the induced three-dimensional forces between both elements, F_s, that according to the research developed by different authors (4), can be determinated from a Fourier series decomposition in the three-space components.

[20] $$F_{p,vert}(t) = P\left[1 + \sum_{i=1}^{n_f} \alpha_{i,vert} \sin\left(2\pi i f_s t - \phi_i\right)\right]$$

[21] $$F_{p,lat}(t) = P\sum_{i=1}^{n_f} \alpha_{i,lat} \sin\left(\pi i f_s t - \phi_i\right)$$

[22] $$F_{p,long}(t) = P\sum_{i=1}^{n_f} \alpha_{i,long} \sin\left(2\pi i f_s t - \phi_i\right)$$

where

$F_{p,vert}$ vertical periodic force due to walking or running
$F_{p,lat}$ lateral periodic force due to walking or running
$F_{p,long}$ longitudinal periodic force due to walking or running
P [N] medium pedestrian weight (internationally considered as P=700.00 N)
$\alpha_{i,vert}$ $\alpha_{i,lat}$ $\alpha_{i,long}$ Fourier coefficient of the ith harmonic for vertical, lateral and longitudinal forces or dynamic load factor (DLF).
f_s [Hz] step frequency
φ_i phase shift of the ith harmonic
n_f total number of contributing harmonics.

Among the contributions of the different authors, for the development of the present document, the vertical dynamic

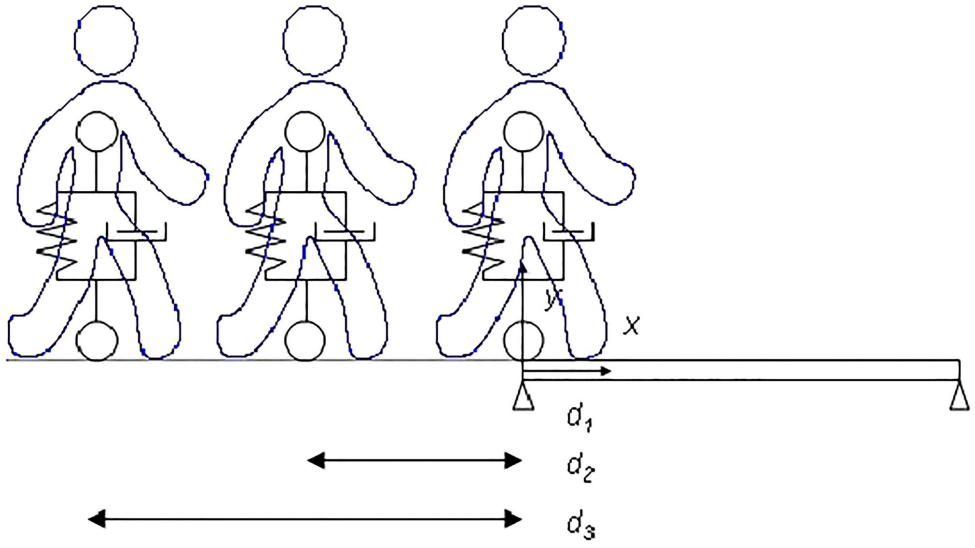

Figure 2. Pedestrians group according to the pedestrian-structure interaction model.

load factors proposed by Setra (5) (see Table 3 and Figure 3) will be considered to construct and validate our model. This criterion is widely accepted by both the scientific community and the designers of this type of structures. These standards obtained the dynamic coefficients from experimental tests performed on mobile platforms. The pedestrian load, according the results of such tests, is adequately characterized by the contribution of the first three harmonics.

The relation between the velocity magnitude, v, and the pacing frequency, f_s, is considered by the empirical relationship based on the work of Bertram and Ruina (3).

[23] $$f_s = 0.35 \cdot v^3 - 1.59 \cdot v^2 + 2.93 \cdot v$$

5. INITIAL ESTIMATION OF THE DYNAMIC PROPERTIES OF THE HUMAN-STRUCTURE INTERACTION MODEL

For the estimation of the dynamic characteristics of the SDOF-system, as a first approximation, a wide bibliographic study has been made. There are several studies that collect the effect of spectators on stadiums stands in the dynamic behaviour of the structure by a SDOF static system (6). In Figure 4 and Table 4, a scheme of the models used and the estimated dynamic parameters are shown, where f_h and ζ_h are the natural frequency and the equivalent damping ratio of the human system.

The above results allow establishing a likely range of variation of the system parameters. Thus, considering the maximum and minimum values (Figure 4) of the sprung mass (m_a), the equivalent human damping ratio (ζ_h) and the vertical natural frequency (f_h) of each pedestrian, it is shown in Table 5 a possible range of variation of the parameters of the proposed model. The sprung mass (m_a) is presented as a percentage of the total mass. A pedestrian type with a mean total mass of 70.00 kg is considered, as established by the European standards (4).

Table 3. Fourier coefficient and phase shift for vertical dynamic load factors (5).

α_1	α_2	α_3	φ_1	φ_2	φ
0.40	0.04	0.04	0.00	90.00	90.00

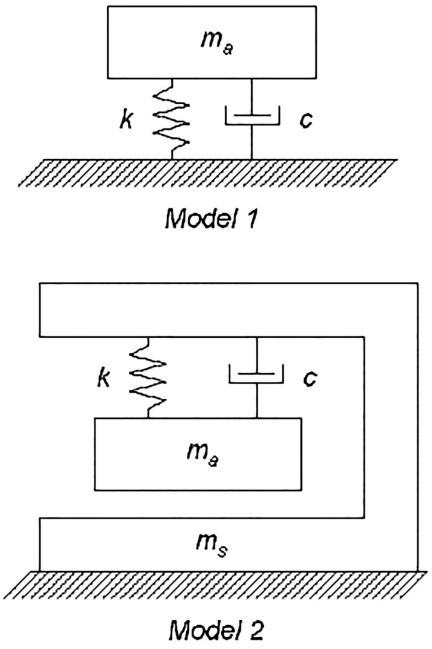

Figure 4. Simplified dynamic representations of the standing human body: (1) SDOF model (2) SDOF model with rigid support.

Table 4. Dynamic properties of SDOF equivalents to standing humans (6).

Human Model	Modal Properties	Human Model	Modal Properties
Foschi et al. (Model 1)	f_h=3.30 Hz ζ_h=53.00 % m_a=91.00 kg	Falati (Model 1)	f_h=10.43 Hz ζ_h=50.00 % m_a=25.00 kg
Al-Foqaha'a (Model 1)	f_h=3.50 Hz ζ_h=34.00 % m_a=83.00 kg	Zheng and Brownjohn (Model 1)	f_h=5.24 Hz ζ_h=39.00 % m_a=85.00 kg
Al-Foqaha'a (Model 2)	f_h=3.70 Hz ζ_h=36.00 % m_a=75.00 kg m_s=8.00 kg	Matsumoto and Griffin (Model 1)	f_h=5.74 Hz ζ_h=69.00 % m_a=76.10 kg
Brownjohn (Model 1)	f_h=4.90 Hz ζ_h=37.00 % m_a=80.00 kg	Matsumoto and Griffin (Model 2)	f_h=5.88 Hz ζ_h=61.00 % m_a=70.60 kg m_s=7.06 kg

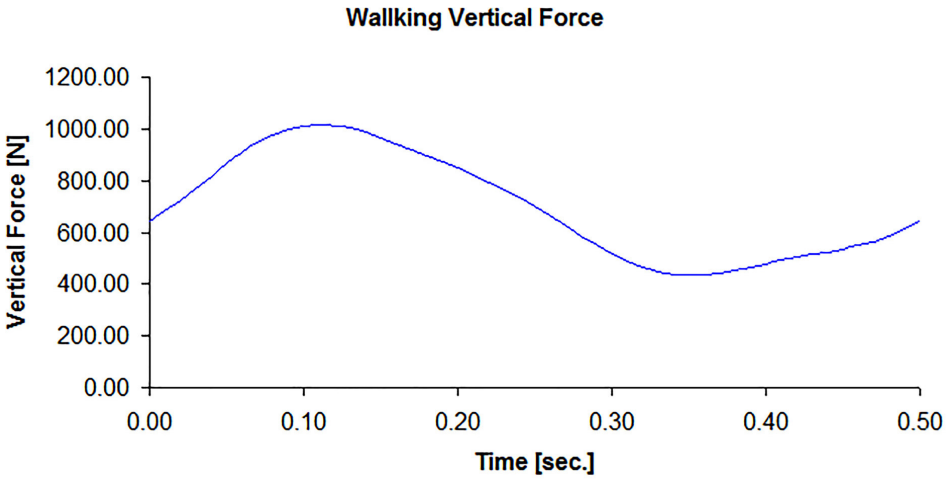

Figure 3. Vertical component of walking pedestrian force (5).

Table 5. Estimated range of the parameters of the human-structure interaction model.

	m_a [%]	ζ_h [%]	f_h [Hz]
Minimum	91.00	34.00	3.30
Maximum	100.00	69.00	10.43

This range of variation is considered as a reference in order to perform a validation of the interaction model in the vertical direction, but provided they are based on a passive pedestrians state, slight variations may be expected.

In order, on one hand, to consider the mass distribution of the human body (3) and on the other hand, the physical understanding of the problem that suggests a reduction of the damping and stiffness of the pedestrian associated with the movement, the above limits are increased, reducing the lower limits to the values set in the following ranges:

- sprung mass, m_a, 80-100 %.
- human damping ratio, ζ_h, 10-69 %.
- human natural frequency, f_h, 1.00-10.43 Hz.

The establishment of a search domain improves the efficiency of the parameter identification methods based on a probabilistic search. The value of the parameters of the pedestrian-structure interaction model will be determined using a probabilistic estimation method applied on the above search domain.

6. EXPERIMENTAL PARAMETERS IDENTIFICATION AND MODEL VALIDATION

6.1. Reference experimental results

Next, we will perform a more efficient estimation of the model parameters and a validation of its reliability by comparing our numerical predictions versus the experimental results obtained by Georgakis and Jorgesen (7). In their work, they studied the change of the dynamic behaviour of a laboratory footbridge due to the step of controlled pedestrians groups.

The laboratory footbridge, considered in (7), is a 16 m-long steel double U simply supported beam. The longitudinal beam profiles are UNP-350, with UNP-200 crossbeams placed at 1400.00 mm intervals. Several masses were added to the footbridge in different point of the structure to increase the modal mass and thus decrease the footbridge's frequency to a level close to the expected mean step frequency of the pedestrians (Figure 5). The total mass of the structure was 5224.00 kg.

A modal analysis was performed in order to identify the footbridge natural frequencies and damping ratio according to the level of vibration. The footbridge was excited by an actuator in the mid-span point to control its level of displacements. Figures 6 and 7 correlate the dependency between the first vertical vibration frequency (f_1) and the damping ratio (ζ_{foot}) with the footbridge vibration level at mid-span, without taking into account the influence of the pedestrians (7).

Subsequently, the structure was subjected to nine different load scenarios (LS), under a continuous flow of 4, 7 and 10 pedestrians (leading to mean flow rates of approximately 0.35, 0.62 and 0.88 P/s), during 180.00 seconds with a step frequency of 1.38 Hz, a step velocity of 1.40 m/s and three different mid-span levels of displacement of 1.00, 5.00 and 10.00 mm. Pedestrians were allowed to walk in both directions along the footbridge.

The estimation of the dynamic properties was performed in each case from a frequency sweep of the actuator. The natural

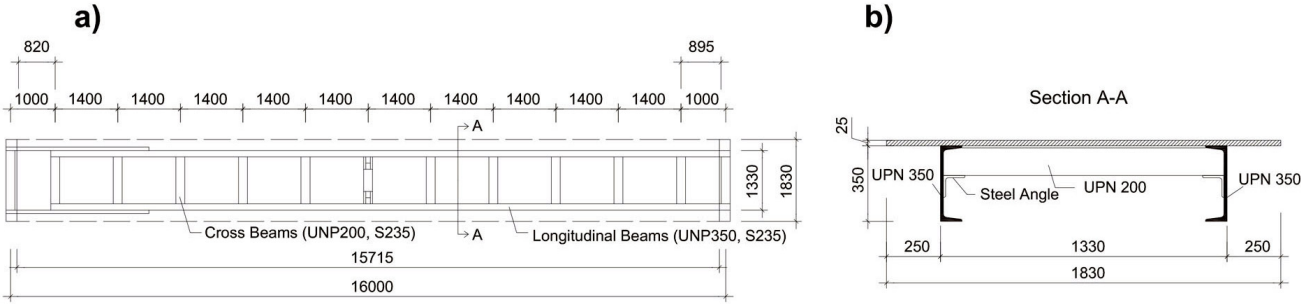

Figure 5. (a) Elevation and (b) cross-section of the laboratory footbridge structure (7).

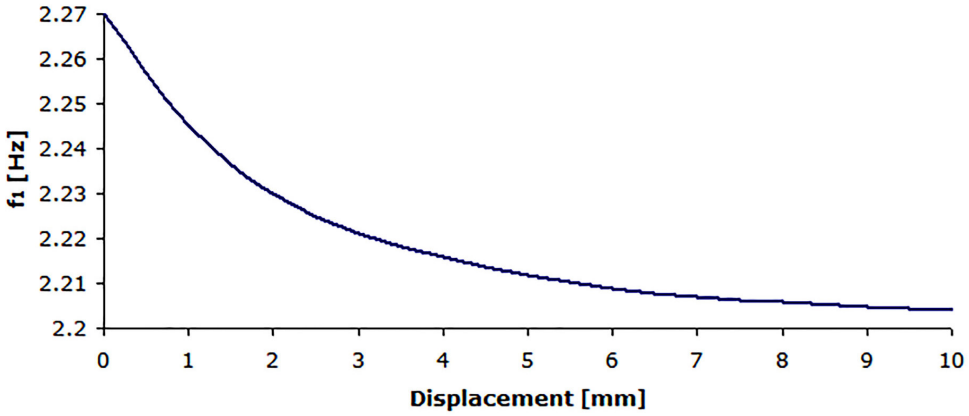

Figure 6. First natural frequency versus vibration amplitude for empty footbridge (7).

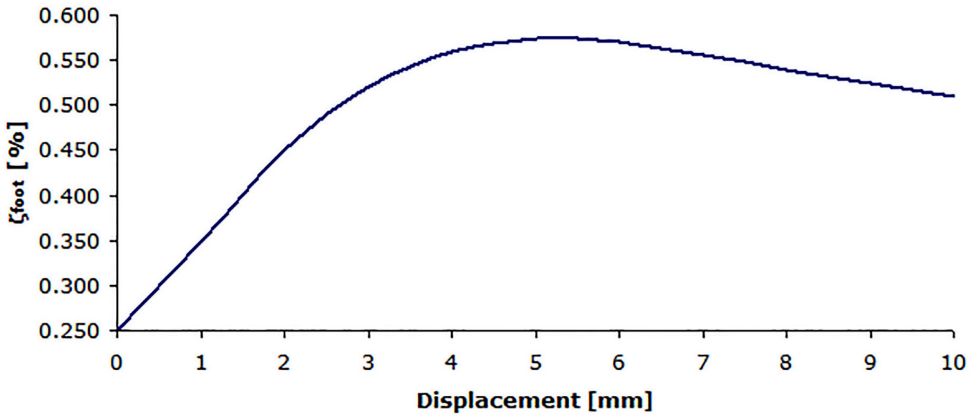

Figure 7. Damping ratio versus vibration amplitude for empty footbridge (7).

frequency was characterized by the frequency where the force exerted by the actuator reaches a minimum value.

The main results of this research, summarized in the Table 6, show the shift of the first natural frequency of the structure, from $f_{1,emp}$ (empty footbridge) to $f_{1,full}$ (full footbridge), versus the level of displacement at the mid-span (A) and the number of pedestrians (N_p).

6.2. Model validation

The above results allow obtaining an experimental estimation of the change in the dynamic behaviour of a laboratory footbridge depending on the pedestrian density. From these data, the different parameters of the proposed human-structure interaction model will be estimated by solving the inverse dynamic problem. The solution of this problem will be made in two phases.

First, a finite element model of the footbridge was developed (see Figure 8), using 3-D beam elements and, adjusting an additional mass distribution so that the value of the first experimental vibration frequency of the footbridge is equal to the one obtained from the numerical modal analysis, considering an empty structure.

Table 6. Change of first natural frequency under the different scenarios.

LS	N_p	A [mm]	$f_{1,emp}$ [Hz]	$f_{1,full}$ [Hz]
1.1	4	1.00	2.280	2.086
1.2	4	5.00	2.270	2.073
1.3	4	10.00	2.220	2.029
2.1	7	1.00	2.280	2.022
2.2	7	5.00	2.270	2.009
2.3	7	10.00	2.220	1.965
3.1	10	1.00	2.300	1.980
3.2	10.00	5.00	2.290	1.970
3.3	10.00	10.00	2.270	1.950

Then in order to estimate the three main parameters of the proposed pedestrian-structure interaction model, sprung mass (m_a), equivalent human damping ratio (ζ_h) and human natural frequency (f_h), the mean square error between the experimental and numerical first vertical natural frequency of the footbridge is minimized (8) for each load scenario (LS). Given the singularity of the minimization function chosen, and in order to avoid local minimums, the genetic algorithms method (a global search method) has been considered (9). The optimization method chosen prevented the solution of the problem from being conditioned by the selected starting point of the search. To avoid ill-conditioning problems, the reduction of the search domain has been developed, constraining the problem. The search range previously proposed has been used.

For each load scenario, a population of 1000 individuals (vectors with three elements) is defined. Each individual modifies through the operations of reproduction, crossover and mutation the values of its elements in order to minimize the value of the objective function. In all the cases, the optimization process reached values of the objective function lower than 10^{-12} Hz. The maximum number of iterations is set to 100. The numerical value of the damped frequency was obtained from the response function of the system in the frequency domain. The experimental value of the damped frequency was determined for each load scenarios according to the pedestrian flow and the level of vibration reached.

It is shown in Figure 9 the flowchart of the human-structure pedestrian model fitting procedure based on genetic algorithms.

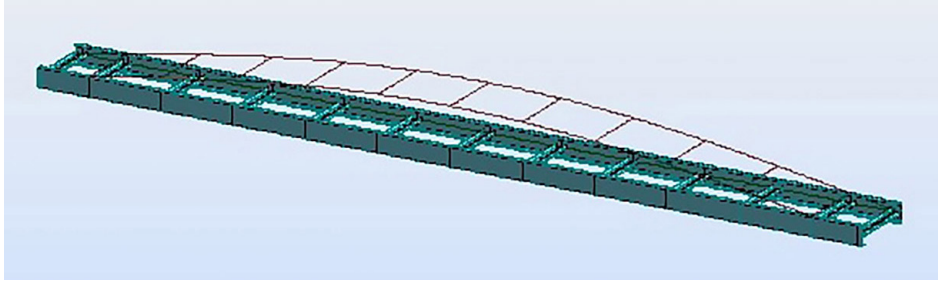

Figure 8. Finite element model and first vibration mode (f=2.27 Hz) of the footbridge.

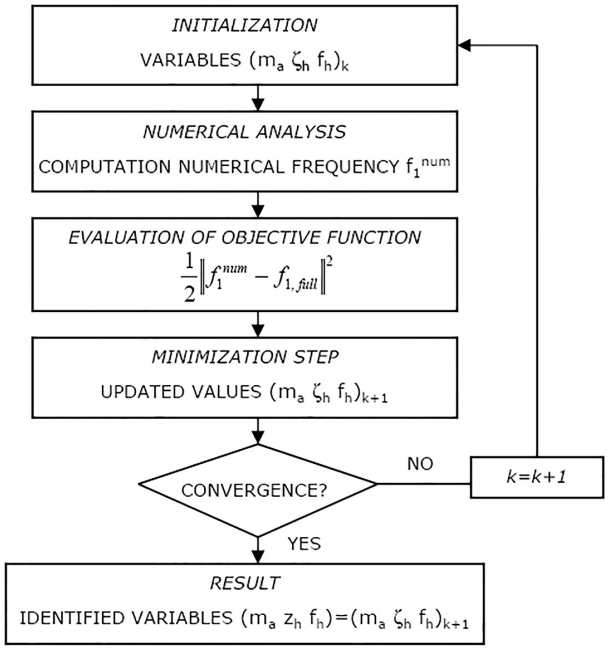

Figure 9. Flowchart of the human-structure pedestrian model fitting procedure.

Table 7. Estimated parameters of the human-structure interaction model.

LS	m_a [%]	ζ_h [%]	f_h [Hz]
1.1	83.046	45.007	2.852
1.2	84.996	45.000	2.600
1.3	84.990	45.583	2.502
2.1	84.861	43.293	2.870
2.2	84.539	49.212	2.759
2.3	84.974	49.975	2.600
3.1	82.139	48.001	2.997
3.2	83.171	51.014	2.908
3.3	83.007	47.486	2.743
Medium	83.969	47.175	2.759
Deviation	1.054	2.611	0.165

In Table 7, the results obtained for the nine load scenarios considered are shown. The last two rows of this table show the medium value and the standard deviation obtained for the different parameters. The values of the parameters that characterize the human-structure interaction model remain slightly constant regardless of the level of the pedestrian flow, the level of vibration reached and the damping ratio of the footbridge. The estimated standard deviations of each model parameter (sprung mass, equivalent human damping ratio and natural frequency) are small and the estimated values are considered as appropriate.

In Figure 10, the numerical estimation of the change of the first vertical vibration frequency ($f_{1,ver}$) of the structure under the crossing of ten pedestrians is shown. In the figure three curves are represented. The "Experimental Results" shows the change of the experimental first natural frequency according to the results of the modal analysis (7), the "Passive Pedestrians" shows the change of the proposed interaction model with the pedestrian parameters estimated from the medium passive pedestrian behaviour (m_a=95.5 %, ζ_h=51.50 % and f_h=6.86 Hz obtained from Table 5), and finally, the "Interaction Model" corresponds to the fitting from the solution of the inverse dynamic problem.

The analysis of the Figure 10 shows that the estimation of first natural frequency of the structure by the proposed model, considering the medium values of the passive pedestrian parameters estimation, produces a relative error of only 5.00 %. Besides the variation of the dynamic properties of the footbridge presents a similar shape to the estimated ones experimentally. Good agreement is observed between the experimental and numerical results.

A comparison of the calculated values with the estimated from the studies on the dynamic effect of passive pedestrians in stadiums, shows mainly a loss of stiffness of each pedestrian when they are in motion.

From the study of the previous results, three main conclusions can be extracted:

- First, the stability that the estimated model parameters present for the different load scenarios, allowing that this model identification may be used as a reliable starting point for the characterization of the effect of the pedestrians on the dynamic behaviour of the structures.
- Then, the appropriately fitting between the experimental and numerical curves that show the change of the first natural frequency of the footbridge, after the adjustment of the pedestrian parameters. The goodness of the correlation verifies the ability of the proposed model to characterize the human-structure interaction problem.

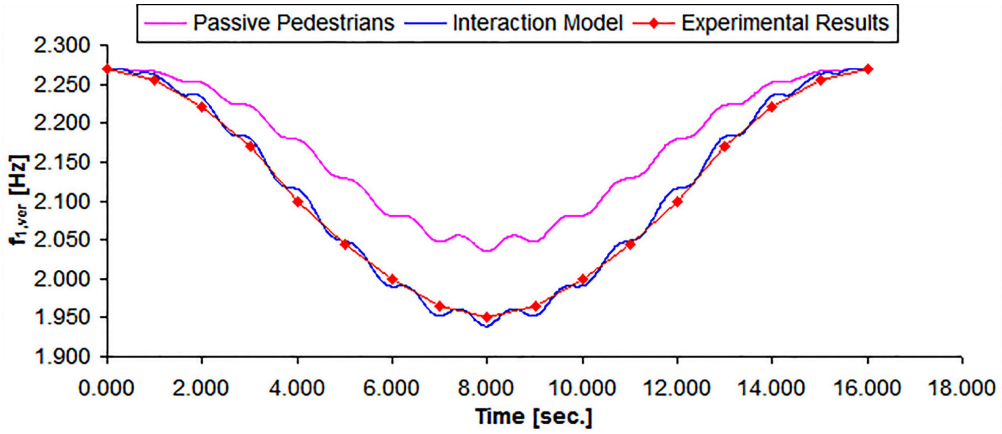

Figure 10. Numerical estimation first natural damped frequency (10 pedestrians).

- Finally, an important result of the present research is that the main parameter that controls, in the vertical direction, the variation of the natural frequencies of a footbridge under a pedestrian flow is the increase of the damping ratio of the system due to the contribution of the human damping.

7. CONCLUSIONS

The models adopted by the current codes for the study of the dynamic behaviour of footbridges do not allow a very accurate estimation of the real response that occurs at the different points of the deck. The most advanced methodology (4) (5), although it is very effective to estimate the sensitivity of the structures to pedestrian flow, it is quite conservative to estimate their effects on the structure. As the acceleration is the main factor that determines the in-service conditions, a pedestrian-structure interaction model has been proposed in order to obtain a more accurate estimation of the response. The model has been presented and its applicability proven in this work. To characterize the accuracy of the presented model, the model parameters are adjusted from the results presented in a scientific study (7) in which the change of the dynamic properties of a laboratory footbridge, under different pedestrian flows, is carried out. The adequate fitting between the experimental and numerical curves that mark the evolution of the first natural frequency of the footbridge under the step of the different group of pedestrians and the stability of the pedestrian parameters for the nine adjustments verify the correct performance of the proposed model to study the problem of human-structure interaction. A medium value, in the vertical direction, for the pedestrian system parameters, is proposed, sprung mass ratio 84.00 %, human damping ratio 47.00 % and human frequency 2.75 Hz. However, further studies are needed in order to characterize the dynamic parameters in the three spatial directions under moving situations in real footbridges and furthermore, others factors must be considered in the model in order to include the synchronization phenomena between the pedestrians and the structure.

REFERENCES

(1) Wolmuth, B., Surtees, J. (2003). Crowd-related failure of bridges. *Civil Engineering*, 156(3): 116-123.
(2) Dallard, P.,Fitzpatrick, A.J., Le Bourva, S., Low, A., Ridsill Smith, R., Willford, M., Flint, A. (2001). The London Millenium Footbridge. *The Structural Engineer*, 79(22): 17-33.
(3) Zivanovic, S., Pavic, A., Reynolds, R. (2005). Vibration serviceability of footbridges under human-induced excitation: a literature review. *Journal of Sound and Vibration*, 279(1-2): 1-74, doi: http://dx.doi.org/10.1016/j.jsv.2004.01.019.
(4) SYNPEX Guidelines. (2007). European Project on Advanced Load Models for synchronous Pedestrian Excitation and Optimised Design Guidelines for Steel Footbridges.
(5) Setra. (2006). *Guide méthodologique passerelles piétonnes (Technical guide footbridges: Assement of vibrational behaviour of footbridges under pedestrian loading)*. Setra.
(6) Jones, C.A., Reynolds, R. , A. Pavic. A. (2011). Vibration serviceability of stadia structures subjected to dynamic crowd loads: A literature review. *Journal of Sound and Vibration*, 330(8): 1531-1566, doi: http://dx.doi.org/10.1016/j.jsv.2010.10.032.
(7) Georgakis, C., Jorgesen, N.G. (2013). Topics in Dynamics of Bridges, Volume 3. En *Proceedings of the 31st IMAC. A Conference on Structural Dynamics, 2013*. Chapter 4. Change in Mass and Damping on Vertically Vibrating Footbridges Due to Pedestrians. The Society for Experimental Mechanics, Inc.
(8) Gonzalez, M.N., Cobo, A., Fuente, J.V. (2013). Obtención de modelos de cálculo de sistemas provisionales de protección de borde mediante la técnica de Análisis Modal Operacional. *Informes de la Construcción,* 65(529): 99-106, doi: http://dx.doi.org/10.3989/ic.11.133.
(9) Ghee, C., Perry, M.J. (2010). *Structural Identification and Damage Detection using Genetic Algorithms: Structures and Infrastructures Book Series,* Vol. 6. London: CRC Press 2010.

* * *

Paper B: Vertical crowd–structure interaction model to analyze the change of the modal properties of a footbridge

The original version of this paper can be found in

doi: 10.1061/(ASCE)BE.1943-5592.0000828

Journal name: Journal of Bridge Engineering (in press)

ISI 2014 Classification: Q2 (54/124) Civil Engineering. Impact Factor: 1.065

SCIMAGO 2014 Classification: Q1 (39/215) Civil Engineering SJR: 1.098

ISSN: 1084-0702

Vertical crowd-structure interaction model to analyse the change of the modal properties of a footbridge.

Javier Fernando Jiménez-Alonso[a*], Andrés Sáez[b] , Elsa Caetano[c] and Filipe Magalhães[d]

[a*]*Assistant professor. Department of Building Engineering and Geotechnical Engineering, University of Seville, Avenida de Reina Mercedes 2, 41012, Seville (Spain). Email: jfjimenez@us.es.*

[b]*Full professor. Department of Continuum Mechanics and Structural Analysis, University of Seville, Camino de los Descubrimientos s/n, 41092, Seville (Spain). Email: andres@us.es.*

[c]*Associate professor. Department of Civil Engineering. FEUP. R. Dr. Roberto Frias, s/n, 4200-465 Porto (Portugal). Email: ecaetano@fe.up.pt.*

[d]*Assistant professor. Department of Civil Engineering. FEUP. R. Dr. Roberto Frias, s/n, 4200-465 Porto (Portugal. Email: filipema@fe.up.pt.*

[*]*Corresponding author:* Assistant Professor: Javier Fernando Jiménez-Alonso. Department of Building Structures and Geotechnical Engineering. University of Seville. Avenida de Reina Mercedes, 2, 41012, Seville (Spain) Ph:+34 954 556 602 . E-mail: *jfjimenez@us.es*.

ABSTRACT

In this paper a biomechanical crowd-structure interaction model is proposed and further implemented in order to adequately estimate the energy exchange between pedestrians and footbridge. The proposed model focuses on the vibrations in the vertical direction and allows taking into account the change of the modal properties of the structure due to the presence of the pedestrians, additionally improving the numerical estimation of the response of the structure under pedestrian flows. The model involves two sub-models, namely (i) a

pedestrian-structure interaction sub-model plus (ii) a crowd sub-model. The first sub-model follows from a modal projection of a system with two d.o.f, that simulates the behavior of each pedestrian, on the vibration modes of the structure. The parameters of this model have been estimated from the accelerations recorded on a real footbridge. For the second sub-model, the crowd behaviour is simulated via a multi-agent method. The performance of the resulting overall model is assessed by correlating the experimental and numerical dynamic of a real footbridge under a group of pedestrians at different controlled step frequencies. In particular, the change in the first natural frequency induced by the pedestrian-footbridge interaction is discussed in detail. The proposed model leads to numerical results that exhibit good agreement with the recorded experimental values. Therefore it is a valuable tool to estimate the change on the modal properties of a footbridge induced by the crowd-structure interaction phenomenon.

Keywords: simplified biomechanical model, human-structure interaction, crowd dynamics, change of natural frequencies, footbridge.

INTRODUCTION.

During the last fifteen years, significant effort has been made by the scientific community to characterize adequately the dynamic response of footbridges under pedestrian flows (Racic et al., 2009; Zivanovic at al., 2005). Although important advances have been achieved in the definition of the pedestrian walking force (Butz et al., 2007; Setra, 2006), some aspects of the crowd-structure interaction problem have not been completely solved and still deserve attention. The study of the crowd-structure interaction problem has been performed according to three key aspects in order to: (i) characterize the walking force transmitted by each pedestrian; (ii) characterize the pedestrian-structure interaction and finally (iii) to characterize the interaction among pedestrians in the crowd. In this way, research efforst focused initially on the determination of analytical expressions for the walking force induced by a pedestrian (Zivanovic et al., 2005; Butz et al., 2007). However, as the increasing sophistication of

this proposed expressions, characterizing the pedestrian walking force, did not lead to significant improvements in the numerical estimations of the response of the footbridge under pedestrian flows, new factors were considered in the models. In that sense, as a result of the research conducted at the Millennium footbridge (Dallard et al., 2001), it was concluded that the effect of a pedestrian flow on the structure involved not only an equivalent pedestrian force but also the modification of the dynamic properties of the structure. Subsequently, this result was validated by other reported works (Ingolfsson et al, 2008) where pedestrians were considered as active damping forces that increased the overall damping of the structure. Following these works, several approaches have been presented in the literature to model de pedestrian-structure interaction problem. The first models maintained the idea of equating the pedestrian to an active viscous damper (Georgakis and Jorgesen, 2013). Subsequently, others modal parameters were considered in the interaction phenomenon leading to the appearance of single degree of freedom systems to characterize the behaviour of each pedestrian (Shahabpoor et al., 2013). According to these latter models, each pedestrian induced a modification of both the damping and stiffness matrix of the footbridge during its crossing. On the other hand, the characterization of the dynamic response of the structure under pedestrian flows motivated the study of how the pedestrians interact in a crowd (Zivanovic at al., 2010). In that sense, both statistical distributions of the step pedestrian frequencies in a crowd (Venuti et al., 2007) and relations between the pedestrian velocity and step frequency (Bruno and Venuti, 2009) were established. In order to characterize the crowd behaviour, the models have evolved from a macroscopic to a microscopic approach. The movement of the crowd simulated originally by the fluid mechanics laws (Venuti et al., 2007), is currently modelled using particle dynamics (Carroll et al., 2012), by considering each pedestrian as an agent whose equilibrium is achieved

through the interaction forces applied by its environment. Currently, several proposals have emerged (Venuti et al., 2014, Tavares et al. 2014).in order to offer a direct and joint response to the three above mentioned key aspects. In all these proposals, the crowd-structure interaction has been simulated through the coupling of two sub-models: a pedestrian-structure interaction model and a crowd model based on multi-agent theory.

In this paper, a new crowd-structure interaction model in the vertical direction is proposed. The model represents an evolution of the existing proposals and aims to improve some shortcomings of the previous reported works. The proposed model involves two sub-models as well. A pedestrian-structure interaction sub-model follows from the modal projection of a two degree of freedom system, where the pedestrian mass is divided in sprung plus unsprung components, on the vibration modes of the structure. The crowd behaviour is simulated via a multi-agent sub-model where the movement of each pedestrian is governed by the experienced interaction forces. A physical interaction force has been included to assess more accurately the crowd behaviour under high pedestrian densities. The interaction between the two sub-models in the vertical direction is achieved by implementing a stop threshold, so that if certain acceleration limit is exceeded the affected pedestrians stop. The estimation of the parameters of the proposed pedestrian-structure interaction model has been experimentally performed based on the results of a pedestrian test conducted at the Viana footbridge (Viana do Castelo, Portugal). Subsequently, the crowd-interaction model has been assessed by correlating the experimental and numerical response of the Viana footbridge under a group of 50 pedestrians. Finally, the model has been applied to study the numerical change of the first vertical vibration mode of the Viana footbridge due to the presence of the group of pedestrians.

The proposed model may further be used to predict the occurrence of the lateral lock-in phenomenon in footbridges or to improve the efficiency of the control devices introduced in a footbridge when vibratory problems are detected.

The paper is organized as follows: The proposed crowd-structure interaction model is presented in section 2, by describing (i) the pedestrian-structure interaction sub-model; (ii) the crowd sub-model as well as (iii) the interaction mechanisms between both sub-models. Section 3 is devoted to the experimental estimation of the main parameters that characterize the pedestrian-structure interaction sub-model. In section 4, the validity and accuracy of the overall crowd-structure interaction model is successfully assessed by correlating both the experimental and numerical results for a real footbridge (Viana do Castelo, Portugal). Finally, some concluding remarks are drawn to close the paper in section 5.

PROPOSAL OF A SIMPLIFIED BIOMECHANICAL CROWD-STRUCTURE INTERACTION MODEL IN VERTICAL DIRECTION.

The complete crowd-structure interaction consists of two individual submodels (Fig. 1), one for the pedestrian-structure interaction (that includes the pedestrian and footbridge dynamic behaviour) and another for the crowd.

The pedestrian-structure interaction model is responsible for modelling, in a simplified way, all the dynamics effects (inertia, damping, stiffness) induced on the footbridge by the crossing of a pedestrian. The vertical acceleration $\ddot{z}_a$ experimented by each pedestrian is obtained as output from this model.

The crowd model is implemented as a behavioural model providing a description of the individual pedestrian position, $\mathbf{x}_p$, walking pedestrian velocity, $\mathbf{v}_p$, and step pedestrian

frequency, f_p, what allows for simulating the overall behaviour of the crowd and its influence in the dynamic behaviour of the footbridge.

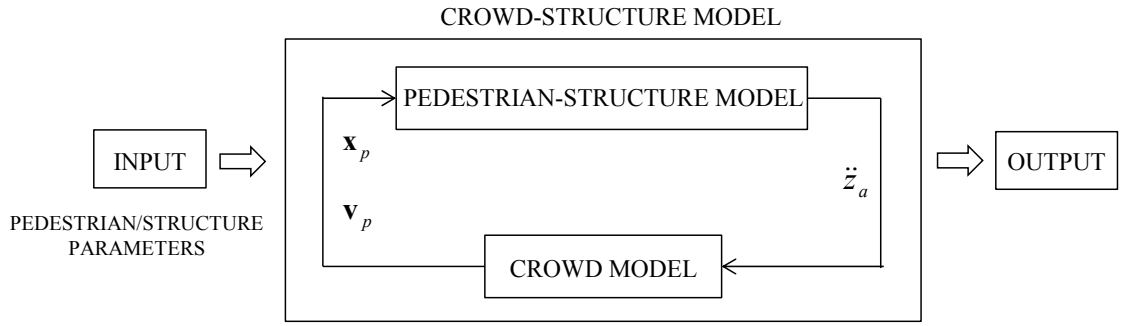

Fig.1. Layout of the biomechanical crowd-structure interaction model.

For each iteration the crowd model determines the position and step velocity of each pedestrian. These two parameters are used as input to define the step frequency and walking force of each pedestrian into the pedestrian-structure model, obtaining as output the pedestrian vertical acceleration. The pedestrian velocity of each individual is then modified according to the level of acceleration experimented by each pedestrian. Finally, the process is repeated with the updated values of the position and the velocity (Fig. 1).

Modelling the pedestrian-structure interaction in the vertical direction.

The proposed pedestrian-structure interaction in the vertical direction follows from the application of dynamic equilibrium equations (Clough and Penzien, 1993; Dominguez, 2001) to a simplified model of interaction (Fig. 2) with sprung (m_a) and unsprung masses (m_s). This methodology has been applied previously by the authors successfully (Jiménez-Alonso and Sáez, 2014), and in this paper it is generalized in order to take into

account the modification of the pedestrian velocity due to the crowd-structure interaction.

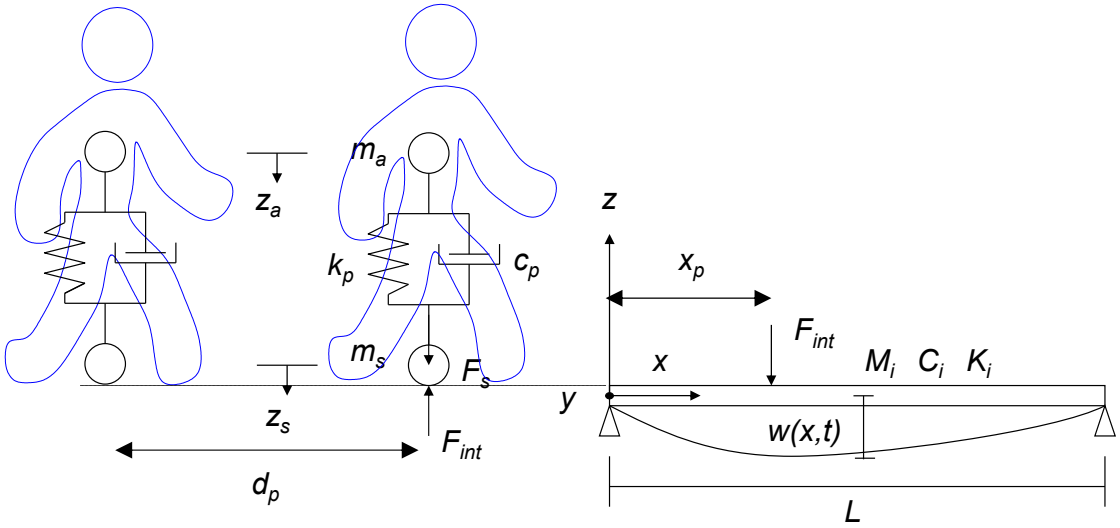

Fig.2. Biomechanical pedestrian-structure interaction model.

Considering the balance of the system, structure and pedestrian model, the following coupled equations are obtained.

$$M_i \ddot{z}_i + C_i \dot{z}_i + K_i z_i = \phi_{NUM\_i}(x_p) \cdot F_{\text{int}} \tag{1}$$

$$m_a \ddot{z}_a + c_p (\dot{z}_a - \dot{z}_s) + k_p (z_a - z_s) = 0 \tag{2}$$

$$m_s \ddot{z}_s + c_p (\dot{z}_s - \dot{z}_a) + k_p (z_s - z_a) = F_{p,ver} - F_{\text{int}} \tag{3}$$

where

m_a is the sprung mass of the pedestrian [kg].

m_s is the unsprung mass of the pedestrian [kg].

$m = m_s + m_a$ is the total mass of the pedestrian [kg].

z_a is the absolute vertical displacement of the sprung mass [m].

z_s is the absolute vertical displacement of the unsprung mass [m].

k_p is the equivalent stiffness of a pedestrian [N/m].

c_p is the equivalent damping of a pedestrian [sN/m].

$F_{p,ver}$ is the vertical pedestrian force due to walking [N].

F_{int} is the interaction force between the pedestrian and the structure [N].

M_i is the modal mass of the vibration mode *i* [kg].

C_i is the modal damping of the vibration mode *i* [sN/m]

K_i is the modal stiffness of the vibration mode *i* [N/m].

ϕ_{NUM_i} is the vertical component of the numerical vibration mode *i*.

$x_p = v_{px} \cdot t$ is the longitudinal position of the pedestrian [m].

v_{px} is the longitudinal component of the pedestrian velocity vector [m/s].

From Eq.(3) the following expression is obtained for, F_{int},

$$F_{\text{int}} = F_{p,ver} - m_s \ddot{z}_s - c_p\left(\dot{z}_s - \dot{z}_a\right) - k_p\left(z_s - z_a\right) \quad \text{.....(4)}$$

and substituting this equation into Eq.(1) yields.

$$M_i \ddot{z}_i + C_i \dot{z}_i + K_i z_i = \phi_{NUM\_i}\left(x_p\right) \cdot \left(F_{p,ver} - m_s \ddot{z}_s - c_p\left(\dot{z}_s - \dot{z}_a\right) - k_p\left(z_s - z_a\right)\right) \ldots (5)$$

Applying, at the contact point the equations of compatibility of displacements, velocity and acceleration between the structure and the simplified pedestrian-model of interaction are obtained.

$$z_s = w(x_p, t) = w(v_{px} \cdot t, t) \quad (6)$$

$$\dot{z}_s = \dot{w}(x_p, t) = \dot{w}(v_{px} \cdot t, t) \quad (7)$$

$$\ddot{z}_s = \ddot{w}(x_p, t) = \ddot{w}(v_{px} \cdot t, t) \quad (8)$$

These quantities may be expressed in terms of the amplitude $z_i(t)$ and the modal shape of the *n* numerical considered vibration modes $\phi_{NUM\_i}(x)$, neglecting the term of variation of the pedestrian velocity over the time, as:

$$w(x_p,t)=\sum_{i=1}^{n} z_i(t)\cdot\phi_{NUM\_i}(x_p) \tag{9}$$

$$\dot{w}(x_p,t)=\sum_{i=1}^{n}\dot{z}_i(t)\cdot\phi_{NUM\_i}(x_p)+\sum_{i=1}^{n} z_i(t)\cdot v_{px}\cdot\phi'_{NUM\_i}(x_p) \tag{10}$$

$$\ddot{w}(x_p,t)=\sum_{i=1}^{n}\ddot{z}_i(t)\cdot\phi_{NUM\_i}(x_p)+\sum_{i=1}^{n}2\cdot\dot{z}_i(t)\cdot v_{p,x}\cdot\phi'_{NUM\_i}(x_p)+\sum_{i=1}^{n} z_i(t)\cdot {v_{p,x}}^2\cdot\phi''_{NUM\_i}(x_p)) \tag{11}$$

$$\phi'_{NUM\_i}(x)=\frac{d\phi_{NUM\_i}(x)}{dx} \tag{12}$$

$$\phi''_{NUM\_i}(x)=\frac{d^2\phi_{NUM\_i}(x)}{dx^2} \tag{13}$$

where

$\phi'_{NUM\_i}(x)$ is the first spatial derivate of the mode of vibration i.

$\phi''_{NUM\_i}(x)$ is the second spatial derivate of the mode of vibration i.

The above relations -Eqs.(6) to (11)- are then substituted in the overall dynamic equilibrium equations -Eqs.(1) to (3)- so that, organizing information in a matrix form, the following model of interaction is obtained (see Appendix I for matrix formulation).

$$\mathbf{M}(t)\cdot\ddot{\mathbf{z}}(t)+\mathbf{C}(t)\cdot\dot{\mathbf{z}}(t)+\mathbf{K}(t)\cdot\mathbf{z}(t)=\mathbf{F}(t) \tag{14}$$

In the previous expressions, the value of the numerical vibration modes is zero, when the pedestrian remains outside the structure.

$$\phi_{NUM\_i}(x_p)=0 \text{ for } \begin{matrix} x_p(t)<0 \\ x_p(t)>L \end{matrix} \tag{15}$$

with L being the length of the structure

The numerical vibration modes, $\phi_{NUM\_i}(x)$, are obtained in a discrete way using the corresponding finite element method as:

$$\phi_{NUM\_i}(x)=\sum_j \phi_i^j\cdot N_j(x) \tag{16}$$

where $N_j(x)$ are the shape functions and ϕ_i^j are the nodal values.

Although the paper focuses on vibrations in vertical direction. The formulation of the proposed model may be further generalized to the other two directions, longitudinal and lateral, by accordingly modifying both the equation that governs the considered pedestrian load in each direction and the value of the modal parameters that define the TDOF (two degrees of freedom) pedestrian model. In this way, the resulting model would be suitable for the more general 3-D problem and it could therefor take into account the possible interaction in the three spatial directions.

For a group of *k* pedestrians (Fig. 2), each of them will be represented by the above simplified interaction model. In the case of a single pedestrian, the proposed model leads to a system *of n+1* equations, corresponding to the considered number of vibration modes *n* plus the simplified interaction equation. Similarly, when considering a group of *k* pedestrians, a system of *n+k* differential equations will need to be solved.

Considering the nature of the resulting system, the use of a method of β-Newmark integration family is proposed, with parameters $\beta = 1/4$ and $\gamma = 1/2$, thus ensuring an unconditionally stable system.

Furthermore, the integration step, Δt, is established according to the usual recommendations (Clough and Penzien, 1993; Dominguez, 2001) for dynamics models based on modal decomposition technique, as the minimum of the following values.

$$\Delta t = \min\left(\frac{1}{8 \cdot f_{\max}}, \frac{L_{\min}}{200 \cdot |v_p|}, \frac{L_{\min}}{4 \cdot n \cdot |v_p|}, 0.01\right) \text{sec.} \tag{17}$$

with $f_{\max}$ [Hz] being the highest considered vibration frequency of the structure (30 Hz according to Dominguez (2001)) and $L_{\min}$ [m] the minimum span length of the pedestrian bridge.

Pedestrian vertical walking force.

The movement of the body mass and the put-down, rolling and push-off of the feet of one pedestrian generate the induced vertical forces between the pedestrian and the structure, $F_{p,ver}$. According to different authors (Butz et al., 2007; Setra, 2006), this force can be determined from a Fourier series decomposition as:

$$F_{p,ver} = P\left[1 + \sum_{i=1}^{n_f} \alpha_{i,ver} \sin\left(2\pi \cdot i \cdot f_s \cdot t - \varphi_i - \phi_p\right)\right] \tag{18}$$

where

$P = m \cdot g$ [N] is the medium pedestrian weight, g being the acceleration of the gravity.

$\alpha_{i,ver}$ is the Fourier coefficient of the *ith* harmonic for vertical forces or vertical dynamic load factor (VDLF).

f_s [Hz] is the step frequency of the pedestrian.

φ_i is the phase shift of the *ith* harmonic of the pedestrian force.

ϕ_p is the phase shift among pedestrians.

n_f is the total number of contributing harmonics.

In order to determine the number of pedestrians that cross the footbridge in phase, a Poisson distribution has been adopted, according to the results by Matsumoto et al. (1978). Further tests performed on Solferino bridge (Setra, 2006), as well as other studies, suggest that lock-in in vertical direction does not seem probable due to the low sensitivity of the pedestrians to vertical vibrations. Thus, when a group of n_p pedestrians arrive at the footbridge, the number of pedestrians randomly synchronized is $\sqrt{n_p}$. This synchronization criterion has been adopted in our crowd-structure interaction model. Its implementation in the model is achieved by the phase shift parameter, ϕ_p. For a given generation/group of pedestrians, the value of the phase shift

of the $\sqrt{n_p}$ randomly synchronized pedestrians has been set equal to zero. For the remaining pedestrians the phase shift has been assigned randomly, using a Gaussian distribution in the range $[0,2\pi]$.

In Table 1 the values of the vertical dynamic load factors (VDLF), the phase shifts and their range of variation provided by different authors are shown (as summarized in Butz et al., 2007; Setra, 2006).

Table 1. VDLF and phase shift according different authors (Butz et al., 2007).

Author	$\alpha_{1,ver}$	$\alpha_{2,ver}$	$\alpha_{3,ver}$	φ_1 [°]	φ_2 [°]	φ_3 [°]
Blanchard	0.257	0.000	0.000	0.00	0.00	0.00
Bachmann	0.450	0.100	0.100	0.00	0.00	0.00
Schulze	0.370	0.100	0.120	0.00	0.00	0.00
Kerr	0.450	0.100	0.100	0.00	0.00	0.00
Young	0.388	0.071	0.056	0.00	0.00	0.00
Charles	0.400	0.000	0.000	0.00	0.00	0.00
EC5	0.400	0.200	0.000	0.00	0.00	0.00
Setra	0.400	0.040	0.040	0.00	90.00	90.00
Minimum	0.257	0.000	0.000	0.00	0.00	0.00
Maximum	0.450	0.200	0.120	0.00	90.00	90.00

Vertical modal parameters of the pedestrian model.

There are several studies, as reported by Jones et al. (2010), describing the effect of passive pedestrians on stadium stands in the dynamic behaviour of such structures in terms of a static single degree of freedom (SDOF) system.

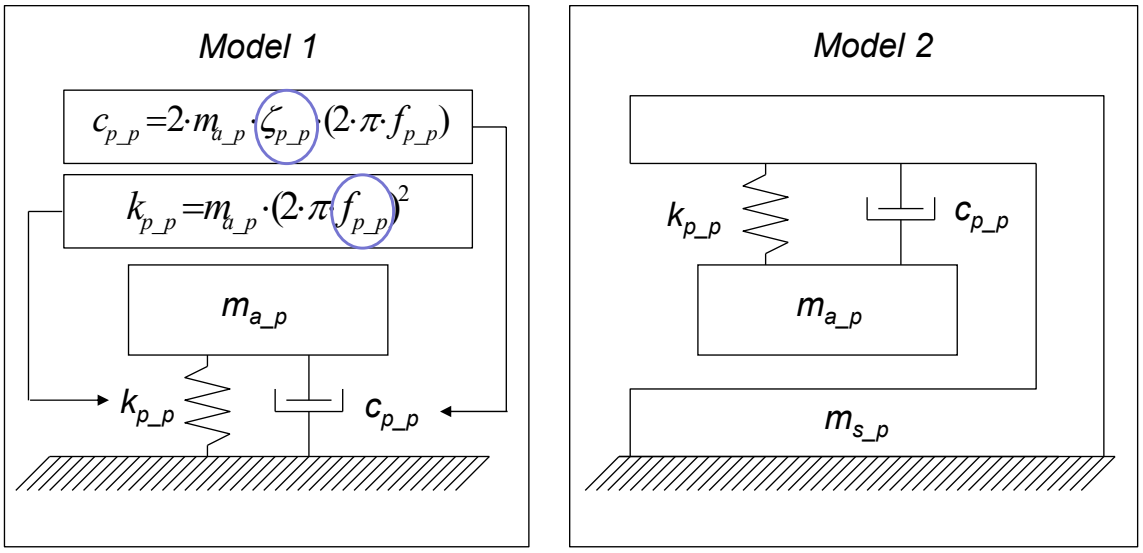

Fig.3. Simplified dynamic models of passive pedestrians on stadiums stands (Jones et al. (2010)).

In Fig. 3 and Table 2, a scheme of the used models, the estimated values of their modal parameters and their range of variation are shown (Jones et al. (2010)), where f_{p_p} is the passive human natural frequency, ζ_{p_p} is the passive equivalent human damping ratio and subsequently m_{a_p}.and m_{s_p} indicate the percentage of passive sprung and unsprung mass respectively of the human body. The main difference between the two passive pedestrian models is the distribution of the total mass of the pedestrian, considering only a sprung component in the "Model 1" and, both sprung and unsprung components in the "Model 2".

Table 2. Dynamic properties for SDOF models of passive pedestrians on stadium stands (Jones et al., 2010).

Author	Model	m_{a_p} [%]	m_{s_p} [%]	ζ_{p_p} [%]	f_{p_p} [Hz]
Foschi et al.	1	100.00	0.00	53.00	3.30
Al-Foqaha'a	1	100.00	0.00	34.00	3.50
Al-Foqaha'a	2	90.00	10.00	36.00	3.70
Brownjohn	1	100.00	0.00	37.00	4.90
Falati	1	100.00	0.00	50.00	10.43
Zheng	1	100.00	0.00	39.00	5.24
Matsumoto	1	100.00	0.00	69.00	5.74
Matsumoto	2	90.00	10.00	61.00	5.88

Minimum		90.00	0.00	34.00	3.30
Maximum		100.00	10.00	69.00	10.43

For our purposes, the parameters characterizing the pedestrian-structure interaction model will be experimentally estimated in Section 3, based on a real footbridge adopted as benchmark.

Modelling the crowd behaviour.

The pedestrian walking inside a crowd may be modelled using the governing equations of particle dynamics (Rapaport, 2004), considering that different social forces interact among pedestrians. This approach has been successfully applied successfully by several authors (Helbing and Molnár, 1995; Carroll et al., 2012). In this way, the different motivation and influences experimented by the pedestrians are described by several force terms. The model is based on Newton dynamics and is able to represent the following rules in relation with the natural pedestrian movement (see (Helbing and Molnár, 1995) for a more involved description): (i) pedestrians normally choose the fastest route, (ii) each pedestrian has an individual speed that may be defined by a Gaussian distribution (iii) and the distance between pedestrians depends on the pedestrian density and the walking pedestrian speed. Fig. 4 sketches the social forces acting on a pedestrian in a crowd, as described in detail in the next sections.

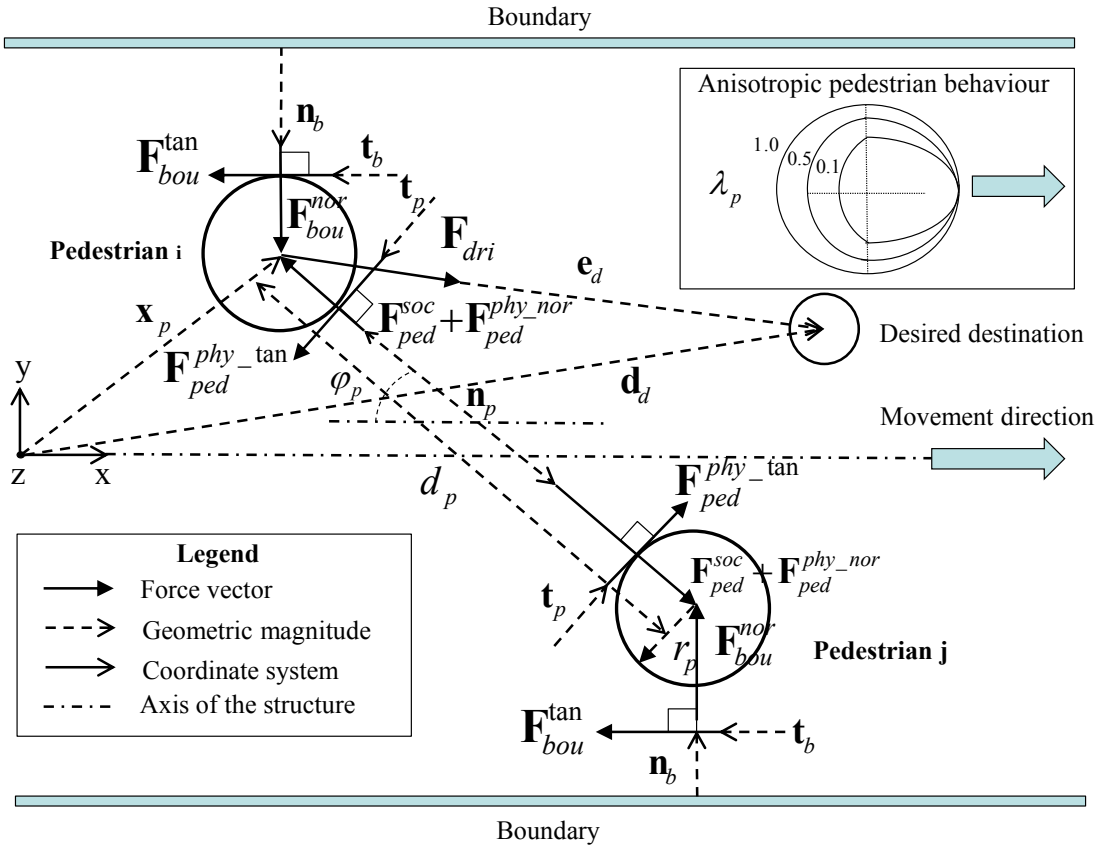

Fig.4. Pedestrian-crowd interaction forces (Helbing and Molnár, 1995).

All the parameters for the crowd model considered in this paper have been obtained from the reported results provided by different authors (Helbing and Molnár, 1995; Carroll et al., 2012), as summarized in Table 3 and briefly described next.

Driving force.

Each pedestrian has a certain motivation to reach his desired destination, $\mathbf{d}_d$, with his desired velocity, v_d, which is represented by the driving force, $\mathbf{F}_{dri}$, as:

$$\mathbf{F}_{dri} = m \cdot \left(\frac{v_d \cdot \mathbf{e}_d}{t_r} - \frac{\mathbf{v}_p}{t_r} \right) \tag{19}$$

where $\mathbf{e}_d$ is the desired direction vector, $\mathbf{v}_p$ is the pedestrian step velocity and t_r is the relaxation time of the pedestrian (Helbing and Molnár, 1995) (Table 3). The desired

direction of the movement may be obtained from the position of the pedestrian in each instant, $\mathbf{x}_p$, and its desired destination according to:

$$\mathbf{e}_d = \frac{\mathbf{d}_d - \mathbf{x}_p}{\left\| \mathbf{d}_d - \mathbf{x}_p \right\|} \tag{20}$$

Interactions among pedestrians.

The interaction among pedestrians originates a repulsive force (Helbing and Molnár, 1995), $\mathbf{F}_{ped}$, with two components, a socio-psychological force, $\mathbf{F}_{ped}^{soc}$, and a physical interaction force, $\mathbf{F}_{ped}^{phy}$, as:

$$\mathbf{F}_{ped} = \mathbf{F}_{ped}^{soc} + \mathbf{F}_{ped}^{phy} \tag{21}$$

The socio-psychological force reflects the fact that the pedestrians try to maintain a certain distance to other pedestrians in the crowd. This socio-psychological force depends on the distance between pedestrians, reaching its maximum value at the lowest established distance and tending to zero as such distance increases. The socio-psychological force is defined as:

$$\mathbf{F}_{ped}^{soc} = A_p \cdot \exp\left(\frac{2 \cdot r_p - d_p}{B_p} \right) \cdot \mathbf{n}_p \cdot s_p \tag{22}$$

where

A_p is the interaction strength between pedestrians (Table 3).

B_p is the range of the repulsive interaction between pedestrians (Table 3).

d_p is the distance between two pedestrians.

r_p is the so-called pedestrian radius (Table 3).

$\mathbf{n}_p$ is the normalized vector pointing between pedestrians.

s_p is a form factor to consider the anisotropic behaviour (the pedestrian action in front of the pedestrian is more important than behind him) of the pedestrians, which value may be obtained from:

$$s_p = \lambda_p + (1-\lambda_p)\cdot\frac{1+\cos(\varphi_p)}{2} \tag{23}$$

where λ_p (Table 3) is a potential factor that considers the influence on the pedestrian movement of other pedestrians situated in front of him (Fig. 4).

φ_p is the angle between two pedestrians (Fig. 4).

The physical interaction force, $\mathbf{F}_{ped}^{phy}$, is only considered in situations of physical contact among pedestrians (if $d_p \le 2\cdot r_p$), associated with situations of high pedestrian densities (≥0.80 P=Person/m2). The physical interaction force is defined by the superposition of two components: (i) the body force, $\mathbf{F}_{ped}^{phy\_nor}$, that describes the counteracting body action that the pedestrians perform to avoid physical damage due to their physical contact with other individuals, (ii) and the sliding force, $\mathbf{F}_{ped}^{phy\_\tan}$, that represents the pedestrians' tendency to avoid passing other individuals with a high velocity at small distances (Helbing and Molnár, 1995). It is defined as:

$$\mathbf{F}_{ped}^{phy} = \mathbf{F}_{ped}^{phy\_nor} + \mathbf{F}_{ped}^{phy\_\tan} \tag{24}$$

$$\mathbf{F}_{ped}^{phy\_nor} = C_p \cdot H\left(2\cdot r_p - d_p\right)\cdot \mathbf{n}_p \tag{25}$$

$$\mathbf{F}_{ped}^{phy\_\tan} = D_p \cdot H\left(2\cdot r_p - d_p\right)\cdot \Delta v_p^t \cdot \mathbf{t}_p \tag{26}$$

where

$\mathbf{F}_{ped}^{phy\_nor}$ is the normal component of the physical interaction force (body force).

$\mathbf{F}_{ped}^{phy\_\tan}$ is the tangential component of the physical interaction force (sliding force).

C_p is the body force strength due to the contact between pedestrians (Table 3).

D_p is the sliding force strength due to the contact between pedestrians (Table 3).

$\mathbf{t}_p$ is a normalized vector perpendicular to $\mathbf{n}_p$.

$\Delta v_p^t = \Delta \mathbf{v}_p \cdot \mathbf{t}_p$ is the tangential component of the relative pedestrian velocity, with $\Delta \mathbf{v}_p$ being the difference of velocities between two given pedestrians.

and function H is defined as:

$$H(\bullet)\cdot = \begin{matrix} \bullet & if & \bullet > 0 \\ 0 & if & \bullet \le 0 \end{matrix} \tag{27}$$

Interactions with boundaries.

The interaction with the boundaries gives rise to forces, $\mathbf{F}_{bou}$. These forces are equivalent to the ones resulting from the interaction with other pedestrian, so they can be formulated in a similar fashion.

$$\mathbf{F}_{bou} = \mathbf{F}_{bou}^{nor} + \mathbf{F}_{bou}^{\tan} \tag{28}$$

$$\mathbf{F}_{bou}^{nor} = \left\{ A_b \cdot \exp\left(\frac{r_p - d_b}{B_b} \right) + C_b \cdot H\left(r_p - d_b\right) \right\} \cdot \mathbf{n}_b \tag{29}$$

$$\mathbf{F}_{bou}^{\tan} = D_b \cdot H\left(r_p - d_b\right) \cdot \left\langle \mathbf{v}_p, \mathbf{t}_b \right\rangle \cdot \mathbf{t}_b \tag{30}$$

where

$\mathbf{F}_{bou}^{nor}$ is the normal component of the boundary interaction force.

$\mathbf{F}_{bou}^{\tan}$ is the tangential component of the boundary interaction force.

A_b is the interaction strength between the pedestrian and the boundary (Table 3)..

B_b is the range of the repulsive interaction between the pedestrian and the boundary (Table 3)..

d_b is the distance between the pedestrian and the boundary.

C_b is the body force strength due to the contact with the boundary (Table 3).

D_b is the sliding force strength due to the contact with the boundary (Table 3).

$\mathbf{n}_b$ is the normalized vector defined perpendicularly from the pedestrian to the boundary.

$\mathbf{t}_b$ is the vector perpendicular to $\mathbf{n}_b$.

$\langle\ \rangle$ denotes scalar product.

Resultant force.

Finally, the proposed multi-agent model that simulates the behaviour of the crowd consists in the sum of all these partial forces that represent the different influences that the pedestrians suffer when interacting in a crowd. Therefore, the resultant force, $\mathbf{F}_{pci}$, describes the movement and direction of each pedestrian in the crowd as:

$$\mathbf{F}_{pci} = \mathbf{F}_{dri} + \mathbf{F}_{ped} + \mathbf{F}_{bou} \tag{31}$$

Table 3. Crowd model parameters considered (Helbing and Molnár, 1995; Carroll et al., 2012).

Parameter	Element	Value
Relaxation time	t_r	0.50 sec.
Interaction strength pedestrians	A_p	2000 N
Interaction range pedestrians	B_p	0.30 m
Potential factor	λ_p	0.20
Contact strength pedestrians	C_p	2000 N
Sliding strength pedestrians	D_p	4800 N
Interaction strength boundaries	A_b	5100 N
Interaction range boundaries	B_b	0.50 m
Contact strength boundaries	C_b	2000 N
Sliding strength boundaries	D_b	4800 N
Radius of pedestrian	r_p	0.20 m

For the generation of pedestrians flows three parameters have been considered, the pedestrian density established by international standards (Butz et al., 2007; Setra, 2006) according to the expected pedestrian traffic on the footbridge, the value of the desired velocity, v_d, of the pedestrians and the distance between pedestrians, d_p. In this paper a one-way traffic has been considered for simplicity in the generation of the pedestrian flows, although the model may be easily generalized for two-way traffic.

The values of the desired velocity of each pedestrian have been obtained from the pedestrian step frequencies, f_s. For the present crowd-structure interaction model the Gaussian distribution of the pedestrian step frequency provided by Zivanovic et al (2010) has been adopted, $N(1.87,0.186)\,\text{Hz}$ (where $N(\mu,\sigma)$ is the Gaussian distribution, μ is the mean value and σ is the standard deviation). After assigning a step frequency to each pedestrian, its desired velocity is determined from the empirical relation given by Bertram and Ruina (2001) (Bruno and Venuti (2009)),

$$f_s = 0.35 \cdot \left|\mathbf{v}_p\right|^3 - 1.59 \cdot \left|\mathbf{v}_p\right|^2 + 2.93 \cdot \left|\mathbf{v}_p\right| \tag{32}$$

so that the initial conditions for each pedestrian assume that the pedestrian velocity, v_p, is equals to the desired velocity, v_d.

Finally, once the pedestrian density and the desired velocity of each pedestrian are established, the original distance among pedestrians is calculated considering the width of the footbridge and assuming a rectangular-shaped mesh of pedestrians.

Solution procedure.

The resultant crowd-structure interaction force, $\mathbf{F}_{pci}$, acts on each pedestrian during each time iteration *j*. The acceleration vector, $\mathbf{a}_p^j$, follows from

$$\mathbf{a}_p^j = \frac{\mathbf{F}_{pci}^j}{m} \tag{33}$$

considering a pedestrian mass, $m\,(= m_s + m_a)$.

The evaluation of the remaining variables that govern the crowd model, $\mathbf{v}_p^{j+1}$ and $\mathbf{x}_p^{j+1}$, is then performed using a multi-step method based on a predictive-corrective method, namely the Gear's algorithm (Heermann, 1986), due to the fact that the social forces depend on the velocity and the position of the pedestrians. The algorithm calculates first an approximate value, called a predictor that subsequently is corrected with a corrector value. The algorithm applied in this case is of fifth order. First, the new locations, velocities, accelerations and higher derivatives are predicted according to -Eqs.(34) to (37)-, where the superscript $^{(p)}$ indicates a predicted value.

$$\mathbf{x}_p^{(p)j+1} = \mathbf{x}_p^j + \Delta t \cdot \mathbf{v}_p^j + \frac{\Delta t^2}{2} \cdot \mathbf{a}_p^j + \frac{\Delta t^3}{6} \cdot \boldsymbol{\alpha}_p^j + \frac{\Delta t^4}{24} \cdot \boldsymbol{\beta}_p^j \tag{34}$$

$$\mathbf{v}_p^{(p)j+1} = \mathbf{v}_p^j + \Delta t \cdot \mathbf{a}_p^j + \frac{\Delta t^2}{2} \cdot \boldsymbol{\alpha}_p^j + \frac{\Delta t^3}{6} \cdot \boldsymbol{\beta}_p^j \tag{35}$$

$$\mathbf{a}_p^{(p)j+1} = \mathbf{a}_p^j + \Delta t \cdot \boldsymbol{\alpha}_p^j + \frac{\Delta t^2}{2} \cdot \boldsymbol{\beta}_p^j \tag{36}$$

$$\boldsymbol{\alpha}_p^{(p)j+1} = \boldsymbol{\alpha}_p^j + \Delta t \cdot \boldsymbol{\beta}_p^j \tag{37}$$

where $\boldsymbol{\alpha}_p$ is the first derivative of $\mathbf{a}_p$ and $\boldsymbol{\beta}_p$ is the second derivative of $\mathbf{a}_p$. From these predicted locations, the difference between the acceleration at time step *j+1* and the predicted acceleration $\mathbf{a}_p^{(p)j+1}$ is obtained (Eq.(38)) from

$$\boldsymbol{\Delta}_{cor} = \mathbf{a}_p^{j+1} - \mathbf{a}_p^{(p)j+1} \tag{38}$$

This correction factor vector, $\mathbf{\Delta}_{cor}$, allows for obtaining the corrected locations, velocities and higher derivations according to

$$\mathbf{x}_p^{j+1} = \mathbf{x}_p^{(p)j+1} + \mathbf{\Delta}_{cor} \frac{\Delta t^2}{2} \cdot \frac{19}{120} \tag{39}$$

$$\mathbf{v}_p^{j+1} = \mathbf{v}_p^{(p)j+1} + \mathbf{\Delta}_{cor} \frac{\Delta t}{2} \cdot \frac{3}{4} \tag{40}$$

$$\boldsymbol{\alpha}_p^{j+1} = \boldsymbol{\alpha}_p^{(p)j+1} + \mathbf{\Delta}_{cor} \frac{1}{3\Delta t} \cdot \frac{1}{2} \tag{41}$$

$$\boldsymbol{\beta}_p^{j+1} = \boldsymbol{\beta}_p^{(p)j+1} + \mathbf{\Delta}_{cor} \frac{1}{12\Delta t^2} \cdot \frac{1}{12} \tag{42}$$

Crowd-structure interaction.

The maximum vertical acceleration experienced by each pedestrian crossing the structure, $\left(\ddot{z}_a\right)_{\max}$ may be compared against the acceleration threshold values established by international codes (Butz et al., 2007; Setra, 2006) in order to modify the individual pedestrian behaviour due to the response of the structure. Due to the good tolerance of pedestrians to vertical vibrations (Racic et al., 2009; Zivanovic at al., 2005) only a stop threshold has been established. In this way, when the vertical acceleration experienced by a pedestrian exceeds the acceleration limite, $\ddot{z}_{\lim} = 2.50$ m/s^2 (Setra, 2006), pedestrians stop walking to maintain balance, and they remain stopped until the acceleration level reduces again, considering for both actions a reaction time, $t_{rea} = 2.00$ sec. A linear variation of the pedestrian velocity during the reaction time has been assumed. In order to avoid meaningless small walking velocities, a practical lower limit on walking velocity magnitude has been imposed as suggested by Carrol et al. (2012).

$$\left|v_p\right| = \begin{cases} 0.1\cdot\left|v_d\right| & if \quad \left(\ddot{z}_a\right)_{\max} < \ddot{z}_{\lim} \cap \left|v_p\right| \le 0.1\cdot\left|v_d\right| \\ 0 & if \quad \left(\ddot{z}_a\right)_{\max} \ge \ddot{z}_{\lim} \end{cases} \tag{43}$$

EXPERIMENTAL ESTIMATION OF THE PARAMETERS OF THE PEDESTRIAN STRUCTURE INTERACTION MODEL.

Inverse dynamic problem methodology implemented.

The estimation of the parameters that characterize the dynamic behaviour of the proposed pedestrian-structure interaction model in vertical direction has been performed from the response of a real footbridge under the crossing of two pedestrians by solving the corresponding inverse dynamic problem methodology. In Fig. 5 the flowchart of the identification procedure is shown.

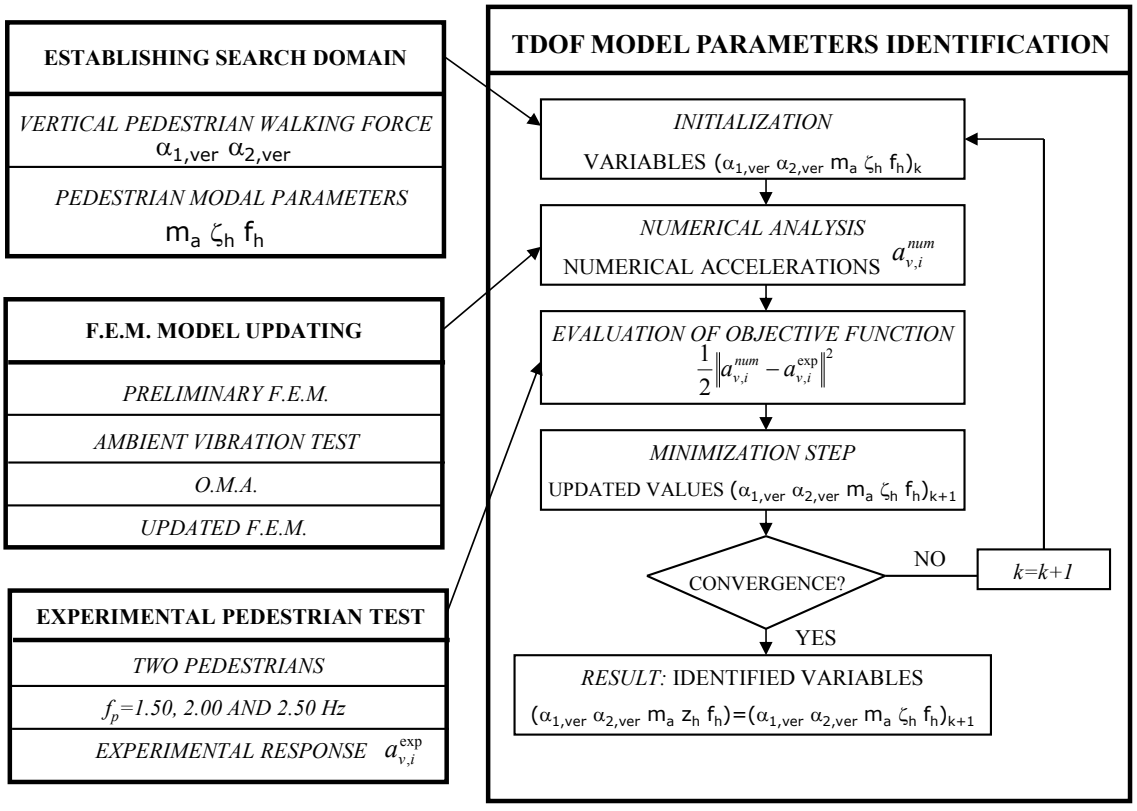

Fig.5. Flowchart of the identification procedure.

As identification method the minimization of a least squares problem has been adopted (Koh and Perry, 2010). The objective function has been defined as the mean square error between the experimental ($a_{v,i}^{\exp}$, where *i* is the considered section) and numerical ($a_{v,i}^{num}$) vertical accelerations obtained, in four points of the Viana footbridge (Barbosa et al., 2012), under the crossing of two pedestrians at controlled step frequencies. Genetic algorithms have been used to ensure a global optimization and a search domain for each parameter has been established. The characterization of the dynamic behaviour of the footbridge has been performed by the finite element model updating (Teughels, 2003; Zivanovic et al., 2007) based on the modal parameters of the structure estimated from the application of an operational modal analysis (Magalhães and Cunha, 2011). An ambient test has been performed on Viana footbridge and the measured signals have been processed by an output-only identification method in the time domain, which provided estimates of the its first four natural frequencies, the corresponding modal shapes and the associated damping ratios (Magalhães et al., 2010). (Fig.6). Later, this test has been reproduced numerically by the implementation of the proposed pedestrian-structure interaction model. An iterative process to reduce the differences between the experimental and numerical vertical accelerations has been performed, under the rules of genetic algorithms (Koh and Perry, 2010; Nocental and Wright, 1999**)**, and considering as design variables the first two VDLF ($\alpha_{1,ver}$ and $\alpha_{2,ver}$) of the pedestrian walking force and the three modal parameters that characterizes the TDOF pedestrian-structure interaction model; the pedestrian sprung mass, m_a, the pedestrian damping ratio, ζ_p, and the pedestrian natural frequency, f_p.

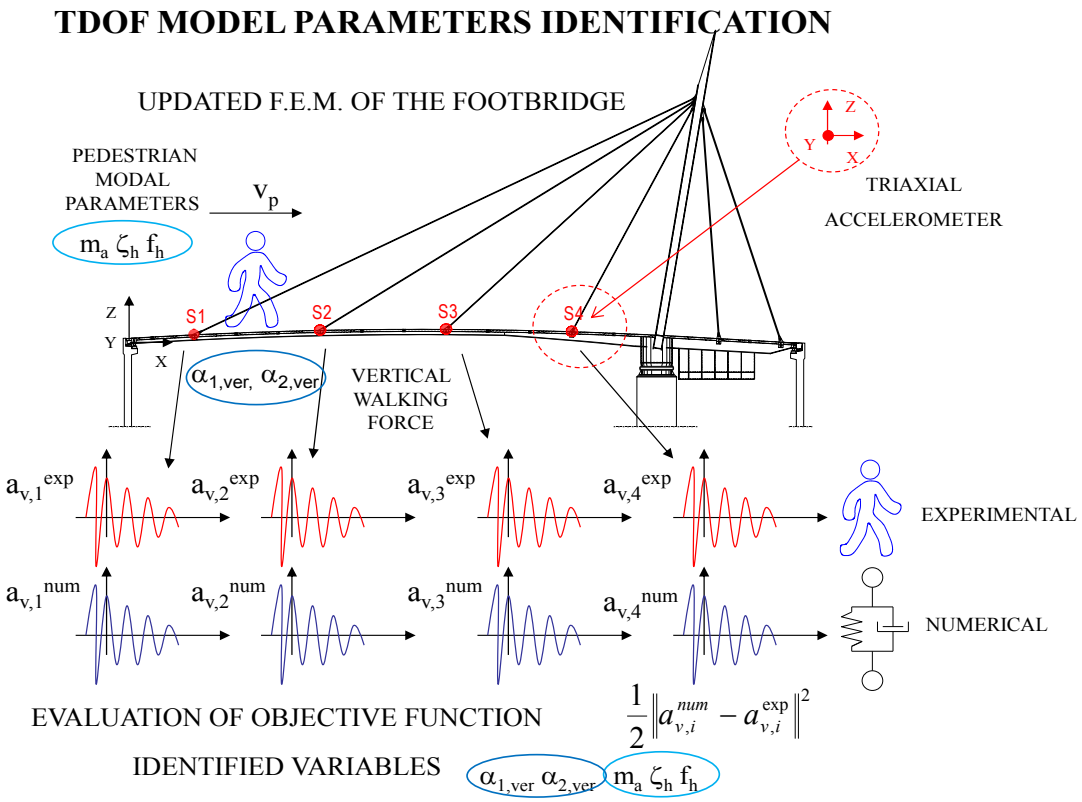

Fig.6. Layout of the identification methodology.

Establishing a preliminary search domain for the parameters of the pedestrian-structure model.

In order to reduce the uncertainty of the estimated values of the five considered parameters and thus prevent an ill-conditioned inverse problem, a search domain has been established.

According to Table 1 the minimum and maximum values of each VDLF allow establishing a search domain for their experimental estimation. In order to take into account that the estimation of these parameters will be performed from measurements carried out on a real footbridge, the above mentioned search domains have been extended. As the value of the third harmonic of the walking pedestrian force proposed by the different authors has a lower magnitude its contribution has been neglected.

Similarly, the phase shifts of the second and third harmonic of the vertical walking force have not been considered.

Similarly, according to **Table 2**, the minimum and maximum values of the parameters of the passive pedestrian models allow defining the search domains for their estimation. The knowledge of the physical problem suggests: (i) a reduction of the damping and stiffness of the pedestrian associated with its movement and (ii) the change in the human body mass distribution between the active and passive states. The search domains of these parameters have been increased to take into account of these facts.

Thus the following search domains have been adopted:

- First VDLF, $\alpha_{1,ver} \in [0.00 - 0.45]$.
- Second VDLF, $\alpha_{2,ver} \in [0.00 - 0.20]$.
- Pedestrian sprung mass, $m_a \in [80 - 100]\%$.
- Pedestrian damping ratio, $\zeta_p \in [10 - 69]\%$.
- Pedestrian natural frequency, $f_p \in [1 - 10.43]$ Hz.

Description and finite element model of the "laboratory" footbridge: Viana footbridge.

The Viana do Castelo footbridge (Barbosa et al., 2012) is a moveable cable-stayed bridge. The longitudinal structural scheme of the footbridge consists of two spans of about 36.50 m and 9.00 m respectively suspended by 6 families of two hangers (two retaining ones) from an inclined mast. The deck, with 2.50 m of width, is configured by two rolled steel beams of variable depth braced by circular hollow profiles. The deck floor is covered with wood. The compensation of the main span weight is achieved by

placing 11 high density blocks (with a weight of 800 kN) placed in the shorter span. The mast is welded in its base to a cylinder that is connected to a wheel gear bearing that allows the rotational movement of the structure. The pylon is connected to a deep foundation that balances the forces transmitted by the mast. A perspective of the Viana footbridge is shown in Fig.7.

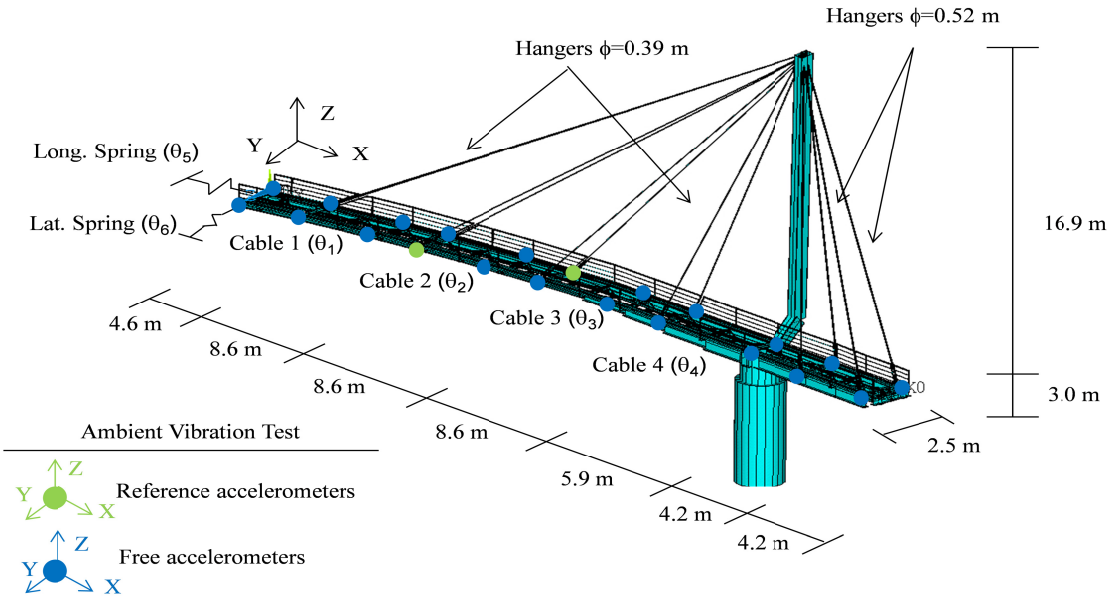

Fig.7. Finite element model, ambient test grid and model updating parameters.

A preliminary numerical finite element (Fig.7) modal analysis was conducted in order to have a first approximation to the dynamic behaviour of the footbridge and a starting point required to perform the ambient vibration test. The software package Ansys (Ansys, 2014) was used, based on a discretization of the structure in 3D-beam elements (BEAM188) except for the hangers where 3D-cable elements (LINK10) were implemented. The nonlinear effects associated with the hangers have been considered for the determination of the numerical natural frequencies and the vibration modes of the structure, by calculating previously the stress level of the hangers under permanent loads and thus estimating its tangent stiffness matrix. The numerical modal analysis of this preliminary FE model leads to the first four numerical vibration modes and associated numerical natural frequencies given in Table 4. In Fig.8 the first two

numerical vertical vibration modes are shown (f_{NUM}_i, with *i* being the vibration mode number).

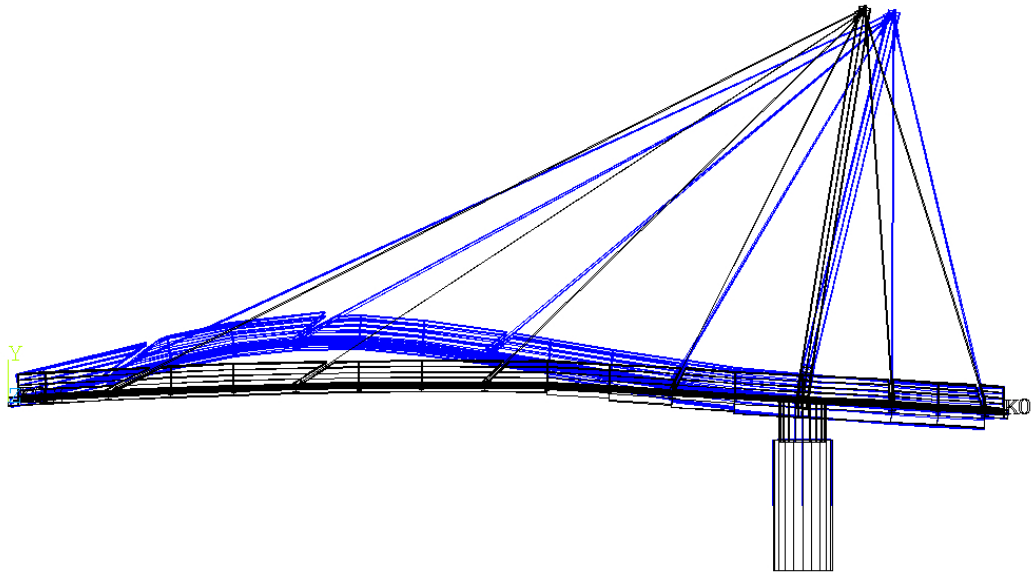

$f_{NUM\ 1}$=3.426 Hz. First numerical vertical vibration mode.

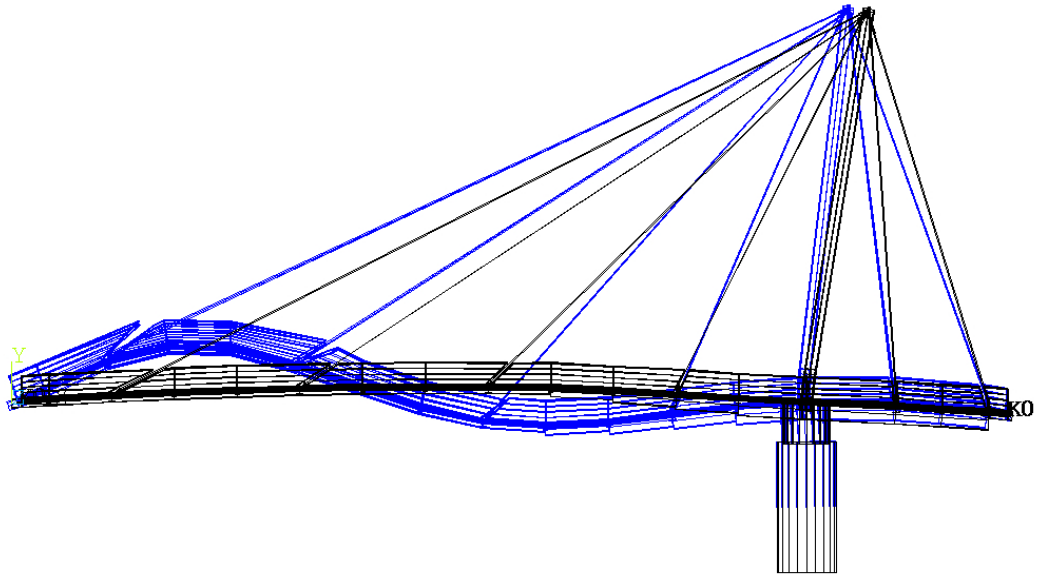

$f_{NUM\ 4}$=7.431 Hz. Second numerical vertical vibration mode.

Fig.8. First two numerical vertical vibration modes. Initial FE model.

Experimental identification of the modal parameters of the footbridge.

In order to obtain experimentally the modal parameters (natural frequencies, damping ratios and modal shapes) of the footbridge, an ambient vibration test was performed.

The measurements were conducted in ambient condition, with the footbridge excited by a light wind. The modal shape coordinates were measured along two gridlines, separated transversally 1.68 m. A total of 2x11 points equally distributed along each longitudinal alignment were instrumented. Four high sensitivity tri-axial force balanced accelerometers were used. Using two of these devices as references, measurements were successively made moving the other two accelerometers to the defined instrumentation locations and recording in each point 1000 sec. time series of acceleration sampled at 100 Hz. (Fig.7). The experimental identification of the modal parameters was done in the time domain using the Stochastic Subspace Identification method (Magalhães and Cunha, 2011), implemented in the software program Artemis (Artemis, 2014). The first four vibration modes were identified and subsequently used for the FE model updating process (see Appendix II). The obtained numerical and experimental natural frequencies and vibration modes shapes are compared in Table 4 and the correlation between the first two numerical and experimental vibration modes in vertical direction is shown in Fig.9 (with the x axis corresponding to the longitudinal direction of the footbridge). In order to validate the correlation between the numerical and experimental modal parameters both the relative difference (Δf) between the numerical and experimental frequencies, Eq. (52), and the modal assurance criterion (*M.A.C.*) , Eq. (53), were analysed (Zivanovic et al., 2007). A good correlation between two modes is achieved when the value of its M.A.C. ratio is greater than 0.90.

Table 4. First four numerical (f_{NUM}) versus experimental (f_{EXP}) vibration modes of the footbridge.

Modes	**f_{NUM} [Hz]**	**f_{EXP} [Hz]**	ζ_i [%]	Δf [%]	**M.A.C.**	**Description**
1	3.426	3.138	1.22	9.17	0.963	First vertical mode
2	4.421	4.068	1.21	8.67	0.985	First lateral mode
3	6.907	6.810	1.10	1.42	0.809	Second lateral mode
4	7.431	7.345	1.39	1.17	0.939	Second vertical mode

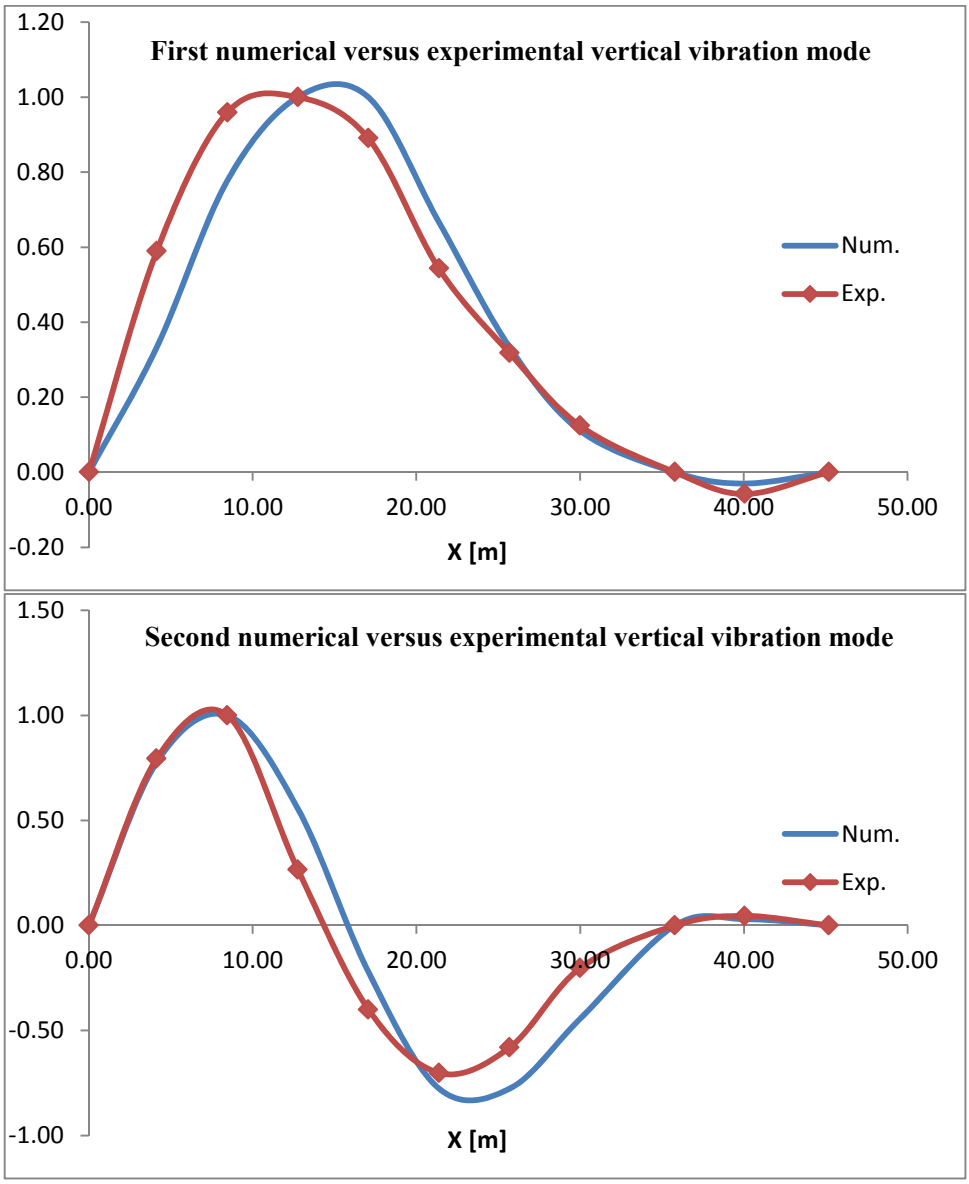

Fig. 9. First two vertical numerical (Num.) versus experimental (Exp.) vibration modes.

Although the shapes of the identified vibration modes are in good agreement (with M.A.C. ratios greater than 0.90 in three of the vibration modes), the relative differences, Δf, between the first two numerical and experimental natural frequencies are still significant. Therefore, the initial estimation made on the physical parameters of the structure is not good enough and it becomes necessary to perform a FEM updating (Friswell and Mottershead, 1995; Teughels, 2003) of the footbridge in order to improve the correlation between the numerical and experimental modal parameters.

Finally, in Table 4 an estimation of the damping ratios, ζ_i, associated with the identified vibration modes is also shown (Magalhães et al., 2010). These values will be adopted later in the identification process of the parameters of the TDOF-pedestrian system.

Model updating of the footbridge.

The finite element model updating of the Viana footbridge has been performed in order to reduce the level of uncertainty of the numerical analysis. Given the good quality of the experimental data, the four identified vibration modes were chosen in the updating process. Both measured natural frequencies and modal coordinate values were taken into account. Therefore, in total 48 residual components were selected for the model updating (the four identified natural frequencies and the eleven coordinates of each identified vibration mode).

In order to adequately select the physical parameters of the FE model with greater influence on the identified vibration modes a sensitivity study was performed, so that the modal sensitivities with respect to some possible physical variables have been obtained numerically (Fox and Kapoor (1968)). The results of this study conclude that the physical parameters that mainly determine the dynamic behaviour of the footbridge are the stiffness of the four families of main hangers and the soil-structure interaction, modelled by two springs (in longitudinal, θ_5, and lateral, θ_6 directions, as Fig.7 illustrates) situated at the extreme of the longer span. As the stiffness of the hangers is conditioned by their stress level, the initial stress state of each mentioned family (θ_1, θ_2, θ_3 and θ_4) has also been considered as physical variable. In Fig.7 and Table 5, the selected physical variables are shown.

The model updating process has been conducted through the implementation of the algorithm described in Appendix II in the software programs Ansys (Ansys, 2014) and Matlab (Matlab, 2011). In each iteration a population of 1000 vectors has been created that using the genetic algorithms rules of mutation, reproduction and crossover have minimized the value of the proposed objective function. The values of the selected parameters have been modified in order to minimize the relative differences between the numerical and experimental modal parameters of the footbridge. In order to increase the efficiency of the genetic algorithms and yet maintain the physical meaning of the finite element model updating, a search domain has been defined to control the variation of each parameter. For the stiffness of the hangers, as a passive behaviour is expected, the medium tension level of the hangers has been determined under permanent loads, with a value of 250 kPa. In order to take into account slight variations of this value, the search domain has been set between 0-500 kPa. For the stiffness of the springs (θ_5 and θ_6), given the uncertainty associated with the stiffness of the soil, a wider search domain has been considered, so considering a variation of the Young's modulus of soil between $E_m = 1-100$ GPa the variation of the equivalent stiffness of the springs has been obtained θ_5 and $\theta_6 \in [10^7 - 10^9]$N/m. The value provided by the geotechnical report for the project of the structure is inside this range. In Table 5 the range of variation of each parameter and its updated values are shown.

Table 5. Updated values of considered physical parameters.

Parameters	Minimum Value	Updated Value	Maximum Value
Tension stress cable 1 (θ_1).	0.00 kPa	112.38 kPa	500.00 kPa
Tension stress cable 2 (θ_2).	0.00 kPa	59.62 kPa	500.00 kPa
Tension stress cable 3 (θ_3).	0.00 kPa	31.62 kPa	500.00 kPa
Tension stress cable 4 (θ_4).	0.00 kPa	147.43 kPa	500.00 kPa
Longitudinal Spring (θ_5).	1.00E7 N/m	6.00E7 N/m	1.00E9 N/m
Lateral Spring (θ_6).	1.00E7 N/m	1.90E8 N/m	1.00E9 N/m

The relative differences between the updated numerical (f_{UPD}) and experimental (f_{EXP}) modal parameters and the *M.A.C.* values achieved after the model updating process are summarized in Table 6, where the improvement with respect to the initial FE model is clear (see Table 4).

Table 6. First four updated numerical (f_{UPD}) and experimental (f_{EXP}) vibration modes of the footbridge.

Modes	**f_{UPD} [Hz]**	**f_{EXP} [Hz]**	Δf [%]	**M.A.C.**	**Description**
1	3.136	3.138	-0.06	0.999	First vertical mode
2	4.052	4.068	-0.39	0.999	First lateral mode
3	6.799	6.810	-0.16	0.998	Second lateral mode
4	7.342	7.345	-0.04	0.999	Second vertical mode

Similarly, Fig. 10 illustrates the correlation between the updated numerical and the experimental vertical vibration modes, with an excellent agreement.

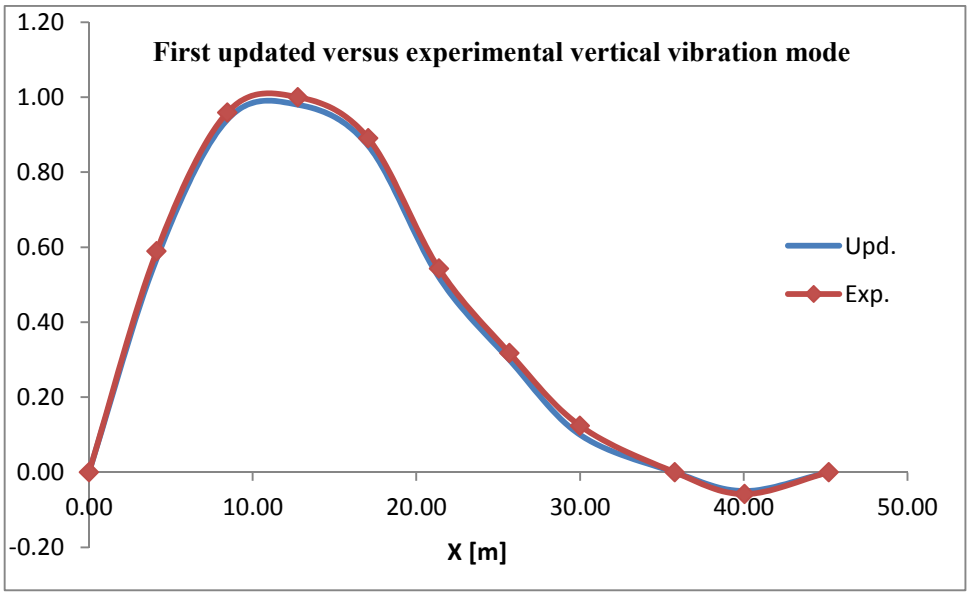

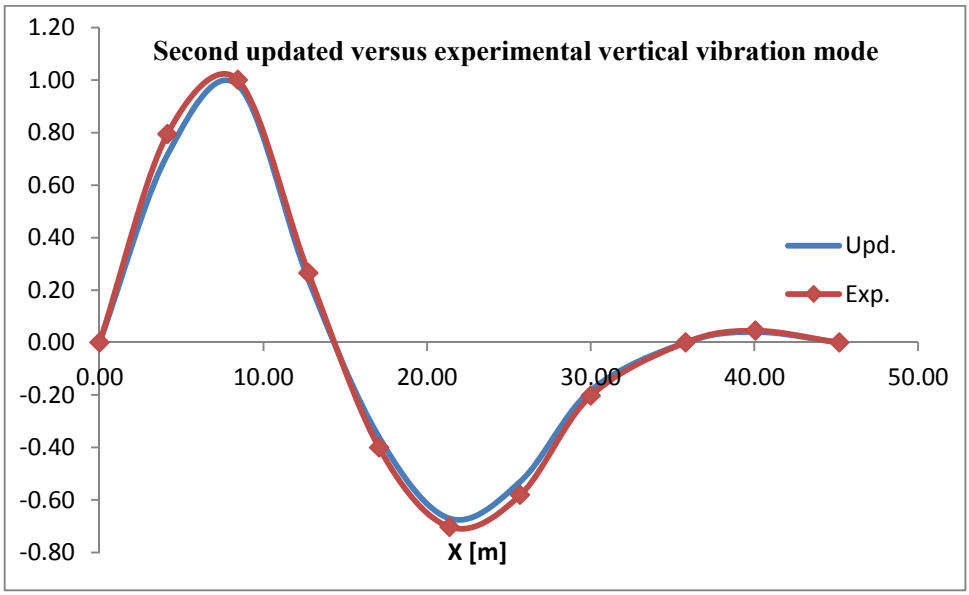

Fig.10. First two vertical updated numerical (Upd.) and experimental (Exp.) vibration modes.

After the development of the model updating, the numerical dynamic behaviour of the footbridge simulates accurately the real response of the footbridge. This detailed knowledge of the dynamic behaviour of the footbridge allows for adopting this real footbridge as a benchmark or "laboratory" footbridge.

Experimental pedestrian test.

The estimation of the parameters that characterize the behaviour of the proposed pedestrian-structure interaction model was made through the results of a pedestrian test. In the test, two pedestrians (A and B) were selected. The mass of each pedestrian was $m_A = 61.70\,\text{kg}$ and $m_B = 100.50\,\text{kg}$. On the deck of the footbridge four triaxial accelerometers were placed at the intersection point between the hangers and the deck (Fig.6). Three series were recorded for each pedestrian, crossing the footbridge three times at different step frequencies, f_s (1.50, 2.00, 2.50 Hz), controlled by a metronome. In the four monitored sections (S_1, S_2, S_3 and S_4 in Fig.6) the dynamic response of the

structure was recorded. In each passage, the initial and end time, that marks the crossing of the pedestrian on the structure, was recorded as well, in order to both localize the forced vibration response corresponding to the passage of each pedestrian and estimate the pedestrian velocity, v_p.

Parameters identification in time domain.

For the estimation of the parameters of the TDOF-system (Koh and Perry, 2010), an inverse dynamic problem was solved, as it has been described previously. As objective function the relative differences between the experimental and numerical vertical accelerations in four sections of the footbridge (S_1, S_2, S_3 and S_4) has been considered. As optimization method, genetic algorithms have been used again. The experimental vertical accelerations correspond to the measurements of the above described pedestrian test. The numerical vertical accelerations have been obtained from the implementation of the proposed pedestrian-structure interaction model on the updated finite element model of the Viana footbridge. Six parameters were adopted as design variables:

(i) the first two VDLF that characterize the pedestrian walking force.

(ii) the three modal parameters (pedestrian sprung mass, pedestrian damping ratio and pedestrian natural frequency) that govern the behaviour of the TDOF-system.

(iii) a time lag that allows adjusting the beginning of the crossing of the pedestrian between the experimental and numerical accelerations.

In order to improve the reliability of the parameters estimation the level of noise of the signal has been reduced (Koh and Perry, 2010). In that way, each measurement record has been decomposed using the Wavelet transform (Gopalakrishnan and Mitra, 2014), choosing as wavelet family, the Daubechies. A level 7 of decomposition has been

applied to each signal. As threshold selection rule, the principle of Stein's Unbiased Risk Estimate has been considered (Gopalakrishnan and Mitra, 2014). Subsequently, the reconstruction of the signal has been carried out using the original approximation coefficients of level 7 and the modified detail coefficients of levels from 1 to 7. For each series, a generation of 1000 individuals has been defined. Each individual modifies, according to the rules of genetic algorithms, the values of its components in order to minimize the defined objective function. In Table 7, the results of the estimation process are summarized, showing the different estimated parameters versus the pedestrian step frequency.

Table 7. Estimation of the parameters of the pedestrian-structural interaction model.

	Pedestrian sprung mass m_a [%]		
f_s [Hz]	**Minimum**	**Medium**	**Maximum**
1.50	84.995	88.367	91.738
2.00	81.636	86.467	91.297
2.50	82.119	86.583	91.048
	Pedestrian damping ratio ξ_p [%]		
f_s [Hz]	**Minimum**	**Medium**	**Maximum**
1.50	22.143	32.115	42.087
2.00	38.908	45.992	53.076
2.50	40.132	46.214	52.295
	Pedestrian frequency f_p [Hz]		
f_s [Hz]	**Minimum**	**Medium**	**Maximum**
1.50	1.923	2.923	3.924
2.00	2.094	2.915	3.736
2.50	2.295	2.962	3.629
	Vertical dynamic load factor $\alpha_{1,ver}$		
f_s [Hz]	**Minimum**	**Medium**	**Maximum**
1.50	0.201	0.203	0.206
2.00	0.214	0.235	0.255
2.50	0.224	0.273	0.322
	Vertical dynamic load factor $\alpha_{2,ver}$		
f_s [Hz]	**Minimum**	**Medium**	**Maximum**
1.50	0.039	0.040	0.041
2.00	0.040	0.042	0.043
2.50	0.043	0.047	0.051

According to the results of Table 7 the parameters of proposed pedestrian-structure interaction model show some dependence on the step pedestrian frequency. However due to the number of pedestrians used during the pedestrian test, only a global mean value, μ, and a standard deviation, σ, have been determined $N(\mu,\sigma)$. For the proposed pedestrian-structure model, the following Gaussian distributions have been considered.

- First VDLF, $\alpha_{1,ver}$, $N(0.237,0.04)$.

- Second VDLF, $\alpha_{2,ver}$, $N(0.043,0.004)$.

- Pedestrian sprung mass, m_a, $N(87.139,3.809)$%.

- Pedestrian damping ratio, ζ_p, $N(41.44,9.776)$ %.

- Pedestrian natural frequency, f_p, $N(2.933,0.728)$ Hz.

The proposed values are inside the range, established by Shahabpoor et al. (2013), that characterizes the modal properties of TDOF pedestrian-structure interaction model. For the generation of the pedestrian flows of the crowd-structure interaction model, the above Gaussian distributions have been considered.

Once obtained the parameters, the definition of the proposed model is complete. This model will be validated in the next section by correlating the numerical and experimental dynamic response of the Viana footbridge under the crossing of a group of pedestrians and the experimental and numerical analysis of the change of the first vertical natural frequency of the structure induced by the pedestrian flow.

MODEL VALIDATION.

The validity and applicability of the proposed crowd-structure interaction model is next assessed through its practical application to a case study. The vertical acceleration at three sections (S_1, S_2, and S_3 (Fig.6)) of the Viana footbridge has been measured under the crossing of a group of 50 pedestrians at different step frequencies (1.30-2.50 Hz). From the forced recorded response, the experimental study of the change of the first vertical natural frequency of the structure, due to the crossing of the group of pedestrians at different step frequencies, has been determined. Subsequently, the crowd-structure interaction model has been applied to the updated FE model in order to obtain first the vertical numerical acceleration at the mentioned sections and later to study numerically the change of the first vertical natural frequencies of the footbridge due to the presence of the pedestrians.

Experimental crowd test: dynamic response and change of the first natural frequency under pedestrian flow.

In the crowd test a group of 50 pedestrians has crossed the footbridge at different step frequencies (1.30-1.40-1.60-1.75-2-00-2.50 Hz) controlled by a metronome, measuring the vertical dynamic response of the footbridge at three sections S_1, S_2 and S_3 with a tri-axial accelerometer (Fig.6). During the crowd test the group of 50 pedestrians has been distributed in three alignments, maintaining a lateral separation among pedestrians around 0.85 m and a longitudinal distance between pedestrians around 0.50 m. A pedestrian with a metronome has led the group in each crossing. A scheme of the pedestrian distribution during the crowd test is shown in Fig.11.

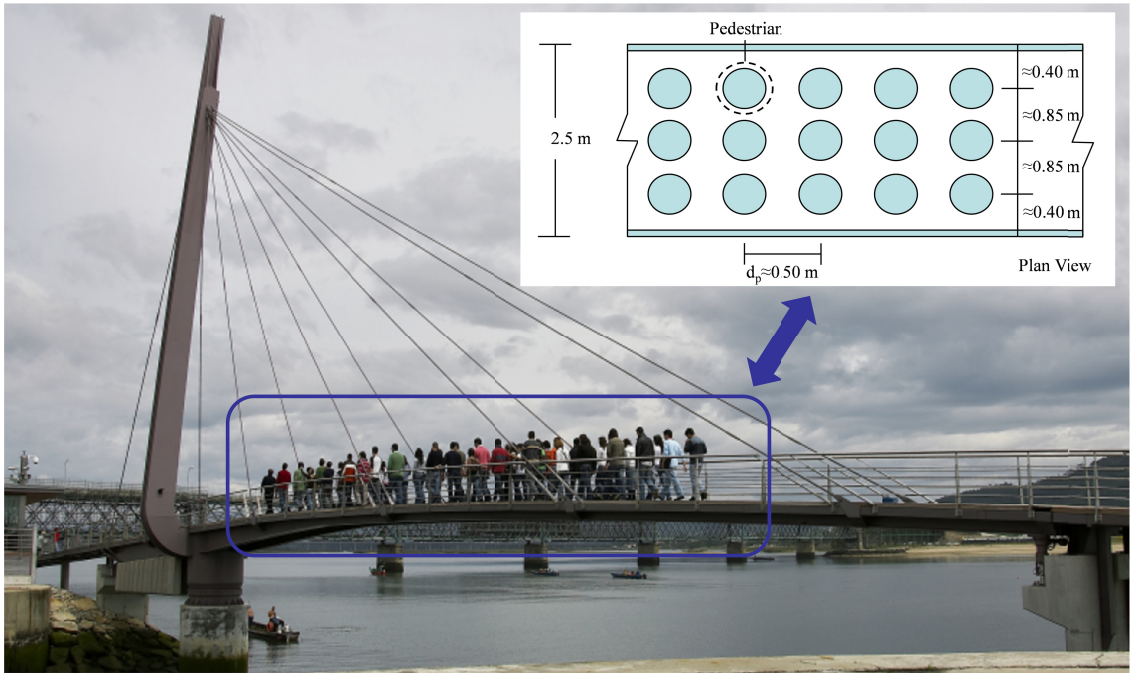

Fig.11. Experimental crowd test at Viana footbridge.

In order to determine the change of the first natural frequency of the footbridge under the crossing of the group of pedestrians at different step frequencies, just the forced vibration response of the structure has been considered. Only the records at section S_2 (higher modal deflection) have been considered. The selected signal has been filtered and processed by the Continuous Wavelet Transform (CWT) (Gopalakrishnan and Mitra, 2014) based on Daubechies family. The maximum value of the wavelet coefficients (Fig.12), in the filtered range of frequencies, is then correlated with the first natural frequency of the structure. This result has been validated by the estimation of the natural frequency through the power spectral density of the above signal (Fig.12) obtained according to the Peak-Picking method (Magalhães and Cunha, 2011). The signal used for the estimation of the power spectral density has been denoised using the methodology previously described.

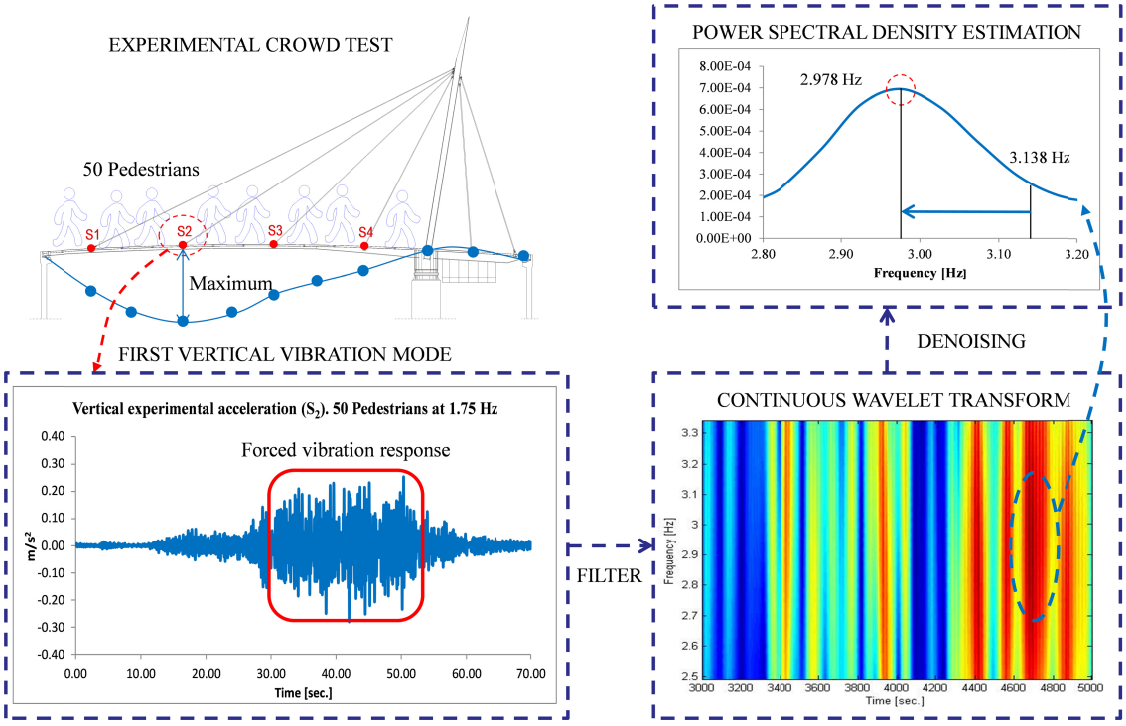

Fig.12. Estimating the change of the first vertical natural frequency of the structure.

To illustrate the recorded results, the measured vertical acceleration of the footbridge in section S_2 under a group of 50 pedestrians at a step frequency of 1.60 Hz is shown in Fig.13.

The experimental study of the change of first vertical natural frequency of the footbridge is summarized in Fig.14.

Numerical crowd test: estimation of the dynamic response and the change of the first natural frequency under pedestrian flow.

The assessment of the model performance has been done correlating the above experimental results with the numerical estimation predicted by the model. For each considered step frequency ten generations of groups with 50 pedestrians have been

simulated. The number of pedestrians in phase in each new simulation has been determined though the evaluation of the parameter ϕ_p. The desired velocity, v_d, of each pedestrian has been assigned according to Eq.(32). A pedestrian mass of 70 kg has been considered according to the French code (Setra, 2006). As initial spatial distribution of the pedestrians, a rectangular grid has been selected, considering an initial distance among pedestrians $d_p = 0.50$ m with an equidistant distribution in the width of the deck. The selected time step is $\Delta t = 0.01$ sec. The numerical vertical acceleration (for three of the 50 pedestrians generations) at section S_2 of the footbridge, for a step frequency of 1.60 Hz, is shown in Fig.13.

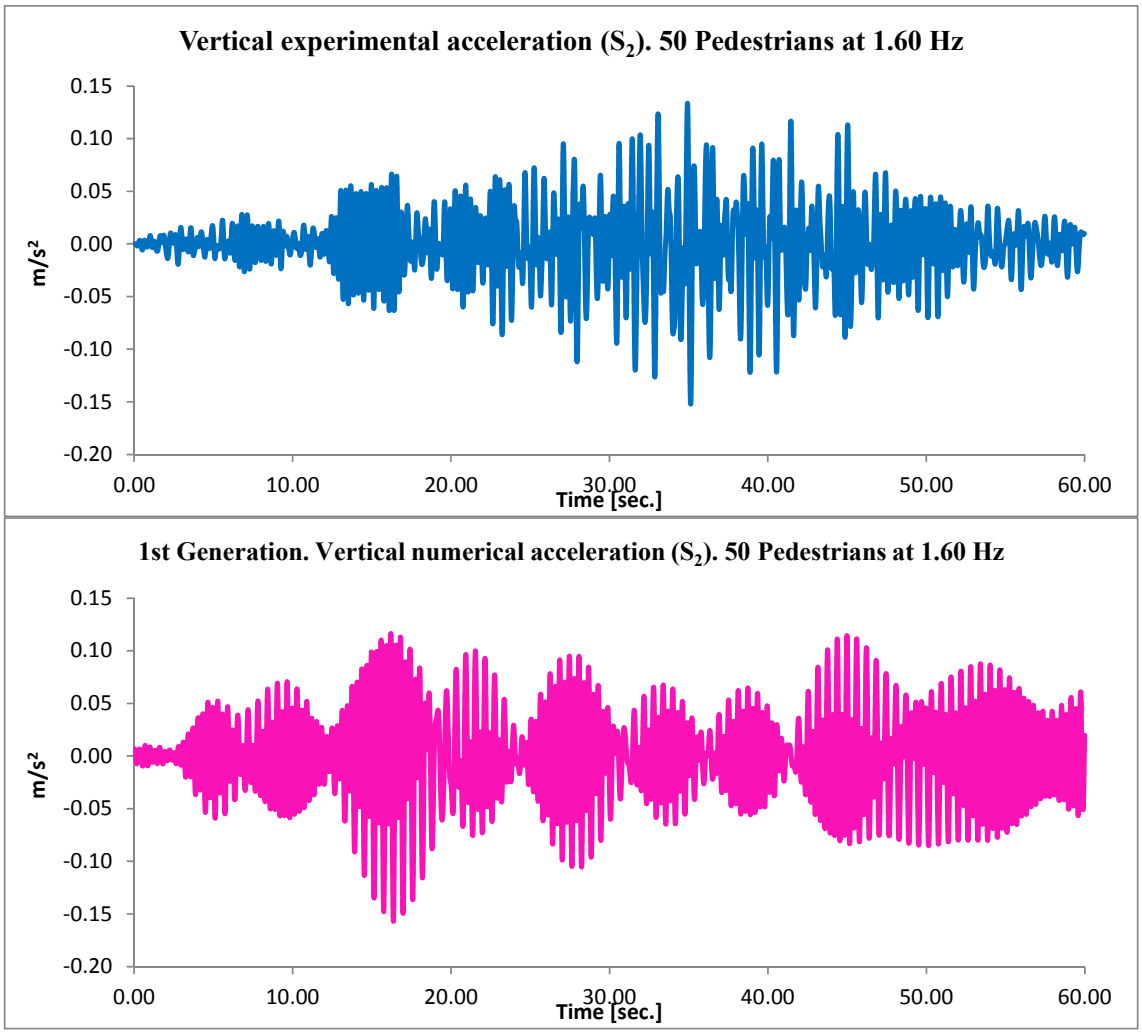

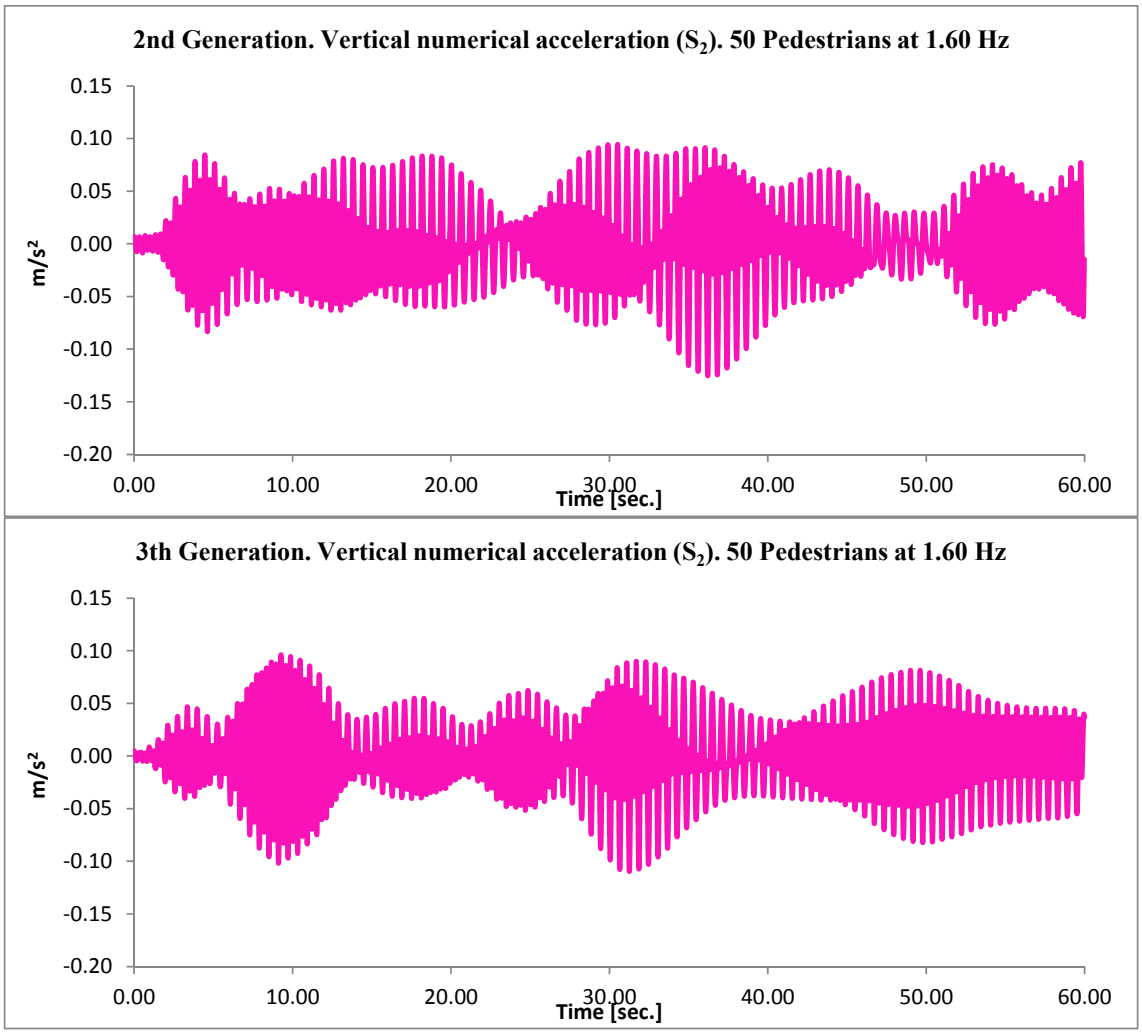

Fig.13. Experimental versus numerical acceleration (three generations) at section S_2 of Viana footbridge under a group of 50 pedestrians (walking frequency of $f_p = 1.60$ Hz).

As Fig.13 shows, the correlation between the experimentally recorded vertical acceleration and the numerically estimated values is adequate, in terms of both the value of the maximum acceleration and its temporal variation.

Finally, the numerically estimated vertical acceleration at section S_2 of the footbridge under a group of 50 pedestrians for different step frequencies has been used to identify the first natural frequency of the structure, following the procedure described in the previous section. Fig.14 illustrates the correlation between experimental and numerical results for the change of first vertical natural frequency of the footbridge induced by the

crowd-structure interaction phenomenon. The numerical estimation of the change of the first vertical natural frequency has been obtained from the mean values of ten simulations for each step frequency. Good agreement between both sets of results is observed, with differences below 1.50 % for all the analysed pedestrian walking frequencies. The first vertical natural frequency corresponding to the empty footbridge is included in Fig.14 for reference.

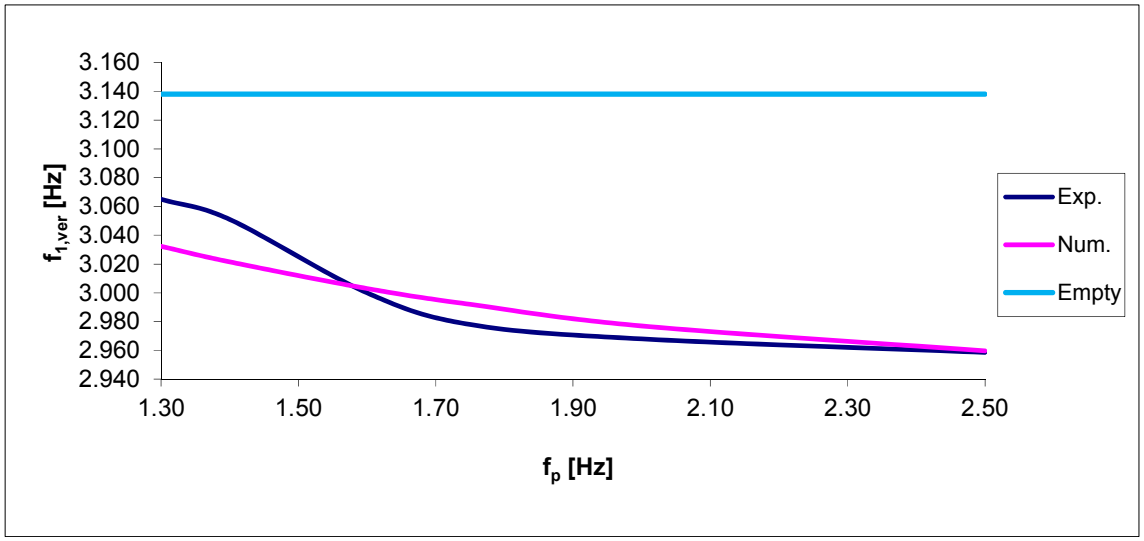

Fig.14. Change of the first vertical, $f_{1,ver}$ [Hz], experimental (Exp.) and numerical (Num.) natural frequency versus the step frequency f_p [Hz].

CONCLUSIONS.

In this paper, a new crowd-structure interaction model in the vertical direction has been presented and further validated through the correlation between the experimental and numerical dynamic response of a real footbridge (Viana) adopted as benchmark. The proposed model has been organized in two sub-models: a pedestrian-structure interaction and a crowd sub-model. The pedestrian-structure interaction sub-model is configured by a TDOF system, with sprung and unsprung masses, whose parameters have been estimated experimentally from the solution of an inverse problem on the

Viana footbridge. The estimated parameters are within the range recommended by previous works. The crowd sub-model is a multi-agent model based on the relationships established by the social force model. The interaction between the two sub-models in the vertical direction is achieved by imposing a stop threshold, so that if certain acceleration limit is exceeded the affected pedestrians stop. The proposed model is formulated under the following hypothesis: (i) the parameter of the pedestrian-structure interaction model are considered as constant, not varying according to the step frequency of each pedestrian, (ii) the dynamic effects of the variation of the pedestrian velocity over the time are neglected and (iii) the direct resolution of the interaction problem has been adapted to walking action. A remarkable application of the model is the analysis of the change of the dynamic properties of the structure due to the presence of pedestrian flows. In that sense, the experimental and numerical change of the first vertical natural frequency of Viana footbridge under a group of 50 pedestrians has been presented. Although the results obtained from the proposed model are adequate, further studies are recommended in order to better characterize the parameters that define the crowd-structure interaction model. In particular for generalizing its use to other directions, the estimation of the parameters of pedestrian model in the longitudinal and lateral direction is needed. Furthermore, additional pedestrian tests, including different pedestrians on different footbridges, would be needed to study the sensitivity of the modal parameters of the pedestrian-structure model versus the step frequency and evaluate experimentally the value of the social forces. Other possible applications of this model lay on improving the efficiency of the damping devices used to control the vibratory problems.

APPENDIX I.

Single pedestrian-structure interaction model matrices and vector.

$$\mathbf{M}(t)=\begin{bmatrix} M_1+\phi_{NUM\_1}(x_p)\cdot m_s\cdot\phi_{NUM\_1}(x_p) & \cdots & \phi_{NUM\_1}(x_p)\cdot m_s\cdot\phi_{NUM\_n}(x_p) & 0 \\ \cdots & \cdots & \cdots & 0 \\ \phi_{NUM\_n}(x_p)\cdot m_s\cdot\phi_{NUM\_1}(x_p) & \cdots & M_n+\phi_{NUM\_n}(x_p)\cdot m_s\cdot\phi_{NUM\_n}(x_p) & 0 \\ 0 & 0 & 0 & m_a \end{bmatrix} \quad (44)$$

$$\mathbf{C}(t)=\begin{bmatrix} C_1 & & & \\ +\phi_{NUM\_1}(x_p)\cdot c_p\cdot\phi_{NUM\_1}(x_p) & \cdots & \phi_{NUM\_1}(x_p)\cdot c_p\cdot\phi_{NUM\_n}(x_p) & -\phi_{NUM\_1}(x_p)\cdot c_p \\ +\phi_{NUM\_1}(x_p)\cdot 2\cdot v_{px}\cdot m_s\cdot\phi_{NUM\_1}(x_p) & & +\phi_{NUM\_1}(x_p)\cdot 2\cdot v_{px}\cdot m_s\cdot\phi_{NUM\_n}(x_p) & \\ \cdots & \cdots & \cdots & \cdots \\ \phi_{NUM\_n}(x_p)\cdot c_p\cdot\phi_{NUM\_1}(x_p) & & C_n & \\ +\phi_{NUM\_n}(x_p)\cdot 2\cdot v_{px}\cdot m_s\cdot\phi_{NUM\_1}(x_p) & \cdots & +\phi_{NUM\_n}(x_p)\cdot c_p\cdot\phi_{NUM\_n}(x_p) & -\phi_{NUM\_n}(x_p)\cdot c_p \\ & & +\phi_{NUM\_n}(x_p)\cdot 2\cdot v_{px}\cdot m_s\cdot\phi_{NUM\_n}(x_p) & \\ -\phi_{NUM\_1}(x_p)\cdot c_p & \cdots & -\phi_{NUM\_n}(x_p)\cdot c_p & c_p \end{bmatrix} \quad (45)$$

$$\mathbf{K}(t)=\begin{bmatrix} K_1 & & & \\ +\phi_{NUM\_1}(x_p)\cdot k_p\cdot\phi_{NUM\_1}(x_p) & & \phi_{NUM\_1}(x_p)\cdot k_p\cdot\phi_n(x_p) & \\ +\phi_{NUM\_1}(x_p)\cdot c_p\cdot v_{px}\cdot\phi'_{NUM\_1}(x_p) & \cdots & +\phi_{NUM\_1}(x_p)\cdot c_p\cdot v_{px}\cdot\phi'_{NUM\_n}(x_p) & -\phi_{NUM\_1}(x_p)\cdot k_p \\ +\phi_{NUM\_1}(x_p)\cdot {v_{px}}^2\cdot m_s\cdot\phi''_{NUM\_1}(x_p) & & +\phi_{NUM\_1}(x_p)\cdot {v_{px}}^2\cdot m_s\cdot\phi''_{NUM\_n}(x_p) & \\ \cdots & \cdots & \cdots & \cdots \\ \phi_{NUM\_n}(x_p)\cdot k_p\cdot\phi_{NUM\_1}(x_p) & & K_n & \\ +\phi_{NUM\_n}(x_p)\cdot c_p\cdot v_{px}\cdot\phi'_{NUM\_1}(x_p) & & +\phi_{NUM\_n}(x_p)\cdot k_p\cdot\phi_{NUM\_n}(x_p) & \\ +\phi_{NUM\_n}(x_p)\cdot {v_{px}}^2\cdot m_s\cdot\phi''_{NUM\_1}(x_p) & \cdots & +\phi_{NUM\_n}(x_p)\cdot c_p\cdot v_{px}\cdot\phi'_{NUM\_n}(x_p) & -\phi_{NUM\_n}(x_p)\cdot k_p \\ & & +\phi_{NUM\_n}(x_p)\cdot {v_{px}}^2\cdot m_s\cdot\phi''_{NUM\_n}(x_p) & \\ -\phi_{NUM\_1}(x_p)\cdot k_p & & -\phi_{NUM\_n}(x_p)\cdot k_p & \\ -c_p\cdot v_{px}\cdot\phi'_{NUM\_1}(x_p) & \cdots & -c_p\cdot v_{px}\cdot\phi'_{NUM\_n}(x_p) & k_p \end{bmatrix} \quad (46)$$

$$\mathbf{F}(t)=\begin{bmatrix} \phi_{NUM\_1}(x_p)\cdot F_{p,ver} \\ \cdots \\ \phi_{NUM\_n}(x_p)\cdot F_{p,ver} \\ 0 \end{bmatrix} \quad (47)$$

$$\mathbf{z}(t)=\begin{bmatrix} z_1 \\ \cdots \\ z_n \\ z_a \end{bmatrix} \quad (48)$$

APPENDIX II.

Basics of model updating.

The model updating procedure (Friswell and Mottershead, 1995) allows adjusting the numerical modal parameters obtained from a finite element model to the experimental identified parameters to characterize more precisely the dynamic behavior of the structure. In the present study, the finite element model updating has been applied defining as objective function the minimization of the relative differences between the experimental and numerical modal parameters (Teughels, 2003) the updating process being conducted from the changes applied on some previously selected structural physical parameters. As optimization method, genetic algorithms (Koh and Perry, 2010), have been used, due to their robustness and limited dependence on the initial point selected to initiate the search process (Nocental and Wright, 1999). The objective function is defined as:

$$f(\theta) = \frac{1}{2} \cdot \sum_{i=1}^{n_r} q_i \cdot \left[z_{NUM\_i}(\theta) - z_{EXP\_i} \right]^2 = \frac{1}{2} \sum_{i=1}^{n_r} q_i \cdot r_i(\theta)^2 \tag{49}$$

where:

$z_{NUM\_i}(\theta)$ are the magnitudes obtained from the numerical model, which are related to the physical parameters of the model, θ (modulus of elasticity, soil stiffness …), θ being the object of the adjustment. The variables z_{EXP_i} represent the same magnitudes obtained from experimental data. The differences between the experimental and numerical parameters are denoted as residues, $r_i(\theta)$. It is advisable that the number of residues, n_r=n_f+n_s (with n_f being the number of natural frequencies considered and n_s being the number of the coordinates of the vibration modes considered), is greater than the number of variables adjusted, θ. A weight variable q_i is established for each

residue to consider the different reliability of the identified modal parameters. In this case, it has been adopted that the weight variable for the natural frequencies is set to $q_f = 1.00$ whilst for the modal coordinates values is set to $q_s = 0.10$., taking into account, as it is recommend by several authors (Teughels, 2003; Zivanovic et al., 2007), the lower reliability of the identified mode shapes in comparison with the measured natural frequencies. Both residues (natural frequencies and vibration modes) are applied according to the following expressions:

$$r_f(\theta) = \frac{f_{NUM\_i}(\theta) - f_{EXP\_i}}{f_{EXP\_i}}, i = 1,2,...,m_f \tag{50}$$

where $f_{NUM\_j}(\theta)$ and f_{EXP_i} are the numerical and experimental natural frequencies of the structure; and

$$r_s(\theta) = \frac{\phi^l_{NUM\_i}(\theta)}{\phi^r_{NUM\_i}(\theta)} - \frac{\phi^l_{EXP\_i}}{\phi^r_{EXP\_i}}, i = 1,2,...,m_s \tag{51}$$

where $\phi^l_{NUM\_i}(\theta)$ and $\phi^r_{NUM\_i}(\theta)$ are the considered and reference component of the numerical vibration mode i, and $\phi^l_{EXP\_i}$ and $\phi^r_{EXP\_i}$ are the same components of the experimental vibration mode i. Finally, the good results of the updating process are checked through the comparison of the experimental and numerical natural frequencies and modal shapes by computing Δf -Eq. (52)- and the *M.A.C.* ratio -Eq. (53)- (Zivanovic et al., 2007).

The relative difference between frequencies may be defined according to Eq.(52).

$$\Delta f = \frac{f_{NUM\_i} - f_{EXP\_i}}{f_{EXP\_i}} \cdot 100 \ [\%] \tag{52}$$

where f_{NUM_i} is the numerical natural frequency and f_{EXP_i} is the experimental natural frequency of the vibration mode i.

The modal assurance criterion is defined from Eq.(53).

$$MAC_i = \frac{\left(\phi^T_{NUM\_i} \cdot \phi_{EXP\_i}\right)^2}{\left(\phi^T_{NUM\_i} \cdot \phi_{NUM\_i}\right) \cdot \left(\phi^T_{EXP\_i} \cdot \phi_{EXP\_i}\right)} \quad (53)$$

where ϕ_{NUM_i} and ϕ_{EXP_i} are the numerical and experimental vibration modes to be compared and ^{T} denotes the transpose. The reliability of the modal parameters identified experimentally has been carefully checked to avoid converge problems of the iterative process. In the same way, the grid of measurements was sufficiently dense to avoid spatial aliasing problems associated with the determination of the M.A.C. ratio (Zivanovic et al., 2007).

ACKNOWLEDGEMENTS

This work was partially funded by the Spanish Ministry for Science under research project DPI2010-21590-C02-02.

REFERENCES

ANSYS Mechanical Release 14.5.

ARTeMIS Extractor Pro 2014.

Barbosa, R., Magalhães, F., Caetano, E. Cunha A. " The Viana footbridge: Construction and dynamic monitoring", *Bridge Engineering*, ICE, Vol. 166, Issue 4, pp. 273-290. 2013.

Bertram, J.E.A., Ruina, A., "Multiple walking speed-frequency relations are predicted by constrained optimization". *Journal of Theoretical Biology*, Vol. 209 (4), pp. 445-453. 2001.

Bruno, L., Venuti, F., "Crowd-structure interaction in footbridges: modelling, application to a real case-study and sensitivity analysis". *Journal of Sound and Vibration*, Vol. 323 (1-2), pp. 475-493. 2009.

Butz CH., Heinemeyer, CH.; Goldack, A.; Keil, A.; Lukic, M.; Caetano, E.; Cunha, A.. Advanced Load Models for Synchronous Pedestrian Excitation and Optimised Design Guidelines for Steel Footbridges (SYNPEX). *RFCS-Research Project RFS-CR-03019*. 2007.

Carroll, S.P., Owen, J.S., Hussein, M.F.M. Modelling crowd-bridge dynamic interaction with a discretely defined crowd. *Journal of Sound and Vibration* 331, 2685-2709, February 2012.

Clough R., Penzien J.. Dynamic of Structures. *McGraw-Hill*, Inc. 1993.

Dallard P., Fitzpatrick A.J., Le Bourva S., Low A., Smith R., Wilford M., Flint, A.. The London Millennium Footbridge. The Structural Engineer, Vol. 79, No. 22, pp.17-33, November 2001.

Domínguez, J.. Dynamic of high speed train bridges: calculation methods and study of the resonance. *Ph. D. Thesis. Escuela Técnica Superior de Ingenieros de Caminos, Canales y Puertos de Madrid (UPM),* 2001 (In Spanish).

Fox, R., Kapoor M.. Rate of change of eigenvalues and eigenvectors. *AIAA Journal*, 6:2426-2429, 1968.

Friswell, M.I., Mottershead, J.E.. Finite Element Model Updating in Structural Dynamics. *Kluwer Academic Publishers*. 1995.

Georgakis, C., Jorgesen, N.G. (2013). *Topics in Dynamics of Bridges, Volume 3: Proceedings of the 31st IMAC. A Conference on Structural Dynamics, 2013. Chapter 4*. Change in Mass and Damping on Vertically Vibrating Footbridges Due to Pedestrians. The Society for Experimental Mechanics, Inc.

Gopalakrishnan, S., Mitra, M.. Wavelet Methods for Dynamical Problems. With Application to Metallic, Composite and Nano-Composite Structures. *CRC Press*, 2014.

Heermann, D. W. Computer simulation methods: in theoretical physics. *Springer-Verlag* New York, Inc. New York, NY, USA 1986.

Helbing, D., Molnár, P.. Social force model for pedestrian dynamics. *Physical Review*, 51(5):4282-4286, May 1995.

Ingolfsson, E.T., Georgakis, C.T., Svendsen, M.N.. Vertical footbridge vibrations: details regarding experimental validation of the response spectrum methodology. Footbridge 2008, Porto, Portugal, 2008.

Jiménez-Alonso, J. F., Sáez, A. (2014). A direct pedestrian-structure interaction model to characterize the human induced vibrations on slender footbridges. *Informes de la Construcción*, 66(extra-1): m007, doi: http://dx.doi.org/10.3989/ic.13.110.

Jones, C.A., Reynolds, P., Pavic, A.. Vibration serviceability of stadia structures subjected to dynamic crowd loads: A literature review. *Journal of Sound and Vibration*, Vol. 330, pp. 1531-1566, November 2010.

Koh Ghee C., Perry M.C.. Structural Identification and Damage Detection using Genetic Algorithms. *CRC Press, Taylor&Francis Group*, 2010.

Magalhães, F., Cunha, A.. Explaining Operational Modal Analysis with data from an arch bridge. *Mechanical Systems and Signal Processing*, Invited Tutorial Paper, Volume 25, Issue 5, pp. 1431-1450 , 2011.

Magalhães, F., Cunha, A., Caetano, E., Brincker, R. Damping estimation using free decays and ambient vibration tests. *Mechanical Systems and Signal Processing*, Volume 24, Issue 5, pp. 1274–1290, July 2010.

Matlab R2011a. . http://www.mathworks.com/.

Matsumoto, Y., Nishioka, T., Shiojiri, H., Matsuzaki, K.. Dynamic design of footbridges. *IABSE Proceedings*, No. P-17/78, pp. 1-15, 1978.

Nocental J., Wright S.J.. Numerical Optimization. *Springer*, New York, USA, 1999.

Racic, V., Pavic, A., Brownjohn, J.M.W. Experimental identification and analytical modelling of human walking forces: Literature review. *Journal of Sound and Vibration*, Vol. 326, pp. 1-49, April 2009.

Rapaport, D.C.. The art of molecular dynamic. *Cambridge University Press*; 2004.

SETRA/AFGC. Guide méthodologique passerelles piétonnes (Technical Guide Footbridges: Assessment of vibration behaviour of footbridge under pedestrian loading). SETRA, 2006.

Shahabpoor, E., Pavic, A., Racic, V.. Modelling effect of pedestrians walking on dynamic properties of structures. *IMAC XXXI: A Conference and Exposition on Structural Dynamics*, 11-14 February, Orange County, California, USA (2013).

Tavares, F., Leal, R., Shubert M. Biodynamic single person and crowd pedestrian model: a worked test case and simulation. *Footbridge 2014*. London, United Kingdom (2014).

Teughels, A., Inverse Modelling of Civil Engineering Structures Based on Operational Modal Data. *Ph. D. Thesis, Katholieke Universiteit Leuven*, 2003.

Venuti, F., Bruno, L., Bellomo, N. Crowd dynamics on a moving platform: mathematical modelling and application to lively footbridges. *Mathematical and Computer Modelling* 45 (3-4), 252-269, February 2007.

Venuti, F., Racic, V., Corbetta, A. Pedestrian-structure interaction in the vertical direction: coupled oscillator-force model for vibration serviceability assessment. *Proceedings of the 9th International Conference on Structural Dynamics, EURODYN 2014*. Porto, Portugal, 30 June - 2 July 2014.

Zivanovic, S., Pavic, A., Ingolfsson, E., Modelling spatially unrestricted pedestrian traffic on footbridges. *Journal of Structural Engineering*, Vol. 136 (10), pp. 1296-1308. 2010.

Zivanovic, S., Pavic A., Reynolds P.. Finite element modelling and updating of a lively footbridge: The complete process. *Engineering Structures*, Vol. 301(1-2), pp. 126-145, March 2007.

Zivanovic, S., Pavic A., Reynolds P.. Vibration serviceability of footbridges under human-induced excitation: a literature review. *Journal of Sound and Vibration*, Vol. 279, Issue 1-2, pp. 1-74, January 2005.

Paper C: Model updating for the selection of the retrofit method of an ancient bridge (Almeria, Spain).

The original version of this paper can be found in

doi: 10.2749/101686615X14355644771333

Structural Engineering International (in press)

ISI 2014 Classification: Q4 (105/124) Civil Engineering. Impact Factor: 0.414

SCIMAGO 2014 Classification: Q2 (106/215) Civil Engineering SJR: 0.417

ISSN: 1683-0350

Model updating for the selection of the retrofit method of an ancient bridge (Almeria, Spain).

ABSTRACT

In this paper we analyse a case study where a finite element model updating is conducted on the basis of the experimental modal parameters recorded for a reinforced concrete truss bridge built in Almeria (Spain) in 1927. The final aim of this study is to help understanding the actual state of structural conservation of the bridge, in order to select an appropriate retrofit technique to reinforce it before the planned widening of its deck. At present, the two most widely used methods for retrofitting consist on either reinforcing the structure with external prestressing or increasing its flexural strength by adhering CFRP laminates. The first method is especially advantageous if the structure is deteriorated to such an extent that the strengthening needs to focus not only on increasing the flexural strength of the bridge, but also on avoiding the deflection problems associated with the reduced inertia of the structure. If this were not the case, strengthening with CFRP would be an adequate option. To this end, and given the monumental character of this ancient construction, it is not possible to apply directly destructive or static load tests to determine the properties of its constituent materials, so that it becomes necessary to estimate its deterioration state indirectly with the use of non-destructive techniques. For this purpose, in the present paper we carry out a finite element model updating of the structure, based on experimental modal parameters, which allows for checking its service condition through the estimation of the value of several physical parameters of the bridge. Subsequently, the resulting updated model constitutes a valuable tool to help establishing which is the most adequate retrofit method.

Keywords: Retrofit methods, operational modal analysis, model updating, ancient reinforced concrete bridge, non-destructive testing.

1. Introduction.

The Molinos Bridge is a reinforced concrete truss girder bridge (Fig. 1) located over the Andarax River at the outskirts of the town of Almería (Spain). It was built in 1927, being at present one of the best preserved achievements of the first reinforced concrete bridges built in Spain. The design of the structure corresponds to one of the schemes proposed by the Spanish engineer Juan Manuel Zafra in the official model of road bridges of the collection of reinforced concrete straight bridge for spans of 32 m, published in 1920 [1-6].

Recently, the Planning Department of the City of Almeria called for a public competition in order to proceed with the repair, reinforcement and widening of this ancient concrete bridge. The growth of the city towards the East and the attempt of promoting the tourism on the East Coast of the province made necessary to improve the road access to those neighbourhoods of the city. Since the construction of a new structure was dismissed due to its high cost, the proposal focused on adapting the existing bridge to the new service conditions.

According to the technical provisions of the competition published by the Planning Department, the works for the rehabilitation and functional adaptation of the Molinos bridge should satisfy the following conditions: (i) widening the existing lanes for vehicles, increasing its width until 3.25 m per lane; (ii) creating a pavement and a cycle lane with a minimum width of 1.50 m; and (iii) the project should maintain the current typology of the bridge and still ensure its adequate bearing capacity under the new loading scenario.

All the presented project proposals addressed three main aspects, namely: (i) design of a structural system to increase the width of the deck; (ii) retrofit of the main

truss girders; and (iii) treatment of the existing cracking on the reinforced concrete elements. Regarding the retrofit method of the main girders, the alternatives presented by the different engineering firms may be grouped in two categories based on: (i) either use external prestressing [7] or (ii) use carbon fiber reinforced polymers (CFRP) laminates [8] to retrofit the reinforced concrete truss girders. The main factor that conditions the choice of the retrofit method is the actual deterioration level of the structure and its influence in the moment of inertia of the girder. In this way, if the structure was seriously damaged, it would be necessary to focus not only on controlling the level of stresses but on reducing the deflection of the girder as well.

Therefore, in order to properly evaluate the different projects and select the most adequate retrofit method, the Planning Department of the City of Almeria decided to conduct a detailed study of the state of deterioration of the structure using non-destructive techniques. The use of the bridge, before its retrofit, was just limited to light traffic, so the Planning Department further established as a requirement the impossibility of performing a static load test, conducted with heavy loads, in order to assess the structural condition of the bridge.

The present paper summarizes the work developed by the authors to evaluate the damage level of the bridge. This study describes an innovative application of the FE model updating method, using it as a valuable tool in order to find the optimum reinforcement method for a ancient bridge. The work mainly focuses on performing a FE model updating [9] of the bridge based on the experimental modal parameters. These parameters are determined from an ambient test, using operational modal analysis [10]. This study focuses on the vertical direction in order to estimate the deterioration state of the ancient bridge comparing two scenarios: (i) one defined by the current structure, from a numerical load test performed on the updated model; and (ii) a second scenario

defined by the original structure, from the original experimental load test at the time of completion of the bridge [4]. The results of the study, and in particular the resulting updated model, are then used as reference for the evaluation of the different project proposals and the selection of the most appropriate retrofit method.

The paper is organized as follows: In section 2, a preliminary study of the structural behaviour of the structure is presented, describing the main structural elements and the level of cracking observed on the structure from visual inspection. Furthermore, a rough estimation of the range of variation of the Young's modulus of the concrete is obtained from a hammer rebound test. At the end of this section, a FE model of the structure is performed in order to obtain an initial estimation of the distribution of the principal stresses of the structure under self-weight and dead load. Later, the results from the hammer rebound test and the static analysis were used to establish both the physical parameters used in the updating process and its range of variation. To make the paper as self-contained as possible, a description and comparison of the two proposed retrofit method is briefly presented in section 3, and further a criterion for its selection is established. In section 4, the modal parameters of a previously selected extreme span are estimated experimentally through the application of operational modal analysis in the frequency domain. In section 5, the FE model updating of the selected span is performed. In section 6, the updated model is employed to assess the structural condition of the bridge, by comparing the results of the original load test of the bridge [4] with the numerical simulation of such load scenario using the updated model. Finally, from the obtained results, the best retrofit method is selected and several conclusions are drawn in section 7.

2. Preliminary study of the structural behaviour of the bridge.

As a preliminary step for the selection of any retrofit system it is of key importance to

understand the actual structural behaviour of the different elements that configure the bridge, as well as to determine the mechanical characteristics of the material and to conduct an in-depth visual inspection of the current state of the bridge.

2.1. Description of the original structure.

The Molinos Bridge over the Andarax River is located along the road between Almería and Níjar (Spain). It is an isostatic structure with five spans (32.64 - 32.72 - 32.72 - 32.68 and 32.78 m) with a total length of 163.54 m (Fig. 1). The width of the original bridge is around 6.20 m, composed by two lanes of 2.20 m and two pavements of 0.20 m.

Fig. 1. Elevation of the Molinos Bridge from the East abutment.

Each span [2, 3 and 11] is configured by two reinforced concrete truss girders separated 2.70 m and connected at the top by a reinforced concrete slab of variable depth (0.18-0.54 m) with a total width of 6.20 m. The total depth of the bridge is about 2.66 m. The width of the different elements that configure the truss girders is 0.40 m. The depth of the lower chord is 0.40 m, but the depth of struts and diagonal varies between 0.18 m in

the mid-span and 0.64 m over the supports. Inside the lower chord of the truss girders there are several rectangular steel plates 300x12 mm, in a number varying from 10 plates in each lower chord at the mid span to 4 plates at the supports [2, 3 and 11]. The force transmission between the lower chords and the struts and diagonals is achieved by the placement of pins of diameter 40-50 mm (Fig. 2). The trusses are jointed at the intersection between the lower chord and the struts by several reinforced concrete rectangular crossbars with 0.40 m of depth and variable width (Fig. 3.a).

Due to the geometric configuration of the bridge the diagonal elements work in compression and are reinforced with longitudinal bars and a high density of stirrups. The struts of the truss girders, always in tension, are reinforced with longitudinal and transversal bars which number increases with the proximity to the supports.

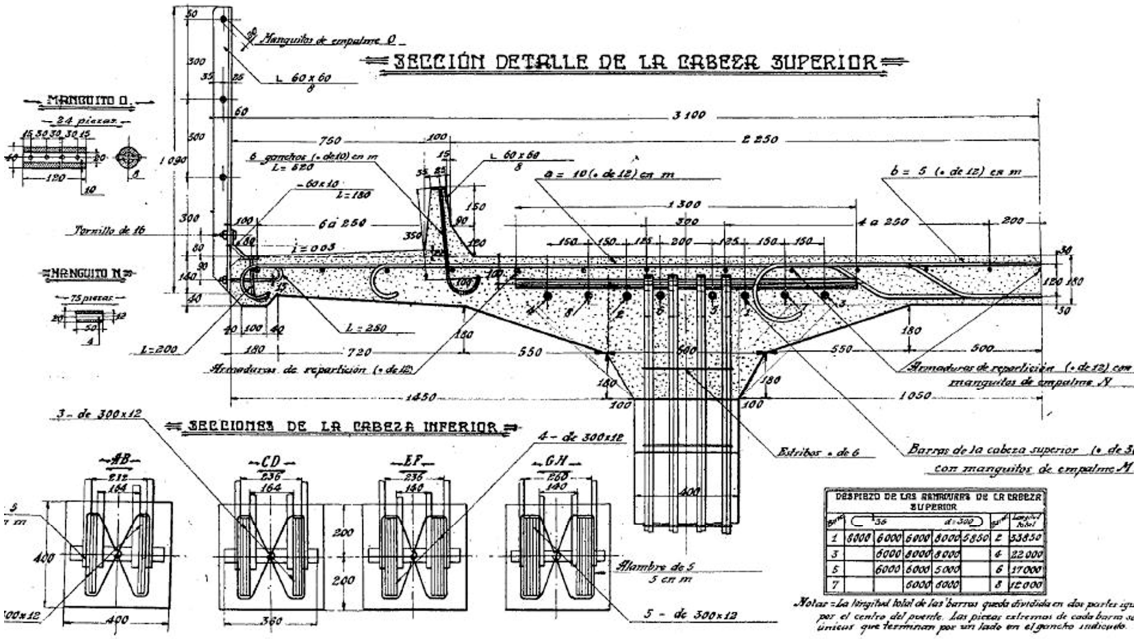

Fig. 2. Original details of the cross section of the bridge [11].

The piers and the abutments have a rectangular cross-section with dimensions 1.60x5.60 m and a height of 6.00 m. Each of these elements rest on a masonry block with

rectangular cross-section 2.00x6.00 m and height around 5.70 m [3]. The foundations of these elements are reinforced concrete slabs with 1.50 m of depth and horizontal dimensions 4.00x8.00 m. The linking between the deck and the piers is achieved by fixed (one hinge) and sliding (two hinges) bearings (Fig. 3.b). To avoid restricting the longitudinal movements of the deck due to the rheological and thermal effects, in each pier these two types of bearings have been installed [3].

Fig. 3. a) Spatial configuration of the truss girder. b) Support on abutments

2.2. Visual inspection of the original structure.

The deterioration state of the bridge was studied, as a first approximation, through its visual inspection. The main damages observed in the structure were the following:

(i) Detachment of the reinforced concrete along of the truss girders. The infiltrations of water and salts, due to the impairment of the waterproofing, in the truss girders have caused the oxidation of the rebars and the appearance of the detachment of the concrete. Detachments around 3.50 cm were measured. The

revised rebars are in general in good condition, with the carbonation front located at an average depth of 5 cm (Fig. 4).

(ii) Cracks and fissures in the lower chord of the truss girders with a variable width of 0.30-0.70 mm, randomly distributed between the supports and the mid spans (Fig. 4).

(iii) With respect to the substructure, the bearings were in clearly poor condition. However the masonry abutments and piers yet maintained a fairly good appearance (Fig. 3.b).

Fig. 4. Cracking of the lower chord of the truss girders.

2.3. First estimation of the stiffness characteristics of the materials.

In the reference literature [1, 2], the required value of the reinforced concrete compressive strength of the structure is reported as $f_{ck} = 20.5\,\text{MPa}$. This value allows establishing a preliminary estimation of the compressive medium strength, $f_{cm} = 28.5$ MPa, and the Young's modulus, $E_c = 30545$ MPa, based on the relationships reported in Eurocode [12].

In order to check preliminary this value, a non-destructive test, namely a rebound hammer test [13], was performed. The test allows defining a preliminary range

of variation of the Young's modulus based on the previous estimation of the compressive medium strength.

The test was performed on the fifth span, the longest one, which is located next to the East abutment (Fig. 1) of the bridge. The test consists on the application of 12 impacts on 10 different points of the girder (Fig. 5).

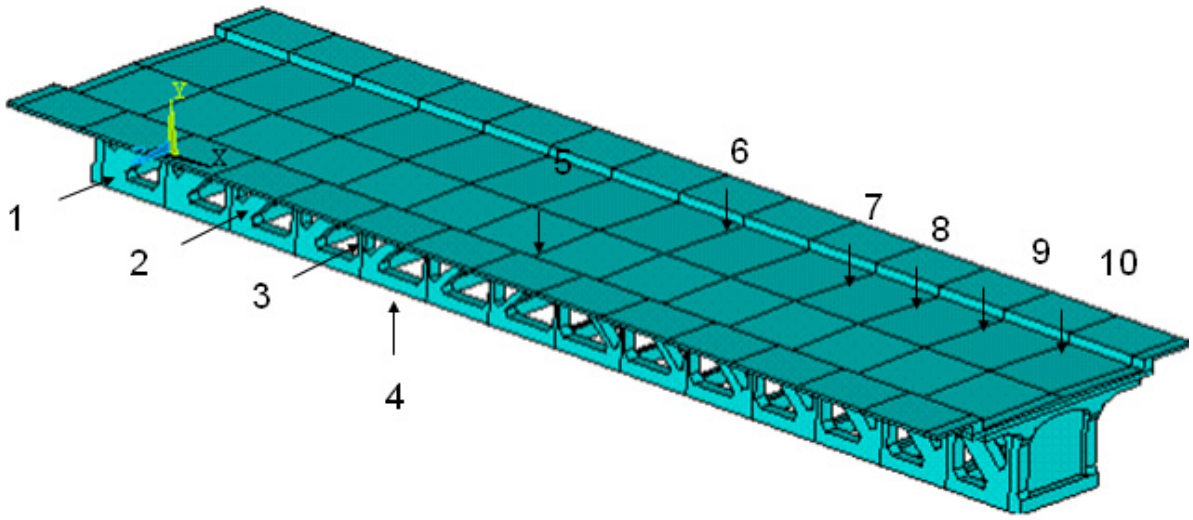

Fig. 5**.** Rebounds hammer test location on one span of the bridge.

The average and standard deviation rate of each series are shown in Table 1. The main factor that conditions the estimation of the compressive strength is the attack angle of the hammer, α [13].

Table 1. Medium compressive strength estimation from rebound hammer test.

	Rebound Number			
Position	Mean	Standard	α [º]	f_{cm} [MPa]
1	31.20	3.50	0.00	25.00
2	48.90	3.10	0.00	55.00
3	37.00	2.30	0.00	35.00
4	37.50	3.10	-90.00	30.00
5	32.00	2.30	90.00	32.00
6	34.80	3.00	90.00	35.00
7	40.60	3.30	90.00	45.00
8	36.00	2.40	90.00	36.00
9	36.20	2.30	90.00	36.00
10	31.30	2.40	90.00	32.00

The range of variation of the value of the compressive medium strength, $f_{cm} = 25 - 55$ MPa, is shown in Table 1. Its variability was justified by the composite character of the reinforced concrete truss girders due to the presence of the embedded steel profiles. Subsequently, using the relationship proposed by Eurocode [12], the range of variation of the Young's modulus was defined as $E_c = 29250 - 38030$ MPa. The value recommend in the original project is inside the range estimated by the non-destructive test. This range will be used later, in section 5, to define the search domain during the finite element model updating, with the aim to estimate more precisely a medium value for the Young's modulus of the reinforced concrete and the deterioration state of the structure.

2.4. Finite element model and preliminary analysis of the behaviour of the structure.

The extreme East span (fifth span) of the bridge was modelled with 3D brick elements (8 nodes per element, 3 d.o.f. in each node) in the finite element (FE) package Ansys [14]. The mesh consists of 870945 elements. For our purpose, the reinforced concrete has been considered as a homogenous material (initial Young's modulus, $E_c = 30$ GPa, and density 2500 kg/m3), modelling only the embedded steel profiles of the lower chord as additional elements. The pavement and barriers were accounted as added masses of 275 kg/m^2 and 75 kg/m, respectively. Each support was modelled by means of one longitudinal spring (with stiffness k_h) and considering that the vertical and lateral displacements were constrained. The initial value for this spring parameter, $k_h = 2.65 \cdot 10^8$ N/m, has been estimated from a simplified FE model of just the pier and abutment, adopting a medium value of Young's modulus of $E_m = 20$ GPa [15] for these elements.

A static analysis of the structure has been performed, obtaining the distribution of principal stresses under self-weight and dead load on the structure. As it is shown in Fig. 6 the lower chord and the struts of the structure are in tension, as expected according to the construction details of the structure. Later, this result will be considered in the selection of the physical parameters used for the FE model updating.

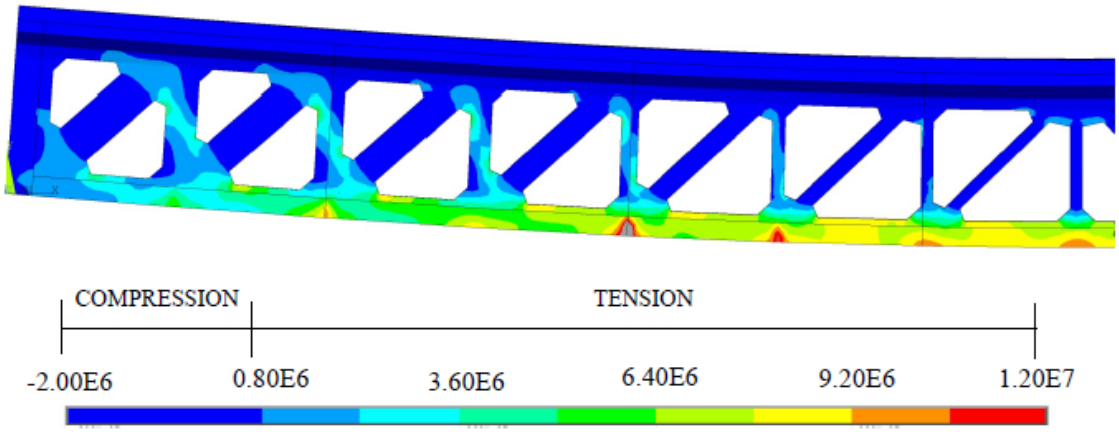

Fig. 6. First principal stress (N/m^2) of the structure under self-weight and dead load.

3. Alternatives to retrofit the structure.

Both the increment of the dead and live loads that the extension of the structure implies, together with the observed cracking at the lower chord of the main girders, make necessary to perform the structural strengthening of the different spans that configure the bridge. As pointed out before, all alternatives proposed by the different engineering firms that participated in the call for proposals may be grouped in two distinct sets of solutions:

- **Externally prestressed reinforcement**. The flexural strength of the main girders can be increased by setting a system of external prestressing [7] configured by tendons arranged in the interior spaces between webs and connected to the lower chord of the truss girders. This alternative has the

advantage of acting directly on the member forces generated in the truss girders, thus improving their behaviour against bending failure, shear failure and cracking of the lower chord. The control of the cracking of the structure makes this alternative very appealing when high levels of deterioration are detected in the bridge to be retrofitted, since it improves the durability of the structure while avoiding the deflection problems associated with the inertia reduction caused by deep cracking. However, it has some disadvantages related to the difficult connection between the tendons and the lower chords of the girders.

- **CFRP laminates reinforcement**. The different elements of the truss girders subjected to tensile efforts (lower chords) may be reinforced by the placement of carbon fiber reinforced polymers (CFRP) laminates attached to the structure with epoxy resin [8]. The resulting increase of the tensile strength of the lower chords improves the bending capability of the whole girders. The main advantage of this alternative is its quick and easy assembly, without any important affection to the existing structure. On the other hand, this retrofit method main disadvantage is that it does not solve both the durability problems and the deflection problems of the structure associated with the concrete cracking, in cases where such cracking has induced a significant inertia reduction of the truss girders.

Considering the advantages and disadvantages of the two proposed retrofit methods, the main differentiating factor to opt for one of them is the level of deterioration of the bridge. In this sense, since it was not possible to perform either destructive tests nor load tests on the structure, its cracking level was estimated in an indirect way, through the development of a finite element model updating of the structure [9] using its actual

modal properties. Such properties were experimentally determined from operational modal analysis [10], after conducting an ambient test developed under service conditions. Due to the isostatic character of all the spans and their similar level of degradation, only the longest one was instrumented, namely the one located next to the East abutment. During the updating process ten physical parameters were considered to estimate the cracking level. The resulting updated model resembles the actual experimental behaviour of the bridge and thus it constitutes a valuable tool to assess its present condition. In particular, it will be used to numerically reproduce the bridge response to a load scenario defined by the original load test carried out at the completion of the bridge, and whose results are available [4]. The comparison of the obtained results for the deteriorated bridge with the observed results for the original bridge will permit to draw valuable conclusions on the actual state of damage, as discussed in the next sections.

4. Experimental modal parameters identification.

4.1. Preliminary numerical modal analysis.

The modal analysis of the above preliminary FE model leads to the first three numerical vibration modes (in vertical direction) and associated numerical natural frequencies (f_{NUM_i}, being i the vibration mode number) given in Fig. 7.

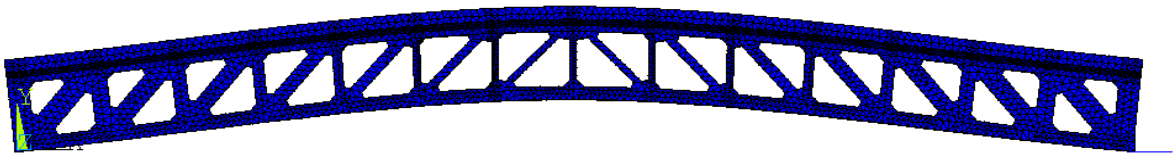

f_{NUM_1}=4.259 Hz. First numerical vibration mode in vertical direction.

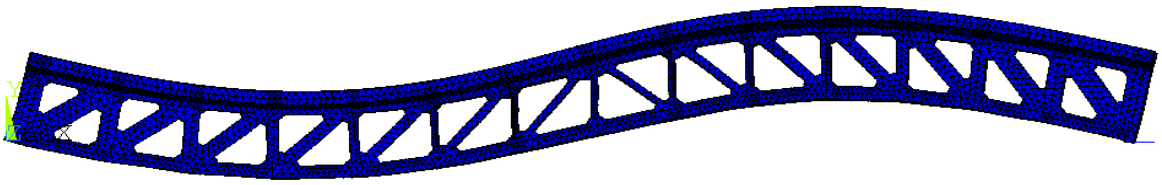

f_{NUM_2}=12.733 Hz. Second numerical vibration mode in vertical direction.

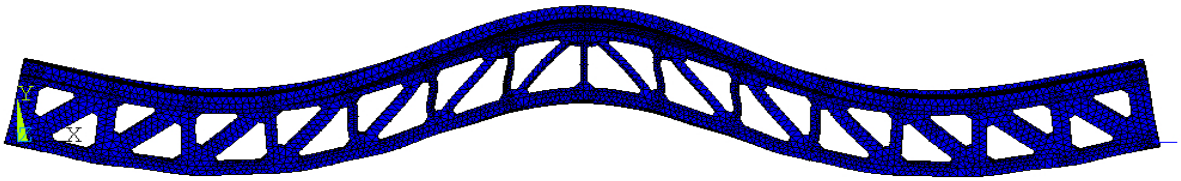

f_{NUM_3}=22.623 Hz. Third numerical vibration mode in vertical direction.

Fig. 7. First three numerical vibration modes in vertical direction. Initial FE model.

4.2. Ambient test and OMA (operational modal analysis).

In order to obtain experimentally the vertical modal parameters (natural frequencies and modal shapes) of the selected span, an ambient test was performed. The measurements were conducted in service conditions under the passage of light traffic. The mode shapes were measured along two gridlines, one at each longitudinal side: 2x15 points were used which were equally distributed in each corridor and separated transversally 6.00 m. Four high sensibility (Kinemetrics Episensor ES-U) uniaxial force balanced accelerometers (two of them as reference) were used. A total number of 14 set-ups were conducted under a sampling frequency of 100 Hz and each series lasting 900 sec.

For the experimental identification of the vertical modal parameters, the above measurements were processed by one of the operational modal analysis methods in the frequency domain, namely the Enhanced Frequency Domain Decomposition method (E.F.D.D.) [10], as implemented in the software Artemis [16]. The first 3 vertical vibration modes were identified and subsequently used for the FE model updating

process. The obtained numerical and experimental natural frequencies and vibration modes shapes are compared in Table 2. In order to validate the correlation between the numerical and experimental modal parameters both the relative difference (Δf) between the numerical and experimental frequencies and the modal assurance criterion (M.A.C.) were analyzed [17]:

- The relative difference between frequencies is defined as:

$$\Delta f = \frac{f_{NUM} - f_{EXP}}{f_{EXP}} \cdot 100 \ [\%] \tag{1}$$

where f_{NUM} is the numerical natural frequency and f_{EXP} is the experimental natural frequency.

- The M.A.C. is defined as:

$$MAC_{j,k} = \frac{\left(\varphi_j^T \cdot \varphi_k\right)^2}{\left(\varphi_j^T \cdot \varphi_j\right) \cdot \left(\varphi_k^T \cdot \varphi_k\right)} \tag{2}$$

where φ_j and φ_k are the two modes to be compared (normally, experimental vs numerical) and ^{T} denotes the transpose. A good correlation between two modes is achieved when the value of its M.A.C. ratio is greater than 0.90.

Table 2. First three vertical numerical (f_{NUM}) and experimental (f_{EXP}) natural frequencies of the selected span. Initial FE model.

Mode	f_{NUM} [Hz]	f_{EXP} [Hz]	Δf [%]	M.A.C.	Description
1	4.259	4.320	-1.412	0.992	First bending mode
2	12.733	10.100	26.069	0.985	Second bending mode
3	22.623	17.840	26.810	0.961	Third bending mode

Although the shapes of the three vertical identified vibration modes are in good agreement (with M.A.C. ratios greater than 0.90), the relative differences, Δf, between the numerical and experimental natural frequencies are still large. Therefore, the initial estimation made on the physical parameters of the structure is not good enough and it

becomes necessary to adjust the FE model in order to obtain a good correlation between the numerical and experimental modal parameters. In this paper, the finite element model updating technique [18] has been used to adjust the numerical results, as detailed in next section.

5. FE model updating of the structure.

As remarked above, the updating procedure was conducted to adjust the modal parameters of the FE model to the experimental identified parameters to, subsequently, estimating the deterioration level of the truss girder of the fifth span of the bridge and, consequently, determine the most suitable retrofit method. For this purpose, the results of a numerical load test using the resulting updated model will be compared with the experimental results recorded on the date of construction of the bridge [4] under the same load scenario, thus estimating the actual state of deterioration of the bridge.

5.1. Basics of FE model updating.

The FE model updating based on the results of the modal parameters of the structure (natural frequencies and vibration modes) may be performed from two different perspectives, via either direct or indirect methods [9]. In the early years of this technique, the adjustment of the FE model was performed directly through the introduction of changes in the mass and stiffness matrices of the structure, what has the advantage of allowing an adjustment between the numerical model and the experimental data through a direct algorithm without the need of iterating. However, this methodology has as main disadvantage that the updating process is performed without necessarily involving the physical knowledge of the problem. This drawback caused the later appearance of other family of methods, iterative methods [18], where the model updating arises from the changes applied on some well-defined structural physical

parameters selected by the users. In this case, the modified parameters are not linearly related to the modal parameters, so that the adjustment process requires the use of optimization algorithms for non-linear problems, thus becoming necessary to undergo an iterative process. A straightforward manner to perform the FE model updating is to define as objective the minimization of the relative differences between the experimental and numerical modal parameters [18]. The objective function resulting from this aim is usually formulated as a least square problem.

$$f(\theta)=\frac{1}{2}\cdot\sum_{j=1}^{m}w_j\cdot\left[z_{NUM,j}(\theta)-z_{EXP,j}\right]^2=\frac{1}{2}\sum_{j=1}^{m}w_j\cdot r_j(\theta)^2 \tag{3}$$

where:

$z_{NUM,j}(\theta)$ are the magnitudes obtained from the numerical model, which are related to the physical parameters of the model, θ (modulus of elasticity, soil stiffness …), being θ the object of the adjustment. The variables $z_{EXP,j}$ represent the same magnitudes obtained from experimental data. The differences between the experimental and numerical parameters are denoted as residues, $r_j(\theta)$. It is advisable that the number of residues, $m=m_f+m_s$ (with m_f being the number of natural frequencies considered and m_s being the number of the coordinates of the vibration modes considered), is greater than the number of variables adjusted, θ. A weight variable w_j is established for each residue to take into account the different reliability of the identified modal parameters.

Both residues (natural frequencies and vibration modes) are applied in the above equation (3) according to the following expressions:

$$r_f(\theta)=\frac{f_{NUM,j}(\theta)-f_{EXP,j}}{f_{EXP,j}},\ j=1,2,...,m_f \tag{4}$$

where $f_{NUM,j}(\theta)$ and $f_{EXP,j}$ are the numerical and experimental natural frequencies of the structure; and

$$r_s(\theta) = \frac{\varphi^l_{NUM,j}(\theta)}{\varphi^r_{NUM,j}(\theta)} - \frac{\varphi^l_{EXP,j}}{\varphi^r_{EXP,j}}, j = 1,2,..., m_s \quad (5)$$

where $\varphi^l_{NUM,j}(\theta)$ and $\varphi^r_{NUM,j}(\theta)$ are the considered and reference component of the numerical vibration mode j, and $\varphi^l_{EXP,j}$ and $\varphi^r_{EXP.j}$ are the same components of the experimental vibration mode j.

The above objective function is to be minimized by the application of an optimization algorithm [19]. Either local or global optimization algorithms could be considered [18]. For our purposes, global algorithms are implemented due to their robustness and controlled dependence on the initial point selected to initiate the search process. In particular, genetic algorithms have been used for the present study. These algorithms are based on the analogy with the natural evolution where the members of a population compete to survive and reproduce, presenting the best individuals a genetic code that allows them to take advantage over the rest of the population [20].

Finally, the validity of the updating process is checked through the comparison of the experimental and numerical natural frequencies and modal shapes by computing Δf – equ. (1)– and the M.A.C. ratio –equ. (2)– [17].

The modal parameters identified experimentally must be carefully considered (checking their reliability) to avoid convergence problems during the iterative process. In the same way, the grid of measurements must be sufficiently dense to avoid spatial aliasing problems associated with the determination of the M.A.C. ratio [17].

5.2. Residual selection.

Given the good quality of the experimental data, the three identified vertical vibration modes were chosen in the updating process. Both measured natural frequencies and modal coordinate values were taken into account. Therefore, in total 48 residual

components were selected for model updating (3 experimental natural frequencies and the 45 coordinates of each vibration mode). To take into account the lower reliability of the identified mode shapes in comparison to the measured natural frequencies, as several authors recommend [17, 18], the weight variable for the natural frequencies is set to $w_f = 1.00$ whilst for the modal coordinates values it is set to $w_s = 0.10$.

5.3. Parameter selection.

Once analyzed the configuration of the structure, the results of the preliminary visual inspection of the bridge and the results of the static analysis of the structure under self-weight and dead load, the study focused on the following three factors, as being the ones with a deeper influence on the dynamic behaviour of the bridge: the medium value of the Young's modulus of the reinforced concrete structure, its damage level and the deck-piers interaction.

Subsequently, ten parameters were considered in the model updating process to take into account these three factors. The cracking level of the structure and the stiffness of the reinforced concrete elements have been simulated by the division of the selected truss girder in nine parts (in order to reduce the number of parameters). In each part, the Young's modulus has been considered as a parameter to be updated, since its variation provides an estimate of the cracking level. In fact, the variation of Young's modulus has been used successfully by several authors [18, 21-23] to simulate the effect of the cracking on the modal parameters of the reinforced concrete structures. Additionally, the influence of the supports on the modal parameters of the bridge has been estimated by varying the stiffness of the longitudinal spring elements (k_h). In Fig. 8 the ten considered parameters to be updated are shown.

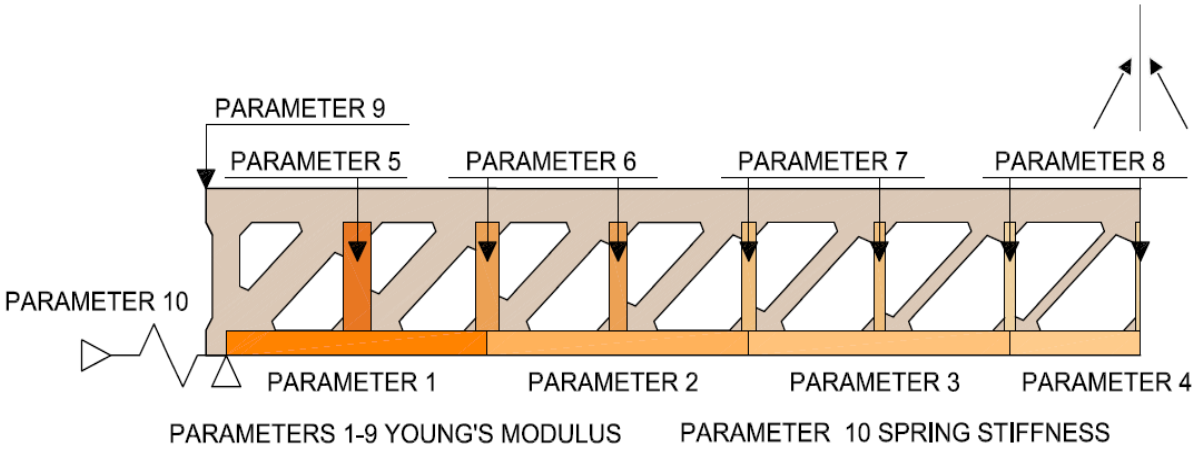

Fig. 8. Parameter selection for the updating process.

5.4. Model updating process and results.

The model updating process has been conducted through the implementation of the above algorithm in the software programs Ansys [14] and Matlab [24]. A population of 1000 vectors has been considered that using the rules of the genetic algorithm have minimized the value of the proposed objective function. In each iteration, the values of the selected parameters have been modified in order to reduce the relative differences between the numerical and experimental modal parameters of the bridge. In order to increase the efficiency of the genetic algorithm and yet maintain the physical meaning of the finite element model updating, a search domain has been defined to control the variation of each parameter. In this sense, the results of the hammer rebound test establish the search domain for the first nine parameters: The minimum value of each search domain has been estimated as ten per cent of the lower estimated Young's modulus, and the maximum as the upper obtained value of Young's modulus. For the remaining parameter, and in order to take account the variation of the effective stiffness of the bearings due to its high friction under reduced vibration conditions, the search domain has been extended to values over more than twice the original estimated value. In Table 3 the range of variation of each parameter and its updated values are shown.

Table 3**.** Range of variation of the considered physical parameters.

Parameter Number	Parameter (Fig. 8)	Minimum	Updated	Maximum
1	Young's modulus lower chord [MPa]	3000	25382	38000
2	Young's modulus lower chord [MPa]	3000	17207	38000
3	Young's modulus lower chord [MPa]	3000	12316	38000
4	Young's modulus lower chord [MPa]	3000	10690	38000
5	Young's modulus strut [MPa]	3000	28712	38000
6	Young's modulus strut [MPa]	3000	29016	38000
7	Young's modulus strut [MPa]	3000	29320	38000
8	Young's modulus strut [MPa]	3000	29628	38000
9	Young's modulus remaining structure [MPa]	3000	30147	38000
10	Long. stiffness spring [N/m]	$1.00 \cdot 10^8$	$3.45 \cdot 10^8$	$7.00 \cdot 10^8$

The differences between the numerical and experimental natural frequencies, after the finite element model updating, are very small and the correlation between the numerical and experimental vibration modes are quite good. The relative differences between the updated numerical (f_{UPD}) and experimental (f_{EXP}) modal parameters and the M.A.C. values achieved after the model updating process are summarized in Table 4 and Fig.9 , where the improvement with respect to the initial FE model looks clear (see Table 2).

Table 4. First three vertical updated numerical (f_{UPD}) and experimental (f_{EXP}) natural frequencies of the selected bridge span.

Mode	f_{UPD} [Hz]	f_{EXP} [Hz]	Δf [%]	M.A.C.	Description
1	4.323	4.320	0.069	0.999	First bending mode
2	10.114	10.100	0.138	0.997	Second bending mode
3	17.853	17.840	0.072	0.996	Third bending mode

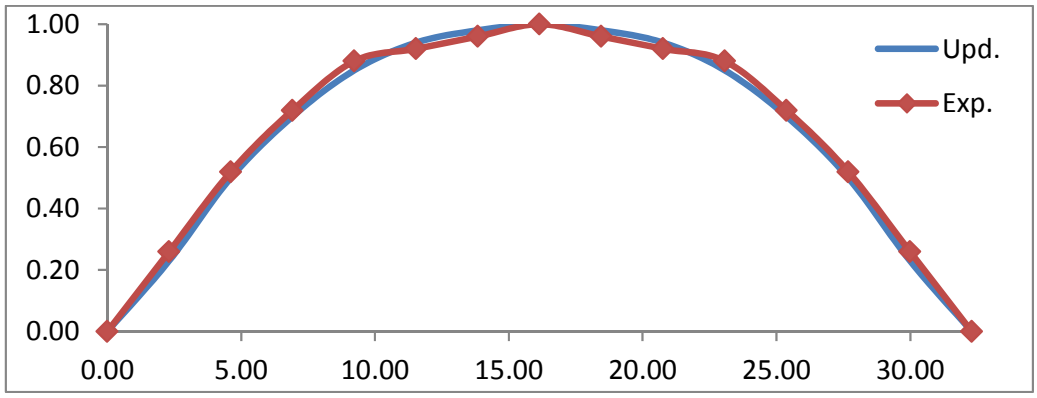

First updated numerical (Upd.) and experimental (Exp.) vertical vibration mode

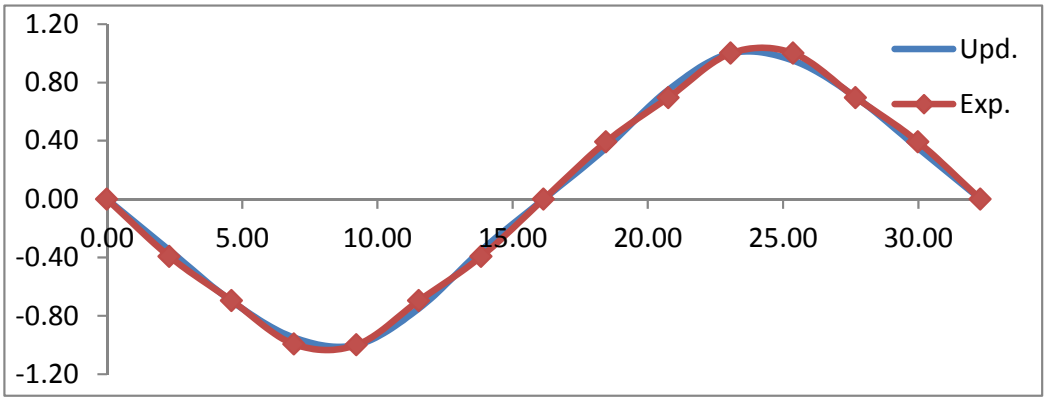

Second updated numerical (Upd.) and experimental (Exp.) vertical vibration mode

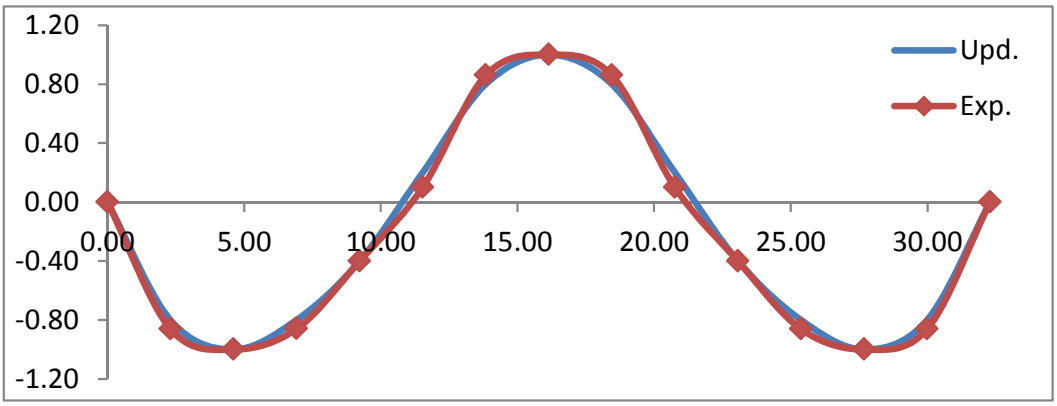

Third updated numerical (Upd.) and experimental (Exp.) vertical vibration mode

Fig. 9. First three vertical updated numerical and experimental vibration modes.

The results of the updated values of the selected parameters (Table 3) shows that, as it was expected, the observed cracking level affects especially the stiffness of the lower chord of the truss girders: the reduction of inertia exhibits a good correlation with the observed cracks. Furthermore, the estimated medium Young's modulus of the reinforced concrete structure maintained an adequate value according to the

recommended value of the original project. The final estimated parameters ensured the updated model provides an improved estimate of the actual bridge behaviour, since excellent agreement is achieved between the numerical and the experimental measurements.

6. Election of the retrofit method.

As pointed out above, two alternative retrofit methods were proposed, based on either external prestressing or strengthening with CFRP laminates. The main advantages and disadvantages of both methods have already been outlined in previous sections, where it was concluded that the main factor conditioning the election focuses on determining whether the bridge in its actual condition is able to ensure a proper deflection of the structure under service loading, and therefore it is not deeply deteriorated.

For this purpose, and in order to evaluate the current state of the bridge and estimate the accumulated deterioration since its original construction, the updated FE model has been used to numerically compute the maximum deflection of the bridge under a load scenario defined by the original load test of the structure, and the obtained results have been compared with the ones recorded experimentally at the time of construction. In case that the correlation between the experimental and numerical deflections was adequate, that would mean that the accumulated damage of the bridge has not affected significantly its stiffness, so that the retrofit method would need to focus mainly on increasing the strength of the structure rather than on controlling the deflections of the bridge and, consequently, the retrofit based on CFRP laminates would become the most reasonable solution.

During the original experimental load test [4] of the bridge, the structure was subjected simultaneously to the following two load trains: (1) two trucks of 65 kN + a cylinder of

200 kN + one truck of 65 kN + a cylinder of 120 kN (total weight of 515 kN); and (2) two trucks of 80 kN + a cylinder of 150 kN + two trucks of 30 kN (total weight of 370 kN). According to the published results of this experimental load test the maximum vertical deflection of the structure at the mid span (for the analysed fifth span) was 8 mm, corresponding to the crossing of the two defined load trains.

These same load conditions have been replicated on the updated finite element model. The distribution and distance between the loads has been established from the standards at the time of construction of the structure [25]. The maximum vertical deflection obtained under this condition was around 7.2 mm.

In spite of the observed cracking on the lower chord of the structure, the numerical deflection is slightly lower than the value obtained experimentally in the original load test of the structure. This fact confirms that the reduction of the stiffness of the truss girders has not caused deflection problems in the structure. The observed differences may be caused by factors like the increase of the concrete Young's modulus with the time, which compensate the bridge deterioration, or the stiffness introduced by the non-structural elements as the safety barriers.

Once characterized the current state of the structure, the retrofit methods based on the use of CFRP laminates appear advantageous, so that the finally selected project opted for this technique. Subsequently, the strengthening of the structure was performed by adhering CFRP laminates to its lower chords. The proposed retrofit is then configured by two components: (i) two longitudinal reinforcements composed of three CFRP laminates of 100x1.4 mm and characteristic tension strength of 2800 MPa and (ii) a fabric FRP system in order to ensure the anchorage and the protection of the above-mentioned longitudinal reinforcements (Fig. 10. a). The procedure for the placement of the laminates consists of the following steps: (i) layout of the reinforcement, (ii) surface

preparation in order to ensure a clean support on the concrete, (iii) application of a layer of epoxy primer, (iv) placement of 2-3 mm of epoxy resin on each previously prepared laminate, (v) placement of the laminate on the element to be reinforced, (vi) application of a new layer of epoxy primer and (vii) finally, placement of the fabric FRP system wrapping the both sides of the lower chord by two layers of epoxy resin. After the completion of the widening and its retrofit (Fig.10. b), the bridge is currently in service without any reported structural incidence.

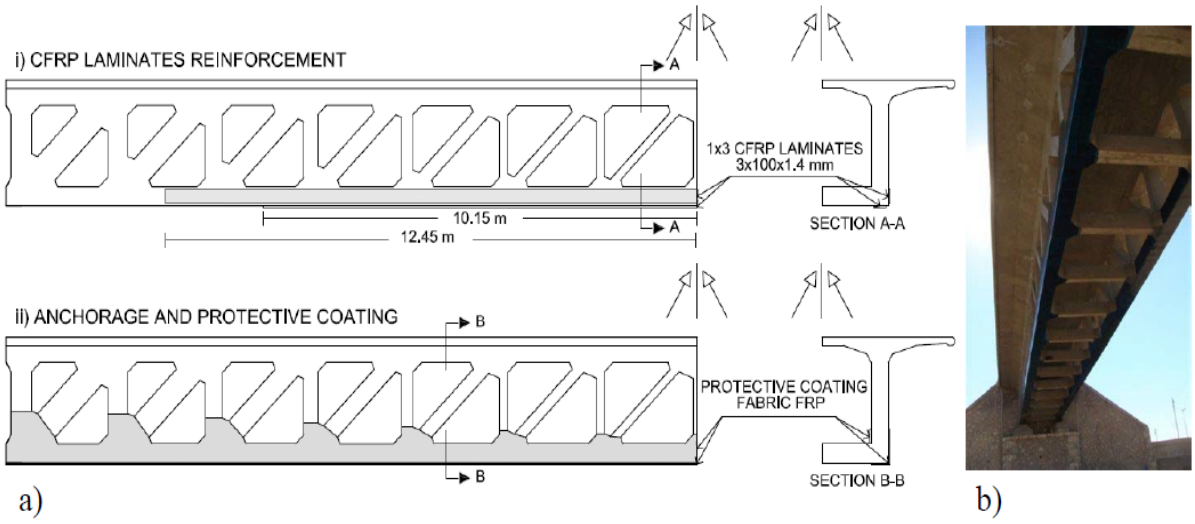

Fig. 10. a) Layout and b) placement of the CFRP reinforcement (courtesy of the Planning Department of the City of Almeria).

7. Conclusions.

In this paper, the finite element model updating technique, based on the modal parameters obtained from operational modal analysis, has been applied to characterize the actual condition of an ancient reinforced concrete truss bridge located in Almería (Spain). The updated model has been further employed to select the appropriate retrofit method, provided that the intended change of the service conditions of the bridge made necessary its strengthening. Different alternatives were proposed based either on the use of external presstressing or on the strengthening with CFRP laminates. The key factor to

select the retrofit method was based on elucidating whether the deterioration state of the structure affected significantly its global stiffness to such an extent that deflection problems could happen, when subjecting the bridge to its new loading conditions.

The use of the updated FE model has allowed for the assessment of: (i) the current behaviour of the bridge; and (ii) the estimation of the reduction in its stiffness due to the existing fissures in the structural members. This was achieved by comparison between the maximum deflection for one span of the structure recorded during the original load test and that numerically estimated based on the finite element updated model. Such analysis concluded that the deterioration state of the structure did not affect significantly its stiffness, so it was enough to strengthen the structure through the addition of CFRP laminates. The structure has been already retrofitted and it is currently in service without any reported structural problems.

Acknowledgements

This work was partially funded by the Junta de Andalucía under research projects P12-TEP-2546 and P12-TEP-2068. The authors also acknowledge the Planning Department of the City of Almería for the support during the development of the experimental tests.

References

[1] Ribera, J.E.. "Puentes de fábrica y hormigón armado. Tomo I (51, 52, 279)". Agencia de Obra Pública de la Junta de Andalucía, 1927.

[2] Ribera, J.E.. "Puentes de fábrica y hormigón armado. Tomo IV (33, 34)". Agencia de Obra Pública de la Junta de Andalucía, 1927.

[3] López Rodríguez, J.. "Puente sobre el río Andarax (o Almería) en la carretera de Almería a la Cuesta de los Castaños, por Nijar". Revista de Obras Públicas vol.75, nº2.469, enero de 1927, pp. 29-32.

[4] López Rodríguez, J.. “Pruebas del Puente sobre el río Andarax (o Almería) en la carretera de Almería a la Cuesta de los Castaños, por Nijar”. Revista de Obras Públicas vol.75, nº2.488, noviembre de 1927, pp. 421-423.

[5] Arenas de Pablo, J.J. “Los puentes en España a lo largo del siglo XX”. Revista de Obras Públicas nº 3388 (1999).

[6] Arenas de Pablo, J.J. “Caminos en el aire. Los puentes. Volumen 2. Capitulo XV (957-963)”. Colegios de Ingenieros de Caminos, Canales y Puertos. Colección ciencias humanidades y tecnología (2002).

[7] Calgaro, J.A., Lacroix, R., “Maintenance et Réparation des Ponts”. Presses de l’école nationale des ponts et chaussées 1997.

[8] Gerard, P., Hewson, N., “ICE manual of bridge engineering”. ICE manuals. Thomas Telford Limited 2008.

[9] Friswell, M.I., Mottershead, J.E., “Finite Element Model Updating in Structural Dynamics, Kluwer Academic Publishers, 1995.

[10] Magalhães, F., Cunha, A. Explaining Operational Modal Analysis with data from an arch bridge", Mechanical Systems and Signal Processing, Invited Tutorial Paper, Volume 25, Issue 5, pp. 1431-1450 , 2011.

[11] del Cuvillo, R.. “Colecciones oficiales de obras de obras de paso de carreteras (siglos XIX y XX) (30-41)”. Colegios de Ingenieros de Caminos, Canales y Puertos. Colección ciencias humanidades y tecnología (2008).

[12] Eurocode 2. Design of concrete structures. EN1992-1-1.

[13] UNE-EN-12504-2:2013. Testing concrete in structures-Part 2: Non-destructive testing-Determination of rebound number.

[14] ANSYS Mechanical Release.

[15] Eurocode 6. Design of masonry structures. EN 1996-1-1.

[16] ARTeMIS Extractor Pro. Structural Vibration Solutions, Aalborg, Denmark.

[17] Zivanovic, S., Pavic A., Reynolds P.. Finite element modelling and updating of a lively footbridge: The complete process. Engineering Structures, Vol. 301(1-2), pp. 126-145, March 2007.

[18] Teughels, A., “Inverse Modelling of Civil Engineering Structures Based on Operational Modal Data”, Ph. D. Thesis, Katholieke Universiteit Leuven, 2003.

[19] Nocental J., Wright S.J., “Numerical Optimization”. Springer, New York, USA, 1999. ISBN 0-387-98793-2.

[20] Koh Ghee C., Perry M.C., “Structural Identification and Damage Detection using Genetic Algorithms” CRC Press, Taylor and Francis Group, 2010, ISBN 978-0-415-46102-3.

[21] Maeck, J. “Damage Assessment of Civil Engineering Structures by Vibration Monitoring”. PhD Thesis, Katholieke Universiteit Leuven, 2003.

[22] Maeck, J., de Roeck, G.. Damage detection on a presstressed concrete bridge and RC beams using dynamic systema identification InProc. DAMAS 99, pp. 320-327, Dublin, Ireland, 1999.

[23] Maeck, J., de Roeck, G.. Description of Z24 benchmark. Mechanical Systems and Signal Processing, 71(1), 127-131. January 2003.

[24] Matlab R2011a. . http://www.mathworks.com/.

[25] del Cuvillo, A., del Cuvillo, R.. “Trenes de carga de puentes de carretera”. Revista de Obras Públicas vol.149, nº3.424, noviembre de 2002, pp. 39-50.

Paper D: Controlling the human-induced longitudinal vibrations of a Nielsen-truss footbridge via the modification of its natural frequencies.

This paper is currently under review.

Controlling the human-induced longitudinal vibrations of a Nielsen-truss footbridge via the modification of its natural frequencies.

Javier Fernando Jiménez-Alonso[a*] and Andrés Sáez[b]

[a]*Department of Building Engineering and Geotechnical Engineering, University of Seville, Reina Mercedes Avenue 2, Seville, 41012, Spain.*

[b]*Department of Continuum Mechanics and Structural Analysis, University of Seville, Camino de los Descubrimientos s/n, Seville, 41092, Spain.*

[*]*Corresponding author:* jfjimenez@us.es (J.F. Jiménez-Alonso).

ABSTRACT

This paper describes a case-study where the human-induced vibrations of a footbridge have been controlled by means of the modification of its natural frequencies. The structure, a Nielsen variable depth truss, is located over a highway on the outskirts of Malaga (Spain), so that it was designed to withstand low pedestrian densities and its dynamic behaviour was just analysed according to Spanish standards at the date of construction. However, the presence of a nearby sports pavilion originated unexpected large pedestrian flows. This new service condition was not properly anticipated leading to significant longitudinal vibration levels. To overcome this problem, experimental and numerical studies were carried out, with the aim of finding a low cost solution that yet maintained the footbridge aesthetic appearance. Following these studies, corrective measures that increased its stiffness were then adopted. Subsequently, experimental tests and a finite element model tuning were performed to obtain: (i) its modified modal parameters; and (ii) a more accurate estimation of its dynamic behaviour under different pedestrian flows. Presently, the footbridge has been in service for more than four years maintaining an adequate comfort level.

Keywords: Longitudinal human-induced vibrations, passive control, natural frequencies modification, slender footbridge.

1. Introduction.

Although the vibration problems caused by the flow of pedestrians on footbridges are well known since the mid nineteenth century [1, 2], it has not been until the early twenty-first century when the scientific community has devoted more attention to this issue [3-17]. However, this effort has not yet been reflected in the standards of many countries, that still either maintain the philosophy of avoiding the problem rather than facing it, or only focus on analyzing the dynamic response of the footbridge in vertical direction without considering the vibration effects in the other directions.

The project of a footbridge over a highway at the outskirts of urban areas is not normally conditioned by its dynamic behaviour under large pedestrian flows, since this load scenario will not be expected during its service life [18]. However, the actual construction of the footbridge may influence the emergence of new pedestrian flows that modify the initially expected pedestrian traffic level of the structure so that its design will be finally conditioned by its dynamic response to pedestrian action.

This is the case analysed in this paper, where the presence of a nearby sports pavilion modified the expected service conditions of a slender footbridge (Fig. 1) built on the outskirts of Malaga (Spain). The construction of the footbridge, which was intended to connect a marginal neighbourhood, “La Concha” (where hardly 200 habitants live), with the urban core of Malaga, originated that this uninhabited area began to be used as parking area for a large number of the spectators who attended the sporting events held in the pavilion located on the other side of the A-7 highway. At the end of these events, high pedestrian traffic levels were recorded on the footbridge, causing the excitation of the vibration modes of the structure in the horizontal plane. The accelerations reached clearly affected the pedestrian comfort and led to closing the

footbridge. Therefore, it became necessary to control its dynamic behaviour in order to guarantee an adequate comfort level. The characterization of the experimental and numerical dynamic behaviour of the footbridge together with the designed implementation and validation of the required remedial measures are the main focus of this paper. This case-study reports one of the first cases where the longitudinal vibrations of the structure have been the cause of the comfort problems and where the control of the vibration problem is achieved by modifying the stiffness of the structure yet maintaining the footbridge appearance and a controlled economical cost. After its reopening, the footbridge has been in service for more than four years, providing an adequate comfort level.

Fig. 1. Lateral view of the footbridge.

The paper is organized as follows: section 2 provides a description of the main structural features of the footbridge. Section 3 is devoted to analyse the dynamic behaviour of the original footbridge: first, a simplified numerical dynamic study conducted using the Spanish standards [19] at the project design date is presented; next, upon the occurrence of the above mentioned vibration problems, a more detailed experimental and numerical dynamic studies were performed, based on the method

proposed by the French code [18] and the Synpex guidelines [20]. Section 4 describes the modifications proposed on the footbridge design in order to stiffen it, thus increasing its natural frequencies and further avoiding the problem of interaction with the pedestrian step action. After the retrofit of the structure, additional experimental tests and numerical studies were performed to validate the goodness of the adopted solution. Due to the inability to test the structure under large pedestrian flows, the experimentally identified natural frequencies of the footbridge were used to perform a finite element model tuning of the structure, and subsequently, the tuned model was used as a start point for a better estimation of the dynamic behaviour of the footbridge under the effect of crowds, as described at the end of the section 4. Finally, some concluding remarks are drawn to close the paper in section 5.

2. Description of the footbridge.

The structure under study is a steel footbridge that crosses over the A-7 highway in the stretch between the cities of Malaga and Torremolinos (Spain). The main factors that conditioned the design of the structure were: (i) the low bearing capacity of the foundation soil, (ii) the construction process should avoid interferences with the traffic and (iii) a maximum width of the deck of 2.10 m was imposed.

The structure finally built has two clearly differentiated parts: (i) A central section that consists of a double Nielsen steel truss of two spans of 65.00 m of length, and an upper parabolic chord, (ii) Two access ramps, composed of a steel box girder with a span distribution of 12.00+8x11.20 m for the north access ramp (“La Concha” neighbourhood), and 16.00 +18.50+18.75 m for the other one (Fig. 2 and Fig. 3).

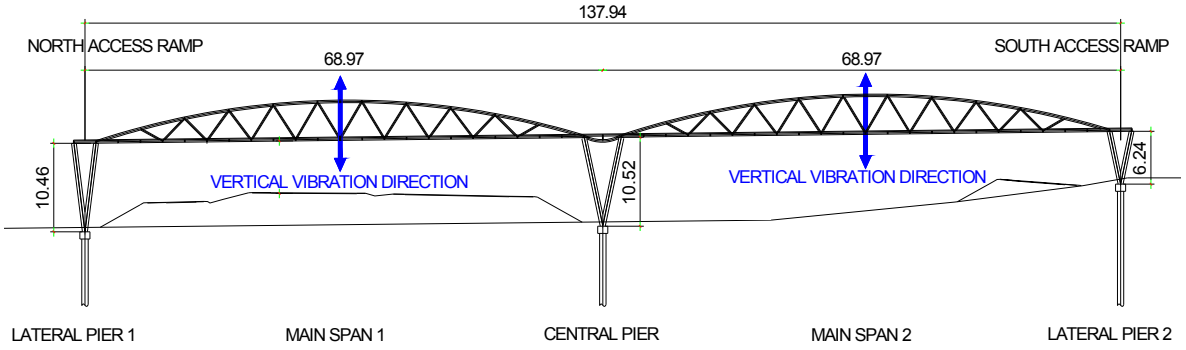

Fig. 2. Original elevation view of the footbridge (dimensions in meters).

Both the main spans and the access ramps are supported on sloping steel piers that are embedded in a deep foundation composed of vertical piles with a diameter of 1.00 m and 40.00 m of length..

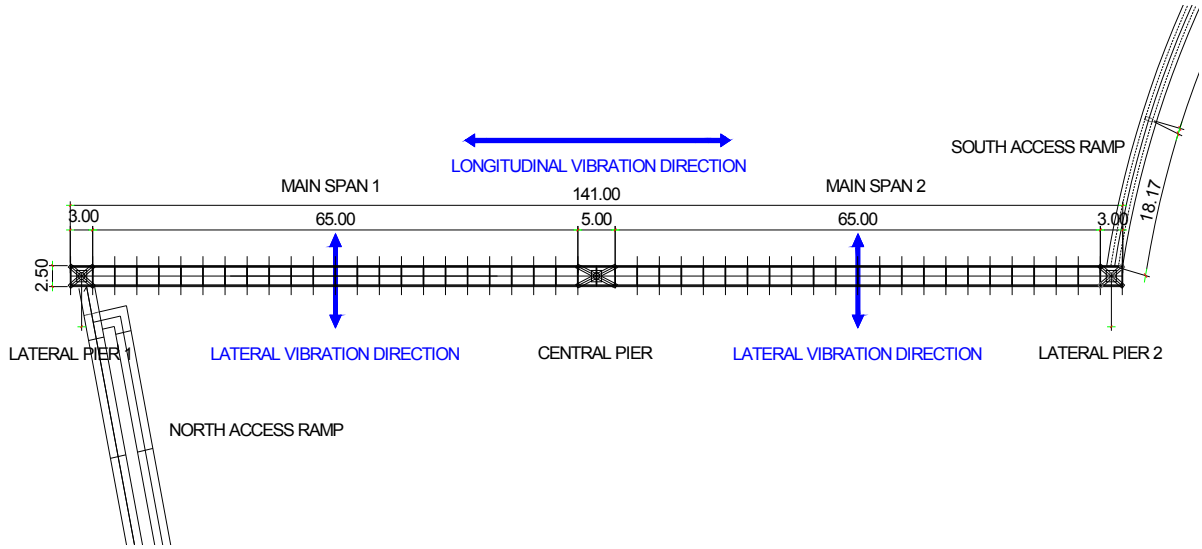

Fig. 3. Original plan view of the footbridge (dimensions in meters).

On these figures (Fig.2 and Fig.3) the reference vertical, longitudinal and lateral directions that characterize the vibration modes of the footbridge have been indicated. This criterion will be maintained for the rest of the paper.

Each of the main trusses, whose dynamic behaviour is the main objective of this study, consists of a curved upper chord formed by rectangular box cross sections 400x200x10 mm, one lower chord formed by the same profiles, and the rest of the members formed by square tubes 200x5 mm. The lateral bracing between arches is achieved by cross struts formed by the square tubes 200x5 mm and spaced about 3.00 m. The lower chord bracing consists of rectangular profiles 200x100x4 mm, on which a composite floor is placed. The depth of the slab is 0.10 m with a corrugated sheet of 1.00 mm of thickness (Fig. 4). The connection of the trusses with the V-shaped piers is achieved by bearings that do not allow any relative displacement between the deck and the piles. The depth of the truss is 4.50 m, reaching an approximate slenderness of L/14.50. The length of the piers ensures a vertical clearance of 5.50 m under the deck

Fig.4. Details of the cross section of the footbridge.

From a structural point of view, the integral footbridge design should be remarked. There are no expansion joints between the deck and the piers, thus improving the response of the deck to vertical loads due to the contribution of the stiffness of piers to bending efforts. The efforts resulting from shrinkage, creep and temperature are controlled by the flexibility of the deep foundations in a low bearing capacity ground.

Both this characteristic structural design and the shape of the piers are the main causes of some coupling effects that happen among the longitudinal and lateral response of the structure under the applied loads and it will be described in next sections.

3. Study of the dynamic behaviour of the original footbridge.

3.1. Preliminary numerical study of the dynamic behaviour of the original footbridge.

In the original project of the structure a simplified dynamic study was carried, based on the Spanish code [19] at that time, like its contemporary British standards [21]. The study simulates the passing of a *single person* by a sinusoidal force F (N) that crosses the footbridge at a speed v (m/s) proportional to the main numerical vertical natural frequency of vibration of the footbridge, f_0 (Hz):

$$F = 180 \cdot \sin\left(2\pi \cdot f_0 \cdot t\right) \tag{1}$$

$$v = 0.9 \cdot f_0 \tag{2}$$

where t (sec) denotes the time variable:

The maximum vertical acceleration, $a_{v,max}$ (m/s^2), at any point of the structure, should not exceed the value of:

$$a_{v,\max} < 0.50 \cdot \sqrt{f_0} \tag{3}$$

The Spanish code also sets a maximum vertical deformation of *L/600* to avoid dynamic problems in steel footbridges, in terms of the live load, being L the footbridge span. The maximum allowed deflection under this criterion, for this footbridge, is about 0.10 m.

The starting point, for the estimation of the comfort level, was the development of a finite element model of the structure (Fig. 5) performed by 3-D beam elements with the commercial software Autodesk Robot Structural Professional [22]. This model serves as basis for determining numerically the natural frequencies and vibration modes of the structure.

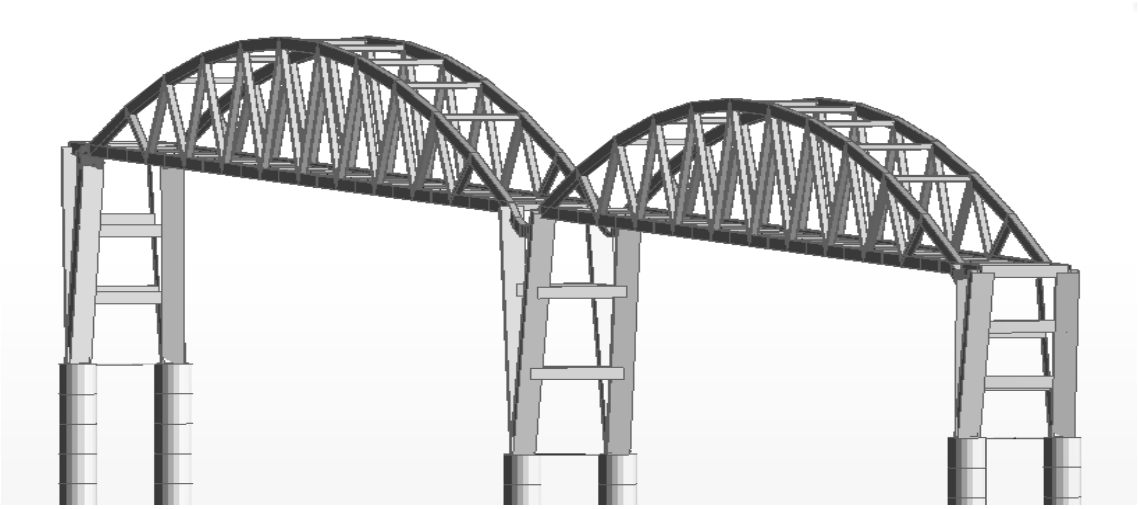

Fig. 5. Original finite element model of the footbridge.

The values of the main physical parameters that concerned the dynamic behaviour of the footbridge were the lateral soil stiffness (7500 kN/m^3), the mass ratio of the deck (200 kg/m) and the hand-railings (100 kg/m). For the characterization of the stiffness of the structure, it has been considered a steel modulus of elasticity of 200 GPa [23] and for a reinforced concrete modulus of 30 GPa [24].

Fig. 6, 7, and 8 illustrate the three first numerical vibration modes for the empty original footbridge.

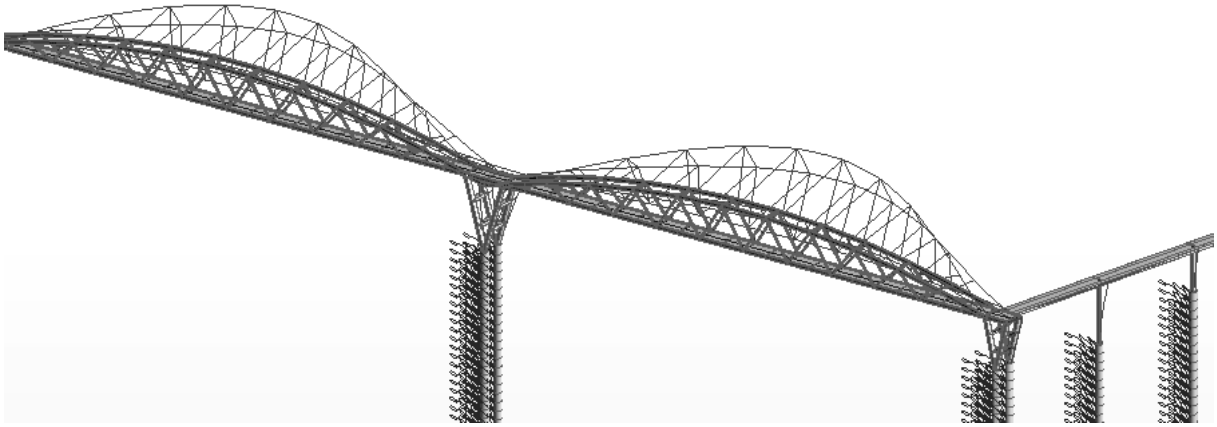

Fig. 6. First lateral bending mode (mode 1, $f_{emp\_ori\_1}$=1.14 Hz).

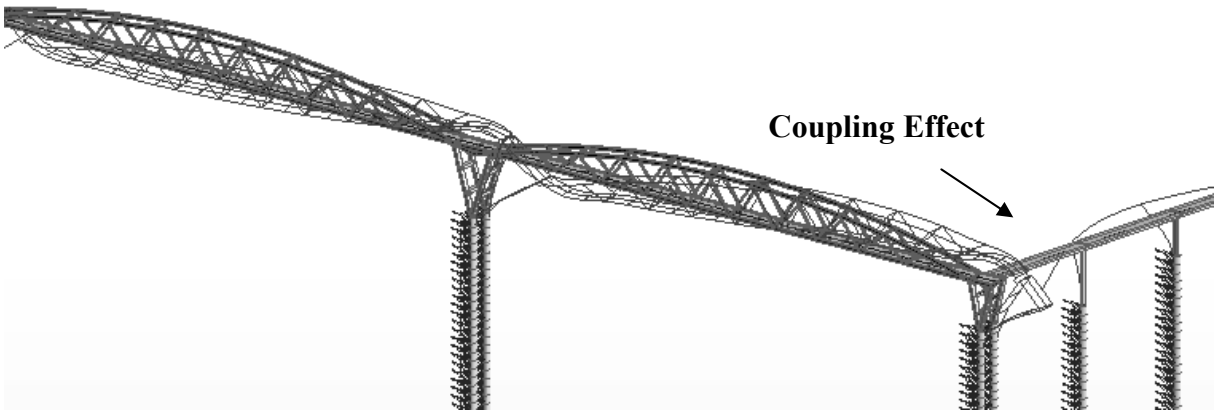

Fig. 7. First longitudinal bending mode (mode 2, $f_{emp\_ori\_2}$=2.22 Hz).

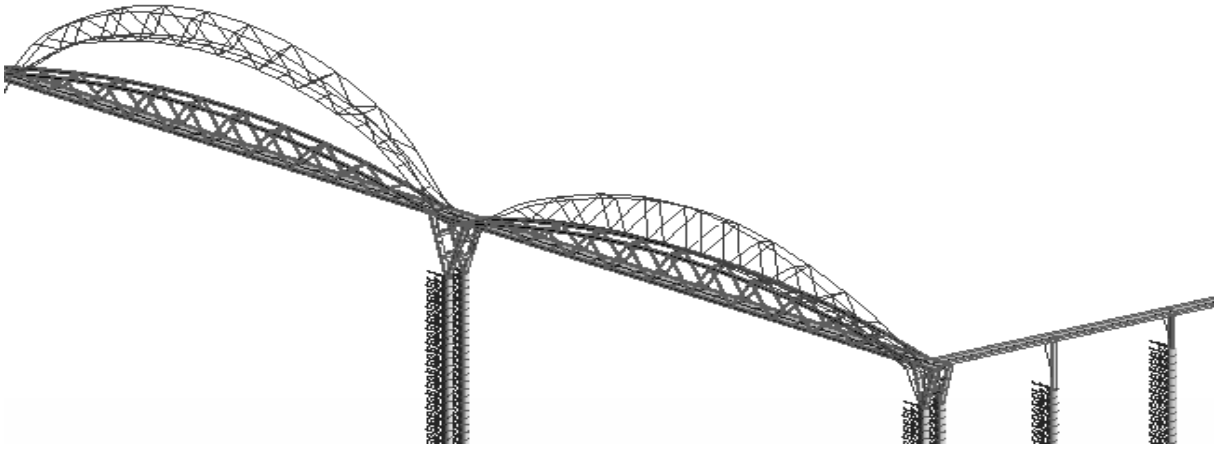

Fig. 8. First vertical bending mode (mode 3, $f_{emp\_ori\_3}$=2.40 Hz).

Analyzing the shape of the vibration modes the following conclusions may be drawn: (i) only the longitudinal vibration mode presents a global behaviour, being controlled by the stiffness of the three piers of the main span, so given certain number of pedestrians, their equivalent effect, considered as the ratio between the sum of the individual action of each pedestrian and the deck surface of the mobilized vibration mode, is reduced to a half value of the applied action on the other to vibration modes (vertical and lateral) (ii) equally, due to this global behaviour, the longitudinal vibration mode presents certain coupling between the main span and the lateral access ramps (Fig. 7).

To estimate the maximum acceleration on the footbridge, the simplified formulation to calculate the dynamic response of an isostatic beam under a moving load was used [20].

$$a_{v,\max} = \frac{\frac{2}{\pi} \cdot P_{mov}}{\frac{1}{2} \cdot \mu \cdot L} \frac{1}{2 \cdot \xi} = 0.41\,\text{m/s}^2 \tag{4}$$

where

L, is the span length (65 m).

ξ, is the damping ratio of the system ($\xi = 0.40\,\%$ according to the international guidelines [20]).

P_{mov} is the amplitude of the sinusoidal force applied (180 N).

μ is the mass of the structure per unit length ($\mu = 1070$ kg/m according to the geometric definition of the project).

Considering $f_0 = f_{emp\_ori\_3} = 2.40\,\text{Hz}$ from the original finite element numerical model of the structure (Fig. 8), the maximum allowable value of the vertical acceleration follows from equation (3)..

$$a_{v,\max} < 0.50 \cdot \sqrt{f_0} = 0.50 \cdot \sqrt{2.40} = 0.77 \text{ m/s}^2 \quad (5)$$

In relation to the maximum deflection criterion [19], the footbridge presented a maximum deflection of 0.05 m (<L/600), under a live load of 4 kN/m^2.

As conclusion of the previous results, the behaviour of the footbridge, under the mentioned Spanish code, was acceptable.

Once the construction was completed and it was opened to the public, the footbridge was in use during several weeks without exhibiting any comfort problem. In November 2009, after a sporting event at the nearby pavilion, a large crowd of people crossed the structure, causing large longitudinal vibrations on it. According to the testimony of some affected pedestrians the footbridge vibrated along a horizontal plan, in the longitudinal direction at the two main spans and laterally at the access ramp (Fig. 7). There was no evidence, according to the witnesses, of excessive vibrations of the footbridge in the vertical direction. This phenomenon occurred only after the completion of the sport event, since the access of pedestrians to the pavilion through the footbridge, before the sport event, happened sequentially. As a consequence, the footbridge was closed to traffic and further studies were conducted in order to find first the cause of the problem and then establishing remedial measures to ensure an adequate comfort level of the footbridge. Therefore, the location of the footbridge near a sports pavilion had modified its design service conditions, giving rise to the longitudinal vibration problems described above.

3.2. Experimental assessment of the dynamic behaviour of the original footbridge.

In order to assess experimentally the dynamic behaviour of the footbridge, both simplified ambient and pedestrian tests were performed. The purpose of these tests was first, simplified ambient test, to measure the response of the footbridge to the environmental noise and processing these signals with an operational modal analysis method, to estimate experimentally the natural frequencies of the structure. In the other hand, from the results of the pedestrian test is possible to check the comfort level of the structure for different loading scenarios and correlate the experimental and numerical simulations.

3.2.1. Simplified ambient test on the original footbridge.

For the simplified ambient test the response (accelerations) of the structure was measured in five locations per span, selected from the previous results of the modal analysis, using five uniaxial force balanced accelerometers (Episensor ES-U2). Due to slight variation of the height the three piers, the development of test was carried out independently in the two main spans. The frequency range of interest was 0.50-5.00 Hz. The sampling frequency was 100 Hz, with time series of 900 sec. Fig. 9 shows the location of the accelerometers on the structure.

Ten sets of measurements, five per span, were carried out; holding fixed the position of the accelerometers in each of them. On the one hand, the accelerometers were placed on the location of maximum numerical modal deformation of the vibration mode under study but also two secondary points were necessary to estimate the modal shape associated with the three identified natural frequency. During the ambient test, the footbridge was only subjected to a slight wind.

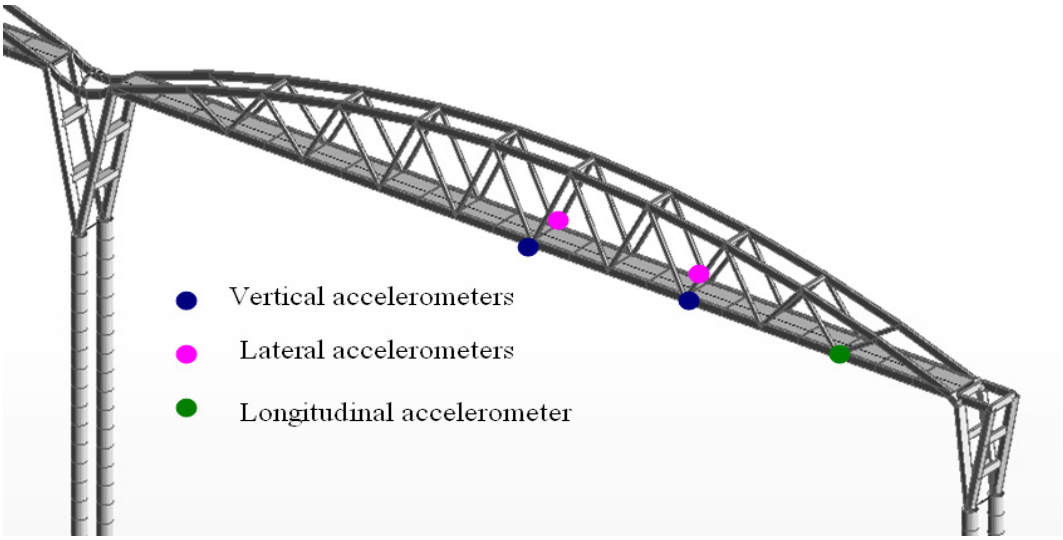

Fig. 9. Location of the five fixed accelerometers on the footbridge.

The treatment of the obtained measurements from the ambient test was conducted by the application of the operational modal analysis technique. To estimate the modal parameters from the response to the ambient excitation the Peak-Picking method was applied [25-28] by its implementation in the commercial program Matlab [29]. The choice of both the above simplified ambient test and the identification method has been motivated by its easy implementation, the adequacy of accuracy of the results to the problem studied and the need to determine experimentally only the natural frequencies of the footbridge given the nature of the vibration problem and the structural typology of the footbridge. The value of the first identified natural frequency, in each direction for each span, has been estimated as the medium value of the five series. The standard deviations obtained for the three identified natural frequencies are lower than 0.01 Hz. The differences between the natural frequencies identified in each span are negligible. The modal shape corresponding to each identified natural frequency has been estimated by the study of the sign of the relative accelerations between each pair of accelerometers situated in the same span. In the case of the accelerometers oriented longitudinally, the ones placed in both spans have been used.

Finally, in order to consider adequately the phenomenon of interaction between pedestrians and structure in the dynamic properties of the footbridge, the numerical modal analysis, described previously, was repeated under two different scenarios, namely empty and full footbridge. In the full footbridge scenario, the entire pedestrian mass is considered attached directly to the modal mass of the structure, with a pedestrian density of 1 P/m^2 (Pedestrian/m^2).

In Table 1 the numerical natural frequencies obtained from the numerical modal analysis of the original footbridge, f_{emp_ori} (empty footbridge) and f_{full_ori} (full footbridge) are shown versus the estimated experimental natural frequencies of the empty footbridge from the Peak-Picking identification method f_{PP_ori}.

Table 1. First three numerical and experimental natural frequencies of the original footbridge.

	Numerical		Experimental
Mode	$f_{emp\ ori}$ [Hz]	$f_{full\ ori}$ [Hz]	$f_{PP\ ori}$ [Hz]
Lateral	1.14	1.10	1.15
Vertical	2.40	2.27	2.43
Longitudinal	2.22	2.11	2.11

The vertical and lateral vibration modes have a good correlation between experimental and numerical values. In the case of the longitudinal frequency, the estimated value is slightly lower than the one predicted by the numerical finite element model. According to the calculation methodology used [18, 20], the difference between the experimental and the numerical longitudinal vibration mode is not relevant for the determination of the equivalent dynamic force generated by a large pedestrian flow (1.00 P/m^2) in that direction.

3.2.2. Pedestrian test on the original footbridge.

An additional pedestrian test was conducted to better characterize the observed vibration problems on the footbridge. This test revealed that the maximum accelerations recorded, under the flow of a group of 30 pedestrians prompted to walk synchronized (with the aid of a metronome) at a normal walk frequency of 2.00 Hz, were: (i) less than 0.40 m/s^2 in vertical direction (Fig. 10), (ii) up to 0.25 m/s^2 in the longitudinal direction and (iii) around 0.10 m/s^2 in the lateral direction without he occurrence of the lateral lock-in phenomenon This number of pedestrians allowed to estimate experimentally the maximum response of the structure versus an equivalent pedestrian density (defined according to international standards [18, 20] as the number of pedestrian divided by the deck surface mobilized by the considered vibration mode) of 0.25 P/m^2 for the first vertical and lateral vibration modes, and 0.12 P/m^2 for the first longitudinal vibration mode.

Fig. 6, Fig.7 and Fig.8 show the global behaviour of the longitudinal vibration mode what reduces the value of the equivalent pedestrian density against the effect of this action to the remaining considered vibration modes.

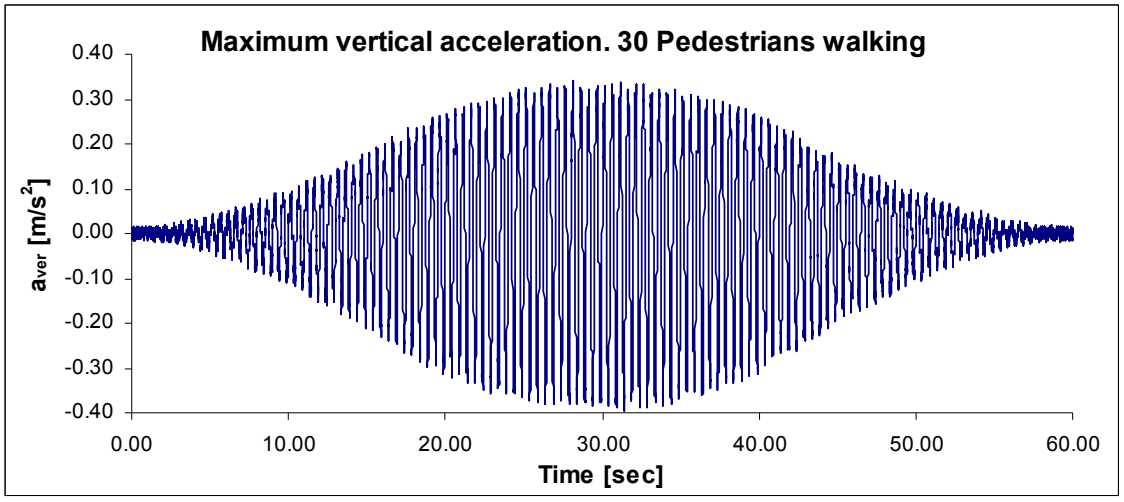

Fig. 10. Maximum vertical acceleration. Group of 30 pedestrians.

Different comfort levels are established in terms of the acceleration ranges for both vertical and horizontal directions, according to international standards [18, 20] as summarized in Table 2.

Table 2. Allowable acceleration versus comfort level.

Comfort Level	Vertical acceleration	Horizontal acceleration
Maximum	<0.50 m/s^2	<0.10 m/s^2
Medium	0.50-1.00 m/s^2	0.10-0.30 m/s^2
Minimum	1.00-2.50 m/s^2	0.30-0.80 m/s^2
Unacceptable	>2.50 m/s^2	>0.80 m/s^2

The results of the pedestrian test ensured a maximum comfort level of the structure under its original design conditions (pedestrian traffic lower than 0.20 P/m^2) in vertical and lateral direction, but only medium in longitudinal direction. Furthermore, considering the greater susceptibility of humans to horizontal vibrations and the extrapolation of the above results to higher pedestrian densities, comfort problems especially in longitudinal direction can be expected for further values of the pedestrian flows.

3.3. Detailed numerical study of the dynamic behaviour of the original footbridge.

To perform the re-evaluation of the structure a detailed numerical dynamic study of the original footbridge was carried out according to the more advanced international standards [18, 20]. These codes establish the range of frequencies that characterizes a pedestrian flow walking is 1.25-2.30 Hz in the vertical and longitudinal direction and 0.50-1.20 Hz for the lateral one, being necessary to check the comfort level of the footbridge if any numerical natural frequency of the structure, f_i, is within the above ranges.

For the determination of the traffic pedestrian level on the structure, the mentioned standards [18, 20] establish a classification of these structures according to their location and their importance, into four types of footbridges. For the type I (1.00 P/m^2), type II (0.80 P/m^2) and type III (0.50 P/m^2), the study of the dynamic behaviour of the structure is required. Subsequently, each traffic level is associated with certain comfort level in order to ensure the proper service conditions of the structure.

For the studied footbridge, the required comfort level is, for pedestrian densities lower than 0.20 P/m^2, maximum, for pedestrian densities lower than 0.80 P/m^2, medium, and minimum in the remaining cases.

The pedestrian induced action, for walking, is represented as an oscillating distributed load *p(t)*, which is applied in accordance with the mode shape considered. This load is defined by:

$$p(t) = \frac{G_i \cdot \cos(2 \cdot \pi \cdot f_i \cdot t) \cdot n' \cdot \psi}{S} \tag{6}$$

where

G_i is the equivalent pedestrian load (280 N for walking, 140 N for longitudinal and 35 N for lateral load).

f_i is the natural frequency under consideration [Hz].

$n' = \begin{matrix} 10.80 \cdot \sqrt{\zeta \cdot n} \\ 1.85 \cdot \sqrt{n} \end{matrix}$ for $\begin{matrix} d < 1.00 \\ d \geq 1.00 \end{matrix}$ P/m^2 is the equivalent number of persons on the deck

being n the number of pedestrian on the structure and ζ the structural damping ratio.

S is the surface of the deck.

ψ is the reduction coefficient that takes into account the probability that the footfall frequency approaches the natural frequency under consideration (Fig. 11).

d, is the pedestrian density [P/m^2].

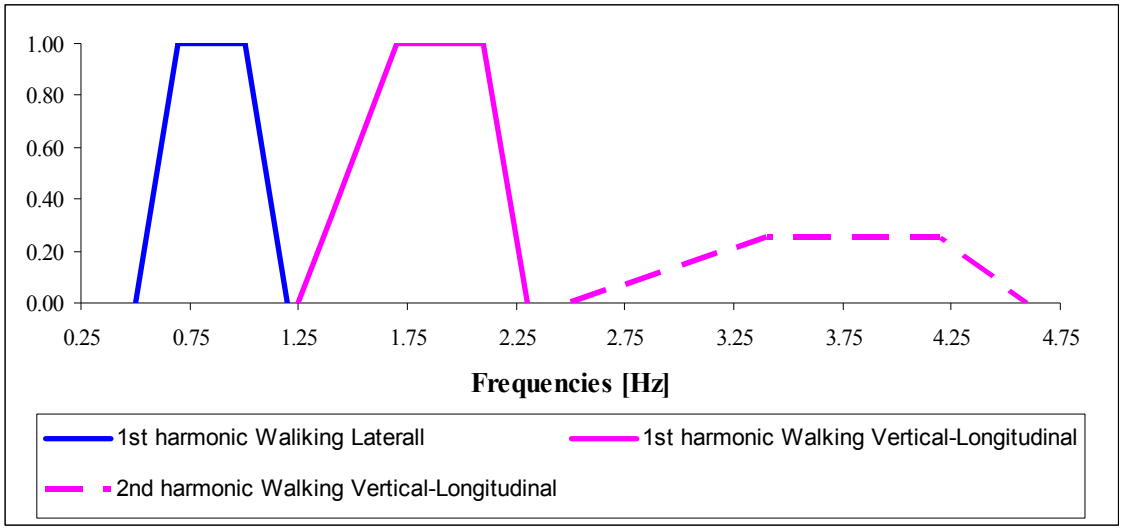

Fig. 11. Pedestrian reduction coefficient ψ.

The three natural frequencies identified experimentally and numerically were inside the ranges that characterize the pedestrian action, therefore being necessary to check numerically the comfort level of the footbridge. In Table 3 it is shown the equivalent pedestrian load p(t), according to the four different considered scenarios (d=0.20 P/m^2, 0.50 P/m^2, 0.80 P/m^2 and 1 P/m^2). These oscillating loads were applied to the finite element model of the structure in order to develop a harmonic calculation [30]. The dynamic response of the footbridge was determined considering that the load is applied with a frequency equal to the natural frequency of the vibration mode under study. Given the impossibility of estimating the damping ratio from a free decay test, all the numerical studies have been made considering a damping ratio ξ=0.40 % according to the recommendations of the international standards [18, 20].

In Table 3 the dynamic response (accelerations) according the different applied loads, a_z vertical direction, a_x longitudinal direction and a_y lateral direction is shown.

Table 3. Pedestrian walking load (eq. (6)) and maximum response of the original structure.

		Lateral			Vertical			Longitudinal		
d [P/m^2]	n' [P]	ψ	p(t) [N/m]	a_y [m/s^2]	ψ	p(t) [N/m]	a_z [m/s^2]	ψ	p(t) [N/m]	a_x [m/s^2]
0.20	4.75	0.35	0.45	0.01	0.00	0.00	0.00	0.55	2.81	0.30
0.50	7.51	0.40	0.81	0.16	0.00	0.00	0.00	0.70	5.66	0.57
0.80	9.50	0.50	1.28	0.25	0.05	1.02	0.18	0.85	8.70	0.85
1.00	28.77	0.50	3.87	0.76	0.15	9.29	1.58	0.95	29.43	2.83

Subsequently, the synchronisation and lock-in phenomena must be checked. To study the synchronization for lateral excitation, between the two methods currently accepted, the criterion established by the French code [18] has been chosen since the lateral natural frequency of the footbridge is slightly out the range of application of Arup's formula [3]. Thus, the pedestrian density that causes a lateral acceleration exceeding the limits established by the French code, 0.10-0.15 m/s^2, is around 0.50 P/m^2 (Table 3)

From the above experimental and numerical results, it may be concluded that the main cause of the vibration problem is the excitation of the first longitudinal vibration mode of the footbridge due to its interaction with the pedestrian step. In this direction, the first natural frequency of the structure is inside the range, 1.25-2.30 Hz that characterizes the pedestrian action so that, due to the large pedestrian flows observed, the footbridge will not be able to meet the required comfort limits. This footbridge appears as one of the first documented cases where vibration problems have their cause in the longitudinal excitation of the piers due to the pedestrian flows. On the other hand, the longitudinal vibration mode caused lateral displacement on the access ramps (Fig. 3 and Fig. 7).

Thus, as a summary of the above results, the dynamic behaviour of the footbridge in the vertical direction is appropriate, as it satisfies the comfort level

associated with each traffic level. However, due to the greater susceptibility of humans to horizontal vibrations, the footbridge need to be reconditioned: (i) increasing the comfort level of the footbridge in the longitudinal direction ensuring at least a medium value for pedestrian densities of 1 P/m^2 and (ii) avoiding the occurrence of the lateral lock-in phenomenon for each design service scenario.

4. Proposal and validation of the structural modifications to improve the dynamic behaviour of the footbridge.

From the above analysis, one may conclude that the two most viable solutions, to control the vibration problem, are either increasing the stiffness of the structure, so that the three first natural frequencies exceed the upper allowable limit values, or increasing the structural damping of the footbridge through the placing of some devices (as usual tuned mass dampers).. Due to the deadlines of the construction, the budged of the estimated tuned mass dampers, the existence of more than one vibration mode affected and the location of the natural frequencies of the structure near the upper limit of the range that characterizes the pedestrian action, the proposed solution focused on stiffening the structure. A modified design was proposed and its performance validated as follows:

- (i) First, the footbridge was stiffened with the objective that the natural frequencies of the structure were upper the range that characterizes the walking pedestrian action.

- (ii) Second, an experimental identification of the natural frequencies of the footbridge was made in order to quantify the value of the stiffness achieved; and

- (iii) Finally, using the results of the previous tests, a finite element model tuning of the structure was carried out. This tuned model allowed a more accurate

estimation of the expected dynamic response of the structure under large pedestrian flows.

4.1. Modification of the stiffness of the footbridge.

In the selection of the stiffening system, there were two limitations: the increase of weight should be mainly resisted by the original structure and foundation; and the overall configuration of the pedestrian bridge, from an aesthetic point of view, should not be deeply affected.

Three stiffening elements were proposed:

(i) Longitudinal stiffening of the central pier.

In order to improve the longitudinal dynamic behaviour of the footbridge, it was proposed to place four inclined elements on rigid footings, attached to the deep piles, in the central piers, so the form of this element is changed, from the V-shaped to M-shaped. Thus, a braking frame is configured in this way; that leads to a significant increase of the longitudinal stiffness of the structure and largely prevents the range of pedestrian vibrations resonance. In the Fig. 12, a scheme of the longitudinal stiffened central pier is shown..

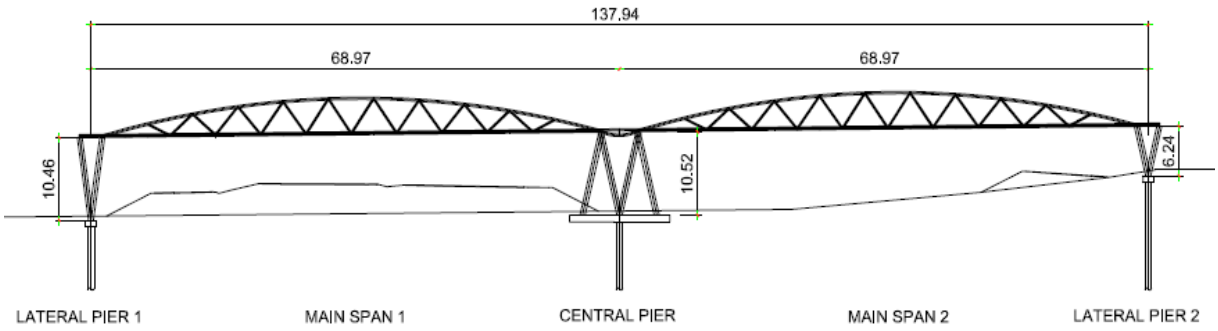

Fig. 12. Scheme of the longitudinal stiffened central pier (dimensions in meters).

(ii) **Lateral stiffening of the three main piers.**

To improve the structural behaviour in the lateral direction, it was decided to operate on the piers, stiffening them by bracings with profiles L100x10 mm, as depicted in Fig 13.

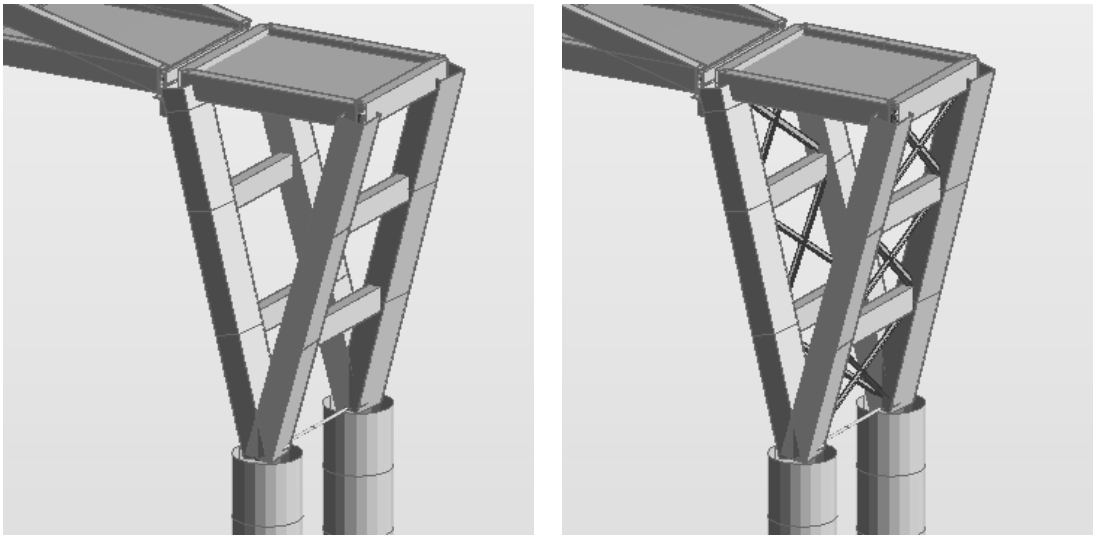

Fig. 13. Scheme of the transversal stiffening of lateral piers.

(iii) Torsion closing of the Nielsen-trusses.

Finally, as an additional action to improve the dynamic behaviour of the footbridge under large pedestrian flows, both vertically and laterally, the torsion stiffness of the Nielsen-trusses was increased. The torsion closing of the trusses was materialized by bracings with profiles L100x10 mm (Fig. 14) on the trusses upper chord.

Fig. 14. Scheme of the torsion closing of the deck.

4.2. Finite element model and numerical modal analysis of the stiffened footbridge.

After the structural modifications were introduced, the first numerical natural frequencies predicted by the finite element model adopted the values shown in Table 4, for both empty (f_{emp_stif}) and full (f_{full_stif}) deck situations.

It follows that the first natural frequencies of the structure, in the three spatial directions fall outside of the interaction range of the first harmonic that characterizes the pedestrian walking action. However, the longitudinal natural frequency is inside the

range that characterizes the second harmonic, 2.50-4.60 Hz. The equivalent harmonic walking load, in longitudinal direction, for pedestrian densities lower than 0.80 P/m^2 originated a longitudinal acceleration of 0.06 m/s^2, which increased to about 0.15 m/s^2 for a pedestrian density of 1 P/m^2. These results guaranteed a maximum comfort level for pedestrian densities lower than 0.80 P/m^2 and a medium comfort level for a pedestrian density of 1 P/m^2, what improves the requirements established in the retrofit project. Furthermore, given the value of the first lateral natural frequency of the footbridge, the lateral lock-in phenomenon is not expected.

After incorporating these modifications on the footbridge, and before its reopening, two types of tests were further performed: (i) ambient test in order to identify experimentally the dynamic characteristics of the structure and (ii) pedestrian test in order to obtain experimental estimations of the maximum accelerations on the deck under a controlled group of pedestrians. Subsequently, a finite element model tuning was performed in order to estimate the dynamic response of the structure under high pedestrian flows.

4.3. Experimental assessment of the modified dynamic behaviour of the stiffened footbridge.

4.3.1. Ambient test on the stiffened footbridge.

The methodology of the ambient test previously made to determine experimentally the natural frequencies of the original footbridge has been replicated after modifying its stiffness. So, the data acquisition equipments, the location of the accelerometers on the structure (Fig. 9), the sets of measurements, the cut-off frequency, the sampling frequency and the duration of each set-up were the same as in the previous ambient test.

In Table 4 the numerical natural frequencies obtained from the numerical modal analysis of the stiffened footbridge, f_{emy_stif} (empty footbridge) and f_{full_stf} (full footbridge) are shown versus the estimated experimental natural frequencies from the Peak-Picking identification methods f_{PP_stif}.

Table 4. First three numerical and experimental natural frequencies of the stiffened footbridge.

	Numerical		Experimental
Mode	$f_{emp\ stif}$ [Hz]	$f_{full\ stif}$ [Hz]	$f_{PP\ stif}$ [Hz]
Lateral	1.30	1.21	1.56
Vertical	2.51	2.35	2.56
Longitudinal	2.86	2.71	3.02

The vertical natural frequencies have a good correlation between experimental and numerical values. In the case of the lateral and longitudinal frequencies the estimated values are higher than the ones predicted by the numerical finite element model. The experimental lateral natural frequency of the footbridge, after the stiffening of the structure, is higher than the numerical one, resulting in this way confirmed that the occurrence of the lateral lock-in phenomenon has been avoided.

4.3.2. Pedestrian test on the stiffened footbridge.

After the completion of the ambient test, an additional pedestrian test was performed in order to measure the response of the structure under controlled groups of pedestrians.

For the study of the dynamic behaviour of the structure, different passages were made with groups of 10 synchronized pedestrians walking (1.50-2.00 Hz). During the performance of this test, the maximum vertical acceleration reached on the structure is

was than 0.20 m/s^2 (Fig. 15), being the corresponding horizontal accelerations less than 0.05 m/s^2

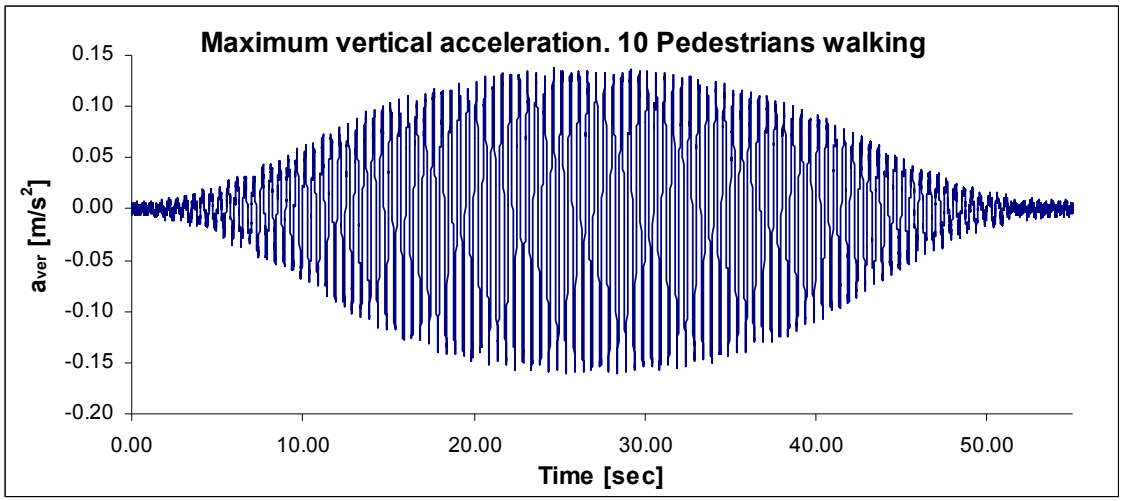

Fig. 15. Maximum vertical acceleration. 10 pedestrians on the stiffened footbridge.

The results of the pedestrian test are within the order of magnitude established by the predictions of the calculation model of the structure.

4.4. Finite element model tuning and prediction of the dynamic response of the stiffened footbridge.

In order to reduce these differences and develop a more precise numerical model, a finite element model tuning was carried out from the identified experimental frequencies. This resulting tuned model will be later used to assess the expected behaviour of the modified footbridge under large pedestrian flows.

The finite element model tuning, based on the results of the experimental identification test, is carried out from the comparison of the natural frequencies values obtained from both the experimental and numerical modal configurations [31, 32]. In this way, the tuning of the finite element model is performed by minimizing the differences between both of the results through a global optimization algorithm [33] (in

this work, the classic genetic algorithms [34]). The objective function and the optimization algorithm have been implemented in the commercial software Matlab [29].

In the model tuning of the footbridge, and provided that three natural frequencies have been identified, three structural parameters have been selected as well; namely the lateral soil stiffness θ_1, the deck mass ratio, θ_2 and the railings mass ratio θ_3.

A summary of the initial values of each parameter, the range of variation during the optimization process, and the values that minimize the objective function are shown in Table 5. The relative mean square error reached, after the adjustment of the parameters, is less than 0.10 %.

Table 5. Different structural parameter values during tuning process

Denomination	Parameter	Unit	Initial	Variation Range	Tuned
Lateral soil stiffness	θ_1	kN/m^3	7500	7500-15000	10000
Deck mass ratio	θ_2	kg/m^2	200	0-250	175
Railings mass ratio	θ_3	kg/m	100	0-200	25

After the finite element model tuning, a more accurate prediction of the dynamic behaviour of the footbridge under large pedestrian flows may be achieved [35, 36]. In this sense, the equivalent harmonic walking load was applied on the tuned finite element model to obtain the maximum acceleration of the footbridge under the different design scenarios. The maximum numerical acceleration obtained from the tuned finite element model is only significant in longitudinal direction, being around 0.10 m/s^2 for pedestrian densities lower than 0.80 P/m^2, which increased to about 0.27 m/s^2 for a pedestrian density of 1 P/m^2. The maximum vertical acceleration obtained in the other two directions is less than 0.05 m/s^2 even for a pedestrian density of 1 P/m^2. These results ensure a maximum comfort level of the structure for the different design scenarios.

Finally, a summary of the numerical estimation of the change of the dynamic natural frequencies of the footbridge and its dynamic response due to the retrofit process is shown in Fig. 16 and Fig. 17.

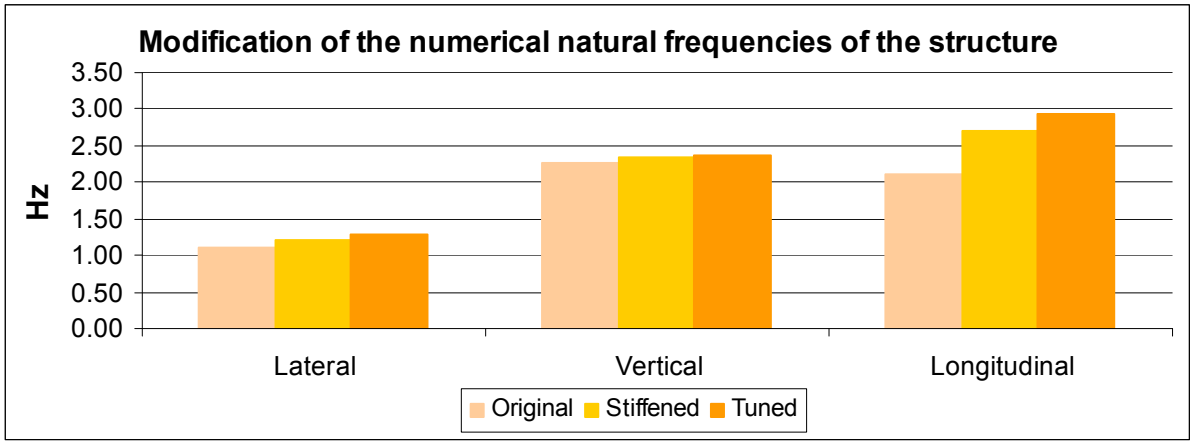

Fig. 16. Summary of the changes of the numerical natural frequencies of the footbridge due to the retrofit process.

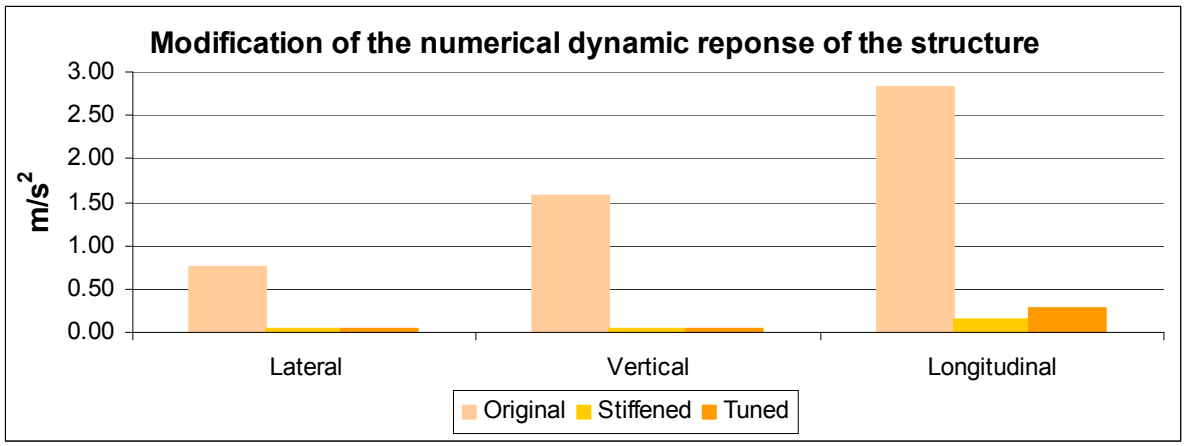

Fig. 17. Summary of the changes of the numerical dynamic response of the structure (accelerations) due to the retrofit process.

These figures (Fig. 16 and Fig. 17) show that a slight variation of the natural frequencies of the structure (due to the retrofit process) leads to a high reduction of the

dynamic response of the footbridge under large pedestrian flows and the corresponding improvement of the comfort level of the structure.

5. Conclusions.

This article describes the vibration problems occurred in a steel footbridge located on the outskirts of Malaga as a result of the change of use experienced by its proximity to a sports pavilion. Both the slenderness of the structure and the unique design of its piers were the cause of its tendency to be excited longitudinally by the effect of the pedestrian flows. Once analyzed numerically and experimentally the natural frequencies of the structure, it was considered that the best option to control the vibration problem was to stiffen the structure while maintaining its overall aesthetics. The action focused on modifying the shape of the central pier from "V" to "M" form, and stiffening laterally the piers and top chord of the truss with the placement of rolled members. In order to check the validity of these modifications, ambient and pedestrian tests were further performed in order to identify experimentally the dynamic properties of the structure. These obtained parameters were subsequently used to tune the finite element model of the footbridge and establish a starting point to estimate more precisely the expected dynamic response of the footbridge under large pedestrian flows. At present, the footbridge has been in service for more than four years without vibration problems.

Acknowledgements

This work was partially funded by the Junta de Andalucia under research project P12-TEP-2546.

The authors acknowledge the construction company, SACYR S.A.U., for the support

during the development of the experimental tests.

References

[1] Bachmann H., Ammann W.. Vibrations in Structures, Induced by man and machines. Structural Engineering Documents, IABSE , 1987. Nº 3e.

[2] Wolmuth, B., Surtees, J.. Crowd-related failure of bridges. Civil Engineering, Vol. 156, No.3, pp. 116-123,2003.

[3] Dallard P., Fitzpatrick A.J., Le Bourva S., Low A., Smith R., Wilford M., Flint, A.. The London Millenium Footbridge. The Structural Engineer, Vol. 79, No. 22, pp.17-33, November 2001.

[4] Fujino Y., Pacheco B., Nakamura S. and Warnitchai P.. Synchronization of human walking observed during lateral vibration of a congested pedestrian bridge. Earthquake Engineering and Structural Dynamics, Vol. 22, Issue 9, pp. 741-758, September 1993.

[5] Barker, C.. Some observations on the nature of the mechanism that drives the self-excited lateral response of footbridges. International Conference on the Design and Dynamic Behaviour of Footbridges. Paris, 2002.

[6] Nakamura, S.. Model for lateral excitation of footbridges by synchronous walking. Journal of Structural Engineering, 130(1): 32-37, 2004.

[7] Brownjohn J., Fok P., Roche M., Moyo P.. Long span steel pedestrian bridge at Singapore Changi Airport – Part 1: Prediction of vibration serviceability problems. Struct Eng 82(16):21-7, 2004.

[8] Brownjohn J., Fok P., Roche M., Omenzetter P.. Long span steel pedestrian bridge at Singapore Changi Airport – Part 2: Crowd loading tests and vibration mitigation measures. Struct Eng 82(16):28-34, 2004.

[9] Zivanovic, S., Pavic A., Reynolds P.. Vibration serviceability of footbridges under human-induced excitation: a literature review. Journal of Sound and Vibration, Vol. 279, Issue 1-2, pp. 1-74, January 2005.

[10] Piccardo G., Tubino F.. Parametric resonance of flexible footbridges under crowd-induced lateral excitation. Journal of Sound and Vibration, Vol. 311, Issue 1-2, pp. 353-371, March 2008.

[11] Ingolfsson, E.T., Georgakis, C.T., Svendsen, M.N., "Vertical footbridge vibrations: details regarding experimental validation of the response spectrum methodology", Footbridge 2008, Porto, Portugal, 2008.

[12] Macdonald JHG. Lateral excitation of bridges by balancing pedestrians. Proceeding of the Royal Society A., First Cite, September 2008.

[13] Racic V., Pavic A., Brownjohn J. M. W.. Experimental identification and analytical modelling of human walking forces: Literature review. Journal of Sound and Vibration, Vol. 326, Issue 1-2, pp. 1-49, September 2009.

[14] Venuti F., Bruno L.. Crowd-structure interaction in footbridges: Modelling, application to a real case-study and sensitivity analyses. Journal of Sound and Vibration, Vol. 323, Issue 1-2, pp. 475-493, June 2009.

[15] Caetano E., Cunha A., Magalhães F., Moutinho C.. Studies for controlling human-induced vibration of the Pedro e Inês footbridge, Portugal. Part 1: Assessment of dynamic behaviour. Engineering Structures Vol. 32, Issue 4, pp. 1069-1081, April 2010

[16] Caetano E., Cunha A., Magalhães F., Moutinho C.. Studies for controlling human-induced vibration of the Pedro e Inês footbridge, Portugal. Part 2: Implementation of tuned mass dampers. Engineering Structures Vol. 32, Issue 4, pp. 1082-1091, April 2010.

[17] Carrol, S.P., Owen, J.S,, Hussein, M.F.M.. Modelling crowd-bridge dynamic interaction with a discretely defined crowd. Journal of Sound and Vibration, 331 (1): 2685-2709, 2012..

[18] SETRA/AFGC. Guide méthodologique passerelles piétonnes (Technical Guide Footbridges: Assessment of vibration behaviour of footbridge under pedestrian loading). SETRA, 2006.

[19] Ministerio de Fomento. "Recomendaciones para el proyecto de puentes metálicos para carreteras, RPM-95". Dirección General de Carreteras. 2003

[20] Butz CH., Heinemeyer, CH.; Goldack, A.; Keil, A.; Lukic, M.; Caetano, E.; Cunha, A.. Advanced Load Models for Synchronous Pedestrian Excitation and Optimised Design Guidelines for Steel Footbridges (SYNPEX). RFCS-Research Project RFS-CR-03019. 2007.

[21] British Standards Institution, Steel, concrete and composite bridges. Part 2: Specification for loads, BS 5400-2: 2006.

[22] Autodesk Robot Structural Analysis Professional. http://www.autodesk.com/products/autodesk-simulation-family/features/robot-structural-analysis,

[23] Eurocode 3: Design of steel structure. Part 2. Steek Bridge. EN1993-2, 2006.

[24] Eurocode 2: Design of concrete structures. Concrete bridges. Design and detailing rules EN 1992-2, 2005

[25] Bendat, J. S., and Piersol, A. G.. Engineering application of correlation and spectral analysis, Wiley, New York. 1993.

[26] Maia N., Silva J.. Theoretical and Experimental Modal Analysis. Instituto Superior Técnico, Portugal, Research Studies Press, LTD,1997, ISBN 0-86380-208-7.

[27] Cunha A., Caetano, E., . Magalhães, F.. Output-only Dynamic Tesing of Bridges and Special Structures. Structural Concrete. Journal of FIB, 8, No. 2, PP67-85, 2007.

[28] Magalhães, F., Cunha, A.. Explaining Operational Modal Analysis with data from an arch bridge. Mechanical Systems and Signal Processing, Invited Tutorial Paper. Volume 25, Issue 5, pp. 1431-1450 , 2011.

[29] Matlab R2011a. . http://www.mathworks.com/.

[30] Clough R., Penzien J., "Dynamic of Structures", McGraw-Hill, Inc. 1993, ISBN 0-07-113241-4.

[31] Friswell, M.I., Mottershead, J.E., "Finite Element Model Updating in Structural Dynamics, Kluwer Academic Publishers. ISBN 0-7923-3441-0, 1995.

[32] Teughels, A., "Inverse Modelling of Civil Engineering Structures Based on Operational Modal Data", Ph. D. Thesis, Katholieke Universiteit Leuven, 2003.

[33] Nocental J., Wright S.J., "Numerical Optimization". Springer, New York, USA, 1999, ISBN 0-387-98793-2.

[34] Koh Ghee C., Perry M.C., "Structural Identification and Damage Detection using Genetic Algorithms" CRC Press, Taylor&Francis Group, 2010, ISBN 978-0-415-46102-3.

[35] Zivanovic, S., Pavic A., Reynolds P.. Modal testing and FE model tuning of a lively footbridge structure. Engineering Structures, Vol. 28, pp. 857-868, January 2006.

[36] Zivanovic, S., Pavic A., Reynolds P.. Finite element modelling and updating of a lively footbridge: The complete process. Engineering Structures, Vol. 301(1-2), pp. 126-145, March 2007.

Paper E: Lateral crowd-structure interaction model to analyze the lateral lock-in phenomenon on a real footbridge.

This paper is currently under review.

Lateral crowd-structure interaction model to analyse the lateral lock-in phenomenon on a real footbridge.

Javier Fernando Jiménez-Alonso[a*], Andrés Sáez[b] , Elsa Caetano[c] and Álvaro Cunha[d]

[a*]*Assistant professor. Department of Building Engineering and Geotechnical Engineering, University of Seville, Avenida de Reina Mercedes 2, 41012, Seville (Spain). Email: jfjimenez@us.es.*

[b]*Full professor. Department of Continuum Mechanics and Structural Analysis, University of Seville, Camino de los Descubrimientos s/n, 41092, Seville (Spain). Email: andres@us.es.*

[c]*Associate professor. Department of Civil Engineering. FEUP. R. Dr. Roberto Frias, s/n, 4200-465 Porto (Portugal). Email: ecaetano@fe.up.pt.*

[d]*Full professor. Department of Civil Engineering. FEUP. R. Dr. Roberto Frias, s/n, 4200-465 Porto (Portugal. Email: acunha@fe.up.pt.*

[*]*Corresponding author:* Assistant Professor: Javier Fernando Jiménez-Alonso. Department of Building Structures and Geotechnical Engineering. University of Seville. Avenida de Reina Mercedes, 2, 41012, Seville (Spain) Ph:+34 954 556 602 . E-mail: *jfjimenez@us.es*.

ABSTRACT

In this paper a biomechanical crowd-structure interaction model is proposed and calibrated in order to take into account the change of the modal properties of the footbridge in lateral direction due to the crossing of pedestrian flows. The model involves two sub-models, namely (i) the pedestrian-structure interaction and (ii) the crowd sub-models. In the first sub-model, a two d.o.f, system, that simulates the behavior of each pedestrian, is projected on the vibration modes of the structure. The parameters of this sub-model have been estimated from the results

of different experimental tests performed on a real footbridge. For the second sub-model, the crowd behaviour is modelled via a multi-agent method. In order to assess the performance of the overall model, the results from an experimental lateral lock-in pedestrian test on a real footbridge, reported in the literature, have been correlated successfully with the numerical estimations obtained from the implementation of the proposed model. In particular, the maximum lateral acceleration of the footbridge and the change of the first lateral natural frequency in terms of the number of pedestrians on the structure are discussed in detail. Therefore, the proposed model is a valuable tool to analyse numerically the lateral lock-in phenomenon and the change of the modal parameters of footbridges due to the presence of pedestrians.

Keywords: simplified biomechanical model, human-structure interaction, crowd dynamics, change of natural frequencies, lateral lock-in phenomenon, footbridge.

1. Introduction.

After vibratory problems happened in the Millennium footbridge (London, U.K.) during its opening (Dallard et al., 2001), the analysis of the sensitivity of footbridges to the lateral lock-in phenomenon has become an essential issue in the design project of this type of structures (Butz et al., 2007). Among the different procedures proposed since that event, three are the methodologies that according to the author's judgement have had more influence on the scientific community and the practical designers. The first proposal comes from the research conducted on the above mentioned footbridge in order to characterize the lateral lock-in phenomenon (Dallard et al., 2001). Its main results were: (i) the establishment of a range, between 0.50-1.20 Hz, of the lateral natural frequency of the footbridge that originates the synchronization between the movement of the pedestrians and the structure and (ii) the consideration of each pedestrian, under this situation, as a device that modifies the modal properties of the footbridge, reducing its structural damping so that an instability dynamic situation may

occur. The practical application of this theory is the well-known Arup formula that allows determining the number of pedestrians that originates the lateral lock-in phenomenon. This relationship has been widely used to analyse the sensitivity of footbridges to the lateral lock-in phenomenon, although it presents the limitation that its coefficients have only been estimated from the experimental tests conducted at one particular footbridge, the Millennium footbridge. Similar expressions have been proposed by different authors (Fujino and Siringoringo, 2014) following the same philosophy. Subsequently, the French standard (Setra, 2006) proposed a compact approach to check directly the comfort level of a footbridge under pedestrian flows and estimate its risk of occurrence of the lateral lock-in phenomenon. This proposal is based on the experimental and numerical tests conducted on the Solferino footbridge (Paris, France) and on mobile platforms. Its main contribution is the establishment of a maximum lateral threshold of the deck, around 0.10-0.15 m/s^2, that determines the occurrence of the lateral lock-in phenomenon. More precisely, if the lateral acceleration of the deck exceeds this value and the lateral natural frequency of the footbridge is inside the range proposed by Dallard (Dallard et al., 2001), the instability phenomenon occurs. According to this standard, the effect of each pedestrian on the structure is simulated by an equivalent harmonic force considering only the pedestrian-structure interaction through a simplified rule that adds passively the pedestrian mass to the modal mass of the structure. The number of pedestrians that originates the lateral lock-in phenomenon may be determined considering both the dynamic response of the footbridge under the pedestrian action and the above threshold. Finally, the model proposed by Macdonald (Macdonald, 2008) considers that the lateral instability dynamic is originated by the increase of the lateral walking pedestrian force associated with the change of the body position of each pedestrian, in order to guarantee his/her

equilibrium, when the lateral accelerations of the footbridge exceed certain level. The model has been accepted internationally in order to predict the beginning of the phenomenon, and it has been the basis for the development of more sophisticated proposals, as the works reported by Carrol et al (2012) and Bocian et al. (2014). However, all these models share a main limitation in commons: they do not take into account the pedestrian-structure interaction appropriately.

In this paper, a crowd-structure interaction model, previously applied successfully by the authors (Jiménez-Alonso et al. 2015) to analyse the vibratory problem in vertical direction, has been generalized in order to analyse the dynamic response of footbridges under pedestrian action in lateral direction. Furthermore, it is implemented to analyse numerically the lateral lock-in lateral phenomenon on a real footbridge. The proposed model, an evolution of the existing proposals, presents as main contributions that it considers the modification of the modal properties of the footbridge induced by the pedestrian-structure interaction and that its parameters have been obtained from experimental tests performed on a real footbridge. The model is configured by two sub-models: (i) a pedestrian-structure interaction sub-model, where each pedestrian is modelled by a two degrees of freedom (TDOF) system that divides the pedestrian mass in sprung plus unsprung components, and (ii) a crowd sub-model, where the movement of each pedestrian is governed by social interaction forces (Helbing and Molnár, 1995). The interaction between the two sub-models in the lateral direction is achieved by implementing two different thresholds, in such way that if certain acceleration limits are exceeded the affected pedestrians change their behaviour. The estimation of the parameters of the proposed pedestrian-structure interaction model has been experimentally performed based on the results of two sets of experimental tests conducted at the Viana footbridge (Viana do Castelo, Portugal) (Barbosa et al., 2012).

Subsequently, the crowd-interaction model has been implemented and its performance assessed by satisfactorily correlating the experimental and numerical analysis of the lateral lock-in phenomenon of Pedro e Inês footbridge (Coimbra, Portugal) (Caetano et al. 2010).

The paper is organized as follows. The proposed crowd-structure interaction model is discussed in Section 2. The experimental estimation of the parameters that characterize the pedestrian-structure interaction model is performed in Section 3. The validation of the model is shown in Section 4. Finally, some concluding remarks are drawn to close the paper in section 5.

2. Proposal of a simplified biomechanical crowd-structure interaction model in lateral direction.

The complete crowd-structure interaction phenomenon has been simulated using two individual sub-models (Fig. 1): (i) the pedestrian-structure interaction and (ii) the crowd sub-model. In the first sub-model, all the dynamics effects induced by the pedestrians on the footbridge are considered. The lateral acceleration $\ddot{y}_a$ experimented by each pedestrian is the output obtained from this model. In the second sub-model, the crowd is simulated as behavioural model providing a description of the individual pedestrian position, $\mathbf{x}_p$, walking pedestrian velocity, $\mathbf{v}_p$, step pedestrian frequency, f_s, and phase among pedestrians, ϕ_p.

In order to consider the change of the pedestrian behaviour associated with the accelerations experienced, two additional conditions have been included in this sub-model: a reduction factor that affects the pedestrian velocity according to the comfort level experienced by each pedestrian; and a lock-in threshold that modifies the step

pedestrian frequency and the phase among pedestrians in order to simulate the synchronization between the movement of the pedestrians and the footbridge (Ronnquist, 2005).

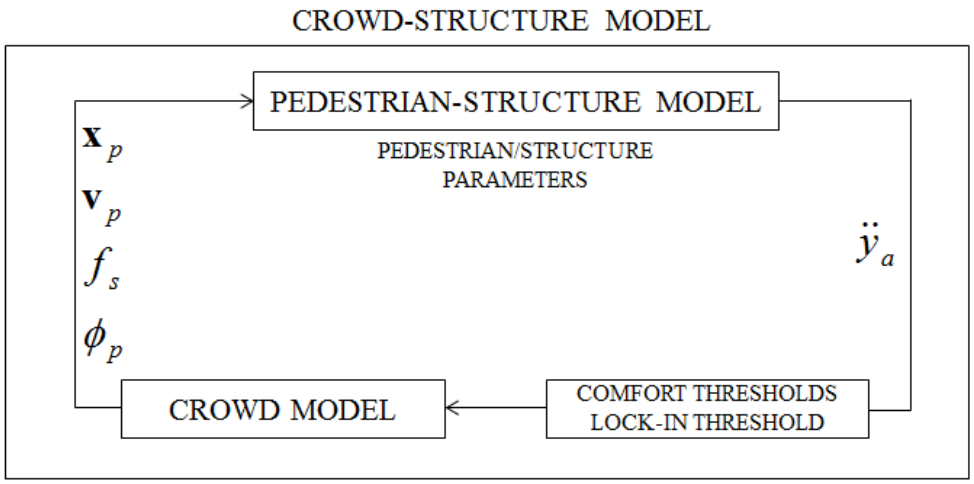

Fig.1. Layout of the biomechanical crowd-structure interaction model.

2.1. Modelling the pedestrian-structure interaction in the lateral direction.

The proposed method is an adaptation of a methodology previously applied successfully by the authors (Jiménez-Alonso and Sáez, 2014) in the vertical direction. The procedure follows from the application of dynamic equilibrium equations (Clough and Penzien, 1993; Dominguez, 2001) to a TDOF-system (Fig. 2) with sprung (m_a) and unsprung masses (m_s).

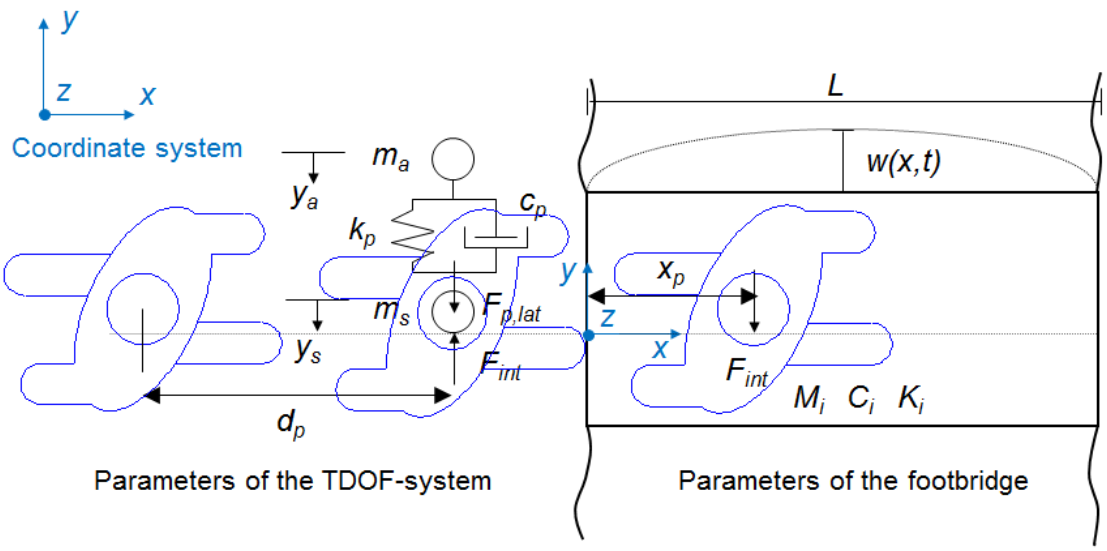

Fig.2. Biomechanical pedestrian-structure interaction model in lateral direction.

The following coupled equation system may be obtained considering the balance of the proposed system.

$$M_i\ddot{y}_i + C_i\dot{y}_i + K_i y_i = \phi_{NUM\_i}(x_p)\cdot F_{\text{int}} \tag{1}$$

$$m_a\ddot{y}_a + c_p(\dot{y}_a - \dot{y}_s) + k_p(y_a - y_s) = 0 \tag{2}$$

$$m_s\ddot{y}_s + c_p(\dot{y}_s - \dot{y}_a) + k_p(y_s - y_a) = F_{p,lat} - F_{\text{int}} \tag{3}$$

where

m_a is the sprung mass of the pedestrian [kg].

m_s is the unsprung mass of the pedestrian [kg].

$m = m_s + m_a$ is the total mass of the pedestrian [kg].

y_i is the lateral displacement of the vibration mode i of the footbridge [m].

y_a is the absolute lateral displacement of the sprung mass [m].

y_s is the absolute lateral displacement of the unsprung mass [m].

k_p is the equivalent stiffness of a pedestrian [N/m].

c_p is the equivalent damping of a pedestrian [sN/m].

$F_{p,lat}$ is the lateral periodic force due to walking [N].

M_i is the modal mass of the vibration mode i [kg].

C_i is the modal damping of the vibration mode i [sN/m]

K_i is the modal stiffness of the vibration mode i [N/m].

ϕ_{NUM_i} is the lateral component of the numerical vibration mode i.

$x_p = v_{px} \cdot t$ is the longitudinal position of the pedestrian [m].

t is the time [sec.].

v_{px} is the longitudinal component of the pedestrian velocity vector [m/s].

d_p is the distance among pedestrians [m]

$w(x,t)$ is the lateral displacement of the footbridge at the position x [m].

L is the length of the footbridge [m].

Thus, F_{int}, follows from the above Eq. (3) to yield.

$$F_{\text{int}} = F_{p,lat} - m_s \ddot{y}_s - c_p\left(\dot{y}_s - \dot{y}_a\right) - k_p\left(y_s - y_a\right) \tag{4}$$

And substituting this equation into the equilibrium equation of the footbridge.

$$M_i \ddot{y}_i + C_i \dot{y}_i + K_i y_i = \phi_{NUM\_i}\left(x_p\right) \cdot \left(F_{p,ver} - m_s \ddot{y}_s - c_p\left(\dot{y}_s - \dot{y}_a\right) - k_p\left(y_s - y_a\right)\right) \tag{5}$$

Applying, at the contact point the equations of compatibility of displacements, velocity and acceleration between the footbridge and the TDOF-system.

$$y_s = w(x_p,t) = w(v_{px} \cdot t, t) \tag{6}$$

$$\dot{y}_s = \dot{w}(x_p,t) = \dot{w}(v_{px} \cdot t, t) \tag{7}$$

$$\ddot{y}_s = \ddot{w}(x_p,t) = \ddot{w}(v_{px} \cdot t, t) \tag{8}$$

These variables may be decomposed in terms of the amplitude $y_i(t)$ and the n considered vibration modes $\phi_{NUM\_i}(x)$, neglecting the term of variation of the pedestrian velocity over the time, as:

$$w(x_p,t)=\sum_{i=1}^{n} y_i(t)\cdot\phi_{NUM\_i}(x_p) \tag{9}$$

$$\dot{w}(x_p,t)=\sum_{i=1}^{n}\dot{y}_i(t)\cdot\phi_{NUM\_i}(x_p)+\sum_{i=1}^{n} y_i(t)\cdot v_{px}\cdot\phi'_{NUM\_i}(x_p) \tag{10}$$

$$\ddot{w}(x_p,t)=\sum_{i=1}^{n}\ddot{y}_i(t)\cdot\phi_{NUM\_i}(x_p)+\sum_{i=1}^{n}2\cdot\dot{y}_i(t)\cdot v_{p,x}\cdot\phi'_{NUM\_i}(x_p)+\sum_{i=1}^{n} y_i(t)\cdot {v_{p,x}}^2\cdot\phi''_{NUM\_i}(x_p)) \tag{11}$$

$$\phi'_{NUM\_i}(x)=\frac{d\phi_{NUM\_i}(x)}{dx} \tag{12}$$

$$\phi''_{NUM\_i}(x)=\frac{d^2\phi_{NUM\_i}(x)}{dx^2} \tag{13}$$

where

$\phi'_{NUM\_i}(x)$ is the first spatial derivate of the mode of vibration i.

$\phi''_{NUM\_i}(x)$ is the second spatial derivate of the mode of vibration i.

In the previous expressions, the value of the vibration modes is assumed zero when the pedestrian remains outside the footbridge:

$$\phi_{NUM\_i}(x_p)=0 \text{ for } \begin{matrix} x_p(t)<0 \\ x_p(t)>L \end{matrix} \tag{14}$$

For our purposes, the vibration modes, $\phi_{NUM\_i}(x)$, are obtained in a discrete way by using the finite element method. For the footbridge, the interpolation functions adopting the hypothesis for the slender beam elements are considered, as:

$$\phi_{NUM\_i}(x)=\sum_j \phi_i^j\cdot N_j(x) \tag{15}$$

where $N_j(x)$ are the shape functions and ϕ_i^j are the nodal values.

When the above relations Eq.(6-11) are substituted in the overall dynamic equilibrium equation of the footbridge, the following interaction model is obtained (organizing the information in a matrix form).

$$\mathbf{M}(t)\cdot\ddot{\mathbf{y}}(t)+\mathbf{C}(t)\cdot\dot{\mathbf{y}}(t)+\mathbf{K}(t)\cdot\mathbf{y}(t)=\mathbf{F}(t) \tag{16}$$

In the case of a single pedestrian, the proposed model leads to a system *of n+1* equations, corresponding to the considered number of vibration modes *n* plus the appropriate simplified interaction equation. For a group of *k* pedestrians (Fig. 2), we may further represent each one by the above TDOF-system. Thus, when considering a group of *k* pedestrians, a system of *n+k* differential equations will need to be solved.

For the numerical evaluation of the resulting system, the β-Newmark integration family method is used, considering as parameters $\beta=1/4$ and $\gamma=1/2$, thus ensuring an unconditionally stable system.

Furthermore, as integration step, Δt, the minimum of the following values has been considered (according to the usual recommendations for dynamics models based on modal decomposition technique (Clough and Penzien, 1993; Dominguez, 2001)).

$$\Delta t=\min\left(\frac{1}{8\cdot f_{\max}},\frac{L_{\min}}{200\cdot|v_p|},\frac{L_{\min}}{4\cdot n\cdot|v_p|},0.01\right)\text{sec.} \tag{17}$$

where

$f_{\max}$ is the highest considered vibration frequency of the structure [Hz].

$L_{\min}$ is the minimum span length of the footbridge [m].

2.1.1. Lateral modal parameters of the pedestrian model.

Unfortunately, there are few studies that provided values for the dynamic effect of the pedestrians on structures in the lateral direction. However, there are several studies, as reported by Jones et al. (2010), describing the effect of passive pedestrians on stadium stands in the dynamic behaviour of such structures in terms of a static single degree of freedom (SDOF) system. In Fig. 3 and Table 1, a scheme of the used models, the estimated values of their modal parameters and their range of variation are shown (Jones et al. (2010)), where f_{p_p} is the passive human natural frequency, ζ_{p_p} is the passive equivalent human damping ratio and m_{a_p} .and m_{s_p} indicate the percentage of passive sprung and unsprung masses of the human body respectively. Two types of models are shown: (i) the "Model 1" that considers that the total mass of each pedestrian is sprung; and (ii) the "Model 2" that divides the total pedestrian mass into a sprung and unsprung components.

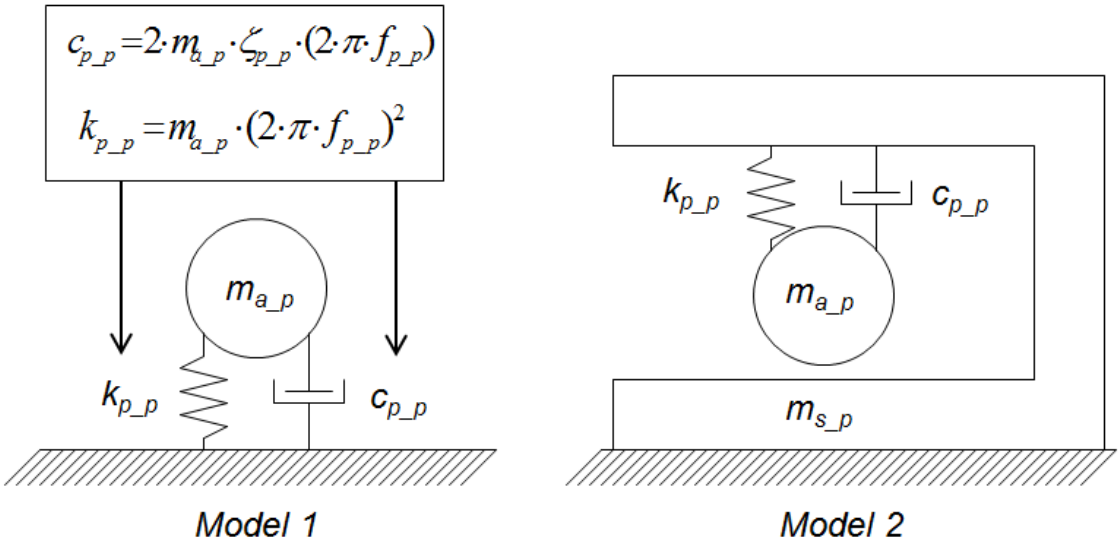

Fig.3. Simplified dynamic representations of the passive pedestrians.

In this paper, the results provided by these passive pedestrians will be used as a starting point in order to estimate experimentally the modal parameters of the model. An inverse dynamic problem methodology has been implemented (Section 3) in order to determine the parameters that characterize the pedestrian-structure interaction model in the lateral direction, based on the results of a crowd test performed on the Viana footbridge adopted as benchmark.

Table 1. Dynamic properties for SDOF models of passive pedestrians on stadium stands (Data from Jones et al. 2010).

Author	Model	m_{a_p} [%]	m_{s_p} [%]	ζ_{p_p} [%]	f_{p_p} [Hz]
Foschi et al. (1995)	1	100.00	0.00	53.00	3.30
Al-Foqaha'a (1997)	1	100.00	0.00	34.00	3.50
Al-Foqaha'a (1997)	2	90.00	10.00	36.00	3.70
Brownjohn (1999)	1	100.00	0.00	37.00	4.90
Falati (1999)	1	100.00	0.00	50.00	10.43
Zheng and Brownjohn (2001)	1	100.00	0.00	39.00	5.24
Matsumoto and Griffin (2003)	1	100.00	0.00	69.00	5.74
Matsumoto and	2	90.00	10.00	61.00	5.88

Griffin (2003)					
Minimum		90.00	0.00	34.00	3.30
Maximum		100.00	10.00	69.00	10.43

2.1.2. Pedestrian walking lateral force.

The movement of the body mass and the put-down, rolling and push-off of the feet of one pedestrian generate an induced lateral force between the pedestrian and the structure, $F_{p,lat}$, that according to different authors (Butz et al., 2007; Setra, 2006), can be determined in terms of a Fourier series decomposition as:

$$F_{p,lat} = P \cdot \sum_{i=1}^{n_f} \alpha_{i,lat} \cdot \sin\left(\pi \cdot i \cdot f_s \cdot t - \varphi_{i,lat} - \phi_p\right) \tag{18}$$

where

$P = m \cdot g$ [N] is the medium pedestrian weight, being g the acceleration of gravity.

$\alpha_{i,lat}$ is the Fourier coefficient of the *ith* harmonic for lateral forces or lateral dynamic load factor (LDLF).

f_s [Hz] is the step frequency of the pedestrian.

$\varphi_{i,lat}$ is the phase shift of the *ith* harmonic of the lateral pedestrian force.

ϕ_p is the phase shift among pedestrians.

n_f is the total number of contributing harmonics.

The number of pedestrians that cross the footbridge in phase has been determined originally adopting the criterion reported by Matsumoto et al. (1978) and later applied successfully applied by the authors (Jiménez-Alonso et al., 2015) . Subsequently, the

phase shift of each pedestrian has been modified if the lateral acceleration experienced by each pedestrian exceeds a lateral lock-in threshold (Setra, 2006).

In Table 2 the values of the lateral dynamic load factors (LDLF), the phase shifts and their range of variation provided by different authors are shown (Butz et al., 2007; Setra, 2006).

Table 2. LDLF and phase shift according different authors (Data from Butz et al., 2007).

Author	$\alpha_{1,lat}$	$\alpha_{2,lat}$	$\alpha_{3,lat}$	$\varphi_{1,lat}$ [°]	$\varphi_{2,lat}$ [°]	$\varphi_{3,lat}$ [°]
Bachmann and Ammann (1987)	0.10	0.10	0.10	0.00	90.00	90.00
Eurocode 5 (2003)	0.10	0.10	0.00	0.00	0.00	0.00
Setra (2006)	0.05	0.01	0.05	0.00	0.00	0.00
Minimum	0.05	0.01	0.00	0.00	0.00	0.00
Maximum	0.10	0.10	0.10	0.00	90.00	90.00

At any rate, as it is point out above, the parameters of the walking pedestrian lateral force of the proposed model will be determined in section 3 by solving an inverse problem on a real footbridge.

2.2. Modelling the crowd behaviour.

The equations that govern the dynamics of particles (Rapaport, 2004) may be applied to define the pedestrian movements inside a crowd. According to this approach, different social forces interact among pedestrians (Helbing and Molnár, 1995), describing the different motivation and influences experimented by them. This type of discrete models has been used by several authors (Helbing and Molnár, 1995; Carroll et al., 2012) to simulate the crowd behaviour and its implementation in the crowd-structure interaction in the vertical direction has been performed successfully by the authors (Jimenez-Alonso et al., 2015). In this section, the behavioural model is now applied in lateral

direction. The proposed multi-agent model that simulates the behaviour of the crowd consists in the sum of three partial forces that represent the different influences that the pedestrians suffer when interacting in a crowd. Thus, the resultant social force, $\mathbf{F}_{pci}$, is defined as:

$$\mathbf{F}_{pci} = \mathbf{F}_{dri} + \mathbf{F}_{ped} + \mathbf{F}_{bou} \tag{19}$$

where

$\mathbf{F}_{dri}$ is the driving force that reflects the motivation of each pedestrian to reach his desired destination.

$\mathbf{F}_{ped}$ is the repulsive force which simulates the interaction among pedestrians.

$\mathbf{F}_{bou}$ is the repulsive force which simulates the interaction among the pedestrians and the boundaries.

A more detailed description of the behavioural model is reported in literature by the authors (Jiménez-Alonso et al., 2015) and references therein.

In order to simulate the pedestrians flows, three parameters must be defined: (i) the pedestrian density [P=Person/m^2], (ii) the value of the desired pedestrian velocity, v_d, and (iii) the distance between pedestrians, d_p.

First, in our model the pedestrian density is determined according to the expected pedestrian traffic on the footbridge, following the recommendations established by international standards (Butz et al., 2007; Setra, 2006).

Second, the values of the desired velocity of each pedestrian is obtained from the pedestrian step frequencies, f_s, defined according to the distributions proposed by several researchers and reported by Bruno and Venuti (2009). For the present model the Gaussian distribution proposed by Zivanovic et al (2010) has been adopted:

$N(1.87,0.186)$ Hz, where $N(\mu,\sigma)$ is the Gaussian distribution, μ is the mean value and σ is the standard deviation. Each assigned step frequency is converted into the desired velocity using the empirical relationship Eq.(20) based on the study developed by Bertram and Ruina (2001) and reported by Bruno and Venuti (2009), considering that initially the pedestrian velocity, v_p, is equal to the desired velocity, v_d.

$$f_s = 0.35 \cdot \left|\mathbf{v}_p\right|^3 - 1.59 \cdot \left|\mathbf{v}_p\right|^2 + 2.93 \cdot \left|\mathbf{v}_p\right| \tag{20}$$

Third, the original distance among pedestrians is calculated assuming an equilateral rectangular-shaped mesh of pedestrians and the considered pedestrian density.

The pedestrian-crowd interaction force, $\mathbf{F}_{pci}$, acts on each pedestrian during each time iteration *j*. The acceleration vector, $\mathbf{a}_p^j$, is determined using Eq.(21) where m is the pedestrian mass (about 70 kg according to international standards (Butz et al., 2007; Setra, 2006).

$$\mathbf{a}_p^j = \frac{\mathbf{F}_{pci}^j}{m} \tag{21}$$

The evaluation of the rest of variables that govern the crowd model, $\mathbf{v}_p^{j+1}$ and $\mathbf{x}_p^{j+1}$, is performed using a multi-step method based on a predictive-corrective method, the Gear's algorithm (Heermann, 1986), due to the fact that the social forces depend on the velocity and the position of the pedestrians. A more detailed description of the algorithm may be found in Jiménez-Alonso et al. (2015).

2.3. Crowd-structure interaction.

The maximum lateral acceleration experienced by each pedestrian crossing the structure, $(\ddot{y}_a)_{\max}$, may be compared against the acceleration threshold values established by international standards (Butz et al., 2007; Setra, 2006) in order to modify the individual pedestrian behaviour inside the crowd. Due to the low tolerance of pedestrians to lateral vibrations (Racic et al., 2009; Zivanovic at al., 2005), two types of thresholds have been considered in our model: (i) comfort thresholds and (ii) a lateral lock-in threshold.

First, in order to reflect in the model the change of the behaviour of each pedestrian due to the modification of his comfort level, a behavioural factor has been applied to the pedestrian velocity. According to the results provided by several studies (Browjohn et al. 2004; Macdonald, 2008; Carrol et al. 2012), a minimum comfort threshold of 0.20 m/s^2 has been selected in our model. In this manner, if the lateral acceleration of each pedestrian exceeds this value, the pedestrian velocity is reduced by a behavioural factor, r_v, which is a function of the acceleration experienced by him. Following the intuitive assumption, reported by Carrol et al. (2012), that the pedestrians are likely to react as more firmly as the experienced lateral acceleration is higher, a third order polynomial is proposed:

$$r_v(\ddot{y}_a) = -0.168 \cdot \ddot{y}_a^{\,3} + 0.1897 \cdot \ddot{y}_a^{\,2} - 0.1443 \cdot \ddot{y}_a + 1.0226 \qquad (31)$$

The function in Eq. (31), has been obtained interpolating the tri-linear function proposed by Carrol et al. (2012) in order to simplify the evaluation of this reduction factor.

Additionally, a maximum lateral limit acceleration of $\ddot{y}_{\lim} = 2.10\,\text{m/s}^2$ has been considered, according to Venuti et al. (2007) so that, when the experienced lateral acceleration becomes too high, pedestrians stop walking to maintain balance and they remain stopped until the acceleration level reduces. A reaction time, $t_{rea} = 2.00\,\text{sec.}$, has been established both to stop walking and to remain stationary before beginning to walk again. The variation of the pedestrian velocity during the reaction time has been modelled by a linear function. In order to avoid meaningless small walking velocities, a practical lower limit on walking velocity magnitude has been imposed as suggested by Carrol et al. (2012).

$$\left|v_p\right| = \begin{cases} 0.1\cdot\left|v_d\right| & if \quad \left(\ddot{y}_a\right)_{\max} < \ddot{y}_{\lim} \cap \left|v_p\right| \le 0.1\cdot\left|v_d\right| \\ 0 & if \quad \left(\ddot{y}_a\right)_{\max} \ge \ddot{y}_{\lim} \end{cases} \tag{32}$$

Second, as lateral lock-in threshold the criterion provided by the French standard (Setra, 2006) has been considered. If the lateral acceleration experienced by each pedestrian is above 0.15 m/s^2 and his step frequency is within ±10 percent of the lateral natural frequency of the structure (Ronnquist, 2005), both his step frequency and phase shift are modified to match the natural frequency of the footbridge and synchronize the movements of the pedestrian and the structure.

3. Experimental estimation of the pedestrian modal parameters in lateral direction.

The estimation of the parameters that characterizes the dynamic behaviour of the proposed pedestrian-structure interaction model in lateral direction has been performed from the accelerations recorded on a real footbridge under two experimental tests, a

crowd test and a pedestrian test, by solving two inverse dynamic problems, as next summarized.

3.1. Inverse dynamic problems.

As identification method of the parameters of the TDOF-system, the minimization of a least squares problem has been adopted (Koh and Perry, 2010) implementing it in the software package Matlab (Matlab, 2015). As minimization method, the genetic algorithms were used (Koh and Perry, 2010). In order to select an adequate objective function the nature of the walking pedestrian lateral force was analysed. Due to its harmonic character, the dynamic response of the structure in the lateral direction, during the crossing of the pedestrian flow, is governed mainly by the steady state component of the dynamic response (Clough and Penzien, 1993), being configured its response function, in the frequency domain, by the different harmonics that characterize the pedestrian step without a remarkable contribution of the free vibration components. On the other hand, as it has been validated by the authors in vertical direction (Jimenez-Alonso et al., 2015), the modal parameters of the TDOF-system were the main cause of the change of the modal parameters of the structure under the presence of pedestrian flows. These two facts forced to divide the identification process in two steps. First, the estimation of modal parameters of the TDOF-system was based on the correlation between the experimental and numerical change of the first lateral natural frequency of a real footbridge under the crossing of a group of 50 pedestrians under different step frequencies. Second, the estimation of the parameters of the walking pedestrian lateral force of the TDOF-system was based on the correlation between the experimental and numerical power spectral density of the dynamic response of a real footbridge under the

crossing of two pedestrians at different controlled step frequencies. In Fig. 4 a flowchart of the identification procedure is shown.

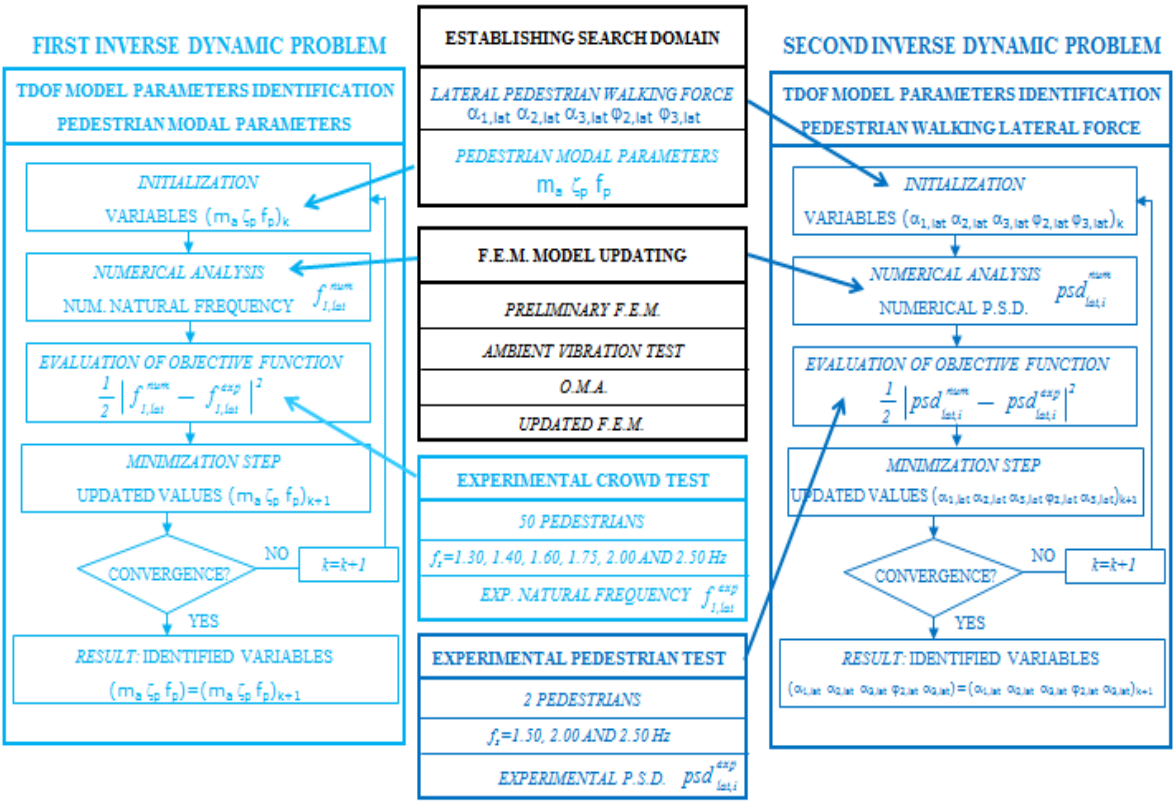

Fig.4. Flowchart of the identification methodology.

In the two inverse problems, the Viana footbridge (Barbosa et al., 2012) has been used as a "laboratory" footbridge. In order to improve the characterization of its dynamic response, the finite element model (Ansys, 2015) of the structure has been updated (Teughels, 2003; Zivanovic et al., 2007) based on the experimental modal parameters of the footbridge estimated from the application of an operational modal analysis (Magalhães and Cunha, 2011) to reduce its uncertainties. An ambient test was performed on the footbridge and the measured signals were processed by an output-only identification method in the time domain, which provided an estimations of the its first four natural frequencies, the corresponding modal shapes and the associated damping ratios (Magalhães et al., 2010) (Fig.5). Subsequently, two experimental tests have been

performed: (i) a crowd test, where the value of the first lateral natural frequency of the Viana footbridge has been estimated experimentally during the crossing of fifty pedestrians at different controlled step frequencies, and (ii) a pedestrian test, where the lateral accelerations at four point of this footbridge have been recorded during the crossing of two pedestrians at different controlled step frequencies. Later, both tests have been reproduced numerically by the implementation of the proposed pedestrian-structure interaction model.

As objective function of the first inverse problem, the mean square error between the experimental, $f_{1,lat}^{\exp}$, and numerical, $f_{1,lat}^{num}$, first lateral natural frequency of the Viana footbridge (Barbosa et al., 2012), obtained during the crossing of 50 pedestrians at different step frequencies, has been considered. Additionally, as design variables of this problem, the three modal parameters that characterizes the TDOF-system; the pedestrian sprung mass, m_a, the pedestrian damping ratio, ζ_p, and the pedestrian natural frequency, f_p, were considered.

As objective function of the second inverse problem, the mean square error between the experimental, $psd_{lat,i}^{\exp}$, and numerical, $psd_{lat,i}^{num}$, power spectral density obtained from the lateral accelerations recorded in four points of the same footbridge under the crossing of two pedestrians at controlled step frequencies, were considered (where i is the considered section). In this case, as design variables the first three LDLF ($\alpha_{1,lat}$, $\alpha_{2,lat}$ and $\alpha_{3,lat}$) and phase shifts of the second and third harmonics ($\varphi_{2,lat}$ and $\varphi_{3,lat}$) of the pedestrian walking lateral force were considered.

Two search domains, one for each inverse problem, were established in order to reduce the uncertainties of the estimated values of the considered parameters and thus prevent

an ill-conditioned inverse problem. Finally, an iterative process to reduce the value of each objective function has been performed (Koh and Perry, 2010; Nocental and Wright, 1999**)**. As a result of this procedure, an estimation of the parameters of the TDOF-system was obtained.

3.2. Establishing a search domain for the parameters of the pedestrian-structure model.

For each inverse problem, a search domain was established. According to Table 1, the minimum and maximum values of the parameters of the passive pedestrian models allow defining the search domains for the estimation of the modal parameters of the pedestrian-structure interaction model. The knowledge of the physical problem suggests increasing the above limits in order to account for the following factors: (i) a reduction of the damping and stiffness of the pedestrian associated with its movement in the lateral direction and (ii) the change in the human body mass distribution between the active and passive states. So, the following search domain has been established for the estimation of the modal parameters of the pedestrian-structure interaction model (first inverse problem).

- Pedestrian sprung mass, $m_a \in [80-100]\%$.
- Pedestrian damping ratio, $\zeta_p \in [10-69]\%$.
- Pedestrian natural frequency, $f_p \in [1-10.43]$ Hz.

Similarly, according to Table 2, the minimum and maximum values of each LDLF allow establishing a search domain for their experimental estimation. In order to take into account that the estimation of these parameters will be performed from measurements carried out on a real footbridge, the above mentioned search domain has been extended. In the case of each lateral phase shift, the search domain has been

defined in a discrete way, considering only the extreme values of these magnitudes. In this manner, the following search domain has been established for the estimation of the walking pedestrian lateral force (second inverse problem).

- First lateral dynamic load coefficient, $\alpha_{1,lat} \in [0.00 - 0.10]$.
- Second lateral dynamic load coefficient, $\alpha_{2,lat} \in [0.00 - 0.10]$.
- Third lateral dynamic load coefficient, $\alpha_{3,lat} \in [0.00 - 0.10]$.
- Second lateral phase shift $\varphi_{2,lat} = 0$ or $90°$
- Third latera phase shift $\varphi_{3,lat} = 0$ or $90°$

3.3. Description and finite element model of the "laboratory" footbridge: Viana footbridge.

The Viana do Castelo footbridge (Barbosa et al., 2012) is a moveable cable-stayed bridge. Two spans of about 36.50 m and 9.00 m respectively configure the longitudinal structural scheme of the footbridge. The deck is suspended by 6 families of two hangers (two retaining ones) from an inclined mast. The deck is composed by two rolled steel beams of variable depth braced by circular hollow profiles. Its width is about 2.50 m. The floor of the footbridge is configured by wooden grids. The main span is compensated by the placement of 11 high density blocks (with a weight of 800 kN) in the shorter span. The mast is welded in its base to a cylinder that is connected to a wheel gear bearing that allows the rotational movement of the structure. The pylon is connected to a deep foundation that balances the forces transmitted by the mast. Different views of the Viana footbridge are shown in Fig.5.

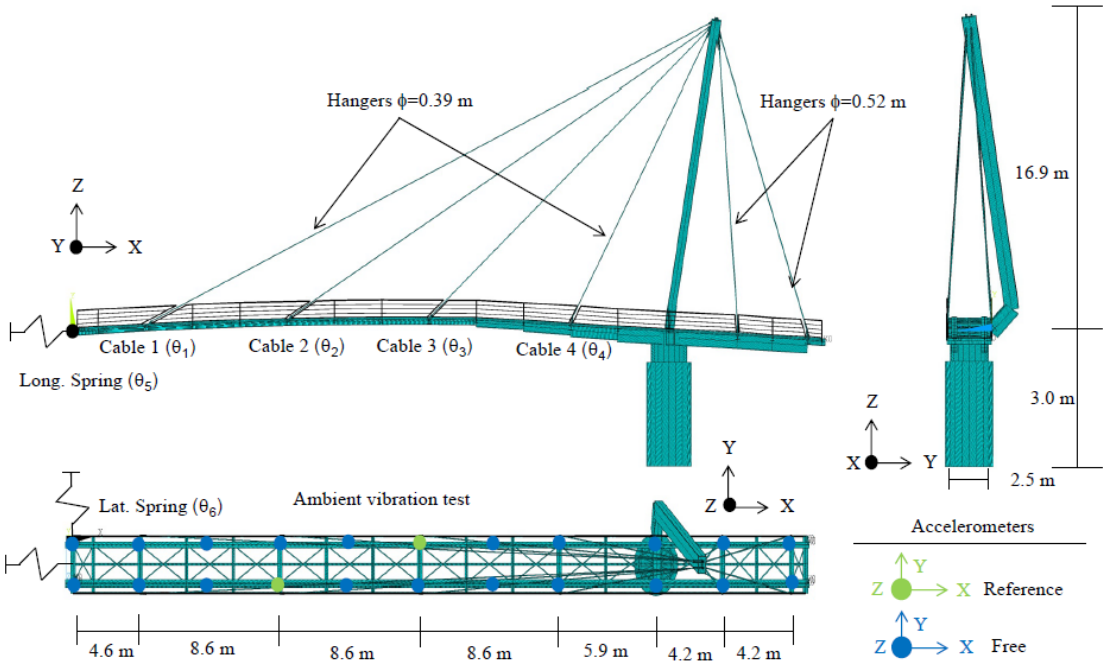

Fig.5. Finite element model, ambient test grid and model updating parameters.

A preliminary numerical finite element (Fig.6) modal analysis was conducted using the software package Ansys (Ansys, 2015), based on a discretization of the structure with 3D-beam elements (BEAM188) except for the hangers and the soil-structure interaction where 3D-cable elements (LINK10) and 1D-spring elements (COMBIN14) were implemented, respectively. The numerical model was then used to have a first approximation to the dynamic behaviour of the footbridge and determine the desired numerical modal parameters to perform the ambient vibration test. The nonlinear effects associated with the hangers have been considered for the determination of the numerical natural frequencies and the vibration modes of the structure, by the estimation of their tangent stiffness matrix, calculating previously the stress level of the hangers originated by the permanent loads. The numerical modal analysis of this preliminary FE model leads to the first four numerical vibration modes and associated numerical natural frequencies given in Table 3. In Fig.6 the first two numerical lateral vibration modes are shown (f_{NUM}_i, with *i* being the vibration mode number in lateral direction).

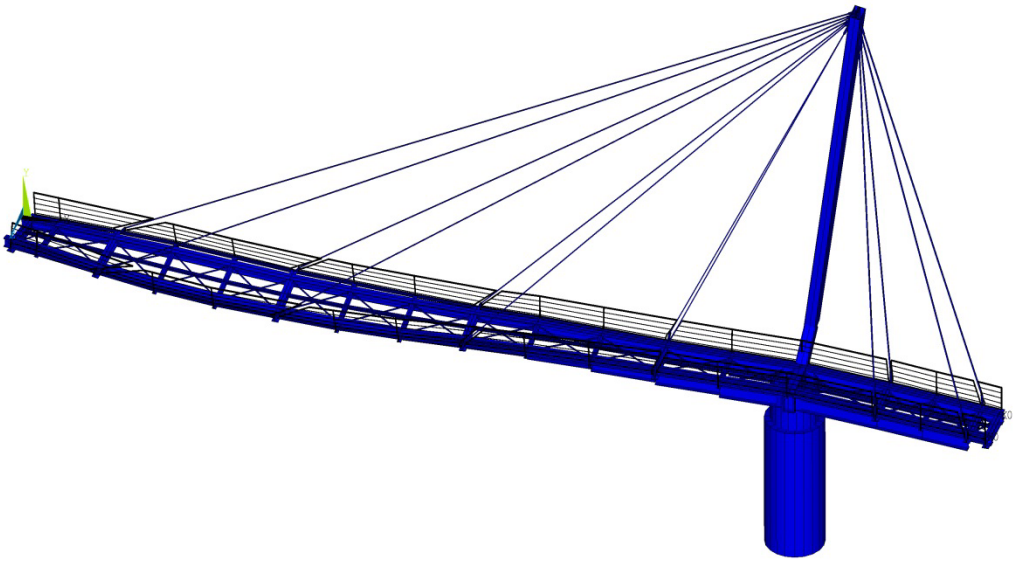

$f_{NUM\ 1}$=4.421 Hz. 1st numerical vibration mode in lateral direction (mode 2 in Table 3).

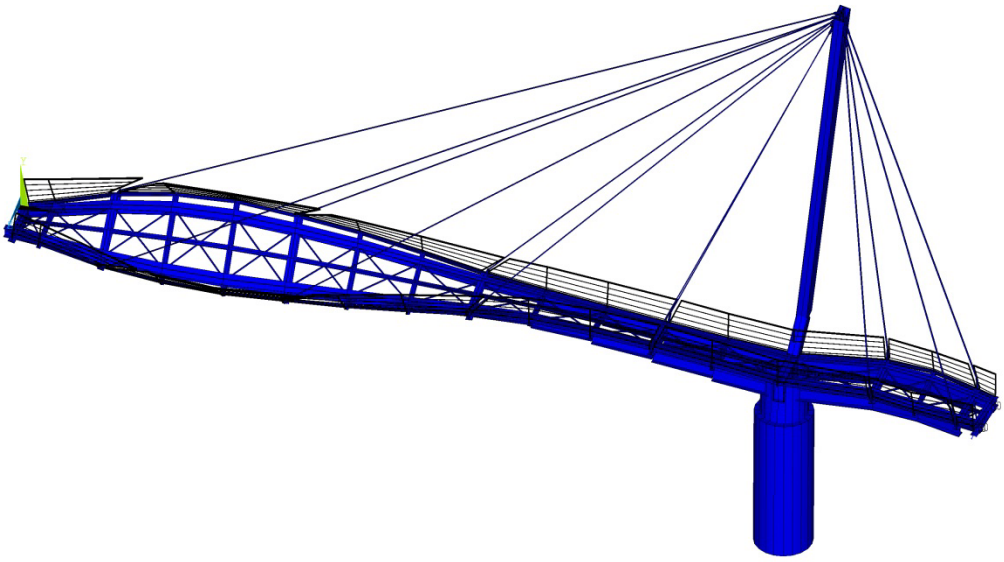

$f_{NUM\ 2}$=6.907 Hz. 2nd numerical vibration mode in lateral direction (mode 3 in Table 3).

Fig.6. First two numerical vibration modes in lateral direction. Initial FE model.

3.4. Experimental identification of the modal parameters of the footbridge.

The modal parameters (natural frequencies, damping ratios and modal shapes) of the footbridge have been estimated experimentally by the performance of an ambient vibration test. The measurements were conducted under ambient conditions, being the

footbridge only excited by a light wind. The modal shape coordinates were measured along two gridlines separated transversally 1.68 m. A total of 2x11 points equally distributed along each longitudinal alignment were instrumented. Four high sensitivity tri-axial force balanced accelerometers were used. Using two of these devices as references, measurements were successively made moving the other two accelerometers to the previously defined locations and recording in each point 1000 sec. time series of acceleration sampled at 100 Hz. (Fig.5). As identification algorithm, the Stochastic Subspace Identification method (Magalhães and Cunha, 2011) has been utilized through its implementation in the software package Artemis. (ARTeMIS, 2015). The first four vibration modes were identified and subsequently used for the FE model updating process. The obtained numerical and experimental natural frequencies and vibration modes shapes are compared in Table 3 and the correlation between the first two numerical and experimental vibration modes in lateral direction is shown in Fig.7 (with the x axis corresponding to the longitudinal direction of the footbridge). Similarly, in Table 3 an estimation of the damping ratios, ζ_i, associated with the identified vibration modes is also shown (Magalhães et al., 2010). In order to validate the correlation between the numerical and experimental modal parameters both the relative difference (Δf) between the numerical and experimental frequencies, and the modal assurance criterion (MAC_i) were analysed (Zivanovic et al., 2007). A good correlation between two modes is achieved when the value of its M.A.C. ratio is greater than 0.90. These two magnitudes may be defined according to Eqs. (33 and 34) as follows:

$$\Delta f = \frac{f_{NUM\_i} - f_{EXP\_i}}{f_{EXP\_i}} \cdot 100 \ [\%] \tag{33}$$

where f_{NUM_i} is the numerical natural frequency and f_{EXP_i} is the experimental natural frequency of the vibration mode i and

$$MAC_i = \frac{\left(\phi_{NUM\_i}^T \cdot \phi_{EXP\_i}\right)^2}{\left(\phi_{NUM\_i}^T \cdot \phi_{NUM\_i}\right) \cdot \left(\phi_{EXP\_i}^T \cdot \phi_{EXP\_i}\right)} \tag{34}$$

where ϕ_{NUM_i} and ϕ_{EXP_i} are the numerical and experimental vibration modes to be compared and ^{T} denotes the transpose

Table 3. First four numerical (f_{NUM}) versus experimental (f_{EXP}) vibration modes of the Viana footbridge.

Modes	**f_{NUM} [Hz]**	**f_{EXP} [Hz]**	ζ_i [%]	Δf [%]	**M.A.C.**	**Description**
1	3.426	3.138	1.22	9.17	0.963	First vertical mode
2	4.421	4.068	1.21	8.67	0.985	First lateral mode
3	6.907	6.810	1.10	1.42	0.809	Second lateral mode
4	7.431	7.345	1.39	1.17	0.939	Second vertical mode

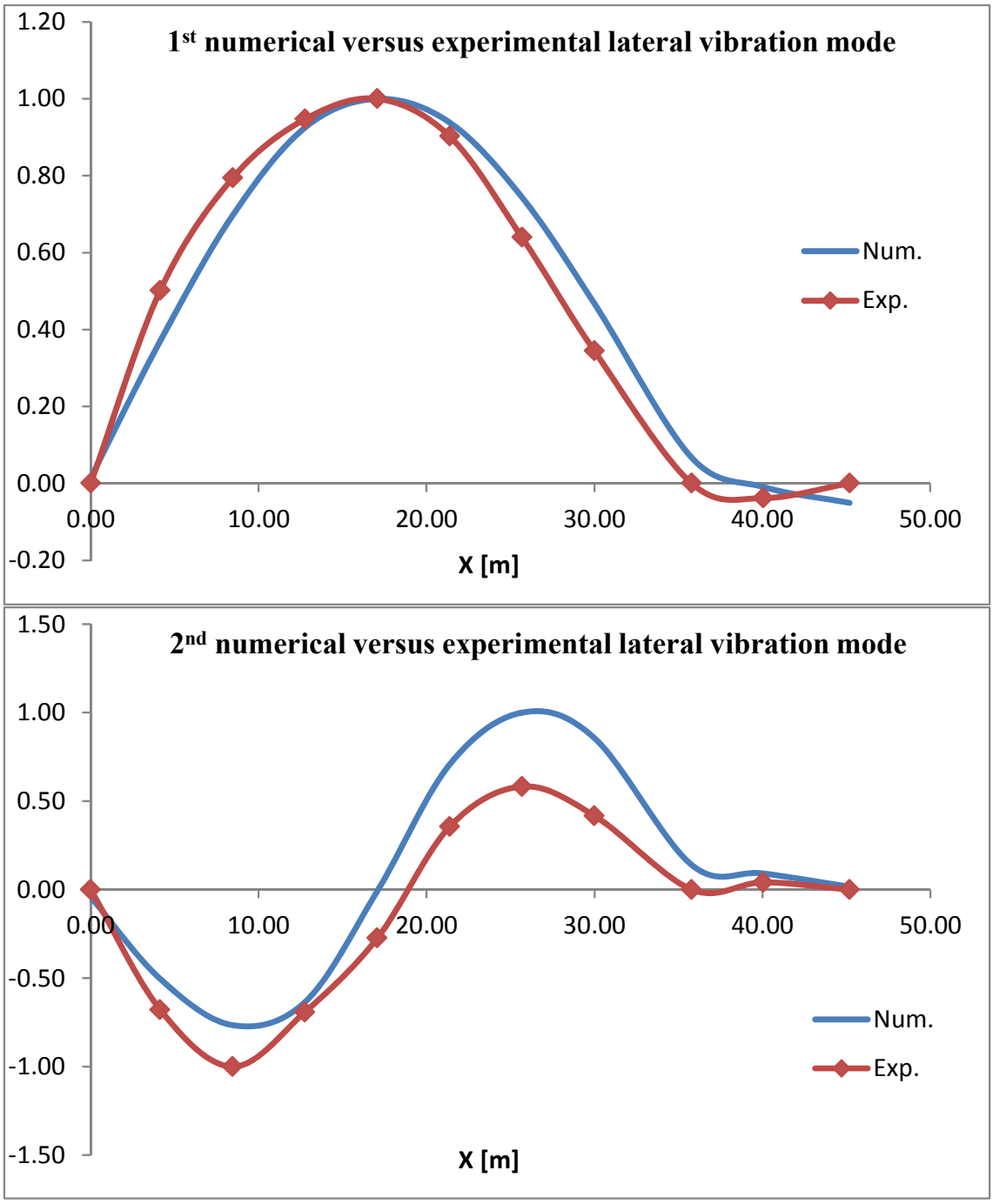

Fig. 7. First two lateral numerical (Num.) versus experimental (Exp.) vibration modes.

Although the shapes of the identified vibration modes are in good agreement (with M.A.C. ratios greater than 0.90 in the first, second and fourth vibration modes), the relative differences, Δf, between the first two numerical and experimental natural frequencies are still significant. Therefore, the initial estimation made on the physical

parameters of the structure is not good enough and it becomes necessary to perform a FEM updating (Friswell and Mottershead, 1995; Teughels, 2003) of the footbridge in order to improve the correlation between the numerical and experimental modal parameters.

3.5. Model updating of the footbridge.

In order to reduce the level of uncertainties of the numerical analysis a finite element model updating (Friswell and Mottershead, 1995; Teughels, 2003; Zivanovic et al., 2007) of the structure has been performed. The four identified vibration modes were considered in the updating process due to the good quality of the experimental data. Both measured natural frequencies and modal coordinate values were taken into account. Therefore, in total 48 residual components were selected for the model updating (the four identified natural frequencies and the eleven coordinates of each identified vibration mode).

A sensitivity analysis was performed in order to adequately select the physical parameters of the FE model with greater influence on the identified vibration modes. In this manner, the modal sensitivities with respect to some possible physical variables have been obtained numerically (Fox and Kapoor (1968)). The results of this study conclude that the most influential physical parameters on the dynamic behaviour of the footbridge are the stiffness of the four families of main hangers and the soil-structure interaction, modelled by two spring elements (in longitudinal, θ_5, and lateral, θ_6 directions, as Fig.5 illustrates) situated at the extreme of the longer span. As the stiffness of the hangers is conditioned by their stress level, the initial stress state of each considered family (θ_1, θ_2, θ_3 and θ_4) has also been taken into account as physical variable. In Fig.5 and Table 4, the selected physical variables are shown.

The model updating process has been conducted through the performance of an optimization problem in the software programs Ansys (Ansys, 2015) and Matlab (Matlab, 2015). As objective function the mean square error between the experimental and numerical modal parameters (natural frequencies and vibration modes) of the Viana footbridge has been considered. A population of 1000 vectors has been generated in each iteration that using the genetic algorithms rules of mutation, reproduction and crossover has minimized the value of the proposed objective function. The values of the selected parameters have been modified in order to minimize the considered objective function. Additionally, a search domain has been defined to control the variation of each parameter, increasing the efficiency of the optimization algorithm and yet maintaining the physical meaning of the finite element model updating. For the stiffness of the hangers, as a passive behaviour is expected, the medium tension level has been determined under permanent loads, with a value of 250 kPa. Slight variations of this value have been considered by increasing the search domain between 0-500 kPa. For the stiffness of the springs (θ_5 and θ_6), given the uncertainty associated with the stiffness of the soil, a wider search domain has been considered. So considering, as it is reported by the geotechnical report, a variation of the Young's modulus of soil between $E_m = 1-100$ GPa and the geometry of the abutments, the variation of the equivalent stiffness of the springs has been established θ_5 and $\theta_6 \in \left[10^7 - 10^9\right]$N/m . In Table 4 the range of variation of each parameter and its updated values are shown.

Table 4. Updated values of considered physical parameters.

Parameters	Minimum Value	Updated Value	Maximum Value
Tension stress cable 1 (θ_1).	0.00 kPa	112.38 kPa	500.00 kPa
Tension stress cable 2 (θ_2).	0.00 kPa	59.62 kPa	500.00 kPa
Tension stress cable 3 (θ_3).	0.00 kPa	31.62 kPa	500.00 kPa
Tension stress cable 4 (θ_4).	0.00 kPa	147.43 kPa	500.00 kPa
Longitudinal Spring (θ_5).	1.00E7 N/m	6.00E7 N/m	1.00E9 N/m

Lateral Spring (θ_6).	1.00E7 N/m	1.90E8 N/m	1.00E9 N/m

The differences between the numerical and experimental natural frequencies, after the finite element model updating, are very small and the correlation between the numerical and experimental vibration modes are high. The relative differences between the updated numerical (f_{UPD}) and experimental (f_{EXP}) modal parameters and the *M.A.C.* values achieved after the model updating process are summarized in Table 5, where the improvement with respect to the initial FE model is clear (see Table 3).

Table 5. First four updated numerical (f_{UPD}) and experimental (f_{EXP}) vibration modes of the footbridge.

Modes	**f_{UPD} [Hz]**	**f_{EXP} [Hz]**	Δf [%]	**M.A.C.**	**Description**
1	3.136	3.138	-0.06	0.999	First vertical mode
2	4.052	4.068	-0.39	0.999	First lateral mode
3	6.799	6.810	-0.16	0.998	Second lateral mode
4	7.342	7.345	-0.04	0.999	Second vertical mode

Similarly, Fig. 8 illustrates the correlation between the updated numerical and the experimental lateral vibration modes, with an excellent agreement.

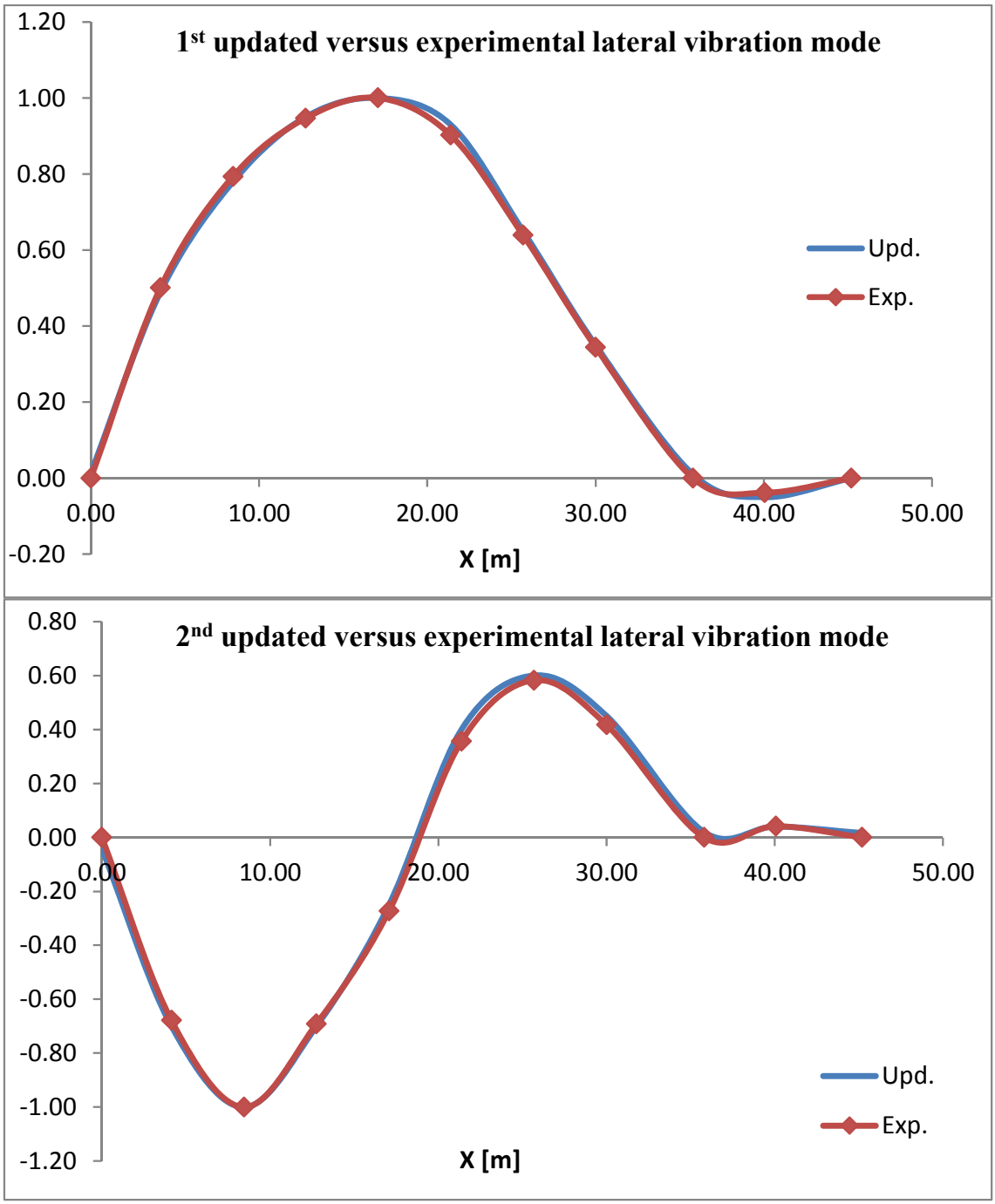

Fig.8. First two lateral updated numerical (Upd.) and experimental (Exp.) vibration modes.

After the development of the model updating, the numerical dynamic behaviour of the footbridge simulates accurately the real response of the footbridge. This detailed knowledge of the dynamic behaviour of the footbridge allows for adopting this real footbridge as a benchmark or "laboratory" footbridge.

3.6. Experimental crowd test.

The estimation of the modal parameters of the proposed pedestrian-structure interaction model was made through the results of an experimental crowd test. In this test, a group of 50 pedestrians crossed the footbridge at different step frequencies (1.30-1.40-1.60-1.75-2-00-2.50 Hz) controlled by a metronome, measuring the dynamic response of the footbridge at four sections (S_1, S_2, S_3 and S_4 in Fig.9) using tri-axial force balanced accelerometers. During the crowd test the group of 50 pedestrians was distributed in three alignments, maintaining a lateral separation among pedestrians around 0.85 m and a longitudinal distance between pedestrians around 0.50 m. A pedestrian with a metronome led the group in each crossing. A scheme of the pedestrian distribution during the crowd test is also shown in Fig.9.

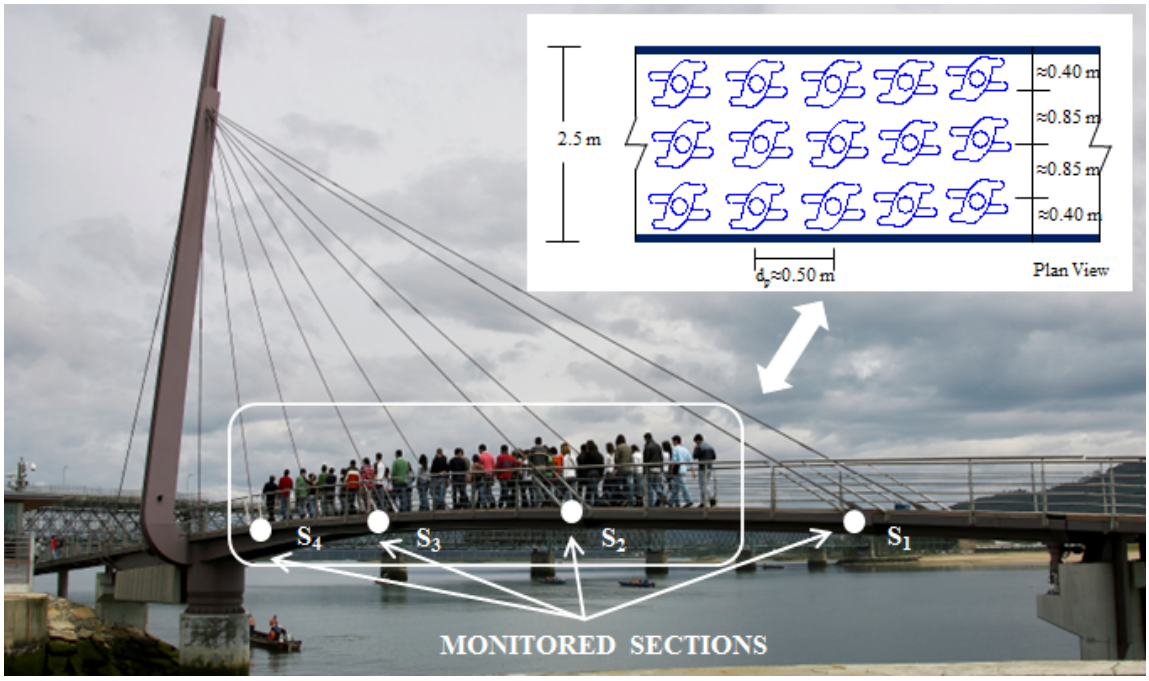

Fig.9. Experimental crowd test at the Viana footbridge.

3.7. Experimental pedestrian test.

The estimation of the walking pedestrian lateral load of the proposed pedestrian-structure interaction model was made through the results of an experimental pedestrian

test. In this test, two pedestrians (A and B), with a pedestrian mass of $m_A = 61.70\,\text{kg}$ and $m_B = 100.50\,\text{kg}$ respectively, were selected. Three time series were recorded for each pedestrian, crossing the footbridge three times at different step frequencies, f_s (1.50, 2.00, 2.50 Hz), controlled by a metronome. In the four monitored sections (S_1, S_2, S_3 and S_4 in Fig.9) the dynamic response of the structure was measured. In each passage, the initial and end time, that marks the passage of the pedestrian on the structure, was recorded for both localizing the force vibration response corresponding to the passage of each pedestrian and estimating the pedestrian velocity, v_p.

3.8. Parameters identification: Modal parameter of the pedestrian-structure interaction model.

For the estimation of the modal parameters of the TDOF-system (Koh and Perry, 2010), an inverse dynamic problem was solved, as it has been point out previously. As objective function the relative differences between the experimental and numerical first lateral natural frequency of the footbridge during the crossing of a group of 50 pedestrians at different step frequencies was considered. As optimization method, genetic algorithms have been used again. In order to determine experimentally the first natural lateral frequency of the footbridge under the crossing of the group of pedestrians, just the forced vibration response of the structure has been considered. Only the records at section S_2 (higher modal deflection) have been considered. The level of noise of the signal has been reduced in order to improve the reliability of the parameters estimation (Koh and Perry, 2010). A level 7 decomposition of the signal using the Continuous Wavelet Transform (CWT) based on Daubechies family has been applied (CWT) (Gopalakrishnan and Mitra, 2014). The principle of Stein's Unbiased

Risk Estimate has been considered as well. The reconstruction of the signal has been performed using the original approximation coefficients of level 7 and the modified detail coefficients of level ranging from 1 to 7. Subsequently, the selected signal has been filtered and processed again by CWT. The maximum value of the wavelet coefficients, in the filtered range of frequencies, is then correlated with the first lateral natural frequency of the structure. This result has been validated by the estimation of the natural frequency through the power spectral density of the above signal, obtained according to the Peak-Picking method (Magalhães and Cunha, 2011). On the other hand, the numerical first lateral natural frequency has been obtained from the implementation of the proposed pedestrian-structure interaction model on the updated finite element model of the Viana footbridge. For the determination of the numerical natural frequencies, the classical formulation of the pedestrian-structure interaction model has been transformed to the state-space formulation which makes easier the determination of these magnitudes. Finally, the adjustment process allowed obtaining an estimation of the modal parameters of the pedestrian-structure interaction model. The considered values are inside the range established by Shahabpoor et al. (2013), that characterizes the modal properties of pedestrian-structure interaction model. The following Gaussian distributions have been considered ($N(\mu,\sigma)$, being μ the mean value and σ the standard deviation).

- Pedestrian sprung mass, m_a, $N(73.216,2.736)$ %.
- Pedestrian damping ratio, ζ_p, $N(49.116,5.405)$ %.
- Pedestrian natural frequency, f_p, $N(1.201,0.178)$ Hz.

Fig.10 illustrates the correlation between experimental and numerical results for the change of first lateral natural frequency of the footbridge induced by the crowd-structure interaction phenomenon. Good agreement between both sets of results is

observed, with differences below 0.70 % for all the analysed pedestrian walking frequencies. The first lateral natural frequency corresponding to the empty footbridge is included in Fig.10 for reference.

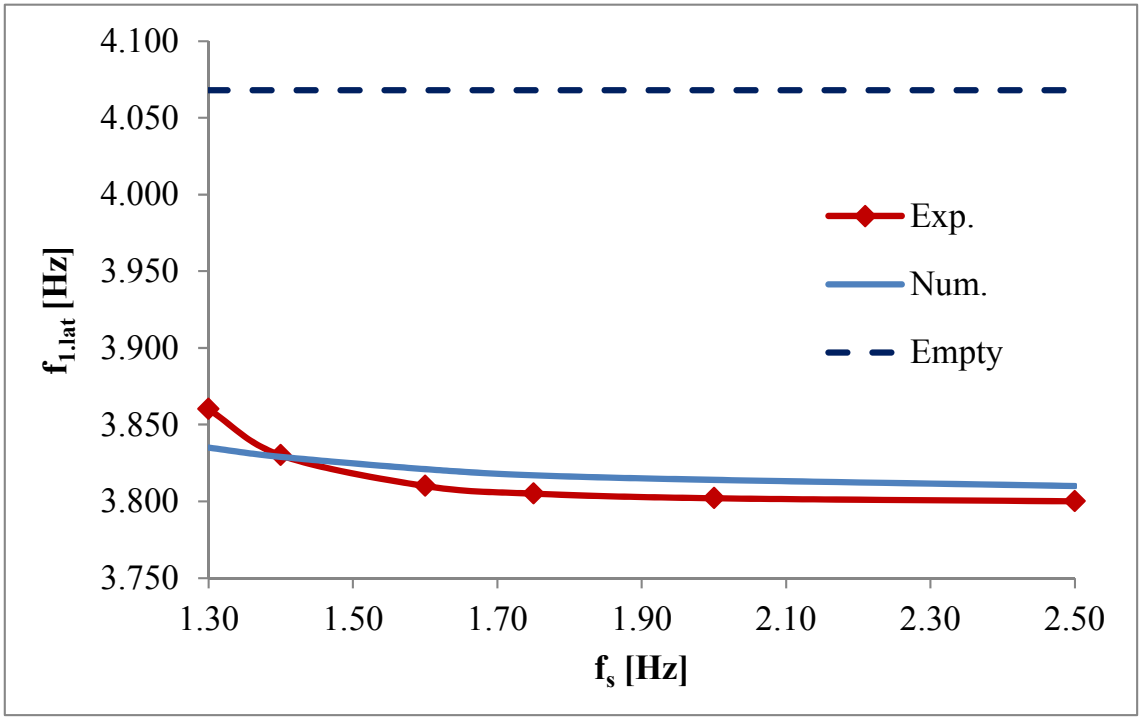

Fig.10. Change of the first lateral experimental (Exp.) and numerical (Num.) natural frequency ($f_{1,lat}$) versus the step frequency [Hz]..

From the previous results the following conclusions may be extracted: (i) the stability that the estimated modal parameters present for the different step frequencies, allowing that the proposed crowd-interaction model may be used as a tool for the characterization of the effect of the moving pedestrians on the dynamic behaviour of footbridges in lateral direction and (ii) the good correlation between the experimental and numerical curves (Fig.10) that show the change of the first lateral natural frequency of the footbridge verifies the ability of the proposed model to characterize the pedestrian-structure interaction phenomenon in lateral direction.

3.9. Parameters identification: Walking pedestrian lateral force of the pedestrian-structure interaction model.

Although there are very recent and comprehensive studies of the walking pedestrian lateral force (Ingólfsson and Georgakis, 2011; Ingólfsson et al., 2011), these research do not include the effect of the pedestrian-structure interaction. In order to consider this fact in our proposal, the estimation of the walking pedestrian lateral force of the TDOF-system was performed based on the solution of an inverse dynamic problem again. In this case, as objective function the mean square error between the experimental and numerical power spectral density obtained from the lateral accelerations recorded in four points (S_1, S_2, S_3 and S_4 in Fig. 11) of the Viana footbridge under the crossing of two pedestrians at controlled step frequencies is considered. The experimental lateral accelerations correspond to the measurements of the above described pedestrian test. The numerical lateral accelerations have been obtained from the implementation of the proposed pedestrian-structure interaction model on the updated finite element model of the Viana footbridge.

The experimental and numerical power spectral density has been obtained from these accelerations. The experimental signals have been previously denoised following the procedure described in the previous section. Six parameters were adopted as design variables:

(i) the first three LDLF that characterize the pedestrian walking lateral force.

(ii) the phase shifts of the second and third harmonic that characterize the pedestrian walking lateral force.

(iii) a time lag that allows adjusting the beginning of the crossing of the pedestrian between the experimental and numerical response.

The estimation of the phase shifts has been made in a discrete way, selecting in each case the option that minimizes the objective function. Fig.11. illustrates the layout of the identification process for the pedestrian walking lateral force of the proposed pedestrian-structure interaction model.

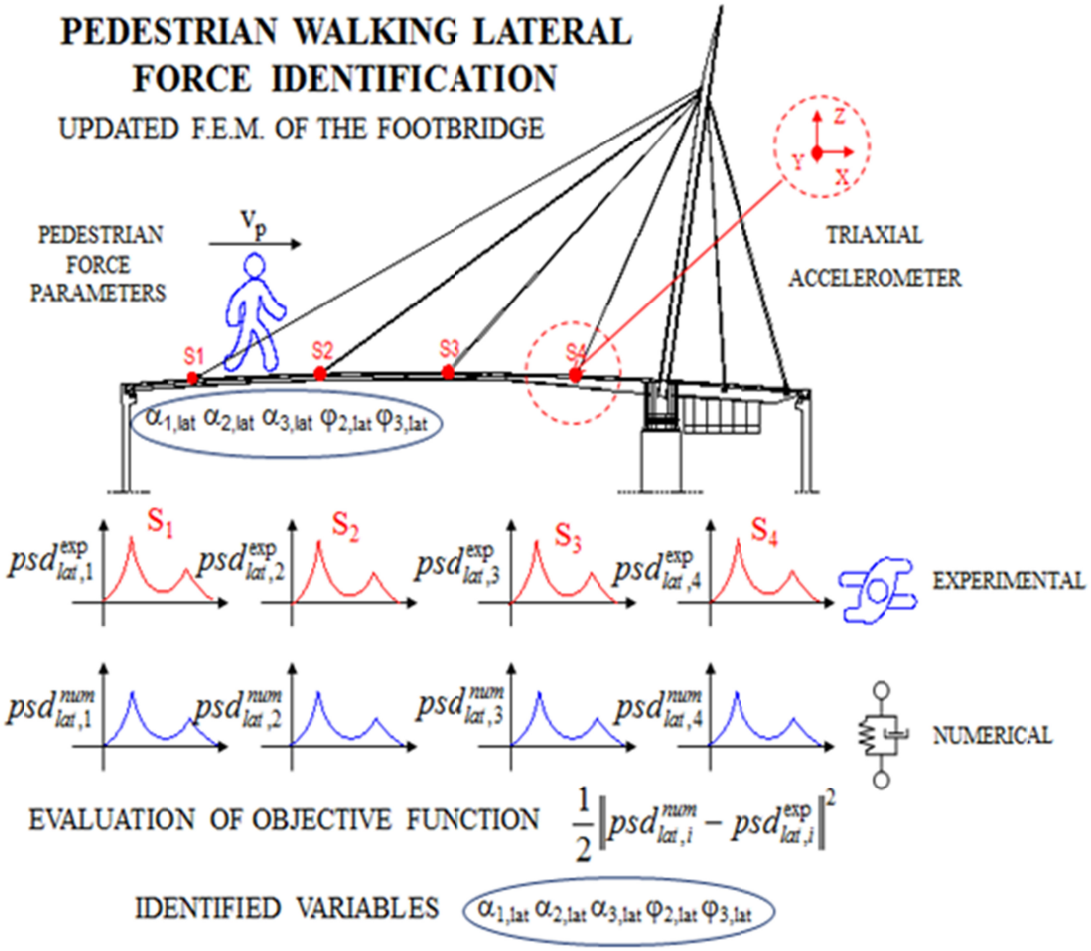

Fig.11. Layout of the walking pedestrian lateral force identification methodology.

In Table 6, the results of the estimation process are summarized, showing the different estimated parameters versus the pedestrian step frequency.

Table 6. Estimation of the LDLF of the lateral walking force of the pedestrian-structural interaction model.

Force Parameters	f_s [Hz]	Minimum	Medium	Maximum
1st LDLF $\alpha_{1,lat}$	1.50	0.079	0.091	0.099
	2.00	0.067	0.088	0.099
	2.50	0.056	0.078	0.099
2nd LDLF $\alpha_{2,lat}$	1.50	0.083	0.096	0.099
	2.00	0.075	0.087	0.099
	2.50	0.095	0.097	0.099
3rd LDLF $\alpha_{3,lat}$	1.50	0.029	0.048	0.074
	2.00	0.027	0.039	0.065
	2.50	0.017	0.032	0.057
2nd Lat. phase shift $\varphi_{2,lat}$	1.50-2.50	0.000	0.000	0.000
3rd Lat. phase shift $\varphi_{3,lat}$	1.50-2.50	0.000	0.000	0.000

According to the results of Table 6 it is possible to obtain a statistical estimation of the design variables that characterize the pedestrian walking lateral force.

- First LDLF, $\alpha_{1,lat}$, $N(0.086,0.017)$.
- Second LDLF, $\alpha_{2,lat}$, $N(0.094,0.009)$.
- Third LDLF, $\alpha_{3,lat}$, $N(0.040,0.019)$.
- Second lateral phase shift, $\varphi_{2,lat} = 0\,^{o}$.
- Third lateral phase shift $\varphi_{3,lat} = 0\,^{o}$.

Once obtained the parameters, the definition of the proposed model is complete. This model will be validated in the next section by correlating the experimental and numerical lateral lock-in phenomenon on another real footbridge, namely Pedro e Inês footbridge (Coimbra, Portugal).

4. Model validation.

4.1. Description of Pedro e Inês footbridge and assessment of its dynamic behaviour.

The Pedro e Inês footbridge is located at Coimbra (Portugal). The total length of the structure is 274.5 m, configured by one central arch of 110 m, two lateral semi-arch of 64 m and two transition spans of 30.5 and 6 m (Fig. 12.a). The main feature of the

footbridge is the anti-symmetrical configuration of the deck and the arches respect of the longitudinal axis of the structure. The deck is a concrete-steel composite box-girder with a variable width between 4 and 8 m, that generates a panoramic square at mid-span of the footbridge (Fig.12.b). From its design phase, the numerical studies indicated that the structure was prone to vibrations induced by pedestrians in lateral direction. This fact motivated the development of a precise and detailed work for the experimental assessment of its dynamic response and the implementation of a control system in order to guarantee an adequate comfort level of the footbridge. This work was performed and reported by Caetano et al. (2010) and its results have been used in this paper in order to validate the proposed crowd-structure interaction model.

Fig.12. a) General view of Pedro e Inês; b) Perspective of the footbridge and c) experimental lateral lock-in pedestrian test on this footbridge (Caetano et al., 2010).

The footbridge presented a first lateral vibration mode with an experimental natural frequency of 0.91 Hz, with an associated damping ratio of 0.55 %, that was easily excited by the pedestrian flows. In order to determine experimentally the number of

pedestrians that originates the lateral lock-in phenomenon an experimental test was performed. The result of this experimental test has been correlated with the numerical simulation based on the implementation of the proposed crowd-structure interaction model on an updated finite element model of the Pedro e Inês footbridge as reported in the literature (Caetano et al. (2010)).

4.2. Experimental and numerical lateral lock-in phenomenon on the Pedro e Inês footbridge.

The analysis focused on the beginning of the lateral lock-in phenomenon, as it is the situation where the effect of the modal parameters of the pedestrians has greater influence on the dynamic behaviour of the structure (Dallard et al., 2001).

In the experimental lateral lock-in test, the lateral acceleration, a_{lat}, at mid-span of the footbridge under the crossing of different group of pedestrians was recorded (Fig.12.c). A graphical representation of the maximum lateral acceleration at this position versus the number of pedestrians on the footbridge (Fig.13) allows for identifying the instability situation associated with the lateral lock-in phenomenon. As it is reported in the literature (Caetano et al. (2010)) and illustrated in Fig.13 the number of pedestrians that originates the beginning of the lateral lock-in phenomenon is around 75.

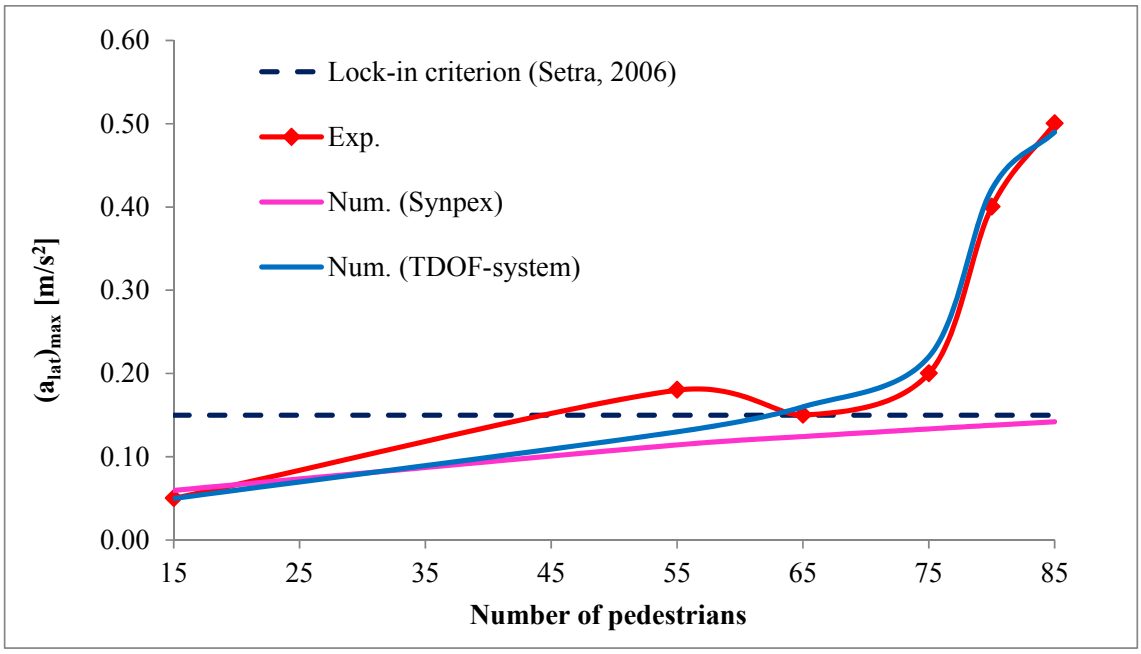

Fig.13. Experimental (Caetano et al. 2010) and numerical variation of the maximum lateral acceleration, $(a_{lat})_{\max}$, at mid-span versus the number of pedestrians.

Subsequently, a numerical lateral lock-in analysis based on the proposed crowd-interaction model was performed. Each considered group of pedestrians has been simulated considering as initial spatial distribution a rectangular-shaped grid with an initial distance among pedestrians $d_p = 0.50$ m with an equidistant distribution in the width of the deck. The coordinates of the considered lateral vibration modes of the structure follow from the results available in the literature (Caetano et al. 2010). In order to account for the change of the structural damping of the footbridge according to its vibration level, a parabolic function has been implemented based on the results obtained by Georgakis and Jorgesen (Georgakis and Jorgesen, 2014) in a laboratory footbridge. The range of variation of the damping ratio was comprised between the experimental value obtained in the previously mentioned free vibration test and the limit value under strong vibrations proposed by the more recent international standards (Butz et al., 2007; Setra, 2006). The maximum numerical lateral acceleration at mid-span versus the

number of pedestrians on the footbridge is shown in Fig.13. As Fig.13 shows, the correlation between the experimental lateral maximum accelerations and the numerically estimated maximum values is adequate. Additionally, the estimation of the numerical maximum acceleration obtained applying the methodology proposed by international standards (Butz et al., 2007) is also shown in Fig.13. It is clear from Fig. 13 that the proposed model allows obtaining a more accurate numerical analysis of the lateral lock-in phenomenon than these standards. The lateral lock-in criterion established by French standards (Setra, 2006) is also illustrated for reference in Fig. 13.

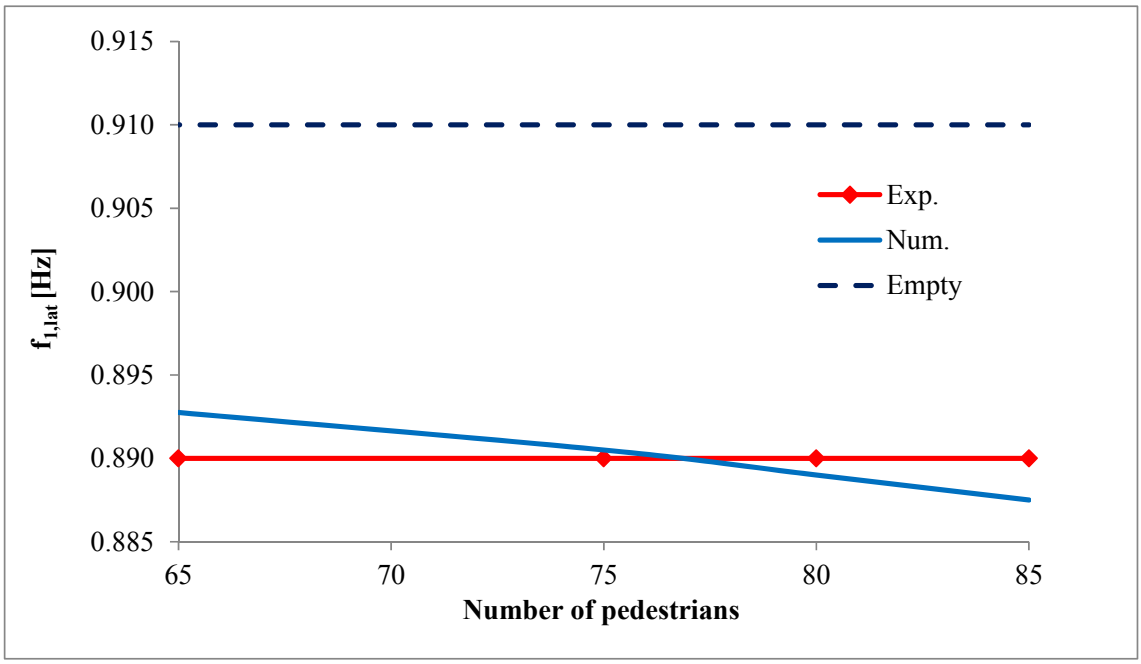

Fig.14. Experimental (Caetano et al., 2010) and numerical variation of the first lateral, $f_{1,lat}$, natural frequency of the footbridge versus the number of pedestrians.

Finally, the first lateral numerical natural frequency of the footbridge during the occurrence of the lateral lock-in phenomenon was obtained and it is shown in Fig.14. The experimental first lateral numerical natural frequency (Caetano et al., 2010) is also shown in Fig.14. Good agreement between both sets of results is observed, with differences below 0.35 % in the studied range of the number of pedestrians.

Additionally, the value of the first lateral natural frequency corresponding to the empty footbridge is illustrated for reference in Fig.14.

5. Conclusions.

In this paper, a crowd-structure interaction model is implemented and calibrated in order to determine the dynamic response of footbridges under pedestrian flows in lateral direction. The proposed model has been validated through the correlation between the experimental and numerical analysis of the lateral lock-in phenomenon on a real footbridge, namely Pedro e Inês footbridge (Coimbra, Portugal). The proposed model is organized in two sub-models: (i) a pedestrian-structure interaction and (ii) a crowd sub-model. The pedestrian-structure interaction sub-model is defined in terms of a TDOF-system, with sprung and unsprung masses, whose parameters have been estimated experimentally from the solution of two inverse problems on another real footbridge, adopted as "laboratory" footbridge, namely Viana footbridge (Viana do Castelo, Portugal). The estimated parameters are within the range recommended by previous works in the literature. The crowd sub-model is defined in terms of a multi-agent model based on the relationships established by the social force model. The interaction between the two sub-models in the lateral direction is achieved by imposing two types of thresholds, comfort and lateral lock-in thresholds, so that if certain acceleration limits are exceeded the affected pedestrians modify their behaviour. As it is described in the manuscript, the proposed model is formulated under the following hypothesis: (i) constant parameters of the pedestrian-structure interaction model; (ii) the dynamic effects associated to the change of the pedestrian velocity are neglected, and (iii) the resolution of the interaction problem does not consider the jogging or jumping action. A

remarkable feature of the model is that it permits an accurate analysis of the lateral lock-in phenomenon on footbridges induced by pedestrians and the estimation of the change of its modal parameters due to the presence of the pedestrians. In this sense, the experimental and numerical analysis of the lateral lock-in phenomenon on the Pedro e Inês footbridge has been studied in detail. Although the results obtained from the proposed model are adequate, further studies, additional pedestrian and crowd test on different footbridges, are recommended in order to better characterize the parameters that define the crowd-structure interaction model.

Acknowledgements

This work was partially funded by the Spanish Ministry for Science under research project DPI2014-53947-R.

References

Al-Foqaha'a, A.A. (1997). Design Criterion for Wood Floor Vibrations Via Finite Element and Reliability Analyses. *PhD Thesis. Washington State University*.

ANSYS Mechanical Release 15.0

ARTeMIS Extractor Pro 2015.

Bachmann, H., Ammann, W. (1987). Vibrations in Structures Induced by Man and Machines, Structural Engineering Documents, Vol. 3e. International Association of Bridge and Structural Engineering (IABSE).

Barbosa, R., Magalhães, F., Caetano, E. Cunha A. " The Viana footbridge: Construction and dynamic monitoring", *Bridge Engineering*, ICE, in press 2012.

Bertram, J.E.A., Ruina, A., "Multiple walking speed-frequency relations are predicted by constrained optimization". *Journal of Theoretical Biology*, Vol. 209 (4), pp. 445-453. 2001.

Bocian, M., Macdonald, J.H.G., Burn, J.F. (2014). Probabilistic criteria for lateral dynamic stability of bridges under crowd loading, *Computers & Structures*, Vol. 136, pp. 108-119.

Brownjohn, J.M.W. (1999). Energy dissipation in one-way slabs with human participation. Asia Pacific Vibration Conference'99. Vol. 1, Nanyang Technological University, 2nd SPIE International Conference on Experimental Mechanics, pp. 155-160.

Brownjohn, J.M.W., Fok, P., Roche, M., Omenzetter, P. (2004). Long span steel pedestrian bridge at Singapore Changi airport part 2: crowd loading tests and vibration mitigation measures. The Structural Engineer 82 (16), pp. 28-34.

Bruno, L., Venuti, F., "Crowd-structure interaction in footbridges: modelling, application to a real case-study and sensitivity analysis". *Journal of Sound and Vibration*, Vol. 323 (1-2), pp. 475-493. 2009.

Butz CH., Heinemeyer, CH.; Goldack, A.; Keil, A.; Lukic, M.; Caetano, E.; Cunha, A.. Advanced Load Models for Synchronous Pedestrian Excitation and Optimised Design Guidelines for Steel Footbridges (SYNPEX). *RFCS-Research Project RFS-CR-03019*. 2007.

Caetano, E., Cunha A., Magalhaes F., Moutinho, C. (2010). Studies for controlling human-induced vibration of the Pedro e Inês footbridge, Portutal. Part 1: Assesment of dynamic behaviour. Engineering Structures, 32: 1069-1081. doi:10.1016/j.engstruct.2009.12.034.

Caetano, E., Cunha A.,Moutinho, C., Magalhaes F. (2010). Studies for controlling human-induced vibration of the Pedro e Inês footbridge, Portutal. Part 2: Implementation of tuned mass dampers. Engineering Structures, 32: 1082-1091. doi:10.1016/j.engstruct.2009.12.033.

Carroll, S.P., Owen, J.S., Hussein, M.F.M. (2012). Modelling crowd-bridge dynamic interaction with a discretely defined crowd. *Journal of Sound and Vibration* 331, 2685-2709.

Clough R., Penzien J. (1993). Dynamic of Structures. *McGraw-Hill*, Inc.

Dallard, P.,Fitzpatrick, A.J., Le Bourva, S., Low, A., Ridsill Smith, R., Willford, M., Flint, A. (2001). The London Millenium Footbridge. The Structural Engineer, 79(22): 17-33.

Domínguez, J. (2001). Dynamic of high speed train bridges: calculation methods and study of the resonance. *Ph. D. Thesis. Escuela Técnica Superior de Ingenieros de Caminos, Canales y Puertos de Madrid (UPM).* (In Spanish).

Eurocode 5 (2003). EN 1995-2. Design of timber structures, Part 2: Bridges European Committee for Standardization.

Falati, S. (1999). The Contribution of Non-structural Component of the Overall Dynamic Behaviour of Concrete Floor Slabs. *PhD Thesis. University of Oxford*.

Foschi, R.O., Neumann, G.A., Yao, F., Folz, B. (1995). Floor vibration due to occupants and reliability based design guidelines. *Canadian Journal of Civil Engineering* Vol. 22 (3) pp- 471–479.

Fox, R., Kapoor M. (1968). Rate of change of eigenvalues and eigenvectors. *AIAA Journal*, 6:2426-2429.

Friswell, M.I., Mottershead, J.E. (1995). Finite Element Model Updating in Structural Dynamics. *Kluwer Academic Publishers*.

Fujino, Y., Siringoringo, D. (2014). Revisiting the pedestrian induced lateral vibration of footbridge and crowd synchronization problem. Footbridge 2014. 5th International Conference. Footbridges: Past, present and future. London (U.K.).

Georgakis, C., Jorgesen, N.G. (2013). Topics in Dynamics of Bridges, Volume 3: Proceedings of the 31st IMAC. A Conference on Structural Dynamics, 2013. Chapter 4. Change in Mass and Damping on Vertically Vibrating Footbridges Due to Pedestrians. The Society for Experimental Mechanics, Inc.

Gopalakrishnan, S., Mitra, M. (2014). Wavelet Methods for Dynamical Problems. With Application to Metallic, Composite and Nano-Composite Structures. *CRC Press*.

Heermann, D. W. (1986) Computer simulation methods: in theoretical physics. *Springer-Verlag* New York, Inc. New York, NY, USA.

Helbing, D., Molnár, P. (1995). Social force model for pedestrian dynamics. *Physical Review*, 51(5):4282-4286.

Ingólfsson, E.T., Georgakis, C.T. (2011). A stochastic load model for pedestrian-induced lateral forces on footbridges. *Engineering Structures*, Vol. 33 (12), pp. 3454-3470.

Ingólfsson, E.T., Georgakis, C.T., Ricciardelli, F., Jönsson, J.. (2011) Experimental identification of pedestrian-induced lateral forces on footbridges. *Journal of Sound and Vibration*, Vol. 330, pp. 1265-1284.

Jiménez-Alonso, J. F., Sáez, A. (2014). A direct pedestrian-structure interaction model to characterize the human induced vibrations on slender footbridges. *Informes de la Construcción*, 66(extra-1): m007, doi: http://dx.doi.org/10.3989/ic.13.110.

Jiménez-Alonso, J. F., Sáez, A., Caetano, E., Magalhães, F. (2015). Vertical crowd-structure interaction model to analyse the change of the modal properties of a

footbridge. Journal of Bridge Engineering, ASCE (in press). doi: 10.1061/(ASCE)BE.1943-5592.0000828

Jones, C.A., Reynolds, P., Pavic, A. (2010). Vibration serviceability of stadia structures subjected to dynamic crowd loads: A literature review. *Journal of Sound and Vibration*, Vol. 330, pp. 1531-1566.

Koh Ghee C., Perry M.C. (2010). Structural Identification and Damage Detection using Genetic Algorithms. *CRC Press, Taylor&Francis Group*.

Macdonald, J.H.C. (2008). Pedestrian-induced vibrations of the Clifton Suspension Bridge, UK. Proceedings of the ICE-Bridge Engineering 161 (2), pp. 69-77.

Macdonald, J.H.C. (2008). Lateral excitation of bridges by balancing pedestrians. *Proceedings of the Royal Society*.

Magalhães, F., Cunha, A. (2011). Explaining Operational Modal Analysis with data from an arch bridge. *Mechanical Systems and Signal Processing*, Invited Tutorial Paper, Volume 25, Issue 5, pp. 1431-1450.

Magalhães, F., Cunha, A., Caetano, E., Brincker, R. (2010). Damping estimation using free decays and ambient vibration tests. *Mechanical Systems and Signal Processing*, Volume 24, Issue 5, pp. 1274–1290.

Matlab R2015a. . http://www.mathworks.com/.

Matsumoto, Y., Griffin, M.J. (2003). Mathematical models for the apparent masses of standing subjects exposed to vertical whole-body vibration. *Journal of Sound and Vibration* Vol. 260 (3) pp. 431-451.

Matsumoto, Y., Nishioka, T., Shiojiri, H., Matsuzaki, K. (1978). Dynamic design of footbridges. *IABSE Proceedings*, No. P-17/78, pp. 1-15.

Nocental J., Wright S.J. (1999). Numerical Optimization. *Springer*, New York, USA.

Racic, V., Pavic, A., Brownjohn, J.M.W. (2009). Experimental identification and analytical modelling of human walking forces: Literature review. *Journal of Sound and Vibration*, Vol. 326, pp. 1-49.

Rapaport, D.C. (2004). The art of molecular dynamic. *Cambridge University Press*.

Ronnquist, A. (2005). .Pedestrian Induced Lateral Vibrations on Slender Footbridges. PhD Thesis. Norwegian University of Science and Technoloy.

SETRA/AFGC. (2006). Guide méthodologique passerelles piétonnes (Technical Guide Footbridges: Assessment of vibration behaviour of footbridge under pedestrian loading). SETRA.

Shahabpoor, E., Pavic, A., Racic, V. (2013). Modelling effect of pedestrians walking on dynamic properties of structures. *IMAC XXXI: A Conference and Exposition on Structural Dynamics*, 11-14 February, Orange County, California, USA.

Teughels, A. (2003). Inverse Modelling of Civil Engineering Structures Based on Operational Modal Data. *Ph. D. Thesis, Katholieke Universiteit Leuven*.

Venuti, F., Bruno, L., Bellomo, N. (2007). Crowd dynamics on a moving platform: mathematical modelling and application to lively footbridges. *Mathematical and Computer Modelling* 45 (3-4), 252-269.

Zheng, X., Brownjohn, J.M.W. (2001). Modelling and simulation of human-floor system under vertical vibration. Smart Structures and Materials 2001: Smart Structures and Integrated Systems. SPIE.

Zivanovic, S., Pavic, A., Ingolfsson, E. (2010). Modelling spatially unrestricted pedestrian traffic on footbridges. *Journal of Structural Engineering*, Vol. 136 (10), pp. 1296-1308.

Zivanovic, S., Pavic A., Reynolds P. (2007). Finite element modelling and updating of a lively footbridge: The complete process. *Engineering Structures*, Vol. 301(1-2), pp. 126-145.

Zivanovic, S., Pavic A., Reynolds P.(2005). Vibration serviceability of footbridges under human-induced excitation: a literature review. *Journal of Sound and Vibration*, Vol. 279, Issue 1-2, pp. 1-74, January 2005.

Paper F: Dynamic testing of Carpinteira footbridge at Colvihã (Portugal).

Conference name: 5th International Operational Modal Analysis Conference

Location and date: Guimarães (Portugal). 13-15 May 2013.

Paper ID: 224 (pp. 1-10).

ISBN: 978-972-8692-83-4.

Scopus: http://0-www.scopus.com.fama.us.es/inward/record.url?eid=2-s2.0-84906259319&partnerID=40&md5=3cd5fcc0518066dbff05cdacdea01d34

IOMAC'13
5th International Operational Modal Analysis Conference
2013 May 13-15 Guimarães - Portugal

DYNAMIC TESTING OF CARPINTEIRA FOOTBRIDGE AT COVILHÃ, PORTUGAL

Javier Fdo. Jiménez-Alonso [1], Elsa Caetano[2], Álvaro Cunha[3]

ABSTRACT

The footbridge over the Carpinteira stream establishes a connection between two steep cliffs, at a height of 52.00 m above the water, having a length of about 220.00 m and being composed of three straight sections with different orientations in plan view, joined by circular curves and supported on four columns. In order to describe the dynamic behaviour of the footbridge, an ambient vibration test was performed, complemented by characterisation tests of the vibrations induced by pedestrians in the loading scenarios assumed as critical for the structure. A detailed finite element model of the structure has also been developed for correlation analysis with the measured values. This paper shows the results of these tests and the main conclusions about the comfort level provided by the footbridge under the service conditions.

Keywords: Footbridge, Operational modal analysis, Human induced vibrations, Ambient dynamic testing.

1. INTRODUCTION

Inserted in the Urbanization Plan of Carpinteira Valley, promoted by the Polis Program, the footbridge over the Carpinteira stream establishes a link between the two steep cliffs of Carpinteira Valley at a height of 52.00 m over the water. The design has been developed by Afassociados, in collaboration with the architect Carrilho da Graça [1], and the construction, performed by the company CERTAR, was finished in September 2009.

The dynamic characteristics of the footbridge, predicted at the design stage, motivated some concern owing to the possibility of occurrence of significant lateral and vertical vibrations, since several of the natural frequencies of the calculated vibration modes, both in lateral and vertical directions, would be apparently located at critical intervals from the point of view of the excitation induced by pedestrians [2]. Accordingly, and as it wouldn't be possible to act on the stiffness or mass of the footbridge in order to achieve significant changes in terms of modifying the dynamic characteristics of the structure, the Designer has foreseen the need to install tuned mass dampers, if after the construction of the structure, there was evidence that they would be really required.

[1] Assistant Professor, University of Seville, Higher Technical School of Building Engineering, jfjimenez@us.es
[2] Associate Aggregate Professor, University of Porto, Faculty of Engineering, ecaetano@fe.up.pt
[3] Full Professor, University of Porto, Faculty of Engineering, acunha@fe.up.pt

The footbridge was constructed in September 2009 and placed at the service of the population without introducing any device to mitigate vibrations, which aroused the interest in conducting the present research.

Thus, using the experimental resources available at the Laboratory of Vibrations and Monitoring (ViBest, www.fe.up.pt) of FEUP, an ambient vibration test was performed with the aim of identifying the dynamic characteristics of the footbridge. Additionally, measurements of the response of the structure under service conditions were made, and also under conditions of use potentially hazardous for the footbridge. This paper presents the main results achieved, which show some differences in the dynamic behavior of the structure in relation to the predicted at the design phase and, in particular, allow the characterization of the comfort level of the footbridge under normal use conditions.

2. DESCRIPTION OF THE STRUCTURE: CARPINTEIRA FOOTBRIDGE

Figure 1 Footbridge over the Carpinteira stream, view from the south side.

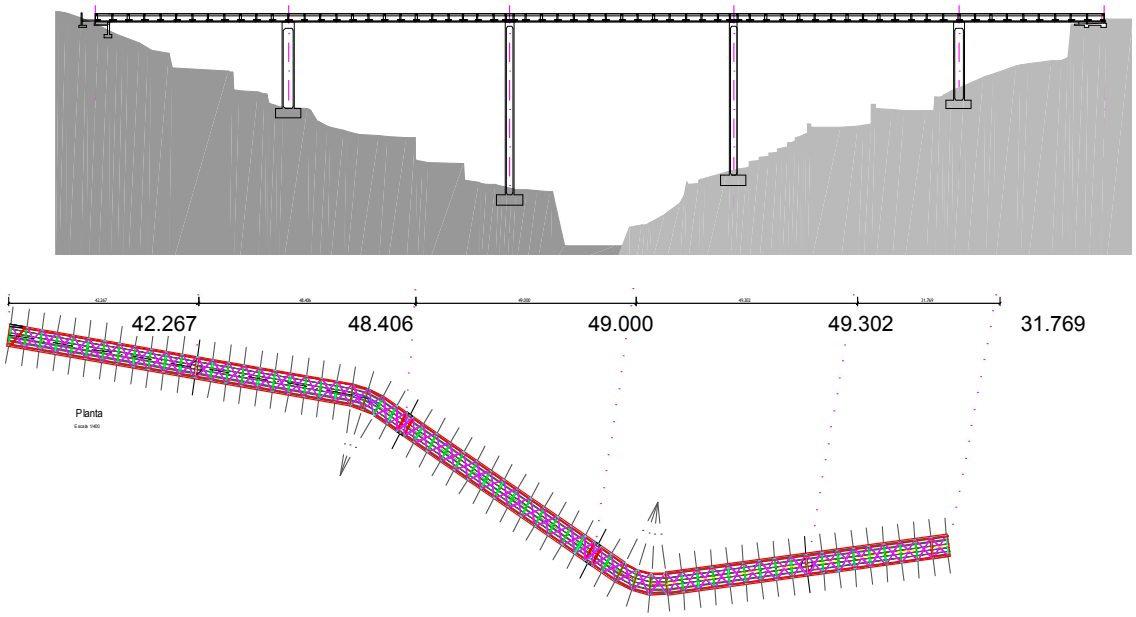

Figure 2 Carpinteira footbridge, lateral and plan views.

The footbridge (Figure 1) is composed of a steel deck that runs at a constant level, being formed by three linear segments with different orientation in plant, connected by circular curves. The total length of the deck is about 220.00 m and it is supported by four composite steel-concrete columns, with a variable height between about 18.00 and 40.00 m. The footbridge is thus divided in five spans, with lengths from about 32.00 to 50.00 m (Figure 2).

The cross-section of the footbridge, with overall dimensions of 4.40 x 1.75 m^2 and 3.50 m of effective width, is formed by two longitudinal steel welded girders and a wooden supporting floor structure that configure the characteristics of the U-shaped section of the footbridge.

3. NUMERICAL MODELLING OF THE FOOTBRIDGE

Due to the complexity of both the geometry and the behaviour of the structure and, with the aim of supporting the development of the dynamic tests and subsequent interpretation of the obtained results, a finite element model of the footbridge was developed using 3-D beam elements [3, 4 and 5]. In Figure 3, the finite element mesh used is presented.

.

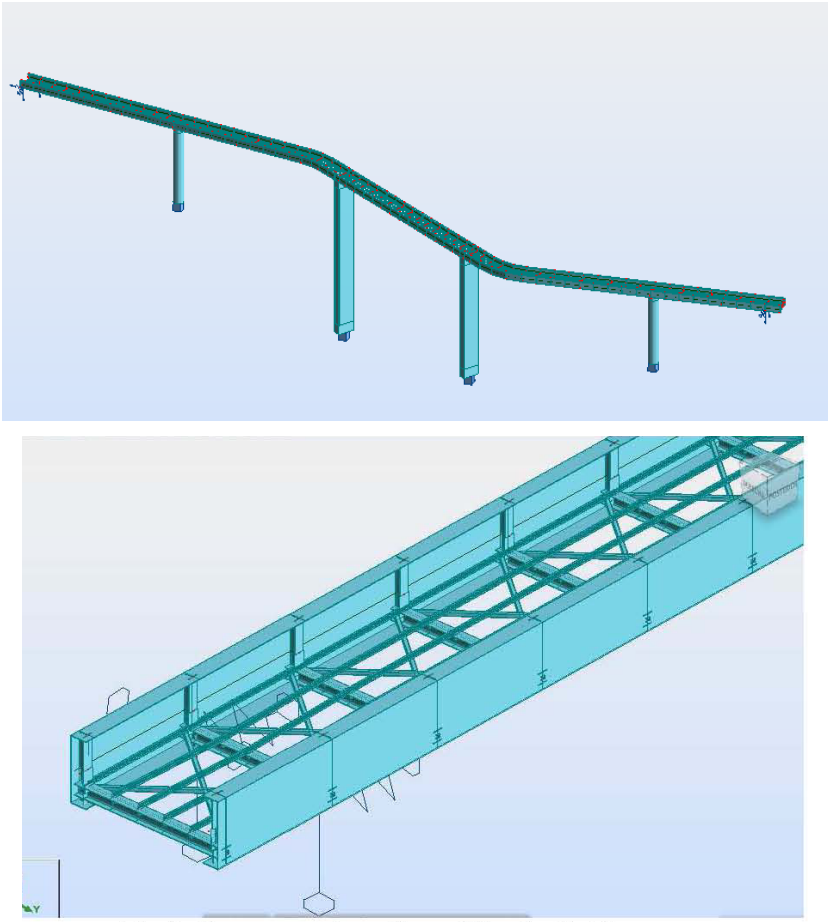

Figure 3 Carpinteira footbridge, finite element mesh used in the numerical model and detail of discretization.

The overall mass of the steel deck is about 300 ton, corresponding to a linear mass of 1250 kg/m. In the design of the footbridge, the associated dynamic effects of a pedestrian flow, with a density of 0.60 pedestrian/m^2, have been considered, which corresponds to an increase of the mass of the deck of about 10 %. Though the whole pedestrian mass is not usually considered in the dynamic characterization of the footbridge, the calculation of the natural frequencies has been made assuming either an empty structure or a loaded state with 0.60 Pedestrian/m^2, in order to frame their natural frequencies. On the other hand, given the relatively low loading levels, it was assumed that during service, the elastic supports at the extremes wouldn't be activated. Accordingly, alternative conditions

of connection were simulated: elastic behaviour associated to neoprene bearings, or constraint movement in longitudinal direction.

Table 1 presents the values of several natural frequencies corresponding to four numerical simulations developed in order to frame the bridge natural frequencies: M1 - empty footbridge, elastic supports; M2 - full footbridge with 0.60 pedestrian/m^2, elastic supports; M3 - empty footbridge, fixed supports; M4 - full footbridge with 0.60 pedestrian/m^2, elastic supports. It is described in Table 1 the main characteristics of the most important vibration modes (L: longitudinal; T: transverse; V: vertical; To: torsion). On the other hand, Figure 4 shows the four most relevant vibration modes, based on the M3 model.

Table 1 Numerical natural frequencies obtained under different assumptions in relation to mass (empty/full deck with a pedestrian density of 0.60 pedestrian/m^2) and the stiffness of the extreme supports (elastic/fixed).

Modes	M1 (elastic/ empty)	M2 (elastic/full)	M3 (fixed/empty)	M4 (fixed/full)
1	1.15 (T)	1.11 (T)	1.21 (T)	1.16 (T)
2	1.34 (L)	1.29 (L)	1.6 (T local)	1.52 (T local)
3	1.38 (T local)	1.3 (T local)	1.97 (To)	1.88 (To)
4	1.79 (T)	1.71 (T)	2.02 (To+ T)	1.93 (To+T)
5/ 6(M3+M4)	2.01 (V+T)	1.9 (V+T)	2.33 (To+T)	2.20 (T+To)
7 (M3+ M4)			2.44 (To+T)	2.32 (T+To)
…	…	…	…	…
14/ 13 (M3+ M4)	3.78 (V)	3.54 (V)	3.83 (V)	3.58 (V)

Freq. 1= 1.21 Hz

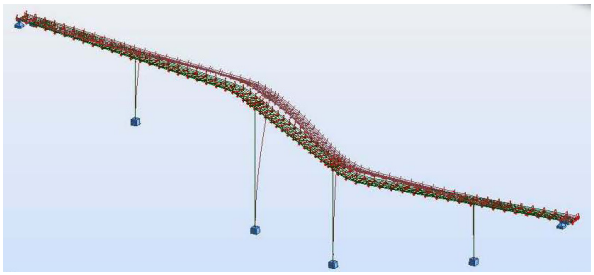

Freq. 3= 1.97 Hz

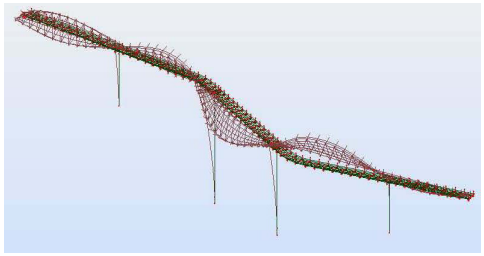

Freq. 7= 2.44 Hz

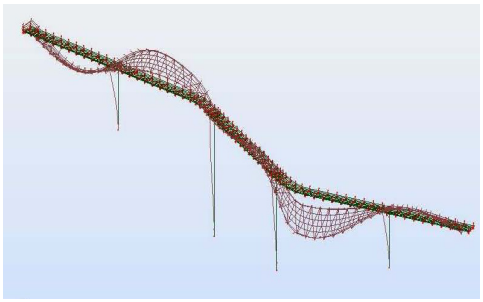

Freq. 13= 3.83 Hz

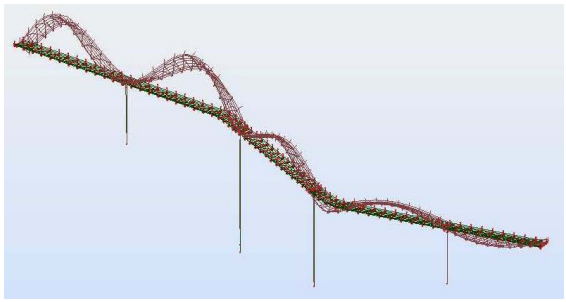

Figure 4 Several modal shapes obtained from finite element model M3 (empty footbridge with fixed longitudinal support at abutments).

4. IDENTIFICATION OF THE DYNAMIC PROPERTIES

The identification of the natural frequencies, vibration modes and modal damping ratios was made performing an ambient vibration test, conducted in July 2011. In this test, 5 seismographs provided with triaxial accelerometers, were used. These elements were successively placed along the positions indicated in Figure 5, keeping two of the devices in sections 6 and 15, in the west side of the footbridge. In each position, records of ambient acceleration have been collected in 15 channels with 13- minute duration, sampled at 100 Hz.

Figure 6 shows two images of the tests performed, held during a normal day and involving the occasional passage of pedestrians, under normal conditions of use.

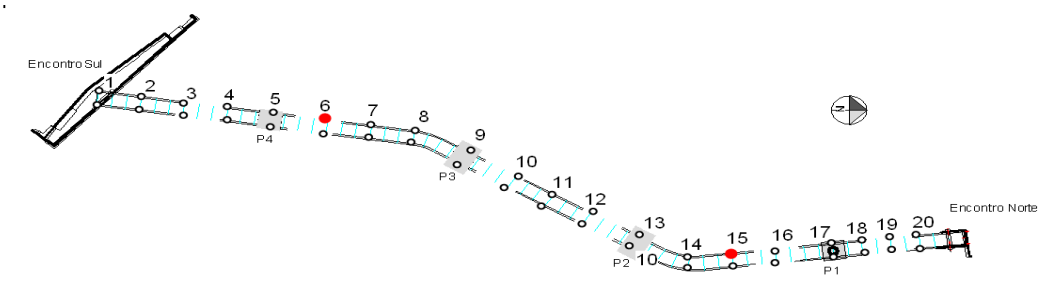

Figure 5 Instrumented points in the ambient vibration test.

Figure 6 Images of the ambient vibration tests.

According to the image of Figure 6, and given the peculiar characteristics of the footbridge, it was decided to dispose systematically the sensors, so that the transverse axis would coincide with the North direction. This permitted the use of a common reference and facilitated the signal processing. The identification of the modal parameters was made using the software ARTEMIS [6]. Table 2 shows a list of the most relevant identified natural frequencies and modal damping ratios, whereas Figure 7 characterizes several of the corresponding vibration modes. It is settled in Table 2 a correspondence between some identified and calculated vibration modes, considering as basis the previously presented M3 model.

The analysis of Table 2 and Figures 4 and 7 shows that, although the main aspects of the dynamic behavior of the footbridge are characterized by the numerical finite element model, in terms of the natural frequencies values of the vibration modes (transverse, vertical and torsion), significant differences exist between the modes calculated and identified.

Indeed, we can notice that the first identified transverse vibration mode has a natural frequency slightly higher than the calculated one, which is indicative of the behavior of the extreme supports, almost fixed to the abutments. Although the numerical modeling has just introduced longitudinal constriction, the natural frequency of the second mode of vibration, of local character, is also higher than the calculated, which certainly also involves the constriction of the transverse motion in the extreme supports at the abutments.

Moreover, it is also observed that the real transverse flexibility of the columns was inferior to the calculated one, since the vertical vibration modes involve generally the torsion of the deck, but not the transverse bending of the columns, contrary to the results of the calculation. Finally, it is noticed some proximity between the natural frequencies of the modes with vertical and torsional components, which is certainly determined by the mechanical characteristics of the deck.

Table 2 Numerical natural frequencies

Modes	Identified natural frequency (Hz)	Numerical natural frequency (Hz)	Damping ratio (%)
1	1.37 (T)	1.21 (T)	0.28
2	2.20 (T local)	1.6 (T local)	0.21
3	2.47* (V+ To)		0.17
4	2.76 (V+To)		0.13
5	2.95 (V+To)		0.33
6	3.59 (V+T)	3.83 (V)	0.07

* Several numerical modes with close frequencies.

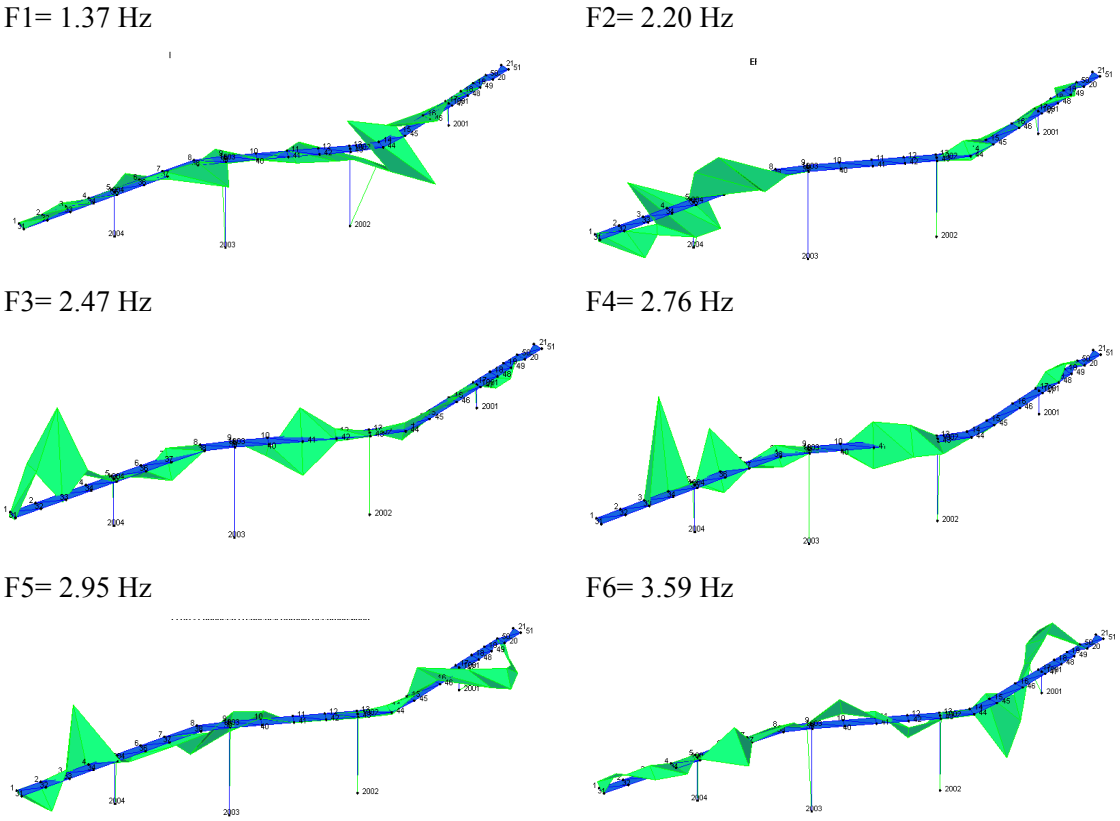

Figure 7 Identified vibration modes using ARTEMIS software.

5. CHARACTERIZATION OF THE DYNAMIC BEHAVIOUR

From inspection of the identified natural frequencies of the footbridge, it can be concluded, firstly, that the footbridge is not vulnerable to the lateral synchronization phenomenon. Indeed, this phenomenon typically occurs with natural frequencies close to 1 Hz. The international codes and recommendations [7, 8] define this synchronization as possible in the range of frequencies from 0.5 to 1.2 Hz, with a critical scenario when the fundamental frequencies are situated between 0.7 and 1.0 Hz. The initial numerical studies [2] suggested a fundamental frequency of 1.14 Hz, so the risk of occurrence of this phenomenon was real. Note that, despite the possible sophistication of the current numerical models, the real boundary conditions of the footbridge and, sometimes, the addition of elements assumed as non-structural, can greatly influence its dynamic behaviour, and there are often differences in the fundamental frequencies of the built structure against the numerical results of the design. In this case, the natural frequency of 1.37 Hz measured in the transverse direction reduces the risk of lateral

synchronization, not avoiding however questions about the comfort level provided by the structure, both in terms of the vertical and horizontal vibrations. This problem is particularly relevant taking in mind the location of the bridge, at a very high level, and also taking into account the characteristics of the pavement, with a slatted wooden relatively sparse.

It is referred, on the other hand, the very low damping identified by the ambient vibration test. It is important to note that the quality of the damping estimates obtained in this way is questionable, particularly since there was no opportunity to validate them using other method. It is noted, however, that the modal damping ratios identified are lower than expected.

In relation to the vertical vibrations, it was also found at the design stage [2] that there were several vibration modes with natural frequencies close to 2 Hz, which could lead to resonant phenomena. In the built footbridge, it was observed that the frequencies of the vertical modes are generally a little higher than calculated, being settled typically above 2.5 Hz.

In contrast, the flexibility of the columns is lower than the modelled one, which reduces their participation in terms of transverse bending in the main vibration modes. This fact leads to a more significant torsional behaviour of the deck.

Also these characteristics become beneficial to the structure, since the resonant phenomena at frequencies around 2 Hz don't occur. In contrast, the dynamic effects induced by pedestrians jogging become more relevant. Moreover, and given that the torsional behaviour of the deck turns out to be evident, also the lateral modes of vibration are associated generally to the components of vertical vibration modes, which may result in more severe vibration levels.

Taking into account the observed dynamic characteristics of the footbridge, previously discussed, it is assumed that the dynamic response may be critical in the following situations:

1) Slow walking of large flows of pedestrians, with frequencies from 1.4 to 1.5 Hz (excitation of vibration mode 1 and modes 3 to 6 (Figure 7) through the second harmonic);

2) Jogging by a pedestrian or a group of pedestrians, with natural frequencies of 2.47 Hz, 2.76 Hz or 2.95 Hz (excitation of vibration modes 3, 4 or 5 (Figure 7)).

Although it has been observed that the use of the footbridge is not intense, it was possible to test a normal operating situation relatively close to the described condition (1) of the above paragraph, although mobilizing a reduced density of pedestrians. The dynamic tests were performed in two days of the summer of 2011. It was found that the footbridge was used merely occasionally during the day. Conversely, and given the warm temperature observed in the late evening, from 19:00 h, a continuous use by pedestrians was detected, characterized by slow walking.

Although an accurate quantification of the density of pedestrians has not been made, it is possible however to say that a density of at least of 0.1 pedestrian/m^2 has been reached, since more than 80 pedestrians were over the structure. Under these conditions, the lateral and vertical vibrations were clearly perceptible, also mobilizing high and low frequencies. Taking as basis the range of 0-8 Hz, both levels of transverse and vertical accelerations were collected, with values of 0.08 m/s^2 and 0.17 m/s^2, respectively, characteristics of the maximum comfort level of the footbridge, in line with the recommendations mentioned above [7, 8].

Figure 8 shows examples of the records of the transverse and vertical acceleration collected in the mark number 16 (see Figure 5) under these conditions, together with their corresponding spectral content.

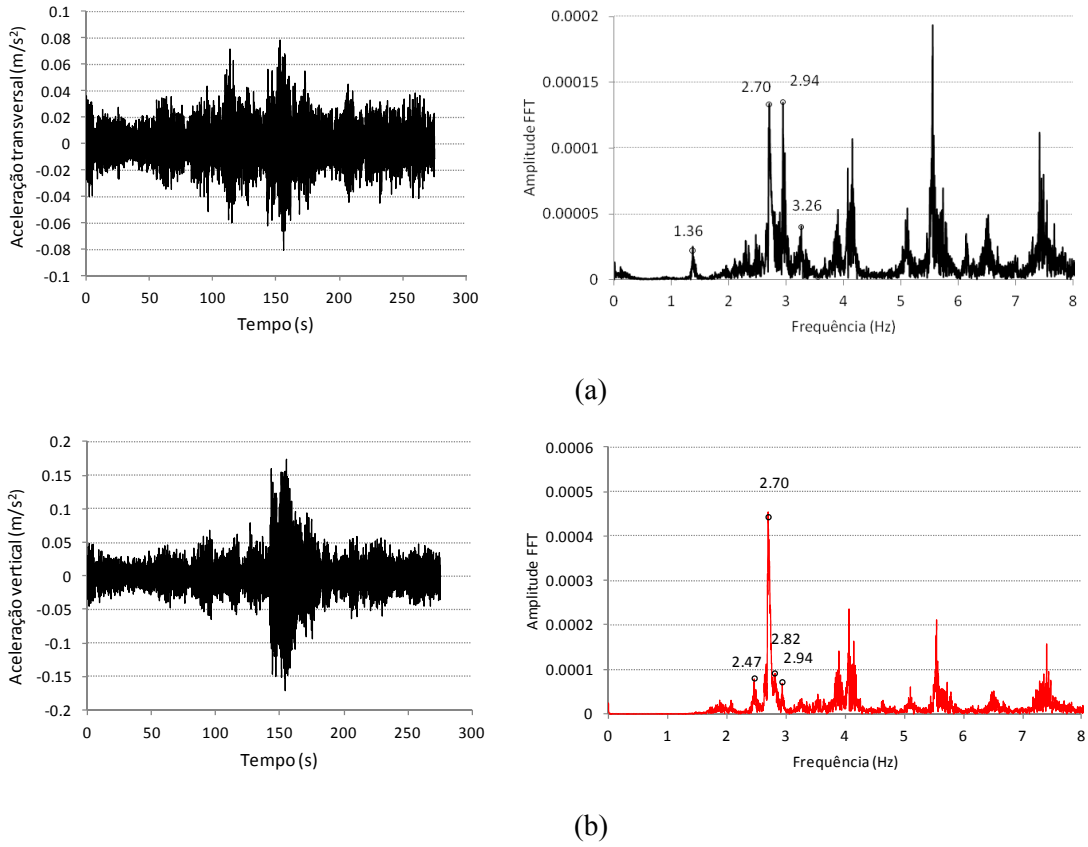

Figure 8 Transverse (a) and vertical (b) accelerations measured during the passage of pedestrians, time series and corresponding spectrum.

With regard to the situatioin of the footbridge under vibrations induced by joggers, several tests were perfomed, using only a single pedestrian running (Figure 9), fixing the step frequency with the help of a metronome. The dynamic response was measured then at sections 7 and 11 (see Figure 5) for step frequencies of 2.45 Hz, 2.70 Hz and 3.00 Hz, considering alternatively passages centered with the axis of the footbridge and eccentric ones. In Figure 10, several examples of the recorded transverse and vertical accelerations are shown.

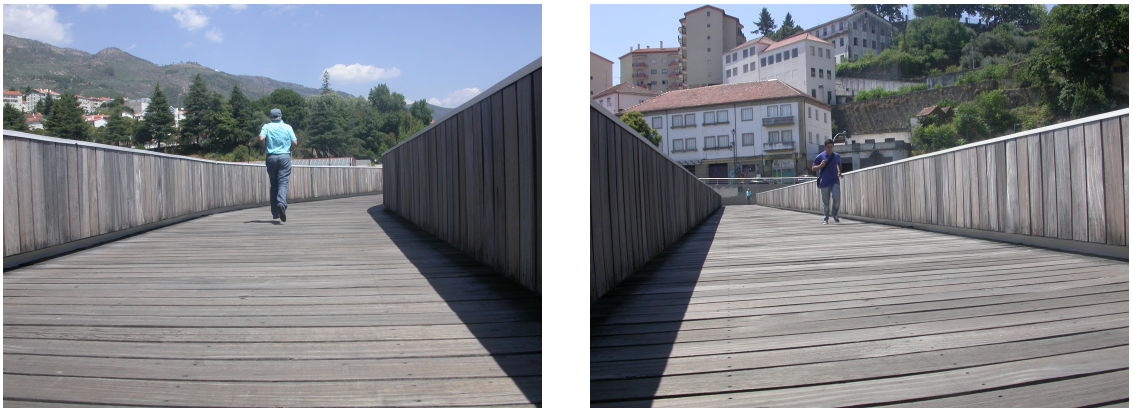

Figure 9 Dynamic test with jogging/running pedestrians.

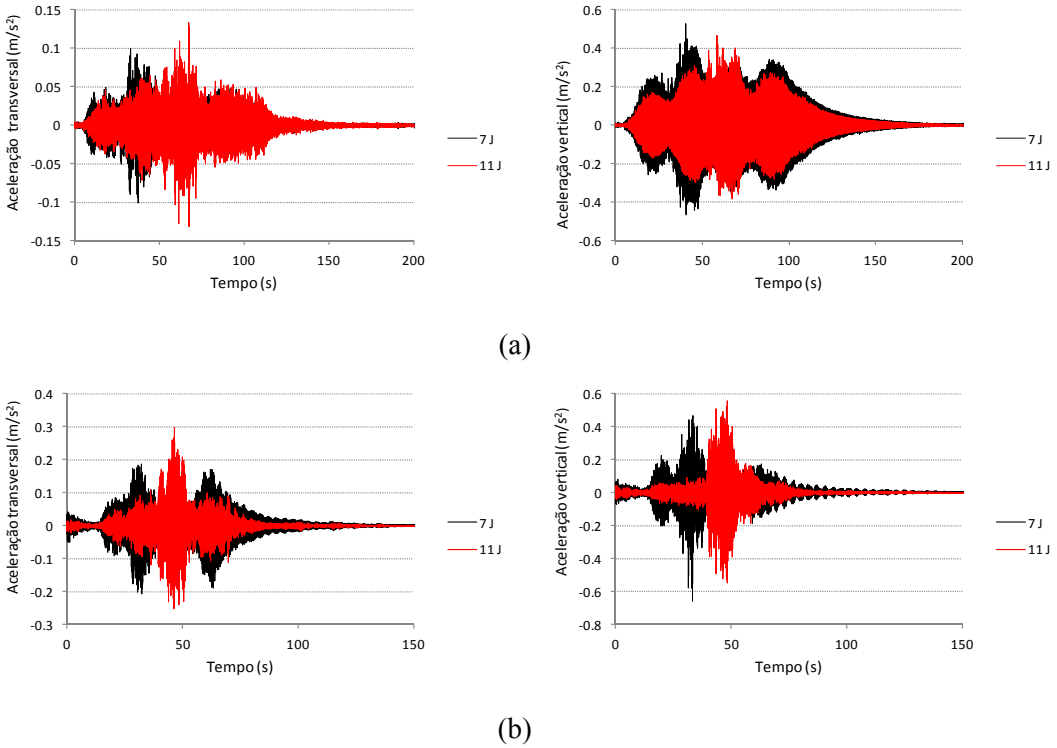

(a)

(b)

Figure 10 Accelerations recorded during the eccentric crossing by a pedestrian with step frequencies of 2.45 Hz (a) and 3.00 Hz (b).

In terms of amplitudes, it's worth mentioning that the transverse acceleration components are generally between 0.1 and 0.2 m/s^2, while the vertical acceleration camponents vary in the range between 0.4 to 0.6 m/s^2. Therefore, for the use by joggers, the footbridge presents a medium comfort level in relation to the transverse accelerations and it is close to the maximum in relation to the vertical ones.

6. CONCLUSIONS

The experimental dynamic study performed in the footbridge over the Carpinteira stream, at Covilhã, has permitted the identification of the main dynamic parameters of the structure (natural frequencies, vibration modes and modal damping ratios). The natural frequencies and vibration modes were compared to the numerical results obtained from a finite element model of the footbridge. The main objective of the work was to get a better understanding of the characteristics of the complex dynamic behavior of the footbridge and analyze the susceptibility of the structure under the dynamic effects induced by the pedestrians.

The analysis of the experimental natural frequencies of the structure, once built, and complementary studies of the vibration measurements under the passage of pedestrians in different situations of regular use or jogging permitted to verify the non-sensitivity of the structure to the lateral synchronization phenomena.

With regard to the comfort levels provided by the footbridge, it was possible to observe that, under the normal use conditions, characterized by a pedestrian flow of less than 0.1 pedestrian/m^2, the structure presents a maximum comfort level, both from the point of view of vertical and transverse vibrations.

The vibration levels observed, under the tested situations, were not clearly disturbing, since they did not prevent the use of the footbridge under service situation, though it may be said that an increase in

the pedestrian flow could lead to relatively high vibrations, particularly in transverse direction, and therefore uncomfortable.

In relation to the use of the footbridge by a "jogger", the comfort level could be classified as medium, essentially due to the more significant acceleration in the transverse direction. However, this classification can only be applied under the situation of a single jogger. In case the bridge is crossed by a group with a significant number of joggers, the expected vibrations may become really high.

ACKNOWLEDGEMENTS

The authors acknowledge the authorization of the Municipal Chamber of Covilhã regarding the performed dynamic tests.

REFERENCES

[1] AFASSOCIADOS Projetos de Engenharia SA, Projeto de Execução da Ponte Pedonal de Cima sobre a Ribeira da Carpinteira, Porto, Dezembro de 2004.

[2] Adão da Fonseca, A., Quinaz, C. Bastos, R., Pereira, M., Concepção e dimensionamento da ponte pedonal sobre a ribeira da Carpinteira, na Covilhã, VI Congresso de Construção Metálica e Mista, Porto, 2007.

[3] Zivanovic S., Pavic A., Reynolds P. (2005) Engineering Structures Modal Testing and FE model tuning of a lively footbridge structure.

[4] Autodesk Robot Structural Analysis Professional 2011. Autodesk 2011.

[5] Manterola J. Puentes: Apuntes para su diseño, cálculo y construcción. Colegio de Caminos, Canales y Puertos. Colección Escuelas, 2006.

[6] SVS (1994-2011). ARTeMIS Extractor Pro 2012. Structural Vibration Solutions, Aalborg, Denmark

[7] SÉTRA/ AFGC, Footbridges: Assessment of vibrational behavior of footbridges under pedestrian loads, 131 pp, 2006.

[8] Butz, C., Heinemeyer, C., Keil, A., Schlaich, M., Goldack, A., Trometer, S., Lukic, M., Chabrolin, B., Lemaire, A., Martin, P. O., Cunha, A., Caetano, E. HIVOSS. Design of Footbridges: Guideline and Background Document. European Commission, HIVOSS Project. 2008.

Paper G: Assessment of the dynamic behavior of Palmas Altas footbridge at Seville (Spain).

Conference name: 37th IABSE SYMPOSIUM MADRID 2014

Location and date: Madrid (Spain). 3-5 September 2014

Paper ID: Madrid-0350-2014.R1 (pp. 2626-2633.)

ISBN: 978-3-85748-134-5

Scopus: http://0-www.scopus.com.fama.us.es/inward/record.url?eid=2-s2.0-84929412609&partnerID=40&md5=49142f5e95b2f411591bf4b38e205cee

ASSESSMENT OF THE DYNAMIC BEHAVIOUR OF PALMAS ALTAS FOOTBRIDGE AT SEVILLE (SPAIN).

Javier JIMENEZ-ALONSO
Assistant Professor
University of Seville
Seville, Spain
jfjimenez@us.es

Javier Jiménez-Alonso, received his civil engineering master degree from the University of Granada, Spain. He worked as Bridge Engineer in Spain before becoming Professor at the University of Seville, Spain.

Andrés SAEZ
Full Professor
University of Seville
Seville,Spain
andres@us.es

Andres Saez, received his Ph.D degree from the University of Seville in 1997. His research mainly focuses on the application of numerical methods, dynamics and structural damage detection in continuum mechanics.

Summary

The behaviour of a slender footbridge is often conditioned by its response to pedestrian flows. This fact is especially relevant when high pedestrian densities are expected on it. The natural frequencies of such structures, that control its dynamic response, are very sensitive to any slight change in the mass or stiffness of the structure. In the case of this footbridge, a frame steel slender (ratio 1/40) structure of three spans (19.25+39.15+19.25 m) its dynamic behaviour was modified by the construction of a flexible cover, which final design was not known during the drafting phase of the project. Although the performed numerical estimations predicted an adequate behaviour, the uncertainty that the cover introduced into its dynamic behaviour, advised conducting a more detailed study of the footbridge response under pedestrian flows. Two types of experimental tests were performed, an ambient test by the application of the operational modal analysis technique to determine the experimental modal parameters of the footbridge, and a pedestrian test in order to determine the dynamic response of the structure under controlled groups of pedestrians. From the obtained experimental results a finite element model updating has been carried out by changing some structural parameters in order to minimize the mean square error between experimental and numerical modal parameters. The updated model was taken as a basis for the prediction of the structural dynamic behaviour under large pedestrian flows and to estimate better the change in the dynamic parameters provided by the steel roof.

Keywords: slender footbridge, human induced vibrations, operational modal analysis, model updating..

1. Introduction

During the design phase, it is a common practice, ensuring that the main natural frequencies of the structure are outside the range of frequencies that characterize the pedestrian walking activity (1.25-2.30 Hz in vertical and longitudinal direction and 0.50-1.20 Hz in lateral direction) and check the comfort level of the structure under the step of one pedestrian jogging [1]. The force exerted by each one of these joggers is characterized by the following equation.

$$p(t,v) = P \cdot \cos(2 \cdot \pi \cdot f \cdot t) \cdot n'_p \cdot \psi \tag{1}$$

where

P is the force component due to a single pedestrian walking/jogging (P=1250 N by SYNPEX [2]).

v, is the velocity of the pedestrian during its step.

f, is the natural frequency under consideration.

n'_p, is the equivalent number of pedestrians on the loaded surface S.

S, is the area of the loaded surface.

ψ, is a reduction coefficient to take into account the probability that the footfall frequency approaches the natural frequency under consideration [2].

In order to check the comfort level of the footbridge under its service condition, it must be ensured that the maximum acceleration that the deck experience under the step of one jogger was less than 1.00 m/s^2 (medium comfort level according to SETRA [1]).

Although, according to the results of the original construction project, the above criterion was checked favorably the dynamic response of the structure was disturbed by the subsequent construction of a steel cover on the footbridge. During the design phase of the footbridge the final geometry of the roof structure had not been adequately defined so its influence on the dynamic behaviour of the footbridge has been considered in a passive form, only modifying the mass matrix of the structure.

Starting from a preliminary dynamic finite element model of the structure, the numerical natural frequencies and vibration modes of the footbridge has been determined. These results have been used to manage an ambient test on the footbridge. The experimental data recollected has been processed by two operational modal algorithms (frequency and time domain) in order to obtain experimentally the dynamic parameters of the structure. The comparison of the experimental and numerical dynamic parameters has been used to update a more detailed finite element model of the whole structure (footbridge and steel cover). The updated model allows a better estimation of the numerical dynamic response of the structure under pedestrian flows and the quantification of the change in the natural frequencies provided by the steel roof.

A pedestrian test was made, in parallel, in order to estimate experimentally the dynamic response of the structure under controlled groups of pedestrians. The values obtained were compared to the numerical results of the normative pedestrian model [3].

2. Description of the structure.

The structure is a composite frame footbridge formed by a corten box-girder steel structure of variable depth interconnected with a reinforced concrete slab of 0.15 m. The length of the structure is about 80.00 m, with three spans (19.25+39.15+19.25 m). The steel box-girder has 3.15 m of width and a variable depth between 0.60-1.40 m. The structure is covered by a stainless steel cover configured by to orthogonal families of arches (formed by tubes) and a 2 mm overhead sheet fixed to these structural elements (Figure 1).

The foundation of the piers and the abutments are made of reinforced concrete pile caps configured each one by four deep piles of 25.00 meters of length and 0.85 m of depth. The average weight of the deck (without the steel cover) is the 2650 kg/m.

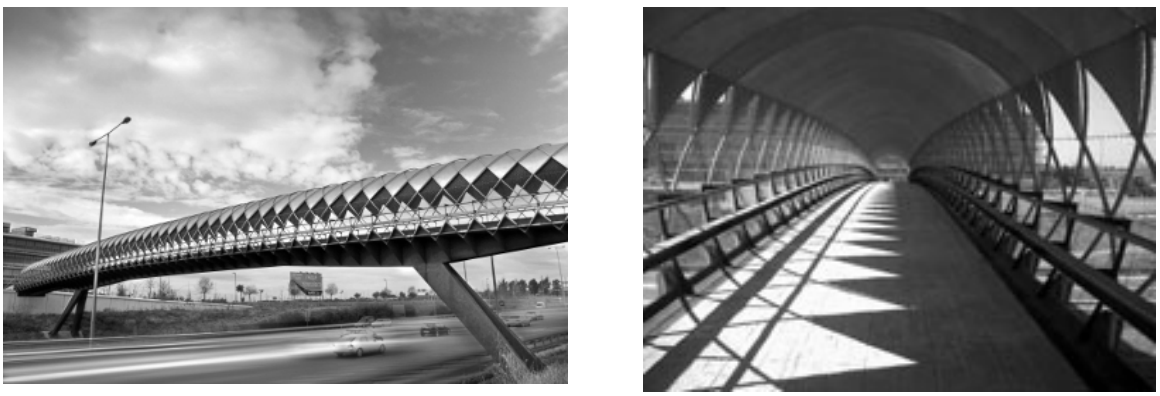

Fig. 1: Lateral view of the footbridge and cross-section.

Due to the slenderness of the structure, the joint between the deck and the piers has been specially stiffened.

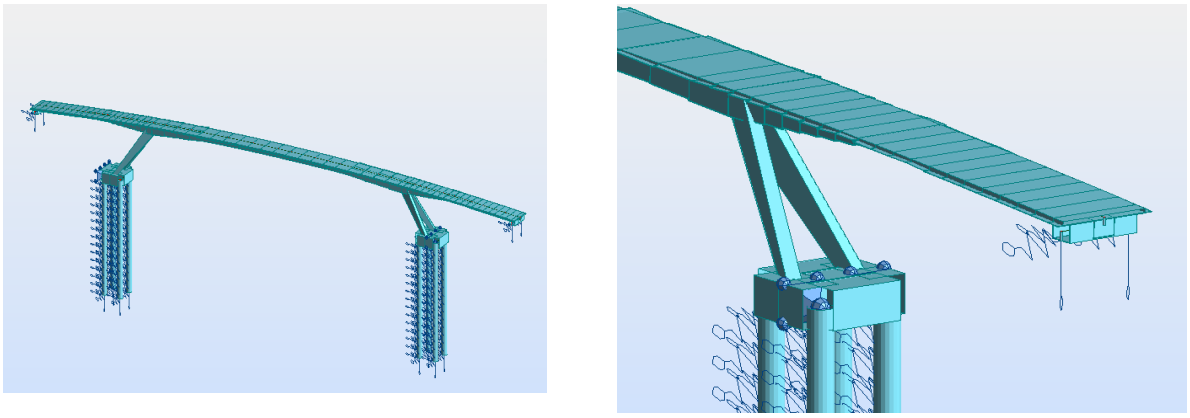

Fig. 2: Preliminary Finite Element Model.

3. Preliminary numerical modal analysis.

Firstly, a numerical modal analysis was developed (Figure 2), where the effect of the steel roof was considered as a passive mass uniformly distributed on the deck (approximately 500 kg/m). The model of the structure was carried out by the finite element software Autodesk Robot Structural Analysis Professional [4]. Under this hypothesis, the numerical vibration modes (Figure 3) of the footbridge has been determined in two scenarios, absence of pedestrians (f_{emp}) and the situation where a pedestrian flow of 1.00 P/m^2 (Pedestrians/m^2) cross the structure (f_{ful}) [2].

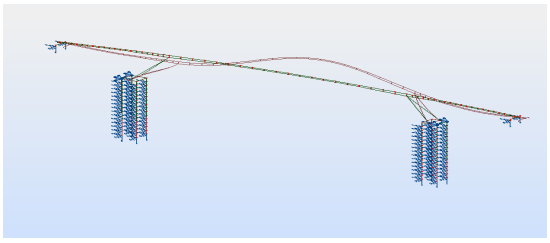

Numerical vertical mode 1 $f_{ful/emp}$=2.34/2.43 Hz

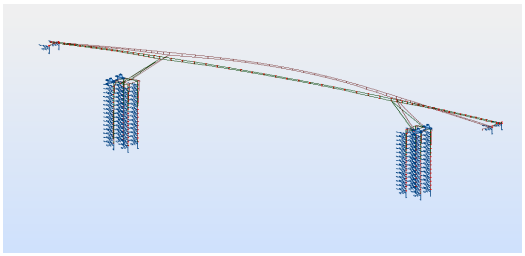

Numerical lateral mode 1 $f_{ful/emp}$ =2.13/2.20 Hz

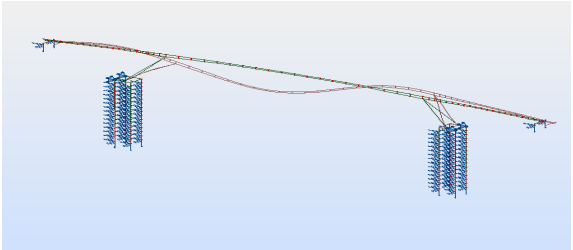

Numerical vertical mode 2 $f_{ful/emp}$=2.56/2.66 Hz

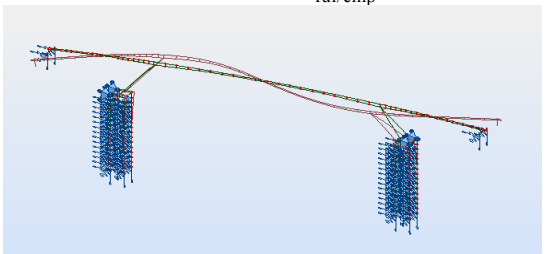

Numerical lateral mode 2 $f_{ful/emp}$=5.08/5.25 Hz

Fig. 3: First four vibration modes. Empty (emp) and full(ful) footbridge.

Given the situation of the footbridge and assuming that on the structure are not expected pedestrians densities above 0.80 P/m^2, the numerical estimated natural frequencies are outside of the normal ranges that characterize the pedestrian walking step. On the other hand, the natural frequencies of the structure are in the range that characterizes the action of jogging or running. The numerical response that produces the crossing of the previously predefined harmonic load on the structure (1) reaches its maximum value under a crossing jogger at 2.56 Hz. In Figure 4 the vertical dynamic response (acceleration) of the structure under the passage of this pedestrian is shown. The maximum value is less than the limit established by the comfort level (1.00 m/s^2).

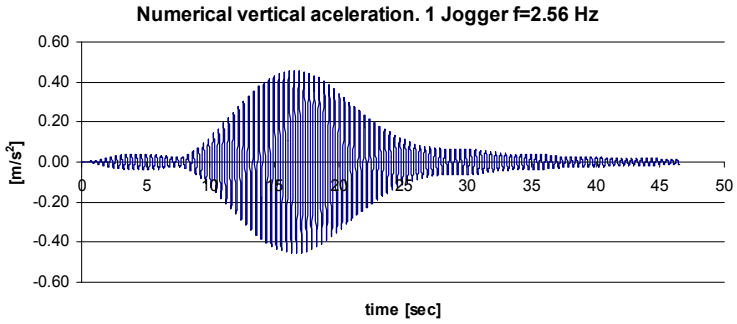

Fig. 4: Numerical vertical acceleration at mid-span due to a jogger step frequency f=2.56 Hz.

4. Ambient and pedestrian tests.

4.1 Ambient test.

The dynamic parameters of the structure have been determined by the measures obtained from an ambient test. The deck of the structure has been divided into a 2x15 grid, being the points separated longitudinally 5.65 m and transversally 3.15 m (see Figure 5, blue arrows are reference accelerometers). Two series of measurements were carried out, each one consisting on 14 set-up, the first one corresponds to the determination of vertical dynamic parameters and the second to estimate the lateral dynamic parameters. The measures were made with 4 uniaxial accelerometers, sensitivity 10 V/g, type Episensor and produced by the company Kinemetrics. The duration of each set-up was 900 seconds and the sampling frequency was 100.00 Hz [5].

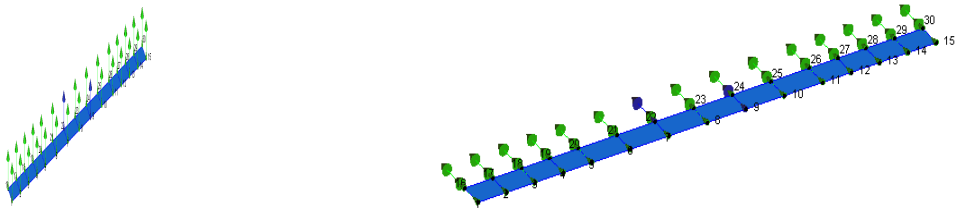

Vertical Ambient Test Layout Lateral Ambient Test Layout

Fig. 5: Measurement grid for the ambient test.

From the above series, the dynamic parameters of the structure have been determined, processing the signals by two different methods, one in the frequency domain, Enhanced Frequency Domain Decomposition (E.F.D.D.), and another in the time domain, Stochastic Subspace Identification (S.S.I.). For the validation of the results [5], the M.A.C. ratio (Modal Assurance Criterion) of certain vibration modes, has been calculated (Table 1) presenting all the identified vibration modes a M.A.C. greater than 0.90.

Table 1: Experimental natural frequencies

Mode	f_{EFDD} [Hz]	f_{SSI} [Hz]	Description	M.A.C.
1	2.372	2.370	Lateral	0.999
2	3.026	3.024	Vertical	1.000
3	3.830	3.844	Vertical	0.890
4	5.508	5.601	Lateral	0.901

In Figure 6 the graphical representation of the first four determined vibration modes is shown. The practical application of the above algorithms was performed using the ARTeMIS Extractor Pro 2012 software developed by SVS A/S [6].

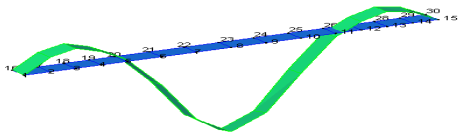

Experimental vertical mode 1 f=3.026 Hz

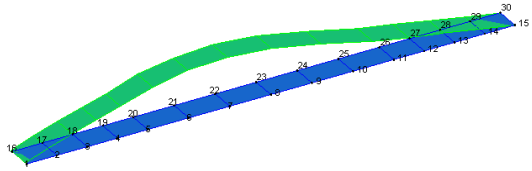

Experimental lateral mode 1 f=2.372 Hz

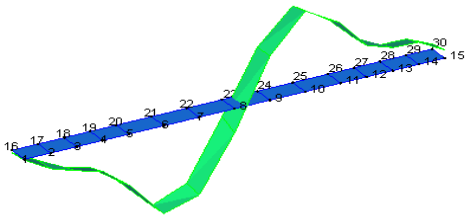

Experimental vertical mode 2 f=3.844 Hz

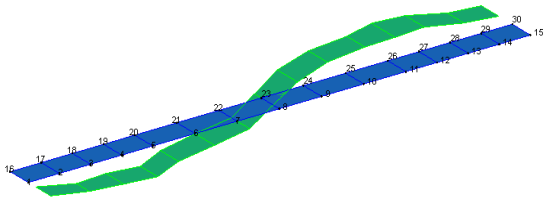

Experimental lateral mode 2 f=5.508 Hz

Fig. 6: Experimental first four modes of vibration (E.F.D.D.).

4.2 Pedestrian test.

Finally, it is performed a test with five different pedestrians, measuring the dynamic response of the footbridge under different step frequencies (*f = 1.50, 2.00, 2.50, 3.00, 3.50 and 4.00 Hz*). In Figure 7, the measured maximum vertical acceleration in the central mid-span for a pedestrian with a weight of 114.00 kg and a step frequency of 3.00 Hz is shown. The maximum measured acceleration is less than the limit established by the medium comfort level and the numerical one estimated previously.

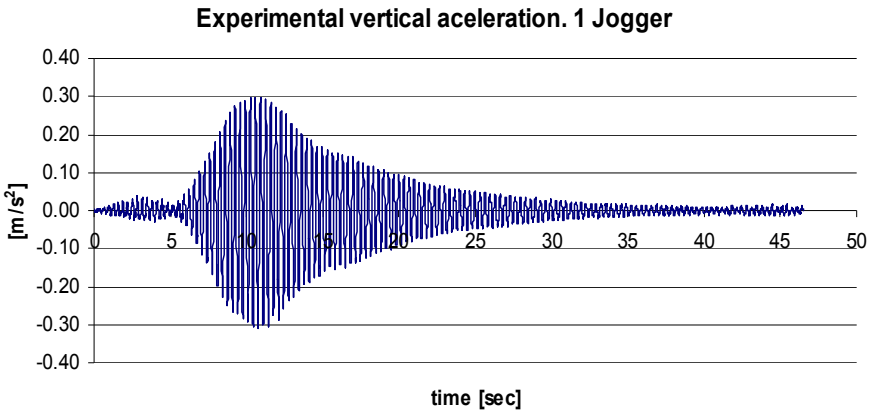

Fig. 7: Experimental vertical acceleration at mid-span due to a jogger step frequency f=3.00 Hz

The stiffening of the structure caused by the presence of the steel roof originates an improvement of the comfort level of the structure.

5. Model updating.

5.1 Detailed finite element model of the whole structure.

In order to have a more accurate understanding of the dynamic behaviour of the structure a detailed finite element model of the whole structure has been developed. Numerical modal analysis has been

developed through the application of the finite element method [7]. In the finite element model of the structure has been necessary to model all the element of the footbridge and the cover to characterize as precisely as possible the mass and stiffness matrices. The model has been carried out using 3D-beam (BEAM188) elements except in the case of the steel cover were 2D-shell (SHELL63) elements has been considered.

5.2 Model updating of the detailed finite element model.

A model updating of the above detailed finite element model has been developed [8] from the results of the above operational modal analysis in order to characterize more adequately the dynamic behaviour of the footbridge. In this sense, 7 physical parameters of the structure (according to Table 2) have been modified in order to minimize the mean square error between the experimental and numerical parameters, considering the identified natural frequencies and their corresponding modal coordinates. After a sensitivity study of the main physical parameters of the finite element model, it was found that the physical parameters with greater influence on the dynamic behaviour of the footbridge are the stiffness of bearings. The stiffness of these elements has been simulated through three springs, one in each direction (longitudinal, lateral and vertical). The objective function, in this case, was defined as the sum of the relative differences between the natural frequencies and the modal coordinates obtained experimentally and numerically. As optimization method the genetic algorithms have been chosen. In Figure 8 the results of the adjustment made on the first four vibration modes are shown.

Table 2: Updated values of considered physical parameters

Parameters	Initial Value	Updated Value
Effective cover thickness	0.003 mm	0.0015 mm
Effective slab concrete thickness	0.15 m	0.10 m
Effective abutment stiffness	30000 MPa	33240 MPa
Soil stiffness	5.00E8 kN/m	4.64E8 kN/m
Longitudinal bearing stiffness	1.00E9 kN/m	2.00E8 kN/m
Lateral bearing stiffness	1.00E10 kN/m	2.64E9 kN/m
Vertical bearing stiffness	1.00E11 kN/m	1.28E11 kN/m

After the adjustment of the selected physical parameters, high correlations between experimental and numerical modal shapes (M.A.C. above 95 %) have been reached in the four modes identified.

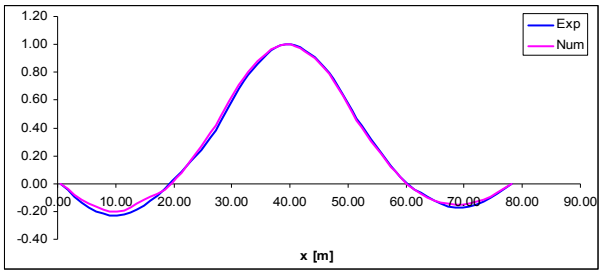

Experimental&numerical 1st vertical mode

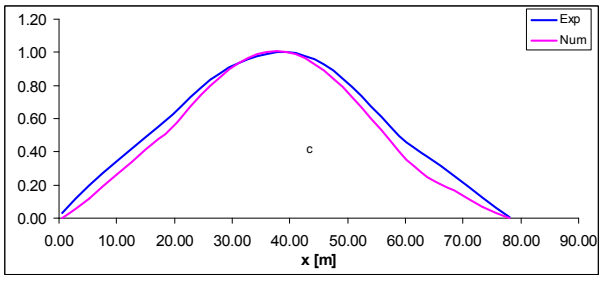

Experimental&numerical 1st lateral mode

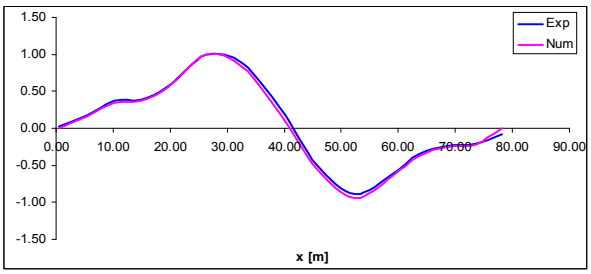

Experimental&numerical 2nd vertical mode

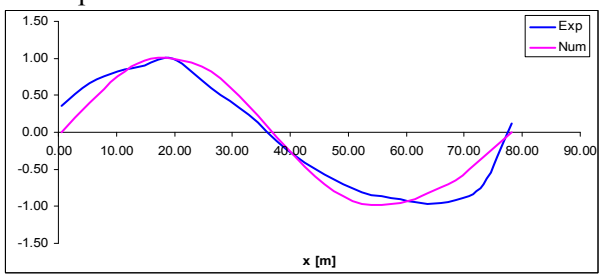

Experimental&numerical 2nd lateral mode

Fig. 8: Comparison between experimental (Exp.) and numerical (Num.) vibration modes

Finally, in Figure 9 the updated four first vibration modes from the detailed finite element method are shown.

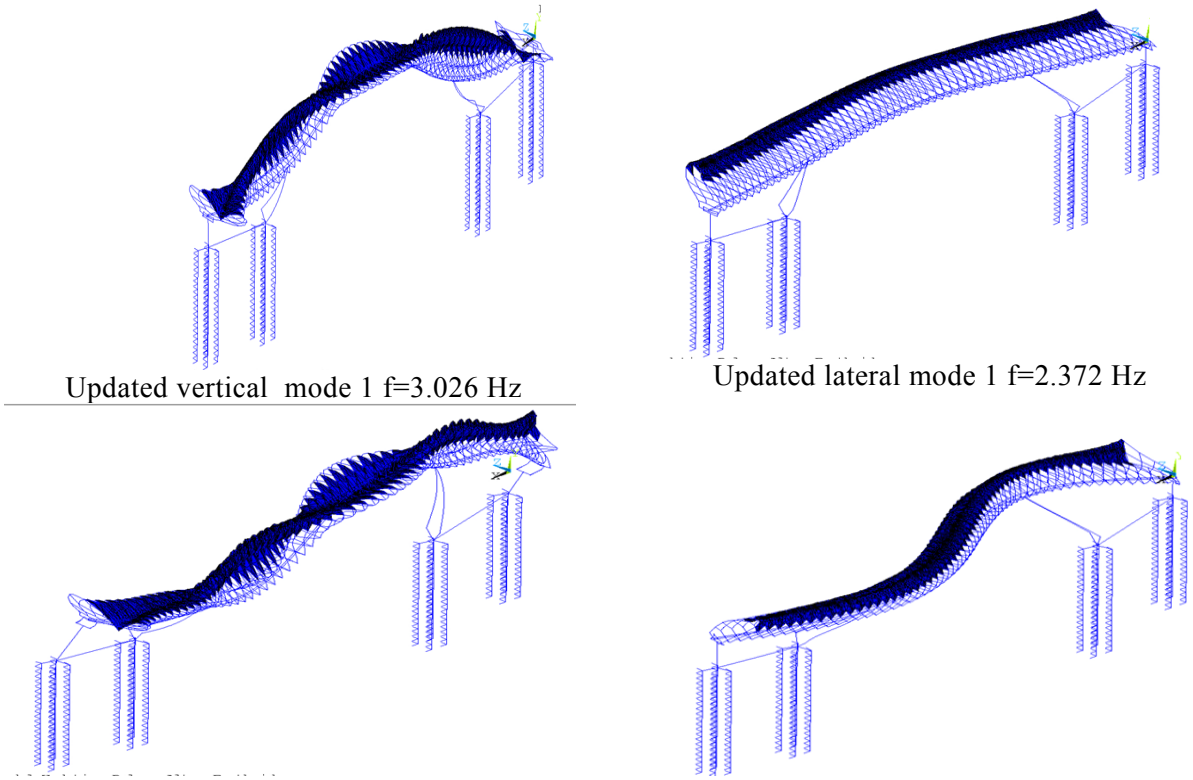

Updated vertical mode 1 f=3.026 Hz

Updated lateral mode 1 f=2.372 Hz

Updated vertical mode 2 f=3.844 Hz

Updated lateral mode 2 f=5.508 Hz

Fig. 9: Updated four first vibration modes.

6. Numerical estimation of the effect of the steel cover construction.

In Table 3 the variation in the natural frequencies of the footbridge due to the construction of the footbridge has been estimated. From the updated finite element model, it has been possible to simulate the behaviour the dynamic behaviour of the footbridge without the steel roof (f_{NUM_INI}) and the current situation (f_{NUM_COV}). Both values have been obtained numerically. The percentage values are representatives of the stiffening effect that the cover presents in each direction.

Table 3: Estimation of the change in the natural frequencies of the footbridge

Mode	f_{NUM_INI} [Hz]	f_{NUM_COV} [Hz]	Description	Δf [%].
1	2.569	2.372	Lateral	-7.69
2	2.839	3.026	Vertical	6.55
3	3.863	3.844	Vertical	-0.51
4	5.722	5.508	Lateral	-3.74

The steel cover increase the stiffness of the footbridge in the vertical direction, however, in the lateral direction the construction of the steel cover reduces the value of the natural frequencies in that direction.

From the point of view of the maximum acceleration values achieved, there is a slight improvement in the comfort level due to the stiffening of the structure. It presents certain safety margin, ensuring that the footbridge reaches a medium comfort level, through even, under a very rare load case as the

circulation on the footbridge of several joggers in parallel (Figure 10).

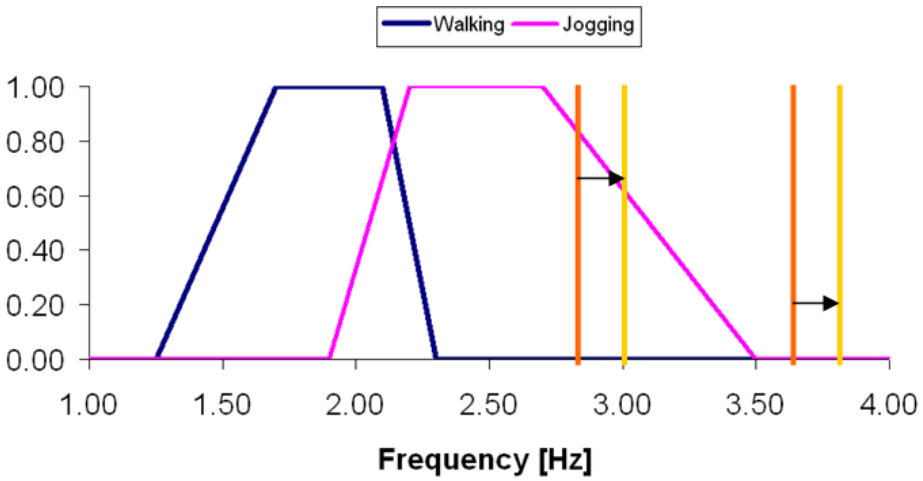

Fig. 10: Change in the first two vertical vibration modes. – without cover -- with cover

7. Conclusions.

In this paper, it has been estimated experimentally and numerically, the change of the dynamic behaviour of a slender footbridge due to the construction of a steel roof over the original structure. The steel roof increases the stiffness of the structure in vertical direction but reduces the value of the natural frequencies of the structure in the lateral direction. This effect is especially relevant in the first two natural frequencies of the structure. However, the values of the current natural frequencies ensure that the structure will not suffer from comfort problems due to pedestrians flow walking. In relation to jogging or running, it has been shown that the structural stiffening improves its behaviour under these types of human action.

8. References.

[1] SETRA, Guide méthodologique passerelles piétonnes (Technical guide footbridges: Assement of vibrational behaviour of footbridges under pedestrian loading), Setra, 2006.

[2] SYNPEX Guidelines, European Project on Advanced Load Models for synchronous Pedestrian Excitation and Optimized Design Guidelines for Steel Footbridges, 2007.

[3] CLOUGH, R and PENZIEN, J. Dynamics of Structures, 2nd. Edition, Mc Graw-Hill, 1993.

[4] AUTODESK ROBOT STRUCTURAL ANALYSIS PROFESSIONAL 2011.

[5] MAGALHÃES, F., CUNHA, A. "Explaining Operational Modal Analysis with data from an arch bridge", Mechanical Systems and Signal Processing, Invited Tutorial Paper, Volume 25, Issue 5, pp. 1431-1450 , 2011.

[6] ARTeMIS Extractor Pro 2012.

[7] ANSYS Mechanical Release 11.0.

[8] ZIVANOVIC, S., PAVIC, A. REYNOLD, P., "Finite element modelling and updating of a lively footbridge: The complete process", Journal of Sound and Vibration, Vol. 301,. nº 1-2, pp. 126-145,2007.